# THERMAL COMFORT UNDER TRANSIENT METABOLIC AND DYNAMIC LOCALIZED AIRFLOW CONDITIONS COMBINED WITH NEUTRAL AND WARM AMBIENT TEMPERATURES

A Dissertation

by

AHMET UĞURSAL

Submitted to the Office of Graduate Studies of
Texas A&M University
in partial fulfillment of the requirements for the degree of

DOCTOR OF PHILOSOPHY

December 2010

Major Subject: Architecture

# THERMAL COMFORT UNDER TRANSIENT METABOLIC AND DYNAMIC LOCALIZED AIRFLOW CONDITIONS COMBINED WITH NEUTRAL AND WARM AMBIENT TEMPERATURES

A Dissertation

by

AHMET UĞURSAL

Submitted to the Office of Graduate Studies of
Texas A&M University
in partial fulfillment of the requirements for the degree of

DOCTOR OF PHILOSOPHY

Approved by:

| | |
|---|---|
| Chair of Committee, | Charles H. Culp |
| Committee Members, | Louis G. Tassinary |
| | Mark J. Clayton |
| | Nancy W. Dickey |
| Head of Department, | Ward V. Wells |

December 2010

Major Subject: Architecture

## ABSTRACT

Thermal Comfort under Transient Metabolic and Dynamic Localized Airflow Conditions Combined with Neutral and Warm Ambient Temperatures.
(December 2010)

Ahmet Uğursal
B.Arch.; M.S., Middle East Technical University;
M.Arch., Ball State University
Chair of Advisory Committee: Dr. Charles H. Culp

Human thermal environments constitute complex combinations of various interacting thermal factors. The transient and non-uniform nature of those thermal factors further increases the complexity of the thermal comfort problem. The conventional approach to the thermal comfort problem has been simplifying the problem and providing steady thermal environments which would satisfy the majority of the people in a given space. However, several problems emerged with this approach. People became finely tuned to the narrow range of conditions and developed expectations for the same conditions which made them uncomfortable when there were slight deviations from those conditions. Also, the steady approach didn't solve the comfort problem because, in practice, people move between spaces, and thermal conditions such as metabolic rate, surface temperatures, airflow speed and direction vary in a typical day.

A human subject test was designed to determine the transient relationship between the people and their environments. In the first part, thermal perceptions of people were taken during various metabolic rate conditions. In the second and the third parts, transient conditions of different thermal factors were created. Various combinations of airflow frequencies, airflow location around the body, metabolic rate, and room temperatures were tested for their individual and interaction effects of providing thermal comfort. The concept of *Localized Dynamic Airflow* was proposed in which room airflow was simply redirected to different parts of the body with a varying airflow speed.

Results showed that males and females respond differently to the thermal conditions. The room temperatures they found neutral were significantly different. People's thermal comfort during transient metabolic conditions was similar to high metabolic conditions. This heightened response extended into the next ten minutes after the high metabolic conditions ended. Test results suggested that people tolerate higher temperatures during transient environmental conditions. The average response was for comfortable even during the high temperature (83°F) and high metabolic rate (4 met) conditions. Low energy use of the localized dynamic airflow and the increased room temperatures has significant potential for monetary savings.

To my mother, father, and sister

# ACKNOWLEDGEMENTS

I had the pleasure to work closely with many people during this research study. Among those people, I owe my deepest gratitude to Dr. Charles Culp, who has first become an advisor, then a mentor for me. The discussions we had in the past five years not only sharpened my critical thinking skills but also significantly improved my problem solving abilities. Without his guidance and support, this dissertation would not have been possible. I am also grateful to my committee members, Dr. Nancy Dickey, Dr. Louis Tassinary, and Dr. Mark Clayton, for their invaluable ideas and input which increased the quality of this study.

I am indebted to my colleagues, Daniel Farmer, Clinton Davis, Erica Salinas, Isaura Perez, and Cem Yuksel who helped me with the thermal comfort tests. I am also indebted to 40 human subjects who helped with the advancement of science by participating in the thermal comfort tests.

I would like to thank the American Society of Heating, Refrigerating, and Air Conditioning Engineers, and the Boston Society of Architects for partially supporting this research. I am also grateful to Dr. Jorge Vanegas, the Dean of the College of Architecture, and to Oscar Munoz, the Deputy Director of the Center for Housing and Urban Development, for providing the space for the thermal comfort test laboratory. I would also like to thank the College of Architecture staff, Melinda Randle, Ginger White, Hala Gibson, and Jill Raupe for their ever-existing help and friendship.

I consider myself lucky for having great friends with whom I shared my time in College Station the past several years. Among them, I am thankful to Ozan, Cansin, Dilhan, Cem, and Olcay whom I know I can always rely on. Finally, I am most grateful to Erin, for always being there and for always supporting me unconditionally.

# TABLE OF CONTENTS


Page

ABSTRACT ..... iii

DEDICATION ..... v

ACKNOWLEDGEMENTS ..... vi

TABLE OF CONTENTS ..... vii

LIST OF FIGURES ..... xii

LIST OF TABLES ..... xx

1. INTRODUCTION ..... 1

1.1 Background ..... 1
1.2 Objectives ..... 7
1.3 Relevance of the Study ..... 8

2. LITERATURE SURVEY ..... 10

2.1 Thermal Comfort and Thermal Sensation ..... 10
2.1.1 Thermal Comfort Variables ..... 13
2.1.2 Thermal Comfort Standards: ASHRAE Standard 55 and ISO 7730 ..... 13
2.1.3 Predicted Mean Vote (PMV) and Predicted Percentage Dissatisfied (PPD) ..... 14
2.1.4 Non-uniform Thermal Conditions ..... 15
2.1.5 Transient Thermal Conditions ..... 16
2.2 Transient and Non-uniform Thermal Comfort Variables ..... 19
2.2.1 Metabolic Rate and Thermal Comfort ..... 19
2.2.2 Dynamic Airflow and Draught Rating ..... 20
2.2.3 Local Airflow ..... 22
2.2.4 Trade-offs between Thermal Comfort Variables for Thermally Comfortable Environments ..... 23
2.3 Physiological Signals of Thermal Comfort ..... 24
2.3.1 Heat Balance and Thermoregulation ..... 24
2.3.2 Thermoreceptors and Thermal Sensation ..... 26
2.3.3 Skin Temperature ..... 29
2.3.3.1 Skin Temperature Response to Thermal Stress ..... 29
2.3.3.2 Skin Temperature Measurements ..... 31

Page


2.3.4 Skin Wettedness .... 34
2.3.5 Heart Rate (HR) .... 35
2.3.6 Electrodermal Activity (EDA) .... 36
2.4 Gender and Thermal Comfort.... 38
2.5 Computational Fluid Dynamics (CFD).... 39
2.5.1 Thermal Comfort Applications of the CFD Methodology .... 40
2.5.2 Review of the Turbulence Models .... 41
2.5.3 Human Geometry in CFD Simulations .... 42

3. METHODOLOGY .... 44

3.1 General Description of the Human Subject Tests.... 44
3.2 Thermal Comfort Test Design .... 44
3.3 Test Conditions.... 48
3.3.1 Ambient Temperature, Mean Radiant Temperature and Relative Humidity.... 49
3.3.2 Mean Airflow and Dynamic Airflow Conditions.... 49
3.3.3 Personal Variables .... 54
3.3.3.1 Determination of Metabolic Rate from Heart Rate .... 54
3.3.3.2 Clothing Insulation Level.... 56
3.4 Test Protocol.... 56
3.4.1 Pre-test.... 57
3.4.2 Session 1 .... 57
3.4.3 Session 2 and Session 3 .... 58
3.4.4 Post-test .... 58
3.5 Thermal Comfort Surveys .... 58
3.5.1 The Background Survey .... 59
3.5.2 The Online Survey.... 62
3.6 Statistical Analysis.... 65

4. INSTRUMENTS AND CALIBRATION.... 68

4.1 Data Collection and Processing.... 68
4.1.1 Data Acquisition (DAQ) System.... 68
4.1.2 Dataset Processing.... 70
4.2 Sensors.... 71
4.2.1 Temperature Measurements and Thermocouples (TCs).... 71
4.2.2 Globe Temperature Sensor .... 73
4.2.3 Dew Point Temperature Measurement and Chilled Mirror Sensor ... 75
4.2.4 Airflow Measurement.... 76
4.2.5 Physiological Measurements: Electrodermal Activity (EDA), Heart Rate, Tympanic Temperature, Weight Loss .... 77
4.2.6 Backpack Design .... 79
4.3 Test Room Design .... 79

Page


4.4 Sensor Calibration ........................................................................................ 84
4.4.1 Thermometer and Thermocouple (TC) Calibration.......................... 84
4.4.1.1 Auxiliary Mercury Thermometer Calibration .................. 85
4.4.1.2 Thermocouple (TC) Calibration for Random Errors (Noise) and Systematic Errors (Offsets)................ 87
4.4.2 Globe Thermometer Calibration...................................................... 91
4.4.2.1 Calibration Conditions .................................................... 94
4.4.2.2 Globe Thermometer Calibration Data .............................. 94
4.4.3 Thermal Comfort Station Airflow Calibration ................................ 95
4.4.3.1 Software Calibration for Target Airflow Speeds.............. 95
4.4.3.2 Thermal Comfort Station Airflow Measurements............ 100
4.4.4 Heart Rate Sensor Calibration ........................................................ 103
4.4.5 Weight Scale Calibration ............................................................... 104

5. GENDER DIFFERENCES OF THERMAL ENVIRONMENT PERCEPTION .......... 106

5.1 Thermal Comfort ........................................................................................ 106
5.1.1 Gender Differences of Thermal Comfort......................................... 106
5.1.2 Interaction Effects of Gender, Room Temperature, and Metabolic Rate on Thermal Comfort............................................... 108
5.2 Thermal Sensation ...................................................................................... 110
5.2.1 Gender Differences of Thermal Sensation....................................... 110
5.2.2 Interaction Effects of Gender, Room Temperature, and Metabolic Rate on Thermal Sensation............................................ 112
5.3 Neutral Temperatures for Males and Females ............................................ 114
5.4 Temperature and Air Movement Preferences ............................................... 116
5.5 Gender Differences of Transient Thermal Comfort and Thermal Sensation ....................................................................................... 117
5.6 Discussion.................................................................................................... 121

6. THERMAL COMFORT AND TRANSIENT METABOLIC CONDITIONS.............. 124

6.1 Overall Thermal Comfort and Thermal Sensation ....................................... 124
6.1.1 Predicted Mean Vote (PMV) and Predicted Percentage Dissatisfied (PPD) Results............................................................. 124
6.1.2 Three Methods of Mean Thermal Sensation Prediction ................... 126
6.2 Subjective Thermal Responses to Transient Metabolic Conditions .............. 128
6.2.1 Thermal Comfort and Thermal Sensation ....................................... 128
6.2.2 Temperature and Air Movement Preferences................................... 129
6.2.3 Environmental Acceptability .......................................................... 130
6.3 Empirical Models for Dynamic PMV.......................................................... 133
6.3.1 Short-term Time Dependent Model................................................. 134
6.3.2 Long-term Time Dependent Model................................................. 135

Page

6.4 Increase in Thermal Sensation Based on Short Durations of High Metabolic Activity Periods ..... 136
6.5 Discussion ..... 138

7. LOCALIZED AND DYNAMIC AIRFLOW FOR TRANSIENT THERMAL CONDITIONS ..... 141

7.1 Airflow Perception ..... 142
7.1.1 Airflow Preferences of Test Subjects ..... 142
7.1.2 Draught Discomfort ..... 146
7.2 Dynamic Airflow and Location of Airflow Stimulus on the Body ..... 147
7.2.1 Dynamic Airflow and Thermal Comfort ..... 148
7.2.2 Localized Airflow and Thermal Comfort ..... 150
7.2.3 The Interaction Effects of Airflow Period and Location on the Body (Localized Dynamic Airflow) ..... 153
7.3 Discussion ..... 155

8. PSYCHOPHYSIOLOGICAL RESPONSES OF THERMAL COMFORT ..... 158

8.1 Skin Temperature ..... 159
8.1.1 Mean Skin Temperature and Thermal Sensation Relationship ..... 159
8.1.2 Mean Skin Temperature Estimation ..... 161
8.1.3 Skin Temperature Setpoints and Variations ..... 163
8.2 Heat Balance and Local Heat Loss of the Human Body ..... 170
8.2.1 Core Body Temperature ..... 170
8.2.2 Evaporative Heat Loss ..... 171
8.2.3 Heat Transfer between the Body Core and the Skin Surface ..... 172
8.2.4 Local Heat Loss from the Skin Surface to the Environment ..... 173
8.3 Heart Rate and Electrodermal Activity (EDA) ..... 174
8.4 Diurnal Variations of Psychophysiological Factors ..... 177
8.5 Discussion ..... 179

9. COMPUTATIONAL FLUID DYNAMICS (CFD) SIMULATIONS OF THE THERMAL ENVIRONMENT ..... 183

9.1 Simulated Human Geometry and the Benchmark Tests ..... 183
9.1.1 Simulated Human Geometry ..... 183
9.1.2 Benchmark Tests for the Simulated Human Geometry ..... 184
9.1.2.1 The Mixing Ventilation Case ..... 186
9.1.2.2 The Displacement Ventilation Case ..... 190
9.2 Airflow Simulations of the Thermal Comfort Test Conditions ..... 196
9.2.1 Head-only Airflow ..... 198
9.2.2 Simultaneous Head/Hands/Feet Airflow ..... 200
9.3 Discussion ..... 204

| | Page |
|---|---|
| 10. CONCLUSIONS | 205 |
| 10.1 Summary | 205 |
| 10.2 Practical Applications | 210 |
| 10.3 Limitations and Future Research | 212 |
| REFERENCES | 214 |
| APPENDIX A: COMFORT STATION DRAWINGS AND CONSTRUCTION PHOTOS | 226 |
| APPENDIX B: TEST PROTOCOL | 229 |
| APPENDIX C: TEST SEQUENCES FOR COUNTERBALANCING | 233 |
| VITA | 237 |

# LIST OF FIGURES

FIGURE Page

2.1 Thermal comfort and sensation scales used in this study .................................... 11

2.2 Thermal sensation vs. thermal comfort graph by Zhang and Zhao (2008b) ......... 12

2.3 The parabolic relationship between thermal sensation and thermal comfort (Zhang 2008a) ......................................................................................... 12

2.4 Base firing of warm thermoreceptors in different ambient temperatures and convection coefficients (Lv and Liu, 2005).................................................. 27

2.5 Static and dynamic responses of TRs to temperature changes (Hensel, 1981)..... 28

2.6 Summary of previous studies by Yao et al. (2008) on skin temperature measurement sites. ........................................................................................ 31

2.7 Skin temperature measurement sites (1: Forehead, 2: Cheek, 3: Neck, 4: Chest, 5: Abdomen, 6: Upper Back, 7: Lower Back, 8: Upper Arm, 9: Lower Arm, 10: Hand, 11: Anterior Thigh, 12: Anterio-medial Thigh, 13: Anterior Calf, 14: Posterior Calf, 15: Instep)....... 33

2.8 The relationship between metabolic rate, oxygen consumption and heart rate (Zhang 2003b)......................................................................................... 36

2.9 Three electrode location alternatives for EDA measurements (Cacioppo et al., 2007) ......................................................................... 37

3.1 Test sequence with online survey instances including the 5 minute breaks between the sessions .................................................................... 48

3.2 Limits of draught discomfort as a function of mean air velocity and turbulence intensity (Mayer, 1987). ............................................................ 51

3.3 Percent of dissatisfied due to draught as a function of mean air velocity for three turbulence intensity bins (Fanger, 1988) .............................................. 51

3.4 Airflow speed pattern of 30-second pulsed air measured between the subjects' head and the nozzle. .................................................................................. 52

3.5 Airflow speed pattern of 60-second pulsed air measured between the subjects' head and the nozzle ......................................................................................... 52

3.6 Sin(30) airflow patterns of Tanabe and Kimura (1994) ...................................... 53

FIGURE Page

3.7 Pulse airflow pattern of Tanabe and Kimura (1994) ........ 53

3.8 Comparison between this study and Zhang et al. (2003b) in estimating metabolic rate from heart rate........ 56

3.9 Background characteristics section of the *Background Survey*........ 60

3.10 Personal control section of the *Background Survey*......... 60

3.11 Health characteristics section of the *Background Survey*........ 61

3.12 Environmental sensitivity section of the *Background Survey*......... 61

3.13 Thermal Comfort *Online Survey* screen......... 64

3.14 Initial input screen of the *Online Survey*........ 64

4.1 NI 6031E I/O Terminal ........ 69

4.2 DAQ software interface ........ 69

4.3 5 second interval data processing scheme........ 70

4.4 *Online Survey* based data processing scheme ........ 70

4.5 T-type thermocouple and INOR Transducers ........ 72

4.6 Medical mesh to secure thermocouples ........ 72

4.7 Schematics of the globe thermometer ........ 74

4.8 Air nozzle, globe thermometer, thermocouple for air temperature and the air velocity probe shown together in the test setup........ 75

4.9 Dew-10 chilled mirror sensor........ 76

4.10 Coulbourn Lablinc V Isolated Skin Conductance Coupler and Bioamplifier....... 77

4.11 MagneTrainer bicycle ergometer ........ 78

4.12 The modified backpack to accommodate the skin thermocouples........ 79

4.13 Test subject’s workstation with the bicycle ergometer ........ 81

4.14 Plan of the test room ........ 82

FIGURE Page

4.15 Three-dimensional drawing of the cubicle design ............................................ 82

4.16 The connection diagram of PCs and PC screens of the researcher and the test subject on both sides of a hypothetical line ..................................... 83

4.17 Subject’s workstation with sensor backpack...................................................... 84

4.18 Schematics of the ice bath and the boiling point calibration setups..................... 86

4.19 Images from the actual ice bath and the boiling point calibration setups ............ 86

4.20 Thermometer measurements during cool-down period....................................... 87

4.21 Modified refrigerator that was used as calibration chamber ............................... 88

4.22 TC copper calibration block.................................................................................. 89

4.23 Raw data and different levels of filtering for reducing the random errors (noise) ......................................................................................... 89

4.24 TC measurements compared to the thermometer data ........................................ 90

4.25 Globe thermometer calibration setup ................................................................. 92

4.26 Procedure diagram of the globe thermometer calibration ................................... 93

4.27 Fan voltage for different software settings......................................................... 95

4.28 Power consumption of the fan for various nozzle opening conditions ................ 96

4.29 The manikin that was used as the human figure during airflow measurements.... 97

4.30 Airflow speeds at the nozzle exit ........................................................................ 97

4.31 Airflow speeds behind the manikin’s neck at different software settings............ 98

4.32 Airflow speed at the head-nozzle exit when all the nozzles are open.................. 98

4.33 Airflow speed behind manikin’s neck when all nozzles are open........................ 99

4.34 Elevation of the thermal comfort unit showing the airflow measurement locations ........................................................................... 101

4.35 Plan of the thermal comfort unit showing the airflow measurement locations..... 101

FIGURE Page


5.1 Thermal comfort responses of males and females under low (1.2 met), medium (2.6 met) and high (4 met) metabolic conditions .................................... 107

5.2 The combined effects of temperature and metabolic activity level on thermal comfort under low (1.2 met), medium (2.6 met) and high (4 met) metabolic conditions for males ........................................................ 109

5.3 The combined effects of temperature and metabolic activity level on thermal comfort under low (1.2 met), medium (2.6 met) and high (4 met) metabolic conditions for females ..................................................... 110

5.4 Thermal sensation responses under low (1.2 met), medium (2.6 met) and high (4 met) metabolic conditions ......................................................................... 111

5.5 The combined effects of temperature and metabolic activity level on thermal sensation under low (1.2 met), medium (2.6 met) and high (4 met) metabolic conditions for males ........................................................ 113

5.6 The combined effects of temperature and metabolic activity level on thermal sensation under low (1.2 met), medium (2.6 met) and high (4 met) metabolic conditions for females ..................................................... 114

5.7 Comparison of thermal sensation models for the given conditions ...................... 115

5.8 Mean temperature preference under low (1.2 met), medium (2.6 met) and high (4 met) metabolic conditions ................................................................. 116

5.9 Mean air movement preference under low (1.2 met), medium (2.6 met) and high (4 met) metabolic conditions ................................................................. 117

5.10 Thermal comfort votes for males and females for the duration of the test............ 118

5.11 Thermal sensation votes for males and females for the duration of the test ......... 120

5.12 Average thermal environment acceptability for the whole test............................ 122

6.1 Correlation between thermal sensation (TS) and thermal comfort (TC).............. 125

6.2 PPD from Fanger's equation and the percentage of dissatisfaction results from the test data plotted together ............................................................ 126

6.3 Mean thermal comfort and thermal sensation based on metabolic rate ................ 128

6.4 Mean temperature preference for three metabolic rate conditions........................ 129

6.5 Mean airflow preference for three metabolic rate conditions .............................. 130

FIGURE Page

6.6 Mean environmental satisfaction votes for three metabolic conditions ............... 131

6.7 The proposed two-staged model of thermal environment perception .................. 132

6.8 Number of instances in which people reported satisfaction or dissatisfaction...... 133

6.9 Thermal sensation, PMV and time-averaged PMVs for the duration of the test... 135

6.10 Long-term (up to 1.5 hours) time effect due to repeated high metabolic rate....... 136

6.11 Increase in thermal sensation as a function of percentage of high metabolic activity period........................................................................................... 137

6.12 Thermal sensation increase factor over the initial thermal sensation................... 138

7.1 Airflow preference percentages grouped by airflow preference class ................. 143

7.2 Airflow preferences as a function of metabolic rate ........................................... 144

7.3 Mean air movement preference for various metabolic and room temperature conditions................................................................................. 144

7.4 The relationship between draught discomfort and the metabolic rate.................. 147

7.5 Thermal sensation and thermal comfort as a function of airflow (83°F Ta, 45% RH, 0.5 clo, 2.13 met) ................................................................ 155

8.1 The relationship between mean skin temperature and the thermal sensation under three metabolic rate conditions ................................................................ 160

8.2 Differences between the skin temperatures and skin temperature setpoints for the course of the test ........................................................................... 165

8.3 Skin temperatures for five locations.................................................................... 165

8.4 Head region temperature differences between the skin temperatures and skin temperature setpoints ............................................................................. 166

8.5 Torso region temperature differences between the skin temperatures and skin temperature setpoints ............................................................................. 166

8.6 Arm region temperature differences between the skin temperatures and skin temperature setpoints ............................................................................. 167

8.7 Leg region temperature differences between the skin temperatures and skin temperature setpoints ............................................................................. 167

FIGURE Page

8.8 Comparison of average skin temperatures for the sedentary/neutral conditions and for the overall test of the current study with Houdas and Ring (1982), Arens et al. (2006a), and Yao et al. (2008) ................. 170

8.9 Correlation between thermal comfort and the difference between core and mean skin temperature as normalized based on body mass index.......... 173

8.10 Thermal responses and EDA data for the duration of the whole test.................... 176

8.11 Transient behavior of physiological signals and thermal responses ..................... 177

8.12 Diurnal variations of mean skin temperature, thermal sensation, thermal comfort and electrodermal activity ........................................................ 178

9.1 Simulated human model shown in rendered and wireframe modes...................... 184

9.2 The mixing ventilation case of the CFD simulation (Nielsen, 2003)................... 185

9.3 The displacement ventilation case of the CFD simulation (Nielsen, 2003).......... 185

9.4 Computer simulated persons (CSPs) that were used by Topp et al. (2002).......... 186

9.5 The simulation domain of the simulated human geometry for the mixing ventilation case.......................................................................................... 187

9.6 Velocity profiles at the virtual data probes located on the x-axis (Topp, 2002)... 188

9.7 Velocity profiles of this study at the virtual data probes located on the x-axis..... 188

9.8 Air velocity profiles on the x-axis........................................................................ 189

9.9 The cross section of the displacement ventilation case and the data probes (Nielsen, 2003)........................................................................................... 190

9.10 Human geometry and the simulation domain of the current study ....................... 191

9.11 Velocity profiles for three grid sizes as simulated at the L1 probe....................... 191

9.12 Velocity profiles at the L2 probe in Deevey et al. (2006).................................... 192

9.13 Velocity profiles for three grid sizes as simulated at the L2 probe....................... 192

9.14 Velocity profiles at the L4 probe in Deevey et al. (2006).................................... 193

9.15 Velocity profiles for three grid sizes as simulated at the L4 probe....................... 193

FIGURE Page

9.16 Velocity profiles at the L5 probe in Deevey et al. (2006) .................................... 194

9.17 Velocity profiles for three grid sizes as simulated at the L5 probe ...................... 194

9.18 Velocity distribution on the central axis of the simulation domain...................... 195

9.19 CFD model of the thermal comfort test room ..................................................... 196

9.20 The structured grid scheme of the simulation domain ......................................... 197

9.21 Probes around the manikin which were used to compare the measured and the simulated data ........................................................................................... 198

9.22 Measured and simulated data at the X-probe for the head-only airflow .............. 199

9.23 Measured and simulated data at the XYnF probe for the head-only airflow ........ 199

9.24 Measured and simulated data at the XYnB probe for the head-only airflow ........ 200

9.25 Measured and simulated data at the XW probe for the head-only airflow ........... 200

9.26 Measured and simulated data at the X probe for the simultaneous airflow .......... 201

9.27 Measured and simulated data at the Z probe for the simultaneous airflow ........... 201

9.28 Measured and simulated data at the XYnF probe for the simultaneous airflow ... 202

9.29 Measured and simulated data at the XYnB probe for the simultaneous airflow ... 202

9.30 Air velocity profiles on the head nozzle cross section ......................................... 203

9.31 Air velocity profiles on the hand and foot nozzle cross section ........................... 203

A.1 Plan drawing of the Thermal Comfort Station ................................................... 226

A.2 Section drawing of the Thermal Comfort Station ............................................... 226

A.3 Construction of the Comfort Station wall ......................................................... 227

A.4 Connection of the fan to the Comfort Station for the test run .............................. 227

A.5 Connection of the wall to the Comfort Station base ............................................ 228

A.6 Completed Comfort Station before the test runs .................................................. 228

FIGURE Page

C.1 The first test sequence used for counterbalancing the treatment effect................ 233

C.2 The second test sequence used for counterbalancing the treatment effect........... 234

C.3 The third test sequence used for counterbalancing the treatment effect .............. 235

C.4 The fourth test sequence used for counterbalancing the treatment effect ............ 236

# LIST OF TABLES


TABLE Page

2.1 Summary of skin temperature measurement sites from the literature .................. 32

3.1 Summary of demographic information of the participants .................................. 45

3.2 Between-subjects variables .................................................................................. 46

3.3 Within-subject variables (metabolic rate, airflow frequency, and airflow location) as triple combinations of treatments during the Session 2 and 3 of the test (Session 1 is the control condition) ........................... 47

3.4 Four test sequences to counter balance the treatment order ................................. 47

3.5 Maximum and mean airflow conditions for two types of airflow patterns ........... 50

3.6 Test constructs for thermal comfort survey and their scales........................ 63

4.1 Ice bath and boiling point measurements after stabilization of the water ............ 86

4.2 Average systematic errors (offsets) between the thermocouples and the thermometer data in Fahrenheit..................................................................... 91

4.3 Offsets between the measured and the calculated MRTs in Fahrenheit................ 94

4.4 Average airflow speeds at various locations around the human body ................. 102

4.5 Heart Rate (HR) data as calculated from the oscilloscope readings and from the Polar system.......................................................................................... 103

4.6 Hourly drift test of the digital scale..................................................................... 104

4.7 Daily drift test of the digital scale ....................................................................... 105

5.1 Mean thermal comfort votes under three metabolic activity conditions .............. 107

5.2 Mean thermal comfort votes under different temperature and metabolic rate conditions ........................................................................................ 108

5.3 Mean thermal sensation votes under different metabolic rate conditions ............. 111

5.4 Mean thermal sensation votes under different temperature and metabolic rate conditions ........................................................................................ 113

TABLE Page

5.5 Thermal comfort drop during the 5-minute exercise sessions (7-point scale) ...... 119

5.6 Thermal sensation drop during the 5-minute exercise sessions (7-point scale) .... 120

6.1 Results from three methods of determining average thermal sensation for 75°F and 83°F room temperatures ........................................................................ 126

6.2 Percentage of people dissatisfied in three metabolic conditions (1 Met = 58.15 W/m$^2$) ........................................................................................ 133

7.1 Airflow preferences for different thermal sensation votes and mean air velocity of 0.21 m/s........................................................................................ 145

7.2 Airflow preferences for different thermal sensation votes and mean air velocity of less than 0.2 m/s (reproduced from Zhang et al. (2007a)) ............. 146

7.3 DR calculation based on Fanger et al.'s formula and the air movement dissatisfaction from the test data ........................................................................ 146

7.4 Normalized and actual thermal comfort votes for three airflow conditions.......... 149

7.5 Normalized and actual thermal sensation votes for three airflow conditions........ 149

7.6 Airflow preference for three airflow conditions (-1: Less Air, 0: No Change, +1: More Air)......................................................... 150

7.7 Normalized and actual thermal comfort votes for three airflow conditions.......... 152

7.8 Normalized and actual thermal sensation votes for three airflow conditions........ 152

7.9 Airflow preference for three airflow conditions (-1: Less Air, 0: No Change, +1: More Air)......................................................... 153

7.10 ANOVA table for the Individual and interaction effects of localized and dynamic airflow for thermal comfort. .......................................................... 154

8.1 ANOVA table for thermal sensation and mean skin temperature with metabolic rate as the grouping factor .................................................................. 160

8.2 Skin temperature sites that are correlated with the mean skin temperature for three metabolic rate conditions...................................................................... 161

8.3 Skin temperature sites that are correlated with the mean skin temperature for two temperature conditions ............................................................................ 163

TABLE Page

8.4 Regression coefficients of deviations of different skin temperatures from setpoints in determining the thermal sensation ..................................................... 168

8.5 Parameter estimates for thermal sensation based on MST and dMST ................. 169

8.6 Body core temperature throughout the test ........................................................... 171

8.7 Weight loss (lbs) of the subjects during the test.................................................... 172

8.8 Evaporative and overall heat loss for males and females...................................... 172

# 1. INTRODUCTION

## 1.1. Background

Providing a thermally appropriate environment for human occupancy has long been a problem of architectural design. According to Badagliacca (2002), the root of this problem lies in the desire of man to provide himself a “sensation of pleasantness in his interaction with any external “Entity”, that may be physical, social or of other kinds”. Man’s desire to provide a sensation of pleasantness in terms of thermal comfort has a physiological basis. The human body can only function within a band of temperatures, and excessive deviations from the normal body temperature have detrimental consequences. Thermal sensation which can be expressed as the feeling of warmth and coolness is the signal to correct potential deviations from the normal body temperatures.

Human body is in constant state of heat exchange with the environment. Thermal comfort is based on the heat balance between the human body and the environment and is regulated through the four environmental and two personal parameters (Zhang et al., 2004). The four environmental parameters are air temperature, humidity, mean radiant temperature and airflow and the two personal parameters are metabolic rate and clothing level (Olesen and Brager, 2004). This approach assumes that a person is thermally comfortable as long as there is a steady heat exchange of the body with the environment. Body temperature rises and a person feels warm if the heat generated inside the body is more than the heat lost to the environment. Similarly, body temperature drops and a person feels cool if the heat generation is less than the heat loss (Houdas and Ring, 1982). The human body is considered as a machine from the energetic point of view with internal heat generation, mechanical efficiency and heat exchange with the environment (McIntyre, 1980). During the heat exchange process, thermoreceptors, which are located largely in the skin and partly in the hypothalamus, send hot or cold warning signals. Based on these signals, the effector mechanisms of the body such as vasodilatation, vasoconstriction, sweating or shivering are activated to maintain homeostasis (Cabanac, 1981; Parsons, 2003).

This dissertation follows the style of *Indoor Air*.

McIntyre (1980), Prek (2006) and Sakoi et al. (2007) stated three conditions of thermal comfort as the heat balance, skin temperature and sweat rate, all of which are directly physiological. Steady-state and transient models of human body exist which take into account effector mechanisms and physiological variables (Gagge et al., 1970; Fanger, 1970; Stolwijk, 1971; Wissler, 1985; Tanabe et al., 2002; Huizenga et al., 2001; Iyoho et al., 2004; Jang et al., 2009).

ASHRAE Standard 55 (2004) defines thermal comfort as the state of mind, where a person expresses satisfaction with the thermal environment. This definition stresses the psychological process that is involved in perception of the thermal environment. In the process of generating a thermal comfort response, the sensory data from thermoreceptors are evaluated by the hypothalamus and a thermal comfort response is generated after processing the data based on the psychological state. The psychological processes involve psychological adaptation, naturalness of the environment, expectations, short and long-term experience, and perceived control (Nikolopoulou and Steemers, 2003). Jones (2002) argued that the relationship between physiological responses and thermal comfort is not established.

The major thermal comfort standards (ASHRAE Standard 55, 2004; ISO 7730, 2005) are based on the steady-state predicted mean vote (PMV) model of Fanger (1972) which has become the *de facto* standard for thermal environment design for human occupancy. As a result, the conventional thermal environment design focuses on steady-state environments at which environmental parameters are constant (Zhao et al., 2004) to achieve 80% satisfaction level with the thermal environment (Brager et al., 2004; ASHRAE, 2004). The aim of the designer became to create uniform environments which provide thermal comfort for the maximum possible number of occupants (Rowe, 2001). However, the steady-state approach is not adequate to explain real-life thermal comfort requirements because transient conditions are more likely to happen during a typical day. Environmental conditions deviate from the steady states, and transient conditions of temperature and air velocity occur (Fiala et al., 2003) such as in a car with air conditioning or in an office space with large windows and temperature gradients (Zhang, 2003a). In addition, people move around, change their clothing and activity levels (Jones and Ogawa, 1992). Bauman et al. (1994) measured in a field study that office workers are away from their workstations 30% of the time. Even when working in a sedentary/neutral environment, metabolic rate changes which creates transient conditions (McIntyre, 1980). In short, transient thermal conditions continuously occur and steady-state relationships of environmental and personal parameters of thermal comfort do not account for the transient conditions (Jones, 2002; Hanqing et al., 2006).

Environmental parameters differ at each moment and therefore a group of lumped indoor physical parameters are not sufficient to explain thermal comfort indoors (Hanqing et al., 2006). The conventional air-conditioning strategy which is preprogrammed to keep the area temperature within a constant range and to keep the airflow at low speeds causes two problems (Zhou et al., 2006). One is the air-conditioning syndrome due to lack of environmental stimulus, which conditions people to expect a very narrow range of thermal condition. The other problem is higher energy costs due to maintaining the temperatures at low levels. According to U.S. Energy Information Administration's (EIA) Commercial Building Energy Consumption Survey (CBECS), heating and cooling energy use constitute about 20% of the total energy consumption in commercial buildings (EIA, 2006). The energy crisis of 1973 raised the awareness to cut back the energy consumption especially in buildings. However, the measures taken by the design engineers were based on sealing the buildings from the outside conditions, which in turn led to the comfort and health problems among occupants (Mui and Chan, 2005). Van Hoof and Hensen (2007) and de Dear et al. (1997) supported Zhou et al. by stating that occupants of the air-conditioned buildings become tuned to the narrow range of comfort temperatures which makes them twice as sensitive to the changes in temperature than the occupants of the naturally ventilated buildings. Building occupants also develop expectations for homogeneous and cool environments. On the other hand, occupants of naturally ventilated buildings are more active in thermoregulatory adaptation through changes in their activity level and clothing (behavioral adaptation). They also tend to be more tolerant to wider ranges of temperatures (psychological adaptation) (Van Hoof and Hensen, 2007). Zhou et al. (2006) and Nikolopoulou and Steemers (2003) supported this point by stating that varying thermal experiences may alter people's expectation and affect their comfort feeling.

In the real world, simultaneous changes in environmental and personal parameters create a dynamic thermal environment. As stated previously, dynamic environments shift people's expectations towards the thermal conditions and their thermal comfort level. Therefore, there is a potential for high thermal comfort due to increased tolerance towards dynamic environments even though the conditions are uncomfortable according to the thermal comfort standards. A thermal comfort test with human subjects was designed to determine the thermal comfort responses under transient thermal environments. The major between-subjects variables are the room temperature and gender, while the major within-subject variables are the metabolic rate, frequency of the air pulse, and the location of airflow on the body. De Dear (2004) compared the advantages and disadvantage of field studies and laboratory studies of thermal comfort research. Our study attempted to use the advantages of both methodologies to increase the external validity as in a field study without compromising the rigor which is the strong point of a laboratory study. To achieve this, an actual office environment was converted into an environmentally controlled room to alleviate the feeling of a laboratory environment and to avoid a shift in subjects' expectations. This is explained in detail in Section 4.3.

This study also differs from the previous studies in terms of the thermal environment conditions and the non-intrusive methods of changing thermal variables. First, realistic scenarios of thermal conditions were designed such as short periods of high metabolic conditions followed by sedentary metabolic conditions as in moving between offices or climbing the stairs. Airflow was directed to different parts of the body since in real environments, airflow is directional and non-uniform around the body. Airflow speed was varied at two different frequencies to emulate the varying airflow speeds in naturally ventilated spaces. Previous studies of thermal comfort focused on one or two variables and their interactions which cannot represent real environments and reduces the external validity. This study focused on the interactions of three within-subject variables for two different temperature conditions which are more realistic and applicable to the actual environments. *Localized Dynamic Airflow* is proposed as the new terminology to represent the coupling of the varying airflow speeds at different locations on the human body.

Gender was chosen as a between-subjects variable because it is a pronounced factor which yields significant differences of thermal comfort and thermal sensation, even when individual variations such as acclimation to physical conditions, age, and expectations are considered. Several laboratory studies showed the gender differences of thermal comfort (Griefahn and Kunemund, 2001a; Fanger, 1972; Parsons, 2002; McNall et al., 1968; Tanabe et al., 2007; Beshir and Ramsey, 1981). In our study, approximately equal number of male and female students participated in the test which allowed a comparative study to be made between the genders.

Room temperature was considered another between-subjects variable since the effect of temperature on thermal comfort has very little variability among different subjects. Higher temperatures yield warmer thermal sensation, and lower temperatures yield cooler thermal sensation.

Duration and location of a stimulus on the body, pre-existing thermal state of the body and temperature intensity are among the factors which affect thermal sensation of people in dynamic environments (Parsons, 2003). In our study, the within-subject variables (metabolic rate, airflow location and frequency) are the variables which were used to create a dynamic thermal environment. Thermal responses of the participants were taken for varying metabolic rate conditions ranging from sedentary (1.2 met) to high metabolic conditions (4 met). Airflow was added a time component by pulsing the air every 30 seconds or 60 seconds. Two different locations on the human body were treated with the dynamic airflow which were head-only or head/hands/feet simultaneously. The worst case thermal conditions in this study fall outside the comfort zone defined by the comfort standards (ASHRAE Standard 55, 2004; ISO 7730, 2005).

Several studies showed that dynamic airflows with higher power spectrum, varying velocities and high turbulence intensities have more cooling effect than the constant airflow (Zhou et al., 2006; Toftum and Nielsen, 1996; Fanger et al., 1988; Tanabe and Kimura, 1994). Dynamic airflow inhibits skin thermoreceptors from adapting to the airflow conditions as occurs with a constant stimulus. Turbulence intensity increases the convection coefficient, and thus increases the convective heat loss on the skin surface. Previous studies also showed that localized thermal sensation at thermally sensitive regions of the body can significantly shift overall thermal sensation of people (Zhang et al., 2004; Arens et al., 2006b; Toftum and Nielsen, 1996; Wang et al., 2007; Pellerin et al., 2004; Huda and Homma, 2005). Among different regions of the body, head, neck, hands and the feet are the most sensitive regions. Sections 2.2.2 and 2.2.3 presents the details of the dynamic airflow and airflow location in more detail.

This dissertation presents the research effort in ten sections as described below.

Section 1, *Introduction,* presents the topic with a brief background literature, sets the objectives and states the relevance of the study.

Section 2, *Literature Survey,* presents the literature survey for various topics related to the thermal comfort. Literature survey is a critical discussion of the previous research based on the analyses presented in the following sections. Fundamental concepts of thermal comfort were also discussed briefly.

Section 3, *Methodology,* presents the human subject test design, test protocol and the thermal conditions that were utilized during the tests. In additions, it presents the two types of questionnaires and the statistical analysis methods.

Section 4, *Instruments and Calibration,* presents the equipments that were used in the tests including the workstation design, various sensors, and the data acquisition (DAQ) system. Also presented are the calibration procedures for various sensors and the airflow conditions around the human body.

Section 5, *Gender Differences of Thermal Environment Perception,* presents thermal comfort requirements, temperature and airflow preferences of males and females in a comparative method.

Section 6, *Thermal Comfort and Transient Metabolic Conditions,* presents three methods of predicted mean vote (PMV) calculation, thermal comfort requirements for transient metabolic conditions and two empirical models for time-dependent PMV calculation.

Section 7, *Localized and Dynamic Airflow for Transient Thermal Conditions,* presents the effects of airflow location and the pulsing on thermal comfort in combination with the transient metabolic conditions and different room temperatures.

Section 8, *Psychophysiological Responses of Thermal Comfort,* presents the relationship between thermal responses and the physiological signals including skin temperature, heart rate, and electrodermal activity. Diurnal variations of thermal comfort requirements were also presented in this section.

Section 9, *Computational Fluid Dynamics Simulations of the Thermal Environment,* presents the development of a simulated human geometry and the benchmark tests to validate the computational fluid dynamics (CFD) models. This section also presents the airflow simulations of the thermal comfort test conditions in comparison with the measured airflow data.

Section 10, *Conclusion,* presents a summary of the study with the concluding remarks, the practical applications of the research findings and the future research possibilities.

The appendices present the supplemental information related to the test design, procedures and the environmental conditions.

### 1.2. Objectives

This research study aims at determining the effectiveness of transient variables to provide thermal comfort in relation to a three-dimensional human body. The specific research question is:

> *What is the alternative environmental conditioning system design and operation method in relation to architectural space that would increase thermal comfort by responding to thermal comfort requirements under transient conditions?*

Once the relationship between the perceived comfort and the transient thermal factors is established, enhanced productivity with reduced energy use should be possible. To accomplish the objectives, a laboratory test station was constructed which contained a workstation, ways to direct and modulate airflow to the test subject, and a computerized and interactive program to query the test subject's comfort level at predetermined times. The objectives of this study are summarized as major and minor objectives.

Major Objectives:

a. To determine the thermal comfort requirements of people during transient metabolic conditions in comparison to the high and low metabolic conditions and to determine the length of transient thermal response period during metabolic cool-down.

b. To determine the thermal comfort responses for increased setpoint temperatures (83°F compared to 75°F) which has the potential for energy savings even when the metabolic conditions vary between high and low metabolic rates.
c. To determine the effectiveness of the localized dynamic airflow in providing thermal comfort for thermal conditions ranging from sedentary (1.2 Met) and neutral temperatures (75°F) to high metabolic rate (4 Met) and warm temperatures (83°F).
d. To determine the optimum airflow location and pulsing frequency combination (localized dynamic airflow) that provides maximum thermal comfort for three metabolic conditions (1.2 Met, 2.6 Met, and 4 Met) and two room temperatures (75°F and 83°F).
e. To determine the gender differences of thermal comfort requirements for three metabolic conditions (1.2 Met, 2.6 Met, and 4 Met) and two room temperatures (75°F and 83°F).
f. To determine the diurnal variations of physiological functions and thermal comfort requirements.

Minor Objectives:

a. To determine the thermal comfort effects of previous thermal experiences, previous sick building syndrome symptoms, and sensitivity to various environmental stimulus.
b. To determine subjects' airflow preferences and their relationship to metabolic condition, room temperature and the gender.
c. To determine the relationship between skin temperature and the thermal sensation for different metabolic conditions.
d. To determine the minimum required skin temperature sites to accurately calculate mean skin temperature.

## 1.3. Relevance of the Study

The deterministic approach to thermal comfort accepts humans as the passive recipients of the external stimulus and humans evaluate the thermal environment based on expectations. Thermal comfort standards are the distilled versions of this deterministic approach to thermal comfort (De Dear, 2004). However, arguably the most important aspects of thermal comfort, i.e. the physiological and psychological drives that generate a subjective evaluation of the thermal environment are missing from the comfort standards. One objective of this study is to determine the relationship between the thermal comfort and the physiological signals. The practicality of using the physiological signals as indicators of thermal comfort and as inputs to thermal environment control is arguable. However, proposals (Mabuchi et al., 1996; Lv and Liu, 2005) for this type of systems had already been made and with the advent of the technology, it will be possible to use psychophysiological signals as input to the environmental conditioning.

This study's objective of increasing setpoint temperatures while maintaining or improving the thermal comfort has a significant potential for energy savings. A 1°C change in temperature setpoints can yield savings of 10% in heating or cooling costs (Tanabe and Kimura, 1994). Zhao et al. (2004) similarly calculated that increasing the temperature setpoint by 3.5°C and providing a dynamic airflow environment can save up to 39% of the total energy in a typical urban office building. Moreover, the perception of the thermal environment has a significant relationship to human productivity (Tanabe et al., 2007; Kosonen and Tan, 2004; Tse and So, 2007). Increasing thermal comfort by creating a dynamic environment can result in increased productivity. This can result in significant monetary gain since worker salaries far exceed the total cost of building energy, maintenance, construction and rental expenses (Kosonen and Tan, 2004; Woods, 1989). Seppanen et al. (2004) showed that better indoor climate conditions improved thermal comfort and workers' productivity which led to monetary gains.

The cooling strategy of this study is based on directing the existing room air to specific locations on the body to maximize the cooling effectiveness. The distribution of the air around the person is decoupled from the room diffuser therefore the air handling unit. The fan power can be reduced at the air handling unit since diffusers don't need the high pressures to distribute the air inside the room. Zhou et al. (2006) states that the higher temperatures can be offset by the cooling effect of airflow which will also help reduce the energy consumption. The total amount of air for comfort can be reduced significantly by using less amount of air at higher speeds directed to the body. In addition, only the existing room air was used in this study without the cooled air from the air handling unit even in warm room temperatures. In conclusion, the findings of this study have significant potential to reduce the amount of cooled air and the fan power.

# 2. LITERATURE SURVEY

## 2.1. Thermal Comfort and Thermal Sensation

The expression of thermal comfort is a result of psychological processes after the evaluation of the thermal signals. ASHRAE Standard 55 (2004) defines thermal comfort as the state of mind, where a person expresses satisfaction with the thermal environment. This definition stresses the significance of psychological state of a person in evaluating the thermal environment. Thermal comfort is essentially an emotional response contrary to the thermal sensation which is a rational response (Tanabe and Kimura, 1994). Thermal sensation which is the feeling of cold or warmth is based on the signals from the thermoreceptors. The thermoregulation center in the hypothalamus collects data from skin thermoreceptors as well as from the internal organs through the blood stream and generates a thermal sensation response which can vary between extremely cold to extremely hot. A thermal comfort feeling is generated after the evaluation of the thermal sensation through psychological processes. Gagge et al. (1967) similarly argued that thermal comfort is the conscious appreciation of warmth or cold and is an interpretation of thermal information from the skin and the inner body.

Parsons (2003) argued that thermal sensation is both a sensory and a psychological phenomenon. Since sensation is about how people feel, it is not possible to define it in physical and physiological terms. However, there are studies which correlate thermal sensation with physical and physiological variables. These studies led to the development of deterministic thermal models which predict thermal sensation for groups of individuals (Parsons, 2003). Epstein and Moran (2006) define three groups of heat indices to determine thermal comfort: rational, empirical, and direct indices. Rational indices involve heat balance equations as in the case of PMV and PPD indices. Empirical indices are based on objective and subjective strain on the occupants. Direct indices are based on direct measurement of environmental variables.

Prediction of thermal comfort led to the development of rational human thermal models which are based on the heat balance equation for the human body. One of the pioneers of these models is the 41-node human physiological model which is also known as the Stolwijk model (1971). This model consists of 10 body segments each having four layers, e.g. core, muscle, fat and skin layers. One node is dedicated to central blood pool. Tanabe et al. (2002) developed the 65-node thermoregulation model based on the Stolwijk's 41-node model. Tanabe's model consists of 16 body segments. Huizenga et al. (2001) developed a human thermal comfort model based also on Stolwijk's model with major improvements of increasing the number of nodes and adding a clothing layer.

Several studies in literature showed that thermal comfort is well-correlated with the thermal sensation (Gagge et al., 1967; Wang et al., 2007; Zhang and Zhao, 2008b; Zhang et al., 2008a). In fact, this relationship is the rationale behind Fanger's PMV-PPD index. Figure 2.1 shows the thermal comfort scales used in this study, and Figure 2.2 and Figure 2.3 show the relationship between thermal comfort and thermal sensation by Zhang and Zhao (2008b) and Zhang et al. (2008a).

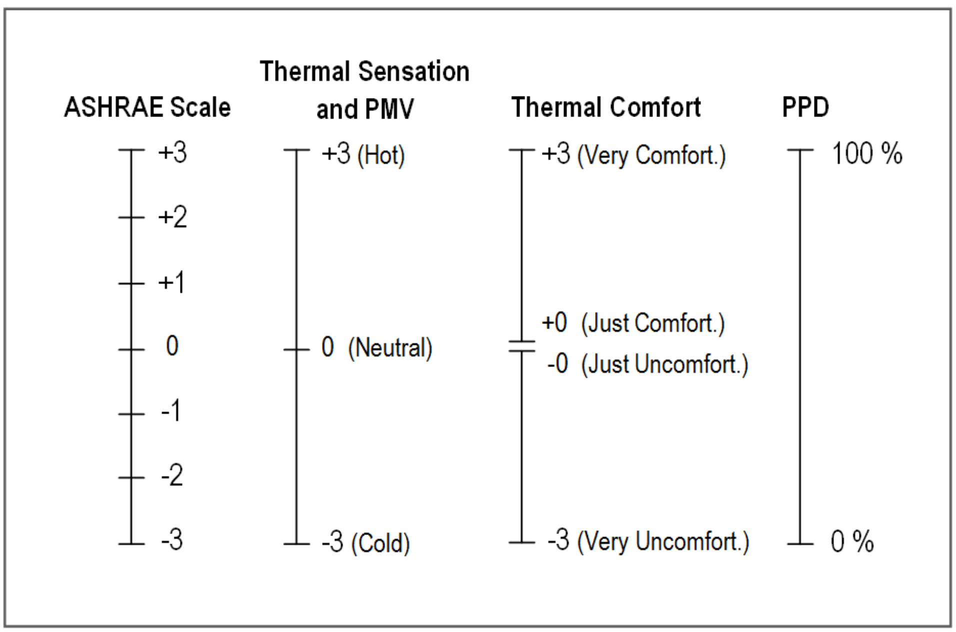


Figure 2.1. Thermal comfort and sensation scales used in this study.

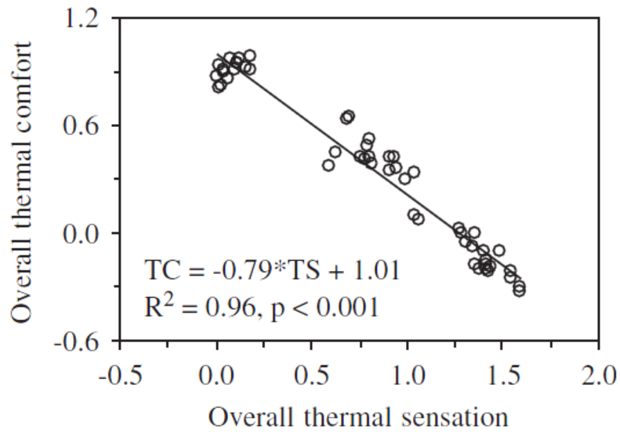


Figure 2.2. Thermal sensation vs. thermal comfort graph by Zhang and Zhao (2008b).

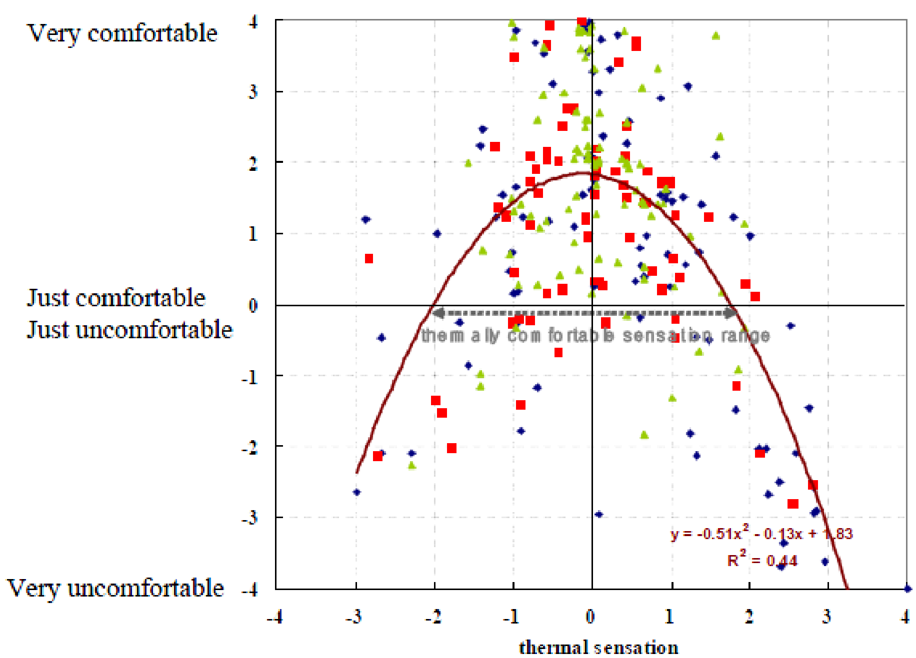


Figure 2.3. The parabolic relationship between thermal sensation and thermal comfort (Zhang, 2008a).

### *2.1.1. Thermal Comfort Variables*

According to Olesen and Brager (2004) there are several contextual and cultural factors which influence comfort sensation of the occupants. In physical sense, thermal comfort depends on the heat exchange of the human body with the surrounding environment (Olesen and Brager, 2004). The conventional understanding of thermal comfort is based on six environmental variables (i.e., ambient temperature, relative humidity, air velocity and the mean radiant temperature), and two personal variables (i.e., clothing insulation and metabolic rate). Lin et al. (2005) added air temperature stratification, radiant temperature asymmetry, and turbulence intensity as additional parameters which regulate heat exchange of the human body with the environment. Parsons (2003) included the following as factors affecting the thermal comfort: area, position and duration of stimulus on the body, pre-existing thermal state of the body, temperature intensity and rate of change of temperature.

Two schools of thought exist in thermal comfort research: conventional and adaptive approach (De Dear and Brager, 2001). Olesen and Parsons (2002) used the term 'western' instead of conventional approach. The 'Western' approach utilizes mechanical means to control the interiors by sealing the building from the outside conditions. This enabled building designers to control the comfort parameters such as temperature, relative humidity, and amount of fresh air according to the standards (ASHRAE Standard 55, 2004; ISO 7730, 2005, ASHRAE Standard 62.1, 2010). On the other hand, an 'adaptive' approach depends on the human behavior, such as adjusting the clothing, activity level and psychology, which can adapt to environmental conditions determined by culture and climate (Olesen and Parsons, 2002).

### *2.1.2. Thermal Comfort Standards: ASHRAE Standard 55 and ISO 7730*

The two most complete and widely used thermal comfort standards are the ASHRAE Standard 55 (2004) and the ISO 7730 (2005). The Standard 55 was developed and maintained by the American Society of Heating Refrigerating and Air Conditioning Engineers (ASHRAE). Whereas, the ISO 7730 was published by the International Standards Organization (ISO).

The description of thermal comfort by the above standards is based on the theoretical analysis of the human heat exchange with the environment. The theoretical analysis was then calibrated with the data derived from the climate chamber experiments (Nicol, 2004). Bouden and Ghrab (2005) added that human energy balance, which is the basis for standards, is assumed to be under steady-state conditions. The ASHRAE Standard 55 and the ISO 7730 use Fanger's predicted mean vote (PMV) method, which predicts a mean thermal sensation on the ASHRAE seven point scale (3=hot, 2=warm, 1=slightly warm, 0=neutral, -1=slightly cool, -2=cool, -3=cold). Predicted percent dissatisfied (PPD), on the other hand, reflects the percentage of people dissatisfied with the thermal conditions.

ASHRAE Standard 55 defines a total level of thermal acceptability at 80% for any occupied space. Ten percent (10%) dissatisfaction accounts for dissatisfaction with general thermal comfort, and the remaining 10% accounts for comfort dissatisfaction due to local conditions in a space (Olesen and Parsons, 2002). Similarly, ISO 7730 (2005) predicts a satisfaction level of more than 80% if the requirements are satisfied. According to the same standard, at most 10% of the occupants should be dissatisfied due to general thermal conditions. Only 5% to 10% of the occupants should feel uncomfortable due to local factors such as vertical air temperature difference, radiant temperature asymmetry. In addition, a maximum 15% of the occupants should feel uncomfortable due to unwanted local cooling around the body, referred to as draught. Toftum (2002) stated that percentages of occupants who are dissatisfied due to different local discomforting factors are not additive because usually a person is dissatisfied by more than one factor.

### *2.1.3. Predicted Mean Vote (PMV) and Predicted Percentage Dissatisfied (PPD)*

Predicted mean vote (PMV) and predicted percentage dissatisfied (PPD) are the two indexes which were developed by Fanger (1970) to characterize the thermal sensation level in a given thermal environment. PMV is essentially a steady-state heat balance equation which is fitted to the extensive subjective thermal response data (Equations 2.1 and 2.2). Equation 2.1 is the simplified version of the actual equation. PMV takes six thermal comfort variables (i.e., ambient temperature, relative humidity, air velocity, mean radiant temperature, clothing insulation, and metabolic rate) as input and outputs the average thermal sensation of a large group of people on the ASHRAE 7-point scale. A thermal sensation vote less than -1 and more than +1 is defined to cause dissatisfaction (Zhang, 2003a). The same 7-point thermal sensation scale was used in our study. Therefore, thermal sensation votes of the test subjects are comparable to the PMV index that is calculated for the same test conditions.

$$PMV = TS * (MW - HL_n) \tag{2.1}$$

$$TS = 0.303 * e^{-0.36*M} + 0.028 \tag{2.2}$$

where,

$MW$ = Net Metabolic Heat, W/m$^2$

$HL_n$ = Heat Loss from the Body, W/m$^2$

$M$ = Metabolic Rate, W/m$^2$

(ASHRAE, 2004).

The *TS* variable in the PMV equation is the term that is used by Fanger (1970) to fit to the thermal sensation responses of test subjects. Improvements to the TS term are possible by introducing a transient term which will match the new subjective data sets. Predicted percentage dissatisfied (PPD) gives the percentage of thermally dissatisfied persons in a large group under the given thermal conditions and is a function of the PMV (ASHRAE, 2004) (Equation 2.3).

$$PPD = 100 - 95 * \exp\left(-0.0335 * PMV^4 - 0.218 * PMV^2\right) \tag{2.3}$$

### *2.1.4. Non-uniform Thermal Conditions*

Sensation of thermal comfort is highly affected by individual differences in activity and clothing level. Therefore, sensitivity to local discomforting factors differs for each individual. Arens et al. (2006a) stated that "there has been limited research on how people respond, physiologically and subjectively, to the thermal non-uniformities encountered in buildings, vehicles, and the outdoors." Arens et al. also mentioned that non-uniformities in the air temperature, air movement, radiation, and conduction to surfaces create a complex relationship between the body and the environment by affecting the skin temperature of various body parts differently. One common source of non-uniformity in the thermal environments is draught, which is defined as 'unwanted local cooling of the body' by Toftum (2002). Fanger et al. (1988) defined draught as a function of mean air velocity, air temperature and turbulence intensity for sedentary persons. Zhang et al.'s (2004) thermal comfort model explains the relationship between local and overall thermal comfort. Local comfort depends on local and overall thermal sensations. If the overall thermal sensation is cold, then warm local sensation is felt comfortable. However, if the overall sensation is warm, then a warm local sensation is felt as very uncomfortable (Zhang et al., 2004).

Standards provide limited information on the prediction of local comfort factors especially for non-sedentary occupants (Toftum, 2002). ASHRAE Standard 55 defines the limits of thermal asymmetries to provide thermal comfort. However, standards still need to consider the occupants who are sensitive, feeling cooler or warmer than neutral and sedentary for long periods (Toftum, 2002). Toftum proposes a high level of individual control of the personal microclimate to accommodate individual preferences. Personal microclimate is also one of the focus points in our study.

### *2.1.5. Transient Thermal Conditions*

Comfort standards, as mentioned previously, are based on theoretical and empirical knowledge derived from the steady-state conditions. However, such studies by Arens et al. (2006a), Zhang (2003a), and de Dear et al. (1993) showed that human interaction with the environment also includes transient conditions which affect human comfort sensation different than the steady-state conditions. Jones and Ogawa (1992) argued that "in real situations people are moving about, changing their activity, changing their clothing etc. The steady-state situation is probably the exception rather than the rule for most people, especially when one leaves the typical office environment." Fiala et al. (2003) supported this point by stating that "human beings are frequently exposed to boundary conditions that deviate from homogeneous mild steady states. Transient changes in ambient temperatures, air velocity, and other environmental parameters characterize our daily life". Transients also happen through local or general thermal stimuli which usually occur over short durations of time. Contrary to the current practice to design fixed thermal environments, a variable environment is preferred by the building occupants (Nikolopoulou and Steemers, 2003). Designing dynamic thermal environments is a viable strategy which can increase people's physiological tolerances to various conditions, and reduce the expectations for fixed thermal environments. Research shows that thermal sensation requires airflow to change to a certain extent and temperature doesn't need to be stationary for comfort (Hanqing et al., 2006). Very comfortable conditions, which cannot be achieved with steady environments, are achieved during transient conditions (Arens et al., 2006a). Arens et al. also point out the practical implications of designing air-conditioning systems that can create dynamic conditions rather than to provide steady-state neutrality.

Transient thermal conditions have been subject to several studies. Zhang et al. (2004) stated that cold or warm stimuli during hypothermia and hyperthermia is felt pleasant by people which otherwise would be unpleasant under steady-state conditions. Gagge et al. (1967) studied subjective temperature sensations and comfort under various ambient temperatures ranging from 53.6°F (12°C) to 118.4°F (48°C). They showed that skin temperature correlates well with thermal sensation under transient conditions. Fiala et al. (2003) supported this point by stating that in sedentary subjects who are exposed to steady-state environmental conditions skin temperature correlated with body core temperature and with other thermophysiological variables. However, this is not applicable to dynamic conditions when there is a step change in temperature. McNall et al. (1967) discussed thermal sensation under three levels of activity and measured thermal sensation of occupants at 30 min. intervals. In a later study, Gagge et al. (1969) studied two types of transients: a sudden rise in metabolic energy production with exercise at the beginning of the experiment and a sudden increase in exercise rate during the experiment. Gagge et al. derived regression equations of sweat rate based on ambient temperature. They also regressed skin temperature on ambient temperature, metabolic rate and sweat rate. One important common point in McNall et al. (1967) and Gagge et al. (1969) is that their results and equations are applicable when the body thermal condition is in equilibrium. Griffith and McIntyre (1974) argued that effect of thermal conditions on comfort can be seen more effectively under dynamic conditions, due to human adaptability. They tested human comfort response to monotonic temperature changes at a rate of 0.15°C/min. under sedentary activity level. Griffith and McIntyre derived the regression equation ($W = 0.395 * T - 4.96$), in which $W$ is the Bedford Warmth Scale Score on a seven point scale from 'much too cool' to 'much too warm', and $T$ is the ambient temperature.

Ring and de Dear (1991) developed a model for dynamic response of skin thermoreceptors to transient conditions and then compared it to human thermal sensation under the same conditions. According to the Ring and de Dear, thermal response has two components. The first one is the static component, which is based on temperature. The second one is the dynamic component, which is proportional to time derivative of temperature (dT/dt) (Ring and De Dear, 1991). In a similar study, Zhang et al. (2004) integrated derivatives of skin and core temperatures of human body to steady-state model to predict local thermal sensation under transient conditions. In a more recent study, Huizenga et al. (2001) developed a human thermal comfort model based on Stolwijk's two-node model. Some of the major improvements are an increased number of nodes from six to unlimited, improved blood flow, addition of clothing node, and addition of radiation heat flux.

Rowe (2001) investigated the effect of time dependent activity level on the present comfort conditions. In his survey, Rowe asked about the activity level at the time of the survey and the activity levels at 10 min, 20 min, 30 min, and 60 min before the survey. He created weighting factors such that activity levels 10 min, 20 min, 30 min and 60 min earlier are 50%, 25%, 15% and 10% effective on the thermal state of a person respectively. Activity level during the preceding one hour of the survey has also been considered as a factor in different ASHRAE projects including RP-921 (Cena and De Dear, 1998).

According to Zhang (2003a) and ISO 7726 (1998) transient and non-uniform conditions occur under two circumstances. The first one is when someone is exposed to changing thermal conditions, such as moving from one space to another or changing the thermal conditions in one space. The second involves occupying a space with varying thermal conditions (Zhang, 2003a). Our study included a third condition, which is changing activity level in a marginally comfortable space. One focus of this research study is to effectively correct discomfort which is due to elevated activity levels. A second focus of the study is creating transient conditions to maximize thermal comfort in neutral environments.

Intentionally creating transient conditions has the potential to provide maximal thermal comfort. Thermal neutrality is not necessary to achieve maximum comfort and intentionally created thermal discomfort should be experienced first so that it can be relieved later (Zhang, 2003a).

Sudden correction of thermal discomfort with a thermal pulse is called overshoot (Arens et al., 2006a). Arens et al. (2006b) found that people felt 'very comfortable' when their thermal stress was alleviated by local stimuli. They also found that local comfort overshoot is more effective in providing thermal comfort than general comfort overshoot. Zhang (2003a) suggested a small step-change supply pattern to achieve maximal comfort. This point is supported by Arens et al. (2006b) who argued that cyclical control of HVAC system to utilize this effect is a possible research area. Fiala et al. (2003) proposed a 'mixed' comfort strategy in which hot warnings of the body due to exercising or environmental transients can be compensated by cold warnings from cutaneous thermoreceptors. In addition, HVAC system oscillating fans and pulsing radiant heaters can be used to create the same effect.

## 2.2. Transient and Non-uniform Thermal Comfort Variables

### *2.2.1. Metabolic Rate and Thermal Comfort*

Metabolic rate is one of the six conventional variables of thermal comfort and is associated with the heat generation inside the body. Since thermal comfort is based on the heat balance between the environment and the body, metabolic heat generation is arguably the most fundamental variable of comfort. The metabolic rate of a person engaged in typical office activity is approximately 1.2 met (1 met = 58.15 W/m$^2$) rather than 1.0 met of the previous laboratory studies (Toftum et al., 2004). Our laboratory study used 1.2 met instead of 1.0 met as the base metabolic rate to better represent the real conditions of an office environment.

Several studies were published on the effect of metabolic rate on thermal comfort. McNall et al. (1968) focused on three metabolic rate conditions (low, medium, high) for different ambient temperature (18.9°C/66°F, 22.2°C/72°F, 25.6°C/78°F). McNall et al.'s high metabolic rate conditions were 247 W/m$^2$ or 4.25 met for males and 234 W/m$^2$ or 4 met for females assuming average body surface areas (1.8 m$^2$ for males and 1.6 m$^2$ for females). Jones et al. (1986) conducted tests for moderate metabolic conditions (2.3 met) with 0.20 m/s (40 fpm) and 1.22 m/s (240 fpm) air velocities in the laboratory environment and found that starting with 19°C/66°F, airflow yields higher comfort votes for moderate activity level for subjects with 0.65 clo insulation. Griefahn and Kunemund (2001a) investigated differences of thermal comfort, thermal sensation and air movement perception between males and females for varying metabolic rate conditions including 104, 128, 156 W/m$^2$ (1.8, 2.2 and 2.7 met respectively). In this study, we studied metabolic activity levels up to a 233 W/m$^2$ level (4 met) combined with two airflow frequencies, two airflow stimulus locations and two temperature conditions.

In higher-than-sedentary metabolic conditions, increasing airflow speed around the body is a viable strategy to increase heat loss from the body. However, draught sensation presents a risk of discomfort in high air velocity conditions. Toftum and Nielsen (1996) investigated the impact of metabolic rate (100 W/m$^2$, 130 W/m$^2$) on draft discomfort for different ambient temperature (11°C/52°F, 14°C/57°F, 17°C/62.5°F, and 20°C/68°F) and airflow conditions (0.05 to 0.4 m/s). Our study used a similar methodology and extended Toftum and Nielsen's study by using higher metabolic rate conditions in neutral (24°C/75°F) and warm (28.3°C/83°F) temperatures and air velocities up to 0.8 m/s to correct discomfort. Draft discomfort decreases with the increased metabolic rate (Toftum, 2002; Toftum and Nielsen, 1996; Griefahn and Kunemund, 2001a) and in theory increased air velocity retains thermal comfort at high heat loads and elevated temperatures (Toftum, 2004).

### *2.2.2. Dynamic Airflow and Draught Rating*

Recent studies on the effect of airflow on thermal comfort suggested that building occupants desire more airflow even when they feel "slightly cool" (Toftum, 2002; Zhang et al., 2007a). Zhang et al. (2007a) showed ,that 60% of the building occupants think airflow enhances their work ability, while only 15% think that airflow interfered with their work; and there are twice as many people preferring more air movement than people preferring less air movement. Our study supports the previous studies such that 18% test subjects preferred more air movement even when they are feeling cool and an average 35% demanded more airflow when feeling between neutral and warm.

Current thermal environment design practices specify constant airflow inside the spaces for relatively extended periods of time. However, skin thermoreceptors adapt to the constant airflow stimulus and the cooling effect is reduced in time (Ring et al., 1993). Varying the airflow speed in the occupied zone is a viable strategy to overcome this problem. Previous studies showed that dynamic airflow yields a higher cooling sensation than the constant airflow (Tanabe and Kimura, 1994; Zhou et al., 2006). Dynamic airflow can work even the comfort conditions of thermal comfort standards are not met. Internal warmth sensations of the body can be balanced with the cool warnings from the skin thermoreceptors (Fiala et al., 2003). Dynamic airflow prevents skin thermoreceptors to adapt and creates repeated cool warnings.

Tanabe and Kimura (1994) compared the thermal sensations for 60-second pulsed air, various sinusoidal air, random and constant air. They found that 30-second and 60-second sinusoidal airflows are more effective in yielding a cooler thermal sensation than the other airflow types. Following Tanabe and Kimura's study, we utilized 30-second and 60-second pulsed air. The airflow speed variation of 30-second pulsed air is identical to the 30-second sinusoidal air of Tanabe and Kimura. Zhou et al. (2006) discussed the mechanisms involved in dynamic airflow and how they work to create a thermal response. They compared three types of airflow patterns which all have 0.8 m/s mean air velocity for 78.8°F (26°C) and 86°F (30°C) room temperatures. A sinusoidal and simulated natural airflow created stronger cooling effect and thermal sensation values 0.4 less than the constant airflow. High turbulence intensity (Tu), in this case, resulted in increased heat transfer coefficient on the skin surface, and in increased fluctuations of skin temperature which generated cool warning signals (Zhou et al., 2006; Toftum and Nielsen, 1996). Ring and de Dear (1991) developed a skin thermoreceptor response model which depends on the temperature difference with respect to the time and the location inside the skin. Fanger et al. (1988) investigated the effect of turbulence intensity on draught sensation and found that highly turbulent airflow increases the sensation of coolness to the point of being uncomfortable. They formulated the percent dissatisfied due to draught equation (Equation 2.4) which became the basis for the draught discomfort sections of the ASHRAE Standard 55 and ISO 7730.

$$DR = \left((34 - t_a)(\bar{v} - 0.05)^{0.62}\right) + \left(0.37 * \bar{v} * Tu + 3.14\right) \quad (2.4)$$

where,

DR = predicted percentage of people dissatisfied due to draft,

$t_a$ = local air temperature, °C,

$\bar{v}$ = local mean air speed, m/s,

Tu = turbulence intensity, %.

### *2.2.3. Local Airflow*

In this study, the airflow stimulus location was tested for airflow's effectiveness to provide a sensation of coolness. The hypothesis is that airflow can be directed to the thermally sensitive locations of the body (hands, feet, and head/neck) to increase its effectiveness. Zhang et al. (2004) reported that hand, forehead and neck cooling in hyperthermia, and warming in hypothermia is felt very pleasant, even more so than the uniform conditions. Results are similar for the foot cooling and warming. Toftum and Nielsen (1996) found that the neck is the most sensitive part to draught when compared to the lower back, hands and face. In general, the sensitivity of the head region is higher than the other parts. Other studies (Zhang, 2003a; Arens et al., 2006b) also showed that the head and hands in cool conditions and the hands and feet in warm conditions significantly affect thermal comfort. One of the reasons for the sensitivity of the neck is the high cold thermoreceptors concentration (Toftum and Nielsen, 1996). The hands and feet are very sensitive to the thermal state of the body because vasodilatation and vasoconstriction at the extremities occur depending on the body's need to retain or lose heat. Hands have the most number of arteriovenous anastomoses (AVAs) which are the valves that control vasodilatation and vasoconstriction (Wang et al., 2007). Pellerin et al. (2004) found that feet, calves, hands and arms have the strongest relationship to cold discomfort. On the other hand, feet and face have the strongest relationship to warm discomfort. Huda and Homma (2005) investigated local airflows to the ankles and the neck and mentioned the possibility of more economical air-conditioning systems by directing the air to the thermally more sensitive parts of the body. They chose those two locations because natural convection produced by the body starts at the ankles and fully develops at the neck. Previous research clearly shows that hands, feet and head are among the most sensitive regions of the body and a careful design of the thermal environment that focuses on those regions can have significant impact on thermal comfort. In our study, two types of airflow were tested: head-only, or head, hands and feet simultaneously. The room air was simply redirected to those parts of the body and no cooled air was used. The air volume was kept constant in both tests in order not to introduce air volume as an additional variable.

### *2.2.4. Trade-offs between Thermal Comfort Variables for Thermally Comfortable Environments*

Among all the environmental factors, ambient temperature is the most important factor that affects thermal comfort. Below neutral temperatures, lower temperature increases discomfort. Above neutral temperatures, higher temperatures increase discomfort. The neutral temperature people find comfortable depends on the mean temperature they experience (Nicol, 2004). However, temperature is not sufficient by itself to ensure thermally comfortable environments since building occupants are exposed to multiple interacting environmental stimuli (Toftum, 2002). Current thermal comfort standards are limited in scope in explaining the interacting thermal factors.

Fountain et al. (1994) studied airflow preferences of test subjects for 77°F (25°C), 78.8°F (26°C), 80.6°F (27°C) and 82.4°F (28°C) with average airflow speed of 41 ft/min (0.21 m/s) (one of the three devices used in this test generated up to 394 ft/min airflow speeds). Fountain et al. found that 50% of the people wanted more air for a given operative temperature where the draught rating (DR) model of ASHRAE 55-1992 specifies 15% dissatisfaction. Therefore, the DR model doesn't necessarily reflect people's preferences for air. ASHRAE Standard 55 allows 3°F (1.7°C) increase in temperature where there is 98 ft/min (0.5 m/s) increase in air velocity. Literature reveals models which take into account the interaction between different factors in providing a thermally comfortable environment. Nicol (2004) proposed the following equation which calculates the allowable increase in comfort temperature where the air velocity is above 20 ft/min (0.1 m/s) (Equation 2.5).

$$7-\frac{50}{4+10v^{0.5}}\,{}^{\circ}C \qquad (2.5)$$

According to this model, 6.1°F (3.4°C) increase above neutral temperature can be compensated with 1 m/s airflow. This value is consistent with Toftum (2004) and Tanabe et al. (1994). Our study also employed 0.8 m/s airflow around the subject.

Epstein and Moran (2006) established tradeoffs between the six thermal comfort factors such that an increase of 17.5 Watt (above resting level) is equivalent to a 1.8°F (1°C) increase in ambient temperature. In addition, a change in 20 ft/min (0.1 m/s) in wind speed is equivalent to a change in 0.9°F (0.5°C) in ambient temperature (up to 2.7°F). Zhang et al. (2007a) also found that comfort temperatures for persons exposed to 39-187 ft/min (0.2-0.95 m/s) air velocity was 1.8°F (1°C) higher than the person exposed to air velocities smaller than 39 ft/min (0.2 m/s).

The dynamic approach to the thermal comfort problem suggests that a time-dependency exists for each thermal comfort variable. Gagge et al. (1967) measured the time-dependency of thermal comfort and sensation of subjects who were exposed to 53.6°F (12°C), 64.4°F (18°C), 71.6°F (22°C) and 82.4°F (28°C) for two hours. Thermal comfort and sensation decreased for all cases except the 82.4°F (28°C) temperature. Gagge et al.'s results proved that even when all the comfort variables are constant, there is still a transient perception of thermal comfort.

## 2.3. Physiological Signals of Thermal Comfort

### *2.3.1. Heat Balance and Thermoregulation*

The human thermoregulation system consists of the control and the controlled subsystems. The controlled subsystem is the physical characteristics of the body. Thermal stress on the controlled subsystem is sensed by the control subsystem through sensor mechanism. The control subsystem then takes the corrective measures to reduce the thermal stress (Neghabat et al., 1989). The first condition of thermal comfort is the existence of heat balance between the human body and the environment. A neutral thermal sensation, which is neither warm nor cool, occurs when there is steady heat exchange of the body with the environment. A transient state of the thermal conditions can be defined as the lack of equilibrium between the heat loss and heat gain. The problem with homeothermy is that the body temperature rises if the excess heat cannot be lost to the environment. The body temperature falls if the heat generated inside the body is less the heat lost to the environment (Houdas and Ring, 1982). Therefore, heat stress results from the imbalance between the body and the environment (Epstein and Moran, 2006).

The heat generated inside the body is carried to the skin surface by conduction, water diffusion or by the blood stream through the counter-current heat exchange of arteries and veins. In a cold environment, blood returns to the heart through the deep veins which are in close contact with the arteries. By doing this, the heat is preserved inside the body without reaching to the skin surface. In a warm environment, blood returns to the heart through the peripheral veins which maximizes heat loss to the environment (Houdas, 1982). In a steady-state model the net heat, after respiration and sweating, is shown as

$$H = K(T_{cr} - T_{sk}) \tag{2.6}$$

where $H$ is the heat transfer (W/m$^2$), $K$ is the body conductance (W/m$^2$K), $T_{cr}$ is the core temperature (°K) and $T_{sk}$ is the skin temperature (°K) (McIntyre, 1980). $K$ includes the effect of skin and tissue conductance and vascular convection (Murray-Smith, 1984) and ranges from 8 W/m$^2$K for maximally vasoconstricted body to 50 W/m$^2$K during heavy sweating (McIntyre, 1980).

Transient models focus on the heat storage inside the body in addition to the heat balance with the environment. Heat storage occurs when the heat generation exceeds the heat loss to the environment. In its simplest form, Houdas and Ring (1982) expresses heat storage with

$$S = mc(\Delta T_b / \Delta t) \tag{2.7}$$

where $S$ is the heat storage (J), $m$ is the mass (kg), and $c$ is the specific heat of the body (kJ/kg), $T_b$ is body temperature (°K), and $t$ is the time. According to McIntyre (1980), the specific heat of the body is 3.49 kJ/kg. For an average man of 70kg and 1.8m$^2$, the heat storage ($S$) produced in 1 hour with 1°K difference is 38 W/m$^2$. In another study, Gagge et al. (1967) formulated heat storage (S) as

$$S = M - (E + 6.0(T_s - T_a)) \tag{2.8}$$

where, $M$ is the metabolic rate (W/m$^2$), $E$ is the rate of evaporative heat loss (W/m$^2$), $T_s$ and $T_a$ are skin and ambient temperatures respectively (°K), 6.0 is the combined heat transfer coefficient for radiation, convection and conduction.

Hypothalamus evaluates the thermal information from the peripheral as well as the central thermoreceptors and initiating the autonomic responses such as shivering, sweating, piloerection, and cutaneous vasomotor control. In addition the thermoreceptor signals, there is an additional implicit signal which is the body setpoint. Information from the central thermoreceptors is compared to the ‘desired’ setpoint temperature signal. The body takes the necessary actions to maintain the central temperature at the setpoint temperature (Cabanac, 1981).

The anterior hypothalamus regulates the heat loss from the body. It functions as a temperature sensor as well as a controller. When the temperature of the anterior hypothalamus exceeds the setpoint temperature, it activates the vasodilatation and the sweating mechanisms. The posterior hypothalamus on the other hand preserves heat. It functions as a controller since it lacks temperature sensors itself. It initiates the efferent responses of vasoconstriction and shivering (McIntyre, 1980).

### *2.3.2. Thermoreceptors (TRs) and Thermal Sensation*

Skin is the largest and the most important sensory organ of the thermoregulatory system and is scattered with cold and warm thermoreceptors that are connected to the hypothalamus (Yao et al., 2008). Cutaneous thermoreceptors are differentiated afferent nerves with different dependence of firing rate on temperature. The firing rate of warm sensing nerves increase as the temperature increases. Conversely, the firing rate of cold receptors increase as the temperature decreases (Lv, 2007). Cold receptors outnumber the warm receptors by 10-15 times regardless of the location on the body (Houdas and Ring, 1982) and they are closer to the skin surface than the warm receptors (0.2 vs. 0.5mm deep) (Lv and Liu, 2007). Shorter response time and larger dynamic peak response of cold TRs together with the number and location explain why humans are more sensitive to cold (Lv and Liu, 2007). Previous research also proved that humans report more discomfort when they are feeling cool (Greenspan et al., 2003; Zhang, 2003a).

The fundamental characteristic of neurons is the base firing which is also called the self-sustained oscillation. The frequency of firing depends on the environmental factors such as temperature and air velocity and their intensity. For warm thermoreceptors, the firing rate increases with the increased temperature. Conversely, the firing rate decreases with the increased convection coefficient (Figure 2.4). Figure 2.4 shows that the firing rate of the warm thermoreceptors in warm environments can be decreased by elevated air velocities which increase the convection coefficient. Decreasing firing rate to the level of 25ºC ambient temperature using air motion has the potential to provide comfortable feeling even when the ambient temperatures are higher. This characteristics of the of the thermoreceptors forms the basis for one of the hypothesis of this study that increased air velocities can create sensation of coolness even though the skin temperature is high.

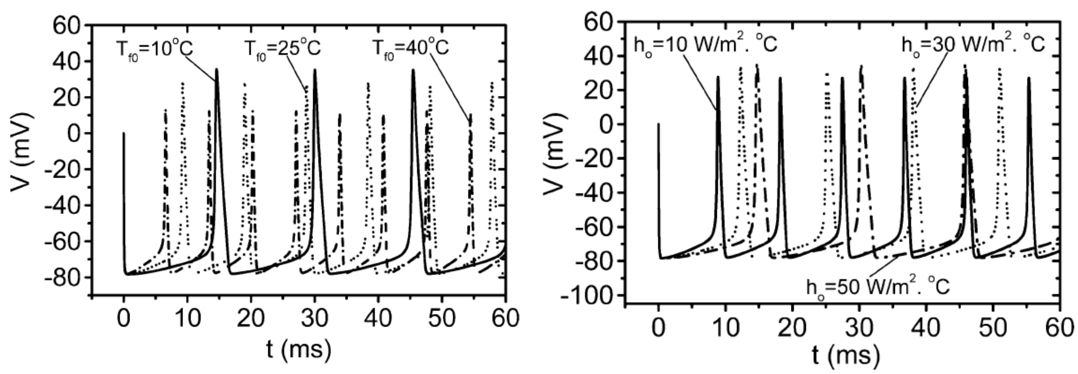


Figure 2.4. Base firing of warm thermoreceptors in different ambient temperatures and convection coefficients (Lv and Liu, 2005).

A second characteristic of the skin thermoreceptors is the static and dynamic response to environmental stimulus. Skin thermoreceptors send signals to the brain at a constant rate under steady state conditions. In transient conditions, thermoreceptors send not only a constant signal but also a dynamic signal which is a function of rate of change in the temperature (dT/dt) (Houdas and Ring, 1982; Fiala et al., 2003; Ring and De Dear, 1991; Zhang, 2003a). This dynamic signal has a high intensity for short amount of time (usually few seconds) which settles down to a steady (constant) level (Figure 2.5).

The dynamic characteristics of the thermoreceptors under transient conditions constitute the basis for the second hypothesis of this study. According to this hypothesis, a sustained peak response condition, thus a higher cooling sensation, can be created by constantly varying the airflow on the skin surface. This could also avoid the adaptation of skin thermoreceptors under constant stimulus (Greenspan et al., 2003) which reduces the effectiveness of the airflow.

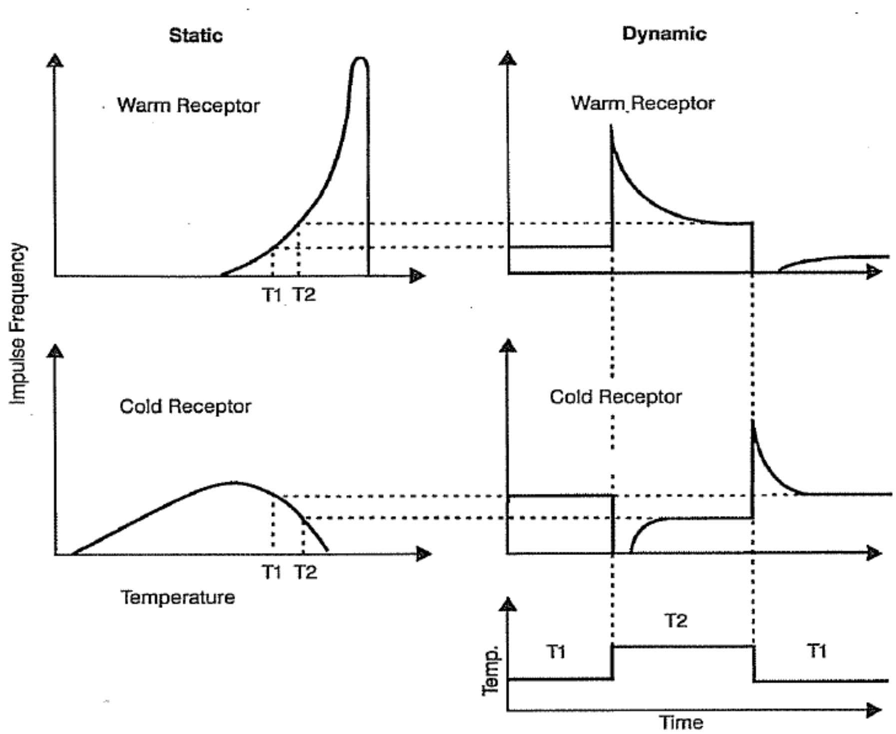


Figure 2.5. Static and dynamic responses of TRs to temperature changes (Hensel, 1981).

Ring and de Dear (1991) suggested that sensation of thermal transients is proportional to thermoreceptor (TR) response in the first 20 seconds of the stimulus onset. This is the period in which central nervous system integrates the response of the TRs (Ring and De Dear, 1991). The firing rate of the neurons is an integrated response of the human body to the thermal comfort parameters such as air temperature, activity level, air velocity, personal health, humidity. Therefore, it is a viable method to evaluate thermal environment. In this study, we used two types of transient airflow conditions one of which has 20 seconds between the two airflow treatments. Fiala et al.'s (2003) findings on thermal sensation of human subjects when temperature changes from 82.4ºF (28ºC) to 64.4ºF (18ºC) is similar to Lv and Liu's results on the cold receptor response to sudden temperature changes. We can infer that thermal sensation under sudden transient conditions follow skin TR response. A practical example is someone who enters a cold environment from warm environment. That person may feel the temperature colder than it actually is due to the dynamic response.

### *2.3.3. Skin Temperature*

*2.3.3.1. Skin Temperature Response to Thermal Stress*

Skin is the largest sensory organ which acts as a selective barrier. It keeps out the foreign material and allows passage of the materials from the bloodstream to the exterior (Cacioppo et al., 2007). In addition, it is the interface between the human body and the environment in the heat transfer processes and is therefore an important variable of thermal comfort (Burton, 1934). Five out of six thermal comfort factors (i.e. ambient temperature, mean radiant temperature, relative humidity, air velocity, and clothing level) affect the heat transfer process of the human body at the skin surface (Sakoi et al., 2007). Skin is also largely responsible of thermal sensation and comfort through the numerous thermoreceptors.

Temperature distribution over the skin is affected by the local heat balance as well as the internal and the external conditions. The basic response of the skin is based on minimizing $\Delta T$ between the ambient temperature and the skin surface, so that a heat balance similar to thermoneutrality can be established. If the external temperature is outside the neutrality, the skin temperature will follow the ambient conditions. If the environment is in a transient state, the skin temperature will first have an amplified response which will recover to a steady level after some time (Houdas, 1982). Zhang (2003a) showed the sudden change in thermal sensation and thermal comfort upon the application of cooling. This sudden response is correlated to the derivative of the skin temperature which is greatest when there is a sudden change in the environment. This overshooting effect is more pronounced for cooling than heating which is also due to the number of cold receptors and their location in the skin. The time constant (i.e. the time required to reach the 64% of the final value) for the recovery of the skin temperature varies between 5-15 minutes depending on ambient temperature and the location of the skin temperature site (Houdas and Ring, 1982). Our tests showed that time constants for skin temperature and thermal sensation are around 4-9 minutes which is on par with Houdas' statement.

Skin temperature shows higher deviations when there is a specific muscle activity. High temperatures are expected on the working muscle (McIntyre, 1980) because when a person starts exercising the blood is first directed to exercising muscles while constricting the skin blood flow.

The body temperature rises if the heat loss to the environment is insufficient which results in increased skin blood flow and sweating (Kistemaker et al., 2006). Gagge et al. (1969) measured muscle temperature 5mm under the skin surface during the exercise and found that there is a sudden increase in muscle temperature within 10 minutes of the onset of exercise. In our study, pedaling utilizes leg muscles and leg skin temperatures are consistent with McIntyre and Kistemaker et al.

Skin temperature shows variations between different skin sites. Houdas and Ring (1982) found the minimum temperatures at the hand and the foot and the highest temperatures at the head for 77°F (25°C) ambient temperature. The temperature difference between the body parts decreased as the temperature increased. The study by Arens et al. (2006a) supported Houdas and Ring and showed that in neutral temperatures (77.9°F / 25.5°C), foot, hand, lower arm and anterior thigh have the lowest temperatures. On the other hand, head region had the highest skin temperature. Yao et al.'s (2008) study is also consistent with Houdas and Ring and Arens et al. and Yao et al. found that in moderate temperatures (24°C to 26°C) head locations and upper back have the highest temperatures. Whereas, foot, hand and arm have the lowest skin temperatures. The difference between the skin temperatures reduces at 29°C and increases at 21°C. Foot and hand temperatures fluctuated most between different ambient temperatures which are also consistent with Houdas and Ring.

Zhang (2003a) established the relationship between skin temperature and the thermal sensation of local body parts. Zhang grouped local body parts into three categories in terms of their influence on the overall thermal sensation: the most, moderate and the least influential. There is an inverse relationship between skin temperature fluctuation and the influence on overall sensation of a body part. The most influential group (i.e. back, chest and pelvis) showed minimal temperature fluctuations, whereas the least influential group (i.e. hand and foot) showed the maximum temperature fluctuations. Moderately influential group's (head, arms, and legs) skin temperature and effect on overall thermal sensation falls between the least and the most influential groups. Zhang concluded that limbs contribute most to the thermoregulation without affecting the overall sensation.

*2.3.3.2. Skin Temperature Measurements*

Yao et al. (2008) presented a summary of skin sites and mean skin temperature calculation methods for different ambient temperatures. They showed that the mean skin temperature doesn't change significantly for twelve or more measurement sites (Figure 2.6). In the literature, weighted and unweighted averaging of skin temperatures were used to estimate the mean skin temperature.

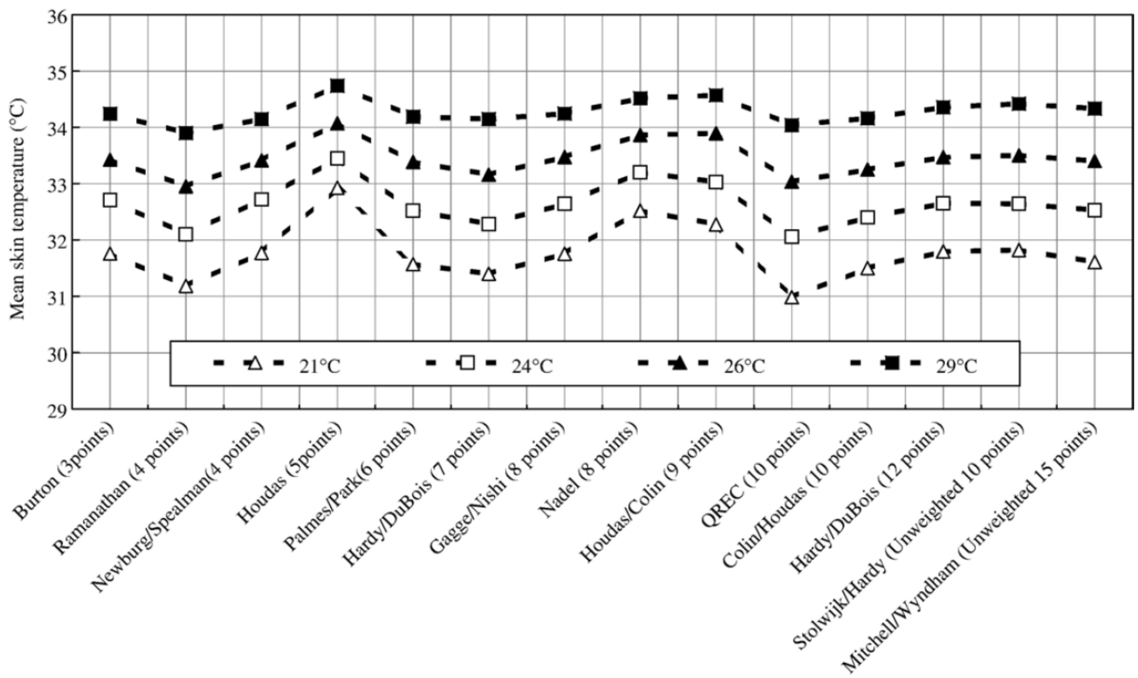


Figure 2.6. Summary of previous studies by Yao et al. (2008) on skin temperature measurement sites.

In estimating the mean skin temperature, as the number of sites increases the relative weighting factor of each site decreases. The early skin temperature measurement dates back to Burton (1934) who measured three sites. A general trend is that the number of skin temperature measurement sites increased in time and recent studies employed up to 28 sites. Table 2.1 presents the common measurement sites. Zhang (2003a) and Arens et al. (2006b) made extra measurements on both sides of the body to test non-uniform conditions.

Based on the previous studies, this study employed unweighted methods of calculating mean skin temperature from 15 skin temperature sites. The sites are forehead, cheek, neck, chest, abdomen, upper back, lower back, upper arm, lower arm, hand, anterior thigh, anterio-medial thigh, anterior calf, posterior calf, instep (Figure 2.7).

Table 2.1. Summary of skin temperature measurement sites from the literature.

| | **Forehead** | **Cheek** | **Chest** | **Upper Arm** | **Abdomen** | **Forearm** | **Hand** | **Anterior Thigh** | **Anterior Calf** | **Foot** | **Neck (Back)** | **Scapula (Upper Back)** | **Lumbar (Lower Back)** | **Postero-medial Thigh** | **Posterior Calf** | **Anterio-medial Thigh** | **Neck (Front)** | **Finger** | **Breathing Zone** | **Posterior Thigh** |
|---|---|---|---|---|---|---|---|---|---|---|---|---|---|---|---|---|---|---|---|---|
| Mitchell and Wyndham (1969) | x | | x | x | x | x | x | x | x | x | x | x | x | x | x | x | | | | |
| Cunningham et al. (1978) | x | | x | x | x | x | x | x | | | | x | x | | x | | | | | |
| Zhang (2003a) | x | x | x | x | x | x | x | x | x | x | x | x | | | | | x | x | x | |
| Pellerin et al. (2004) | | x | x | x | | x | x | x | | x | | x | x | x | x | | | | | |
| ISO 9886 (2004) | x | | x | x | x | x | x | x | x | x | x | x | x | | x | | | | | x |
| Arens et al. (2006b) | x | x | x | x | x | x | x | x | x | x | x | x | | | | | | | x | |
| Sakoi et al. (2007) | x | | x | x | x | x | x | x | x | x | | x | x | x | x | | | | | |
| Jay et al. (2007) | x | | x | x | x | x | x | x | x | | | x | x | x | x | | | | | |
| Yao et al. (2008) | x | x | x | x | x | x | x | x | x | x | x | x | x | x | x | x | | | | |
| Hashiguchi et al. (2010) | x | | x | | x | x | x | x | x | x | | x | | | x | | | | | x |
| Uğursal (Current Study) | x | x | x | x | x | x | x | x | x | x | x | x | x | | x | x | | | | |

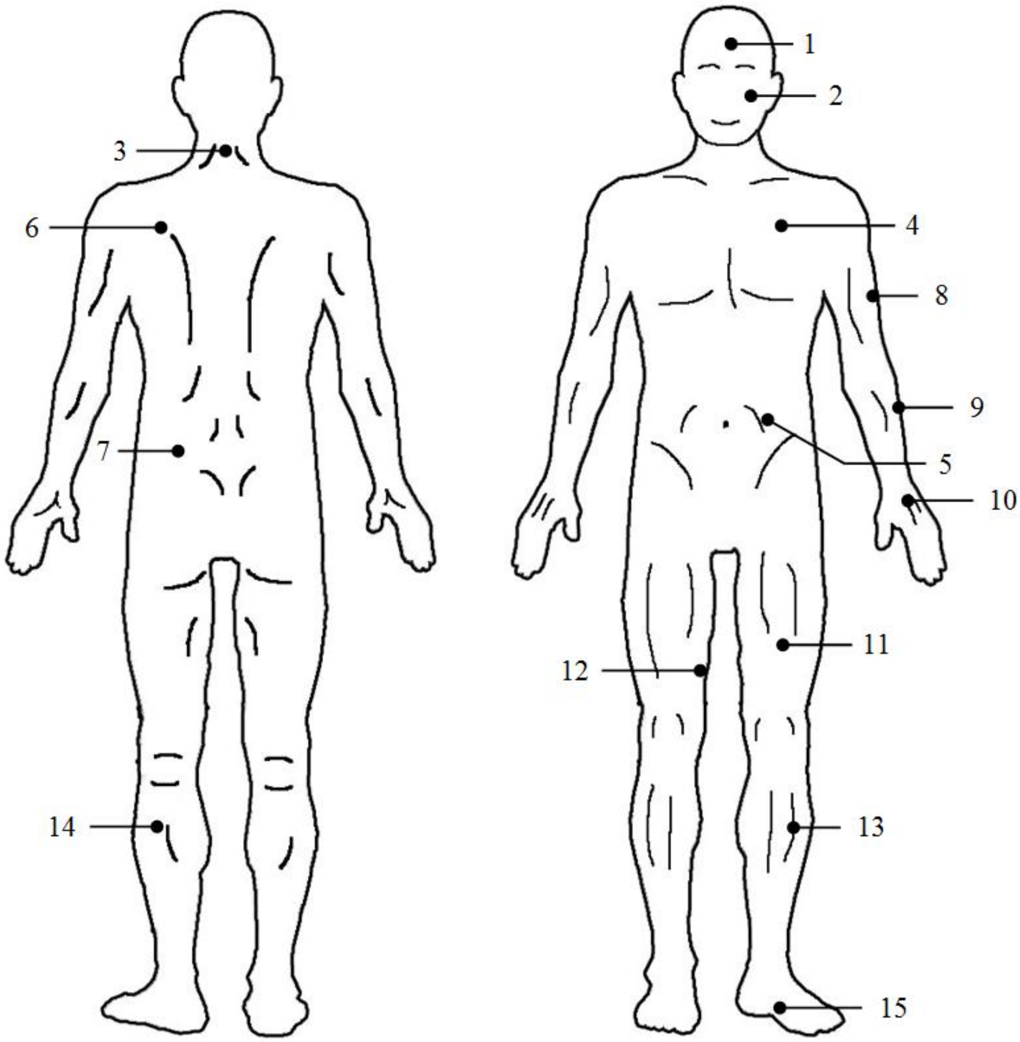


Figure 2.7. Skin temperature measurement sites (1: Forehead, 2: Cheek, 3: Neck, 4: Chest, 5: Abdomen, 6: Upper Back, 7: Lower Back, 8: Upper Arm, 9: Lower Arm, 10: Hand, 11: Anterior Thigh, 12: Anterio-medial Thigh, 13: Anterior Calf, 14: Posterior Calf, 15: Instep).

### *2.3.4. Skin Wettedness*

Skin wettedness is one of the three comfort conditions as put forward by several researchers (McIntyre, 1980, Prek, 2006, Sakoi et al., 2007) and is defined as the ratio of wet skin to overall skin surface area (McIntyre, 1980). To maintain homeostasis, sweating mechanism is activated when the heat loss from the body is not sufficient even after the vasodilatation. Sweating increases the body's heat loss through the evaporation of sweat on skin (Kaynakli and Kilic, 2005). Increasing the air velocity increases rate of evaporation and convective heat loss. This is represented in the heat transfer equations as the increased convective and evaporative heat transfer coefficients. Increased evaporation from the skin surface drops the skin temperature and a sense of comfort is resumed. Therefore, skin wettedness is part of the latent heat loss mechanism of the body (Kaynakli and Kilic, 2005). The accepted minimum skin wettedness (w) for the nude body parts is 0.06 and it increases for the clothed regions (Atmaca and Yigit, 2006). However, in an earlier study, Tanabe et al. (1993) proposed 0.028 as the minimum value instead of 0.06 which resulted in closer agreement of the standard effective temperature with the thermal sensation of a group of people. Atmaca and Yigit (2006) plotted the skin wettedness values of different body parts for different relative humidity conditions under 26°C ambient temperature. They found that skin wettedness increases with the clothing insulation and it reaches to 0.44 at the pelvis for relative humidity below 90%.

Gagge et al. (1969) investigated the relationship of high metabolic rate, air temperature, skin temperature, skin wettedness and thermal comfort. They found that the warm sensation increases with the average skin temperature and the discomfort increases linearly with the increased skin sweat. This point was supported by McIntyre (1980) and Cabanac (1981) such that warmth discomfort is correlated with the skin wettedness, and the onset of warm discomfort corresponds to the onset of sweating. An interpolation of Gagge et al.'s data revealed that at 233 $W/m^2$ (which is the high metabolic rate condition of our study) and 25°C ambient temperature, the skin wettedness is approximately 0.45 which was reached after 30-40 minutes of exercising.

### *2.3.5. Heart Rate (HR)*

Exercise and psychological stress both contribute to the cardiovascular response of the body. If both exercise and psychological stress exist at the same time, they create a higher cardiovascular response than the individual ones (Andreassi, 2000). Heart rate decelerates with the mental incorporation to an external stimulus (stimulus intake), whereas heart rate accelerates with the rejection of the stimulus as during the solution of a problem (Andreassi, 2000; Steele and Lewis, 1968). The psychological stress yields increased blood pressure, heart rate, and respiration rate. Energy expenditure increases with the increased heart rate due to psychological stress. Andreassi (2000) considered this as the high physiological cost of psychological stress.

Exercise intensity and heart rate have a fairly straightforward relationship. Heart rate increases with the intensity of an activity to supply the necessary oxygen to the muscles. Berggren and Hohwu (1950) suggested that the oxygen consumption during work is closely related to the heart rate. Zhang et al. (2003b) established the relationship between the oxygen consumption, metabolic rate and the heart rate (Figure 2.8). A nearly linear relationship exists between the metabolic rate and the heart rate. ISO 8996 (2004) also presents equations for the estimation of metabolic rate using the heart rate for both genders. Section 3.3.3.1 explains how the metabolic rate is calculated from the heart rate.

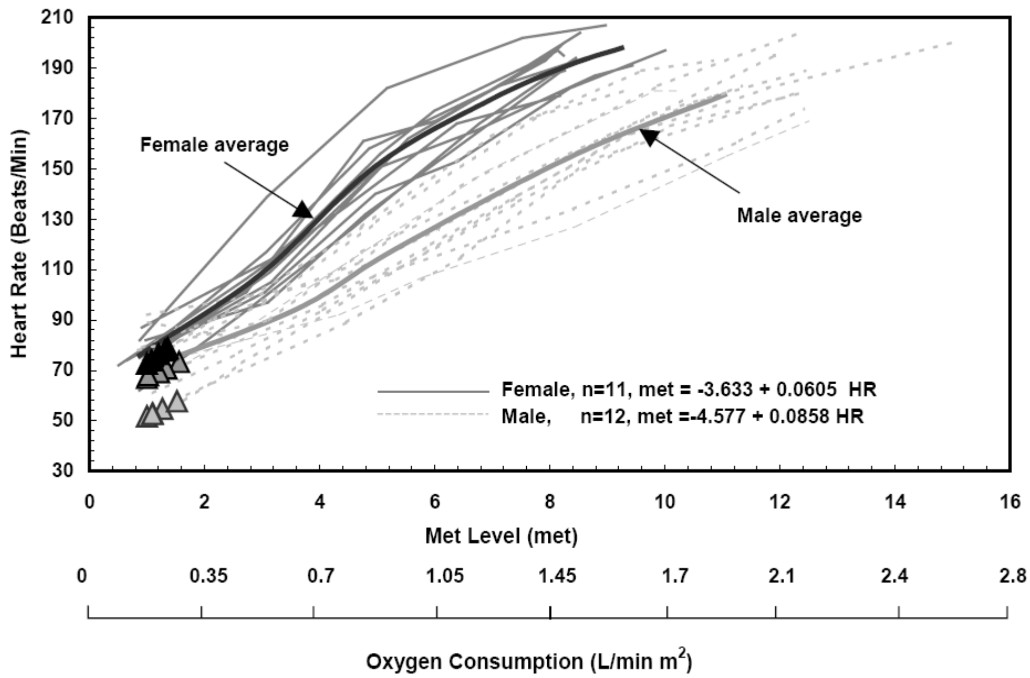


Figure 2.8. The relationship between metabolic rate, oxygen consumption and heart rate (Zhang et al., 2003b).

### *2.3.6. Electrodermal Activity (EDA)*

The human body houses two forms of sweat glands, namely apocrine and eccrine glands. Apocrine sweat glands are found in the armpit and the pubic region and they discharge a complex mixture of substances. Eccrine sweat glands are distributed to the whole body and they produce a watery sweat (McIntyre, 1980). The primary function of the eccrine gland is thermoregulation although Edelberg (1972) argued that the activity of the eccrine glands in the palmar region is more related to the grasping behavior than thermoregulation. Eccrine gland activity of this area is more sensitive to the psychological stimuli than the thermal stimuli except during extreme heat stress (McIntyre, 1980).

To understand the mechanism of EDA and its measurement, Cacioppo et al. (2007) made an analogy between the skin and a variable resistor. The sweat rises in the sweat ducts due to the level of activation of the sympathetic nervous system. As more sweat fills the ducts, skin becomes more conductive which creates observable changes in EDA. This sweating response is very rapid and is measured by a small amount of current passed through the skin between two electrodes (McIntyre, 1980). Cacioppo et al. (2007) presented alternative electrode locations for electrode placements (Figure 2.9). In this study, we used the third alternative which is the thenar and hypothenar eminences of the palm.

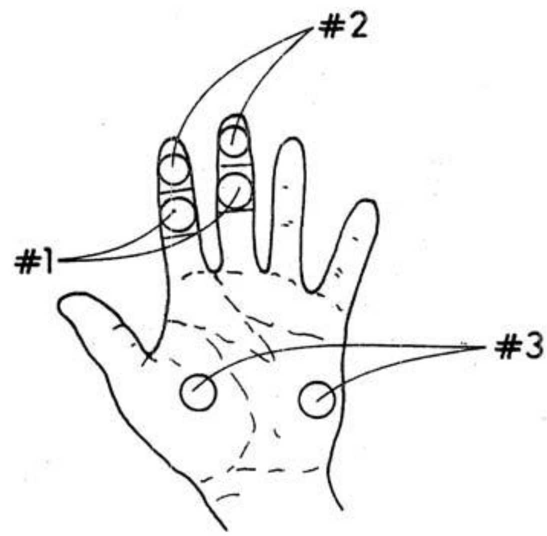


Figure 2.9. Three electrode location alternatives for EDA measurements (Cacioppo et al., 2007).

The EDA measurement in this study was used to determine the level of psychological stress of the participants. One hypothesis of this study is that thermal comfort decreases with the increased psychological stress. We also tested whether EDA is an indicator of satisfaction with the thermal environment. Another analysis we conducted was based on Hot et al. (1999) who found diurnal variations in the skin conductance level. People have significantly higher skin conductance level in the afternoons than in the morning. We repeated this analysis to investigate whether the thermal environment should account for the increased mental load.

Skin conductance was traditionally measured in mho, which is the backward spelt version of the unit of resistance (ohm). The measured level of skin conductance is in the order of μmho which corresponds with the 1,000,000 ohm of skin resistance (Andreassi, 2000). Analyses of this study use microsiemen (μS), which is the more recent use of the units and which is identical to μmho.

## 2.4. Gender and Thermal Comfort

Interactions between different comfort variables have been the subject of both laboratory and field studies. The combined effects of activity level and airflow were studied by Toftum (2002) and Jones et al. (1986). Toftum analyzed the combined effects of draught and activity level (1.1 to 1.4 met) under moderate conditions for field studies. Toftum found high correlation between (Pearson correlation 0.91) draught discomfort and preference for less air movement. Jones (Jones et al., 1986) studied moderate metabolic conditions (2.3 met) with 40 ft/min and 240 ft/min air velocities in the laboratory environment and adjusted temperature to result in thermal sensations ranging from slightly cool (-1) to slightly warm (+1) on predicted mean vote scale. His results showed that females are more sensitive to temperature changes in the 2.3 met activity level range. Our study covered Toftum's and Jones' combined metabolic rate conditions as well as the airflow speeds and temperatures. In addition, our study extended the conditions to 4 met and 83°F (28.3°C) which is 4°F (2.2°C) higher than the Jones' maximum temperature range. Erlandson et al. (2003) reported thermal sensation votes of males and females from two buildings which were studied in an ASHRAE field study research. Female workers in one building reported higher thermal sensation (corrected for indoor environmental conditions), whereas male workers reported higher thermal sensation in the other buildings. Erlandson et al. suggested that overall perception of the thermal environment biases the instantaneous thermal sensation votes. The same proposition was tested in our study and it was shown with 99.9% confidence ($p<0.001$) that the thermal experience of a person in his/her usual work environment affects his/her thermal sensation in a laboratory environment. This shows the effects of previous thermal experiences and built-in expectations on the thermal sensation of building occupants.

Griefahn and Kunemund (2001a) investigated the differences of thermal comfort, thermal sensation and air movement perception between males and females for varying metabolic rate conditions including 104, 128, 156 W/m$^2$ (1.8, 2.2 and 2.7 met respectively). They found significant differences and showed that females felt more uncomfortable by draught and reported a feeling of "rather cool." McNall et al. (1968) conducted a thermal comfort study which focused on three metabolic rate conditions (high, medium, low) under different ambient temperature (18.9, 22.2, 25.6°C). McNall et al. studied metabolic rates up to 1599 Btuh for males and 1277 Btuh for females (247 W/m$^2$ or 4.25 met and 234 W/m$^2$ or 4 met respectively assuming body surface areas are (1.8 $m^2$ and 1.6 $m^2$ for males and females). In our study, we studied metabolic activity levels up to 233 $W/m^2$ level (4 met) combined with two airflow and temperature conditions and compared results with the two studies.

Parsons (2002) compared the thermal sensation of males and females for different environmental temperatures (65.3°F/18.5°C, 73.4°F/23°C, 84.2°F/29°C). Parsons concluded that females tend to feel cooler in cold conditions and tend to feel warmer in neutral and warm conditions. This is also supported by Karjalainen (2007) who found that males are more satisfied with normal room temperatures. This is more pronounced in office environment than the home. On the other hand, Tanabe et al. (2007) found that on 7-point scale sedentary females' thermal sensation votes (–0.6±1.03) were significantly lower than the sedentary males' votes (0.1±0.83) for 25.5°C ($p<0.01$). This contrasts to the previous studies which concluded higher thermal sensation votes for females under neutral and warm conditions. A similar study by Beshir and Ramsey (1981) showed that males tend to feel warmer in neutral to hot conditions ($0.1090T_a$-3.807, R=0.995), whereas females feel cooler under the same conditions ($0.1359T_a$-6.478, R=0.984), where $T_a$ is the room temperature. The literature review showed contrasting conclusions on the thermal sensation tendencies of males and females. For this reason, we conducted analysis regarding the gender differences of thermal responses.

## 2.5. Computational Fluid Dynamics (CFD)

The thermal characteristics of an environment are variable due to various driving forces such as surface temperatures, heat sources, or air pressure. Airflow is alone driven by wind, mechanical fan, or thermal buoyancy, which create a complex environment with flow characteristics such as separation, circulation, and vortices (Zhai et al., 2007). The computational fluid dynamics (CFD) emerged as the solution to determine the conditions in thermal environments of which experimental methods are costly and impractical.

CFD is the general term to describe the numerical methods which solves partial differential equations for the conservation of mass, momentum, energy, species concentrations and the turbulence. The resulting simulation provides information on the spatial distribution of pressure, air velocity, temperature, particle concentration and turbulence (Chen, 2004; Zhai et al., 2007).

CFD has been in use to simulate the thermal comfort conditions from component scale, such as heating and cooling equipment to atmospheric scales. A summary of the development of the CFD methodologies were presented by Nielsen et al. (2004).

### *2.5.1. Thermal Comfort Applications of the CFD Methodology*

At the component scale, Zhao et al. (2003) developed efficient simulation methodologies and utilized the CFD to simulate room air diffusers. Uğursal and Culp (2007) simulated the pressure losses in ventilation ducts which affect the energy consumption and thermal comfort of the buildings. On a larger scale, Abanto et al. (2004) studied the airflow characteristics in a complex room with several computers and equipments, different human figures and various diffusers. They also calculated the predicted mean vote (PMV) for specific locations in the simulation domain using the simulated mean radiant temperature and other thermal comfort factors. In a similar study, Lin et al. (2005) studied the effectiveness of the displacement ventilation system in a computer laboratory which is composed of various furniture and heat generating elements. They also studied the PMV as well as the carbondioxide distribution in the simulation domain. In a following study, Lin et al. (2007) studied the effect of the door opening on the displacement ventilation system. Hanqing et al. (2006) utilized CFD simulations in conjunction with the time-dependent changes of the comfort parameters. They used large eddy simulation (LES) to determine the instantaneous thermal comfort parameters rather than the Reynolds averaged Navier-Stokes (RANS) which is the time-averaged solutions. They, then, determined the changes in thermal comfort in 0.1 second time steps. Stamou and Katsiris (2006) simulated the airflow characteristics in an office type environment using a cuboid human geometry. They compared the simulation results to the measured data and concluded that SST, standard k-ε, and RNG k-ε models all predict the general flow characteristics satisfactorily. Nielsen et al. (2004) studied the room air distribution based on the diffuser characteristics, furniture layouts and the complexity of the human geometry. Chen (2004) applied the CFD methodology to the outdoor wind simulations at the urban scale. In addition, Chen simulated the airflow inside the buildings induced by the natural wind.

### *2.5.2. Review of the Turbulence Models*

As mentioned previously, CFD is the numerical solution to the fundamental flow equations which are the three momentum equations, and the equations of continuity, energy and transport. Turbulence is expressed with turbulent viscosity which is a function of the turbulence kinetic energy (k), and the dissipation rate of the turbulence (ε) (Nielsen et al., 2004). The outcome of the CFD simulation depends highly on the selection of the turbulence model which is characterizes the flow properties. Direct numerical simulation (DNS), large eddy simulation (LES) and the Reynolds Averaged Navier-Stokes (RANS) equation with turbulence models are the three main approaches (Zhai et al., 2007). An extensive review of the turbulence models was presented by Zhai et al. (2007) and Zhang et al. (2007c).

DNS is based on the direct calculation of all the transport equations at each grid point. However, DNS is not feasible because it requires a very fine grid resolution which is a limitation due to demand for excessive computing power for the time being. The two other methodologies are the filtering and Reynolds averaging. Large eddy simulation is essentially the filtering of the small scale eddies which are usually smaller than the grid size. Large eddies are computed and the small eddies are modeled which are universal and independent of the general flow characteristics (Stamou, 2006). In Reynolds averaging, all the scales of the turbulence are modeled, therefore is the least demanding approach in terms of computing power. This approach has been used in the form of algebraic-stress models and zero, one and two equation models.

The CFD simulations in this study employed the $k$-$\varepsilon$ turbulence model which is a two-equation model and is based on the transport equation of turbulence kinetic energy ($k$) and turbulence dissipation rate ($\varepsilon$). The turbulent viscosity in this model is calculated based on $k$ and $\varepsilon$ (Fluent Inc., 2005). Zhang (2005) stated that the standard $k$-$\varepsilon$ model is able to give satisfactory results for complex flows in various types of applications. Drori et al. (2005) used the standard k-$\varepsilon$ model at the room scale to simulate airflow inside a 7.7 ft x 7.7 ft x 19.5 ft (2.35 m x 2.35 m x 5.94 m) test room. The standard $k$-ε model has been the most popular of two-equation models and has given satisfactory results for certain complex flows (Zhang, 2005). The RNG $k$-ε model has an additional term in the turbulence dissipation rate (ε) which results in more accurate simulations for rapidly strained flows. In addition, the effect of swirling is added to the RNG model which improves its accuracy in swirling flows (Fluent Inc., 2005). The RNG model provides an analytically derived formula for effective viscosity which improves the model in low-Reynolds number flows compared to the standard *k*-ε model which is a high-Reynolds number model. In this study, standard k-e model with near-wall treatment was used due to its satisfactory performance for the low-Reynolds number flows.

### *2.5.3. Human Geometry in CFD Simulations*

The geometry of the human figure in the simulation domain affects the simulation results depending on the variables of interest. Topp et al. (2002) compared a cuboid and a lifelike human geometry for their effects on the simulation of the micro environment and the environment at a distance. They resulted that simplified cuboid geometry is adequate for the flow characteristics away from the human body. However, a detailed geometry is required for the accurate representation of the thermal environment. Gao and Niu (2004) developed a female human geometry by laser scanning an actual mannequin. They reduced geometrical complexity by not including the hand and foot digits as well as the hair. Gao and Niu used the standard k-ε model to simulate a personalized ventilation system which is directed to the breathing zone. Deevy et al. (2008) utilized a standing nude female human geometry to simulate the displacement ventilation in an empty space. They considered 76 Watts of heat flux from the body half of which due to radiation and the other half due to convection. Dygert et al. (2009) simulated the personal microenvironment using a realistic human geometry. Authors stressed the importance of the chin, shoulder and neck in simulating the microenvironment around the breathing zone, and the general body posture and geometry in simulating the thermal plume around the human body. Abanto et al. (2004) generated human geometries using the Rhinoceros NURBS modeler and assigned 60 $W/m^2$ and 85 $W/m^2$ heat generations for the simulation. Same software was used in our human figure modeling.

Based on these studies, we designed a simplified human figure with significant body parts such as the head, neck, arms, and legs with adjustable joints. The extremities of the body such as finger, nose, and ears were simplified since they don’t affect the airflow characteristics after few inches of distance from the body. Nielsen et al. (2003) devised a benchmark test for evaluating the thermal environments with human figures. They designed two scenarios for displacement and mixing ventilation conditions. The validation of our human geometry based on Nielsen et al.’s study is presented in Section 9.1.

# 3. METHODOLOGY

## 3.1. General Description of the Human Subject Tests

Thermal comfort tests with human subjects were conducted to test the thermal comfort and sensation of people for various transient thermal conditions. Tests were administered from October 2009 to April 2010 with 40 volunteer (21 male, 19 female) graduate and undergraduate students of the Texas A&M University. This thermal comfort test was approved by the Institutional Review Board (IRB) of the Texas A&M University.

The thermal comfort test lasted approximately 2.5 hours including the pre-test period. Subjects filled out a computerized survey form at predetermined intervals during the test. Subjects exercised a total of 25 minutes in five sets using a bicycle ergometer that was placed under their workstation. Three types of data were collected during the test. The first type is the background information and the subjective responses of the test participants. The second type of data is the environmental measurements including ambient, globe, and room surface temperatures, dew point temperature, and air velocity. The third type of data is the physiological measurements including the skin temperature, heart rate, and the electrodermal activity.

## 3.2. Thermal Comfort Test Design

Thermal comfort research has taken two distinct paths in the second half of the twentieth century. De Dear (2004) called those paths deterministic engineering and holistic architectural approaches. Deterministic engineering approach is based on environmental chamber studies which led to the development of thermal comfort standards. The shortcoming of this approach is that it is not possible to determine how multiple sources are combined to create dissatisfaction. Architectural approach is based on the holistic person environment systems and led to the development of field studies. The shortcoming of this approach is the lack of control over the environmental parameters. This study was designed to combine the advantages of both methodologies which are the controlled conditions of the laboratory studies and applicability and external validity of the field studies. To achieve this, a regular office environment which is located at the Center for Housing and Urban Design (CHUD) of the Texas A&M University was converted to an environmentally controlled test room. The office environment was designed to alleviate the feeling of a laboratory environment as mentioned by McIntyre (1980). Multiple environmental factors were tested simultaneous as explained below.

Human thermal environments are complex web of relationships between different thermal factors. Transient conditions increase the complexity by adding a time component to each variable. Explaining thermal comfort with individual variables has proven to be useful and was used as a methodology in developing thermal comfort standards. However, this approach has limitations due to the interaction effects between the thermal factors. A thermal comfort test with human subjects was designed to test the individual as well as the interaction effects of dynamic personal and environmental comfort variables. 21 male and 19 female Texas A&M University graduate and undergraduate students whose ages ranged between 18 and 34 participated in the test (Table 3.1). This study was approved by the Institutional Review Board of Texas A&M University. The research design and the methodology were adapted from the previous studies by Astrand et al. (2003), Kistemaker et al. (2006), Zhang (2003a), Van den Heuvel et al. (2004), Gagge et al. (1967) and Strigo et al. (2000).

Table 3.1. Summary of demographic information of the participants.

| | **Male (21 subjects)** | | **Female (19 subjects)** | |
|---|---|---|---|---|
| | **Mean** | **St. Dev.** | **Mean** | **St. Dev.** |
| **Age** | 23.5 | 3.8 | 24.2 | 4.7 |
| **Weight (lbs)** | 168.3 | 27.2 | 133.6 | 29.7 |
| **Height (inches)** | 70.4 | 2.6 | 64.5 | 2.9 |
| **Time lived in College Station (months)** | 34.7 | 27.9 | 35.2 | 23.1 |
| **Exercise per Week (hours)** | 3.4 | 1.8 | 2.2 | 1.7 |

This research is a 2x2x2 factorial design with two levels of metabolic rate, airflow frequency and airflow location as the within-subject variables. Participants responded to a thermal comfort survey for various combinations of within-subject variables. Metabolic rate had two levels which are sedentary (1.2 Met) or high (4 Met). Airflow frequency had two levels in which airflow condition changes with a period of 30 seconds (10 seconds on, 20 seconds off) or 60 seconds (10 seconds on, 50 seconds off). Airflow location had two levels one of which was head-only and the other one was head/hands/feet simultaneously. Therefore, eight tests were conducted with each participant which totaled to 308 tests after the invalid cases were removed. Responses were also taken during metabolic transient conditions; however, they were not included in the three way interaction analysis of thermal comfort variables. Room temperature (75°F, 83°F) and gender (male, female) are the between-subject variables with two levels each. Temperature and gender were considered as between-subject variables since the literature has sound evidence on the subjective response differences for gender and temperature.

Table 3.2 and Table 3.3 present the between-subjects and within-subject test variables respectively. Table 3.3 is the detailed version of each cell in Table 3.2. Each male or female subject was randomly assigned to one the temperature conditions. Each combination of gender and temperature has approximately equal number of subjects (between 9 and 11). Therefore, each cell in Table 3.2 was tested a minimum of nine times for each temperature and gender combination. Each cell in Table 3.3 was tested a total of 40 times since all the subjects went through the same combinations of treatments. The treatment order was altered to counterbalance the treatment order effect. Each subject was randomly assigned to one of the four test sequences as presented in Table 3.4.

Table 3.2. Between-subjects variables

| | **Male** | **Female** |
|---|---|---|
| **Neutral Room Temperature (75°F)** | 8 Tests per Subject (2x2x2) | 8 Tests per Subject (2x2x2) |
| **High Room Temperature (83°F)** | 8 Tests per Subject (2x2x2) | 8 Tests per Subject (2x2x2) |

Table 3.3. Within-subject variables (metabolic rate, airflow frequency, and airflow location) as triple combinations of treatments during the Session 2 and 3 of the test (Session 1 is the control condition).

| | **First 15 minutes** | | **Second 15 minutes** | |
|---|---|---|---|---|
| **Session 2** | Met Rate 1<br>Air Freq. 1<br>Air Loc. 1 | Met Rate 2<br>Air Freq. 1<br>Air Loc. 1 | Met Rate 1<br>Air Freq. 2<br>Air Loc. 1 | Met Rate 2<br>Air Freq. 2<br>Air Loc. 1 |
| **Session 3** | Met Rate 1<br>Air Freq. 1<br>Air Loc. 2 | Met Rate 2<br>Air Freq. 1<br>Air Loc. 2 | Met Rate 1<br>Air Freq. 2<br>Air Loc. 1 | Met Rate 2<br>Air Freq. 2<br>Air Loc. 2 |

Table 3.4. Four test sequences to counter balance the treatment order.

| | **Session 2** | | **Session 3** | |
|---|---|---|---|---|
| | **First 15 minutes** | **Second 15 minutes** | **First 15 minutes** | **Second 15 minutes** |
| **Test Sequence 1** | 60 seconds Head-only | 30 seconds Head-only | 60 seconds Head/Hands/Feet | 30 seconds Head/Hands/Feet |
| **Test Sequence 2** | 30 seconds Head-only | 60 seconds Head-only | 30 seconds Head/Hands/Feet | 60 seconds Head/Hands/Feet |
| **Test Sequence 3** | 60 seconds Head/Hands/Feet | 30 seconds Head/Hands/Feet | 60 seconds Head-only | 30 seconds Head-only |
| **Test Sequence 4** | 30 seconds Head/Hands/Feet | 60 seconds Head/Hands/Feet | 30 seconds Head-only | 60 seconds Head-only |

Tests subjects were selected through classroom announcements. Group meetings were held prior to the test dates with the volunteers who signed up during classroom announcements. They were given information about the nature of the study and how to fill the background and online survey forms. Volunteers who wanted to participate in the study after the information session were assigned a test date based on their preferences. Subjects were also assigned one of the three test times which are 8.30 am, 11.30 am, and 2.30 pm.

Tests were conducted one subject at a time. On the test date, verbal explanations about the test were given a second time and the consent form was signed after all the questions of the participant were answered. Subject spent 30 minutes at the test station prior to the test to acclimatize with the room temperature (Gagge et al., 1969; Strigo et al., 2000; Tanabe et al., 2007). The actual test had three sessions and lasted 1 hour 40 minutes with two 5 minutes break between the three sessions (Figure 3.1). The first session is the control period without the treatment during which subjects' thermal responses were recorded. The second and the third sessions are the treatment periods during which subjects were exposed to multiple thermal conditions. Thermal comfort tests totaled to 100 subject hours excluding the group meetings before the tests.

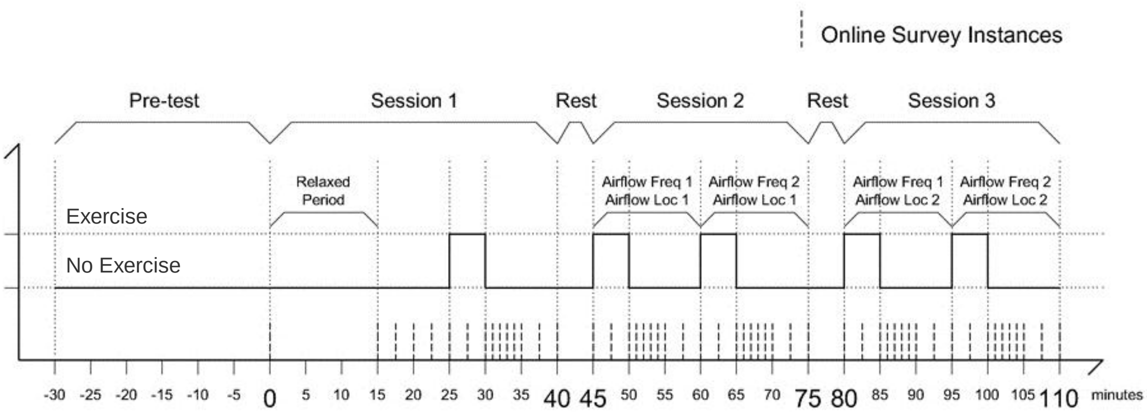


Figure 3.1. Test sequence with online survey instances including the 5 minute breaks between the sessions.

### 3.3. Test Conditions

Thermal conditions of this test range from sedentary activity and neutral room temperatures to high metabolic activity and high room temperatures which fall clearly outside the comfort zone based on ASHRAE Standard 55 (2004). One of the premises of this study is that thermal comfort is a psychological phenomena and can be achieved even the physical conditions suggest otherwise.

Subjects read magazines or played simple card games on the computer throughout the test except the first 15 minutes which was the relaxed period. For those first 15 minutes, subjects were asked to relax as much as possible while they leaned back with their eyes closed. Owing to the design of the thermal comfort unit, subjects were able to carry on the reading and the playing activities during the exercise periods.

### *3.3.1. Ambient Temperature, Mean Radiant Temperature and Relative Humidity*

Subjects evaluated their thermal states for either 75°F (St. Dev. 0.4°F) or 83°F (St. Dev. 0.6°F) ambient temperatures while relative humidity was kept between 40% and 50%. Temperature of the test room was brought to the test conditions at least 1 hour prior to the test for the room surface temperatures to stabilize. The room surfaces were constructed out of dry wall which has low thermal capacity. Therefore, mean radiant temperature reached the target room temperature within 1 hour before the test and stayed at that level for the duration of the test. Room surface temperatures were monitored with thermocouples.

### *3.3.2. Mean Airflow and Dynamic Airflow Conditions*

Two types of airflow patterns were used in the thermal comfort tests, of which one is directed to the head-only and the other one is directed to head/hands/feet simultaneously. The volume of air delivered to the subject was kept constant in those two cases. Since the number of open nozzles were three times less (two compared to six), higher air velocities were experienced during the head-only flow. Maximum air velocities which occurred during air pulsing next to the subject's neck and the face are presented in Table 3.5 together with the mean air velocities. This air speed is consistent with the high temperature tests found in the literature (Zhou et al., 2006; Toftum, 2004; Tanabe and Kimura, 1994).

Table 3.5. Maximum and mean airflow conditions for two types of airflow patterns.

| | **Head-only** | | **Head/Hands/Feet** | |
|---|---|---|---|---|
| Nozzle Exit | 420 ft/m | 2.13 m/s | 214 ft/m | 1.09 m/s |
| Neck (2” away) | 156 ft/m | 0.79 m/s | 81 ft/m | 0.41 m/s |
| Face (2” away) | 66 ft/m | 0.34 m/s | 57 ft/m | 0.29 m/s |
| Mean Air Velocity | 55 ft/m | 0.28 m/s | 44 ft/m | 0.22 m/s |
| Maximum Tu | 38% | | 31% | |

Turbulence intensity is closely related to the sensation of draught which is the unwanted cooling of the body. Airflows with high turbulence intensities are perceived as uncomfortable by people (Mayer, 1993; Fanger et al., 1988). Turbulence intensities which have occurred during the tests were calculated using Equation 3.1 (Wessel et al., 2006; Mayer, 1987). Maximum turbulence intensities (Tu) were 38% and 31% for head-only and head/hands/feet respectively.

$$Tu = \frac{\sigma_u}{\bar{u}} * 100 \qquad (3.1)$$

where,

$\sigma_u$, is the standard deviation of the air velocity,

$\bar{u}$, is the mean air velocity.

Mayer (1987) published the allowable turbulence intensity limits as a function of mean air velocity to avoid draught discomfort (Figure 3.2). Draught is less of a problem in higher temperatures and we used the 23°C curve which is conservative for our 24°C and 28.3°C room temperatures. The test conditions of our study which was 0.28 m/s and 38% turbulence intensity is shown on Mayer’s plot. Our turbulence intensities were within the comfort limits and should not cause draught discomfort according to Mayer’s findings. Fanger et al. (1988) investigated the effect of turbulence intensity on draught sensation and determined the dissatisfaction levels as shown in Figure 3.3. The test conditions of our study are also shown on Fanger’s figure. This figure suggests that for 0.28 m/s airflow and medium turbulence intensity, 15% of the people are dissatisfied due to draught. Fanger et al. formulated the draught dissatisfaction formula (DR) which is still in use by ASHRAE Standard 55 (2004) and ISO 7730 (2005).

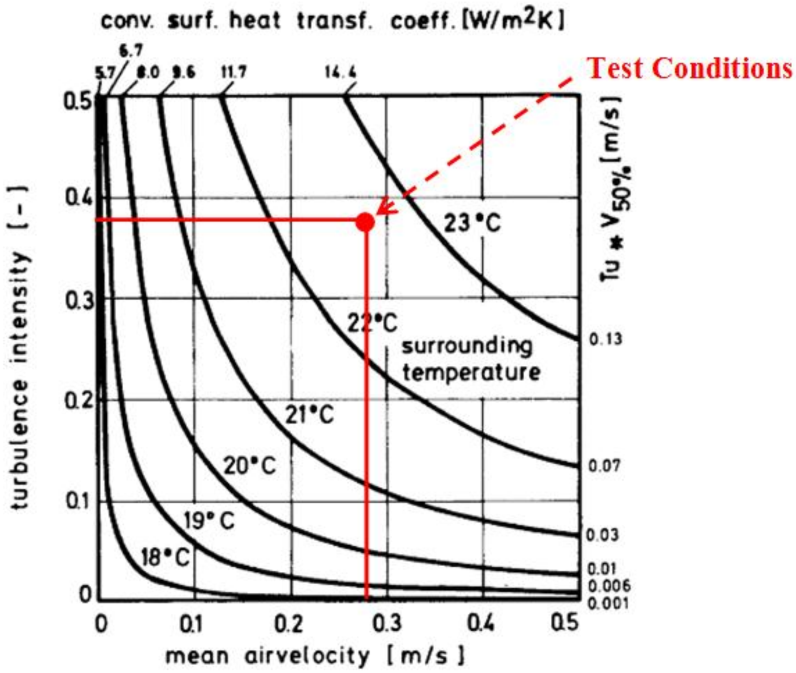


Figure 3.2. Limits of draught discomfort as a function of mean air velocity and turbulence intensity (Mayer, 1987).

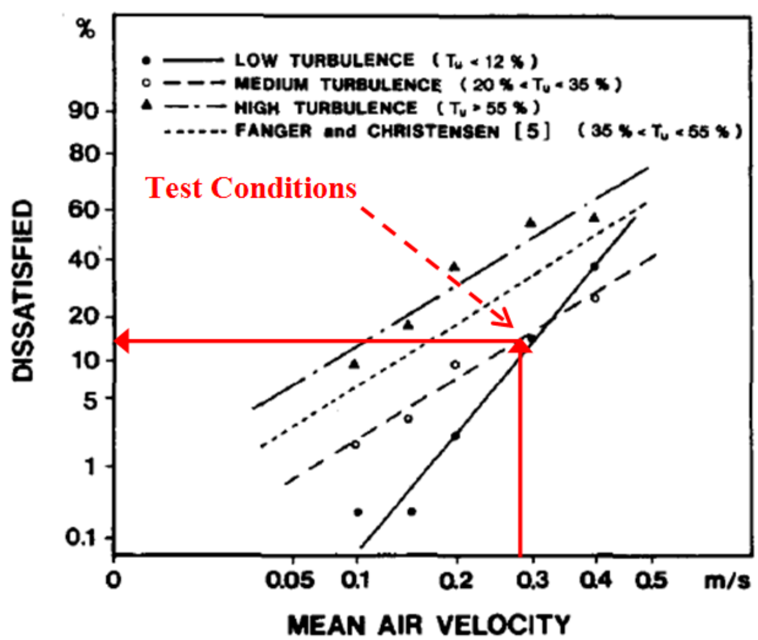


Figure 3.3. Percent of dissatisfied due to draught as a function of mean air velocity for three turbulence intensity bins (Fanger et al., 1988).

Fiala et al. (2003) and Zhou et al. (2006) suggested that warm sensation can be compensated with the cold warnings from the skin thermoreceptors. Following this proposition, we hypothesized for this study that stimulation of the cold receptors can provide comfort in warm temperatures and in high metabolic conditions. In order to achieve this, we designed a dynamic airflow sequence of 30-second and 60-second pulsing which would prevent skin thermoreceptors to adapt to the thermal conditions (Figures 3.4 and 3.5).

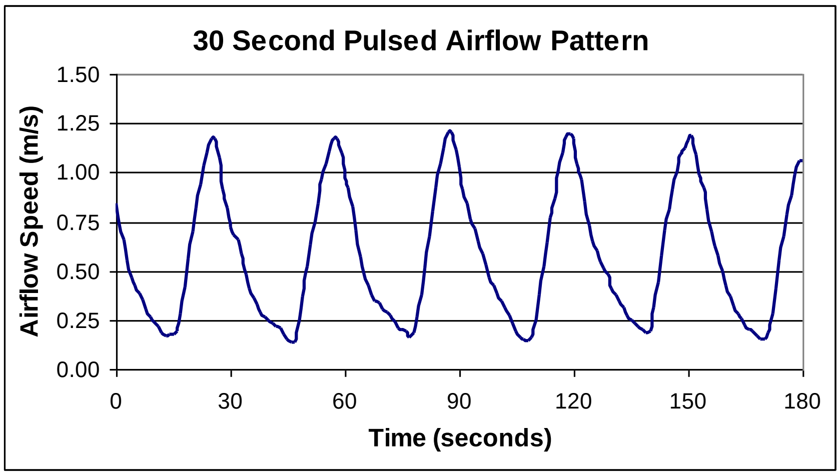


Figure 3.4. Airflow speed pattern of 30-second pulsed air measured between the subjects' head and the nozzle.

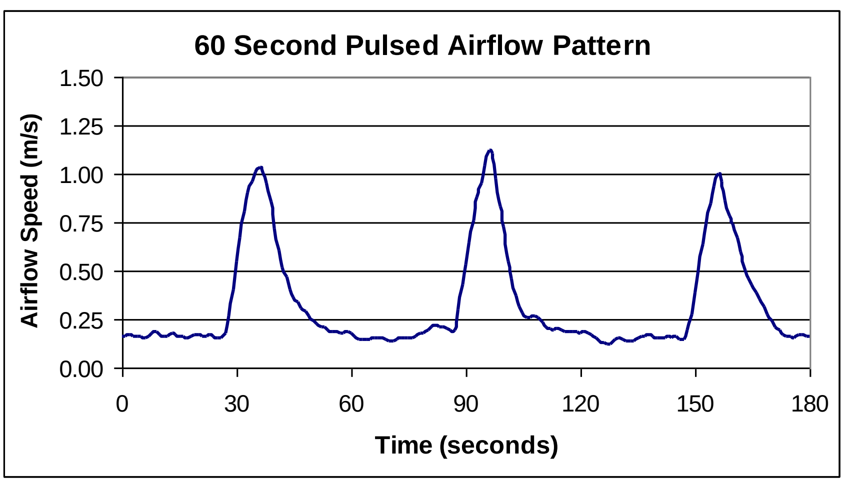


Figure 3.5. Airflow speed pattern of 60-second pulsed air measured between the subjects' head and the nozzle.

Tanabe and Kimura (1994) compared different patterns of dynamic airflow in terms of their effectiveness to provide thermal comfort. Our 30-second airflow pattern is similar to the sin(30), and 60-second airflow is similar to the pulsed air of Tanabe and Kimura except their pulsed air has a longer high airflow period (Figures 3.6 and 3.7).

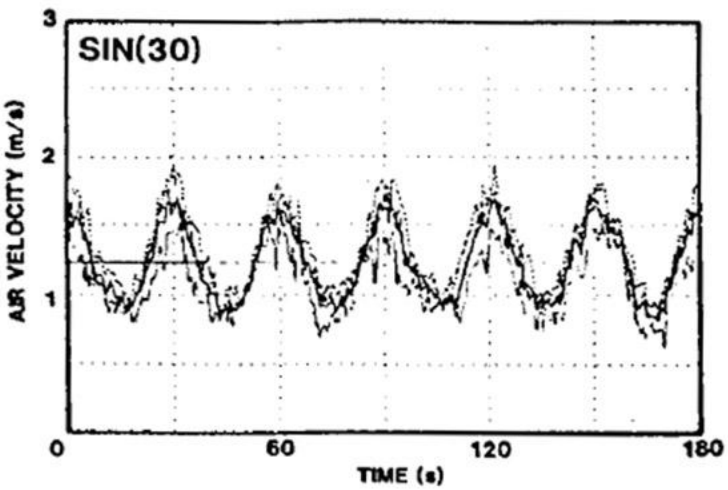


Figure 3.6. Sin(30) airflow patterns of Tanabe and Kimura (1994).

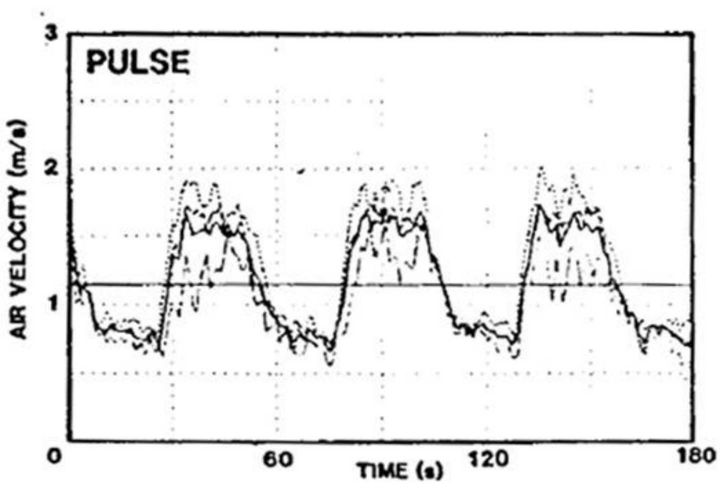


Figure 3.7. Pulse airflow pattern of Tanabe and Kimura (1994).

### *3.3.3. Personal Variables*

Physiological and psychological stimuli invoke several physiological responses including blood pressure, heart rate, electromyogram, skin conductance level, electroencephalogram, skin temperature, and body core temperature (Boregowda and Karwowski, 2005). Cacioppo et al. (1987) stated that heart rate is the most favored measure of physiological arousal. In this study, heart rate was used as the main indicator of the metabolic activity.

#### *3.3.3.1. Determination of Metabolic Rate from Heart Rate*

Subjects were asked to bring their heart rate to the target heart rate level which corresponded with a 232 $W/m^2$ (4 met) metabolic activity. Target heart rate was calculated using Equations 3.2 through 3.6 as presented in ISO 8996 (2004). In order to account for individual variations, the resting metabolic rate was calculated using Mifflin et al.'s (1990) resting energy expenditure (REE) formula (Equations 3.7 and 3.8) which takes into account age, height, weight and gender of the subject. REE was then used as the basal metabolic rate ($M_0$) which was used in the target heart rate equation. Basal heart rate ($HR_0$) was measured during the first 15 minutes of the test which was the relaxed period.

$$HR_{target} = HR_0 + RM * (M_{target} - M_0) \quad (3.2)$$

$$RM = (HR_{max} - HR_0)/(MWC - M_0) \quad (3.3)$$

For males, $$MWC = (41.7 - 0.22A)P^{0.666} \quad (3.4)$$

For females, $$MWC = (35.0 - 0.22A)P^{0.666} \quad (3.5)$$

$$HR_{max} = 205 - 0.62A \quad (3.6)$$

For males, $$REE = 10 * P + 6.25 * H - 5 * A + 5 \quad (3.7)$$

For females, $$REE = 10 * P + 6.25 * H - 5 * A - 161 \quad (3.8)$$

where,

$HR_{target}$, target heart rate, beats per minute (bpm),

$RM$, increase in heart rate per unit of metabolic rate, bpm/(W/m$^2$),

$HR_0$, heart rate at rest, bpm,

$M_{target}$, target metabolic rate, W/m$^2$,

$M_0$, basal metabolic rate, W/m$^2$ (calculated from REE),

$MWC$, maximum working capacity, W/m$^2$,

$P$, weight, kg,

$H$, height, cm,

$A$, age, years,

$REE$, resting energy expenditure, kcal/day,

*REE* (kcal/day) was converted to the $M_0$ (W/m$^2$) using the Equations 3.9 and 3.10. Average body surface areas were accepted as 1.8 m$^2$ for males and 1.6 m$^2$ for females based on ISO 8996 (2004) and Havenith et al. (2002).

For males, $$M_0 = REE * 1.162/(24 * 1.8) \quad (3.9)$$

For males, $$M_0 = REE * 1.162/(24 * 1.6) \quad (3.10)$$

In order to validate our calculation of target heart rate, we compared the calculated heart rates to the measured heart rate data that were presented in McNall et al. (1968) and Zhang et al. (2003b). Our mean predicted target heart rate to reach 4 met level matched with McNall et al. and Zhang et al. within 5 beats/min, which is considered less than margin of error for this estimation. A comparison between this study and Zhang et al.'s study is presented in Figure 3.8. Zhang et al.'s data was reconstructed from their original graph that is presented in Section 2.3.5.

Time-averaged metabolic rates based on ISO 8996 (2004) were 1.55 met for the first session, 2.13 met for the second and the third sessions, and 1.9 met for the whole test. Metabolic rate was averaged to 2.6 for the transient conditions during which metabolic rate dropped from 4 met to 1.2 met within 5 minutes.

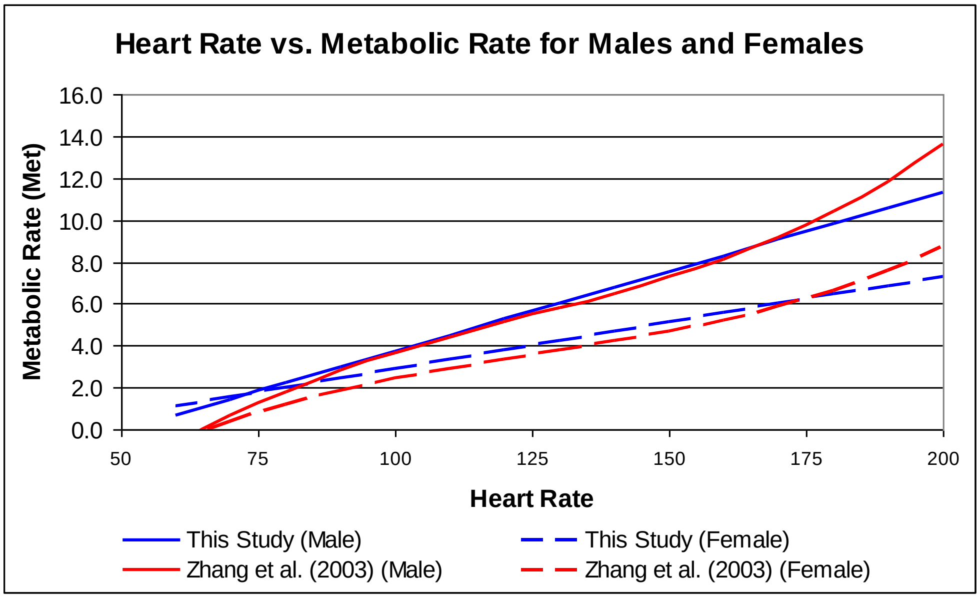


Figure 3.8. Comparison between this study and Zhang et al. (2003b) in estimating metabolic rate from heart rate.

*3.3.3.2. Clothing Insulation Level*

Subjects wore t-shirts, long shorts, and ankle size sports socks during the test. Based on ISO 9920 (1995), clothing insulation level was calculated as 0.5 clo, including the chair insulation and the backpack. This insulation level corresponds with the summer clothing ensemble based on ASHRAE Standard 55 (2004).

**3.4. Test Protocol**

The thermal comfort test had three sessions. The first session was the control case which aimed at determining subjects' responses towards thermal environment during transient metabolic rates for two temperature conditions. The second and the third sessions aimed at testing interaction effects airflow location, air pulsing frequency and metabolic rate on thermal comfort and thermal sensation. Test protocol of the study is based on the studies by Gagge et al. (1969), Astrand et al. (2003), Kistemaker et al. (2006), Zhang (2003a), and Van den Heuvel et al. (2004). The complete itemized test protocol is presented in Appendix B. One male and one female researcher was present at the laboratory at all times during the tests.

### *3.4.1. Pre-test*

The pre-test phase consisted of getting participants ready for the experiment and collecting the background data. Previous studies suggested between 10 minutes and 60 minutes (30 minutes being the norm) in the environmental chamber to acclimatize with the environment (Greenspan et al., 2003; Strigo et al., 2000; Jones and Ogawa, 1992; Huda and Homma, 2005; Yao et al., 2008). Participants in this study spent 30 minutes in the test room at the test temperature before the test started for their body to acclimatize with the environment.

Upon arrival, the participant was given a verbal briefing of the test procedure. Time was provided for the questions and the consent form was signed should the participant agreed to participate. During pre-test period, the subject filled out the *Background Survey* and familiarized himself with the *Online Survey* and the computer environment. The subject was given a standard amount of water (3 oz.) to avoid dehydration during the test. The Subject's weight was measured with the test clothing ensemble. Thermocouples, heart rate sensor, and electrodermal activity (EDA) electrodes were attached to the subject during the pre-test period.

### *3.4.2. Session 1*

The subject filled out the first *Online Survey* with the start of the test to record the initial thermal responses. The first session of the test lasted 40 minutes, the first 15 minutes of which the subject was asked to completely relax with eyes closed. During this period, the basal heart rate was measured and the target heart rate of the subject to reach 4 met (233 $W/m^2$) of metabolic activity was calculated using basal heart rate, age, weight and height of the subject (Section 3.3.3.1). At the end of the 15-minute period, the subject was asked to wake up and he was allowed to start reading magazines or playing games. Subject exercised between the $25^{th}$ and $30^{th}$ minutes and rested between $30^{th}$ and $40^{th}$ minutes. Pilot studies showed that it takes 2-4 minutes for the subjects to resume normal metabolic rate after the exercise session. It was then assumed that 5 minutes after the exercise period is the metabolic transient phase and all the subjects recovered to the base metabolic level by the end of the 5 minute transition period.

Subjects filled out the Online Survey every 2.5 minutes with the exceptions that there were no surveys during the first 15 minutes and the survey was filled every 1 minute within the 5 minutes after the exercise period ended. Therefore, more subjective response data exist for the transient metabolic rate periods. A 5-minute break was given after Session 1 ended during which the tympanic temperature of the subject was measured.

#### *3.4.3. Session 2 and Session 3*

Session 2 and 3 aimed at measuring subjects' subjective thermal and physiological responses to transient conditions and lasted 30 minutes each. Thermal comfort responses were taken for combinations of airflow frequency (30-second and 60-second), airflow location (head-only and head/hands/feet together), and metabolic rate (low and high). Airflow frequency was changed in 15-minute periods. Subjects exercised for 5 minutes and rested for 10 minutes in each 15-minute period which totaled to two exercise periods per session. There was a 5-minute break between the sessions during which the researcher adjusted the nozzles to change the airflow location. The tympanic temperature of the subject was also measured during the break.

#### *3.4.4. Post-test*

The tympanic temperature of the subject was measured immediately after Session 3 ended. The sensors were detached from the subject and the subject's weight was measured. The subject was asked to evaluate his/her test experience on a 7-point discrete scale which ranged from very negative to very positive with a neutral response in the middle.

### 3.5. Thermal Comfort Surveys

This study aimed at quantifying thermal comfort and thermal preferences of subjects based on two types of independent variables: (1) background of the test participant, (2) environmental and personal variables at the time of the experiment. A *Background Survey* and an *Online Survey* were designed to gather information regarding the subject's background and his/her perception of the thermal environment.

### *3.5.1. The Background Survey*

The *Background Survey* is a modified and computerized version of a background survey of a previous ASHRAE report (Cena and De Dear, 1998) (Figures 3.9 through 3.12). ASHRAE field study's questions on the perception towards the current work environment were slightly modified for our test to cover subject's usual work environment. This survey aimed at collecting data on the background characteristics of the subjects, environmental control over their usual workplace, health characteristics, and the sensitivity to different environmental stimulus. Figure 3.9 shows the background characteristics that were collected from the test subjects. These include demographic attributes including age, gender, year in college and physical attributes such as weight and height. Figure 3.10 shows the questions on thermal environment control. These were used to determine the test subject's degree of environmental control over their usual workspaces as well as the different control strategies that they can apply. Figure 3.11 shows the health characteristics which the subject might experience at their workplace. These questions provided information on some of the sick building syndromes that subjects experience in their usual work areas. Finally, Figure 3.12 shows the questions on sensitivity to environmental stimulus. This data will help categorize the subjects' sensitivity to environmental stimulus such as light, airflow, noise and temperature.

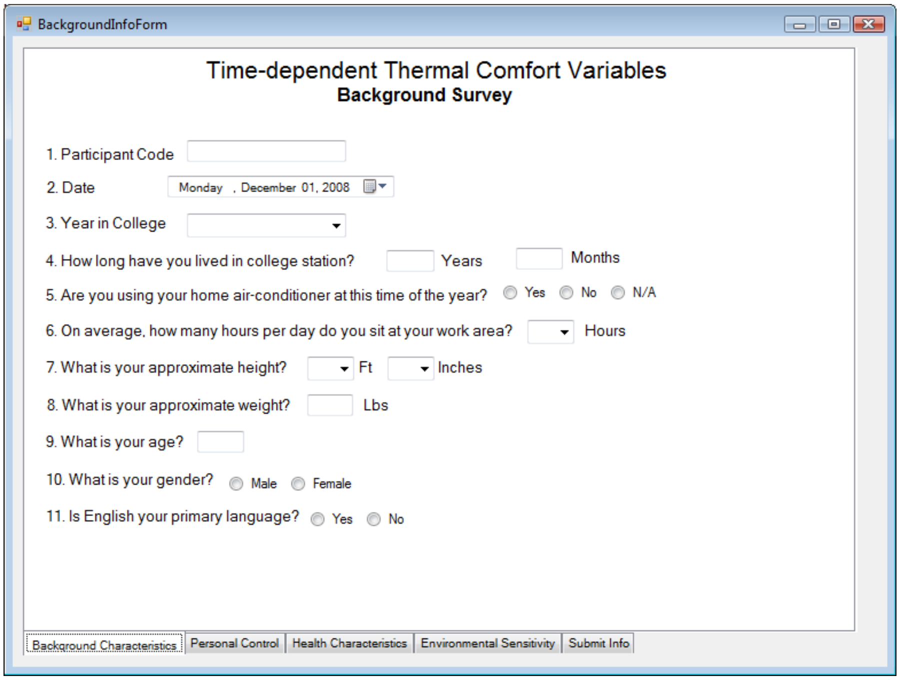


Figure 3.9. Background characteristics section of the *Background Survey*.

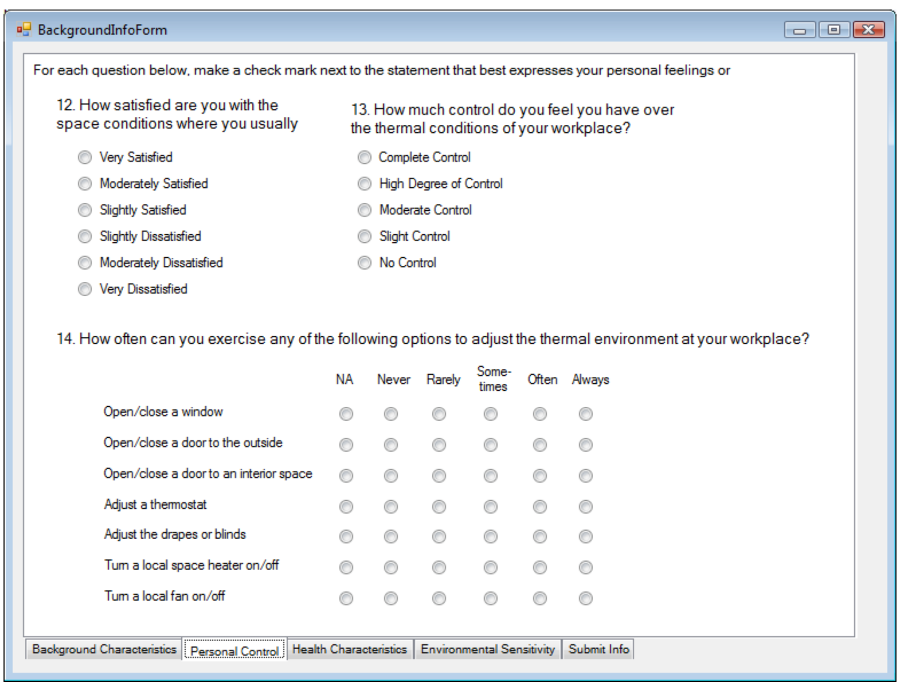


Figure 3.10. Personal control section of the *Background Survey*.

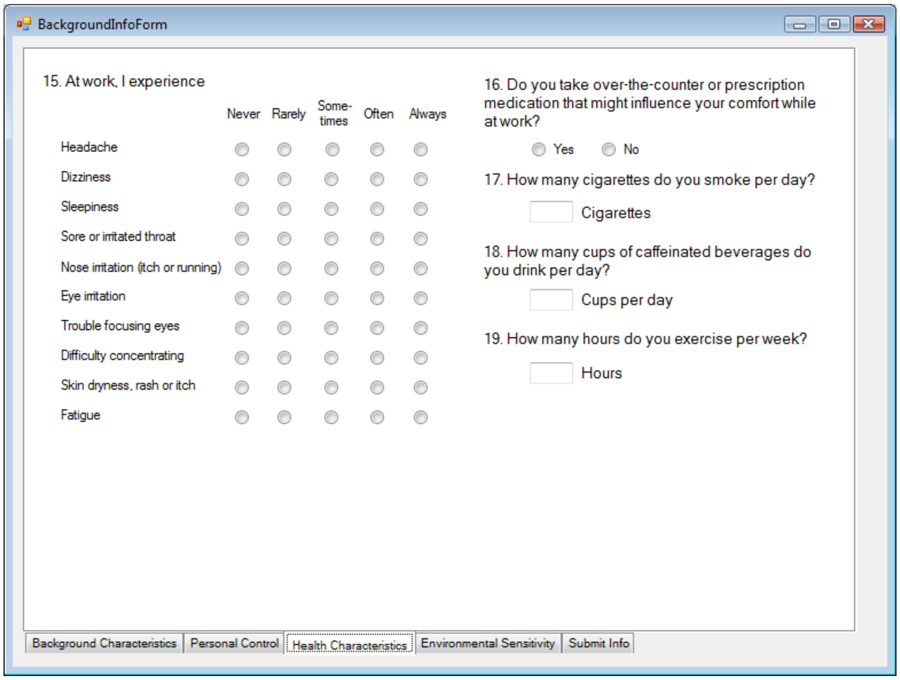


Figure 3.11. Health characteristics section of the *Background Survey*.

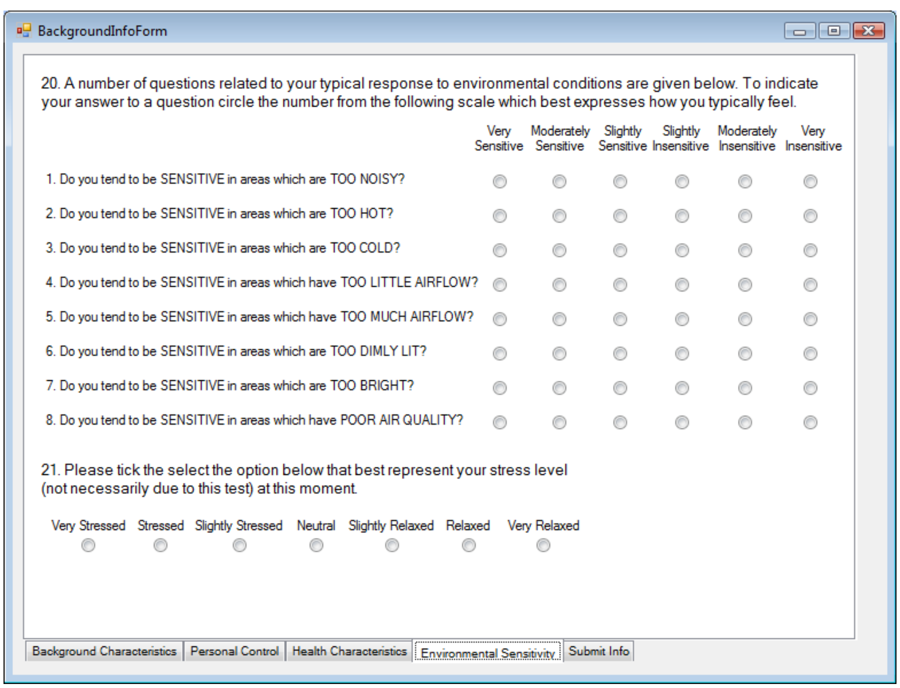


Figure 3.12. Environmental sensitivity section of the *Background Survey*.

### *3.5.2. The Online Survey*

The *Online Survey* was used to collect data on subjects' perception of thermal comfort and thermal sensation during the tests. The literature survey showed variations in the thermal comfort surveys which are summarized in Table 3.6. Scale column in Table 3.6 shows the minimum, maximum and the midpoint values of each scale. The accepted norm for thermal sensation and thermal comfort is the ASHRAE 7-point scale. The predicted mean vote also has values from -3 to +3 which is the same as the 7-point thermal sensation scale. McIntyre (1980) provided a physiological explanation as the rationale to the 7-point scale by stating that people can only identify seven levels of sensation without confusion. The early version of the 7-point scale is the Bedford scale which goes from which has seven discrete levels from 'much too cool' to 'much too warm'. McIntyre also mentioned that both the new 7-point scale and the old Bedford scale gave similar correlations and neutral temperatures in an environmental study.

The *Online Survey* of this study had analog scales for thermal comfort and thermal sensation. Discrete scales were used for thermal environment acceptability, temperature and air movement preference (Figure 3.13). A break was placed between the two halves of the thermal comfort scale to encourage the subjects to make a decision for their thermal comfort level. Thermal sensation and thermal comfort were based on continuous 7-point scale, whereas other questions had discrete scales. The thermal comfort scale covered values from (-3) very uncomfortable to (-0) just uncomfortable and from (+0) just comfortable to (+3) very comfortable. The thermal sensation scale covered values from (-3) very cold to (+3) very hot with (0) neutral in the middle. The thermal environment acceptability question had (1) acceptable, and (0) unacceptable as answers. The temperature preference question had (1) warmer, (0) no change, (-1) cooler, and airflow preference has (1) more air movement, (0) no change, (-1) less air movement as answers. This version of the *Online Survey* is the result of several design iterations. User behavior studies were conducted for different designs to avoid response biases. The Online Survey was designed to appear on the computer screen of the test subject at predetermined times during the tests. Figure 3.14 shows the input screen to setup the behavior of the *Online Survey*.

Table 3.6. Test constructs for thermal comfort survey and their scales.

| | Test Construct | Scale |
|---|---|---|
| Kacmarczyk et al. (2004) | Thermal Sensation | (-3) (0) (+3) |
| | Air Movement Acceptability | (-1) (0) (+1) |
| Huda et al. (2005) | Thermal Sensation | (-2) (0) (+2) |
| | Thermal Comfort | (-2) (0) (+2) |
| Melikov (2007) | Thermal Sensation | (-3) (0) (+3) |
| | Thermal Acceptability | (-1) (-0) (+0) (+1) |
| Yao et al. (2008) | Thermal Sensation | (-3) (0) (+3) |
| Zhang et al. (2007b) | Thermal Satisfaction | (-3) (0) (+3) |
| | Thermal Sensation | (-3) (0) (+3) |
| Zhang and Zhao (2008b) | Thermal Sensation | (-3) (0) (+3) |
| | Thermal Acceptability | (-1) (-0) (+0) (+1) |
| | Thermal Comfort | (-2) (-0) (+0) (+2) |
| Zhang et al. (2008a) | Thermal Sensation | (-4) (0) (+4) |
| | Thermal Comfort | (-4) (-0) (+0) (+4) |
| | Air Movement Acceptability | (-4) (-0) (+0) (+4) |
| Hashiguchi et al. (2010) | Thermal Sensation | (-4) (0) (+4) |
| | Thermal Comfort | (-3) (0) (+3) |

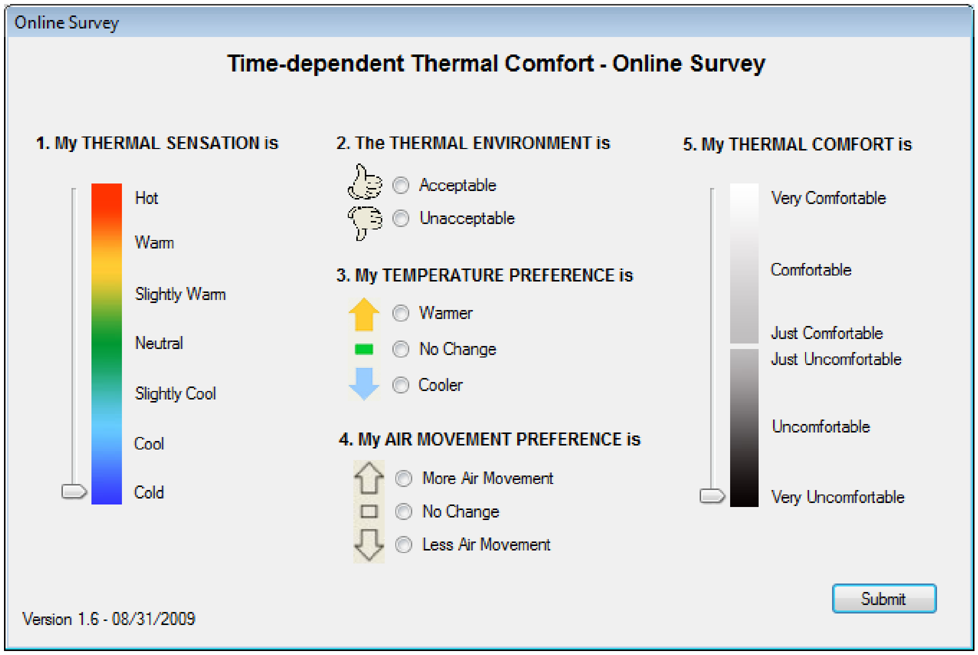


Figure 3.13. Thermal Comfort *Online Survey* screen.

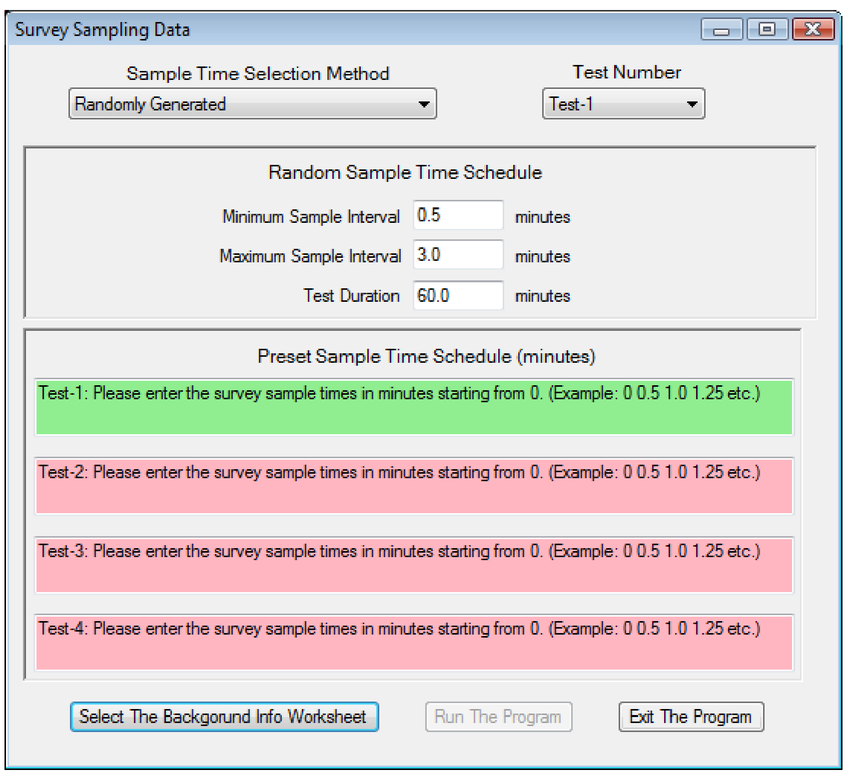


Figure 3.14. Initial input screen of the *Online Survey*.

### 3.6. Statistical Analysis

The main methodology of this study is based on investigating the relationships between the measured environmental data and user responses to the environmental conditions. A major focus point is the predictability of the subjective responses by physiological conditions and environmental factors. The effects of airflow frequency and airflow location in restoring thermal comfort have been subject to numerous studies (Zhao et al., 2004; Fiala et al., 2003; Ring et al., 1993; Zhang, 2003a; Arens et al., 2006b). To date, pulsing air and local cooling have been studied independently for sedentary subjects. In this research, their combined effectiveness was tested for various metabolic conditions. In addition, the interaction effects of the airflow frequency and the airflow location were tested for the sedentary and transient activity levels.

The environmental, physiological, and the subjective thermal data was analyzed using several statistical analysis techniques including three-factor analysis of variance (ANOVA), multivariate regression analysis, independent samples t-test for pairwise comparisons, and correlation analysis. This research was a mixed design with temperature and gender as between-subject variables and metabolic rate, airflow frequency and location are the within-subject variables. The main dependent variables were the thermal comfort, thermal sensation, thermal satisfaction, and the airflow and temperature preferences. In all statistical analysis, the results were accepted significant at $\alpha=0.05$ or $p<0.05$.

Assuming that the null hypothesis of a statistical analysis is the equality of two values; the p-value is the probability of rejecting the equality when the two values are actually equal. Rejecting the null hypothesis in such a case is also called the type I error (Ott and Longnecker, 2001). $\alpha$ is then the maximum allowable probability that something is a result of a random variation in the data instead of the result of an investigated cause.

Shapiro-Wilk's for data counts less than 2,000 and Kolmogorov-Smirnov for data counts more than 2,000 were used to test the normality with a null hypothesis that the data is normally distributed (Kacmarczyk et al., 2004; Melikov and Knudsen, 2007; Zhang and Zhao, 2008b).

Each subject was exposed to all combinations of treatments in the same session. Therefore, three-factor repeated measures analysis of variance (ANOVA) was used in which within-subject variables (repeated measures) were metabolic rate, airflow location and frequency (Kistemaker et al., 2006; Kacmarczyk et al., 2004; Hot et al., 1999; Melikov and Knudsen, 2007; Toftum and Nielsen, 1996; Zhang and Zhao, 2008b). The null hypothesis was that the mean value of the dependent variable was the same across all the combinations of factor levels. ANOVA tables were presented as the analysis report. The sphericity of the data was checked with the null hypothesis that the relationships between different combinations of factors were the same. Likeliness of the relationship was based on equal variances of the differences between different combinations of the factors. The dependent variables in these analyses were the thermal responses of the test subjects. For some of the analysis Tukey's Post Hoc model was used for pairwise comparisons (Yao et al., 2008).

Independent samples t-test was used to compare the results from two different populations. The null hypothesis of this test was that the means of the two populations are the same. The independent samples t-test was used to compare subjective responses or physiological data for known groups such as two different room temperature conditions, two genders, three levels of metabolic rate, or two levels of airflow conditions. The t-test was also used to follow up some of the ANOVA test for group differences to determine which group was different than the others.

The regression analysis, which is predicting a quantitative data using another quantitative data (Ott, 2001), was used to determine the causal relationships between various environmental, physiological, and subjective data. The unit of association in these analyses is the time. Models were developed in the form of

$$y = \beta_0 + \beta_1 x + \varepsilon \qquad (3.11)$$

in which, $y$ is the predicted variable, $\beta_0$ is the intercept, $\beta_1$ is the slope of the fitted line, and $\varepsilon$ is the random error term. The regression analysis was mainly used for predicting thermal comfort from thermal sensation votes, and thermal sensation from various skin temperature sites. A stepwise regression analysis was used to determine which skin temperature sites correlated best with the mean skin temperature (Olesen, 1984). In stepwise regression analysis, the combinations of independent variables that had the highest correlation with the dependent variable were determined.

The initial analysis of the subjective thermal response data showed similar variability for each subject. However, offset between subjects existed due to the differences in subjective interpretation of the *Online Survey* question scales. Z-normalization was applied to the subjective response data to eliminate the offsets and to better determine the overall response trends. The following formula was applied for Z-normalization which essentially brought individual mean responses to 0 and scaled individual standard deviations to 1 (Equation 3.12).

$$z = \frac{x - \mu}{\sigma} \tag{3.12}$$

where,

$x$ is the raw score to be normalized,

$\mu$ is the mean of the population,

$\sigma$ is the standard deviation of the population.

# 4. INSTRUMENTS AND CALIBRATION

This section presents the various instruments that were used for the environmental and physiological measurements and their calibration procedures. In the first part, sensors were explained with their measurement principles. In the second part, test room design was explained with operational principles and equipment connections. In the third part, calibration procedures of various equipments were explained.

The environmental parameters, including ambient temperature, air velocity, relative humidity, and room surface temperatures were measured with the laboratory grade equipment according to the ISO 7726 (1998), ISO 7730 (2005), and ASHRAE Standard 55 (2004) specifications.

## 4.1. Data Collection and Processing

### *4.1.1. Data Acquisition (DAQ) System*

All the data, except the heart rate and the *Online Survey*, was collected using National Instruments 6031E Data Acquisition (DAQ) input/output (I/O) terminal (National Instruments, 2010) at 100 millisecond sampling and 1 second recording intervals (Figure 4.1). This specific terminal has 64 single ended or 32 differential, 2 analog outputs with 16-bit resolution and 8 programmable digital input/output channels. A custom LabView program was used to collect data and to control the fan sequence for air pulsing effect that was used in the tests (Figure 4.2). DAQ software converted the 4-20 mA and 1-5 V signals from various thermocouples and transducers to the actual measurand.

The heart rate data was recorded separately every 5 seconds which was the average of the preceding 5 seconds. MagneTrainer's (2010) propriety software which interfaces POLAR system was used for the heart rate measurements. The *Online Survey* was recorded on a separate computer which was used by the subject. All the data was matched based on their time stamps as explained in Section 4.1.2.


Figure 4.1. NI 6031E I/O terminal.

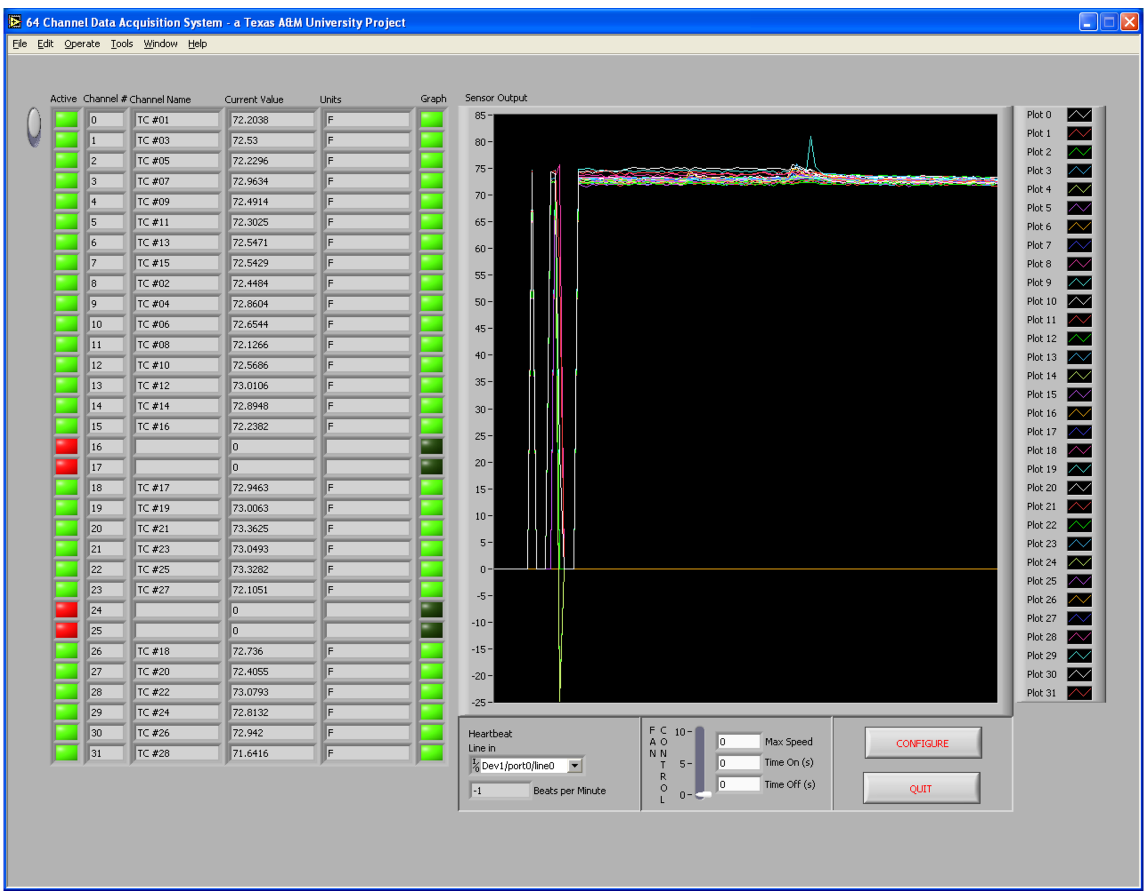


Figure 4.2. DAQ software interface.

#### *4.1.2. Dataset Processing*

Two types of datasets were prepared from the raw DAQ, heart rate and survey data. In the first dataset, the heart rate time stamp was used as the basis and the DAQ data was matched to the heart rate data as presented in Figure 4.3. This data set was used for analyzing the transient environmental conditions. A total of 50,560 data points existed in this dataset. A second data set was prepared to analyze the *Online Survey* results (Figure 4.4). In this dataset, heart rate and DAQ data were matched to the *Online Survey* time stamp with different processing techniques. The methods to process the individual data types in Figure 4.4 were chosen to project their impact on the subjective response on the particular *Online Survey* instance. A total of 53 data points per test subject exist in this data set. The total number of points in this data set was 2,101 after the invalid data were removed.

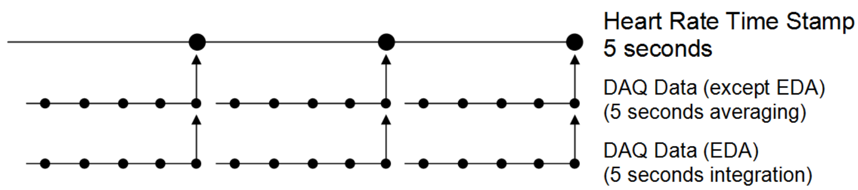


Figure 4.3. 5 second interval data processing scheme.

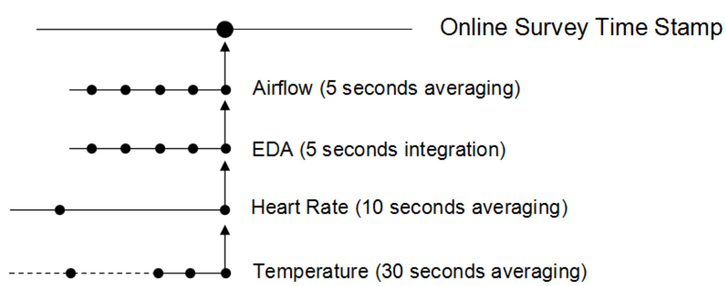


Figure 4.4. *Online Survey* based data processing scheme.

## 4.2. Sensors

### *4.2.1. Temperature Measurements and Thermocouples (TCs)*

Thermocouples are thermoelectric devices which measure temperature based on the Seeback effect (Nicholas and White, 1994). Two dissimilar metal wires are welded on one end are connected to a measurement device on the other. The temperature of the welded end creates a potential difference which can be measured with a voltage measuring device. One of the junctions is kept at a known temperature which is usually 0°C and is called the cold junction. Then, the net potential difference can be calibrated to an absolute temperature over the cold junction. In earlier measurement systems, the cold junction was literally an ice bath which provided a temperature of 0°C. However, modern data acquisition systems can apply cold junction compensation (CJC) electronically.

Omega T-type thermocouples having 28-gauge wire (OMEGA, 2010) with INOR $^{MIN}$IPAQ-HLP transducers (INOR, 2010) were used for the tests (Figure 4.5). T-type thermocouples are made of copper-constantan which can measure temperatures of human thermal environment with high accuracy. The specific thermocouple used in this test has special limits of error (SLE) with an accuracy of 1°F or 0.4% whichever is greater. T-type thermocouples with SLE have higher accuracy than regular T-type thermocouples. Zhang (2003a) used 28-gauge thermocouples for skin temperature measurements. Yao et al. (2008) used copper-constantan thermocouples for skin temperature and environmental measurements. Copper-constantan thermocouples have the highest resistance to measurement errors due to wire flexing (Nachtigal, 1990) which could occur during the tests since legs were used to exercise. INOR transducers were used to amplify and convert the thermocouple voltage, which is usually in the order of few millivolts, to a 4-20 mA level. The INOR transducers also have built-in CJC. A total of 25 thermocouples were used for the test. Fifteen thermocouples were used for skin temperature, eight were used for environmental, and two were used for globe temperature measurements. Three thermocouples were dedicated as spares in case any of the thermocouple broke during the tests. Thermocouples were attached to the skin surface with porous medical tapes (Hot et al., 1999). The subjects also wore a mesh for the thermocouples to be securely held in place. This mesh allowed airflow over the skin surface (Figure 4.6).

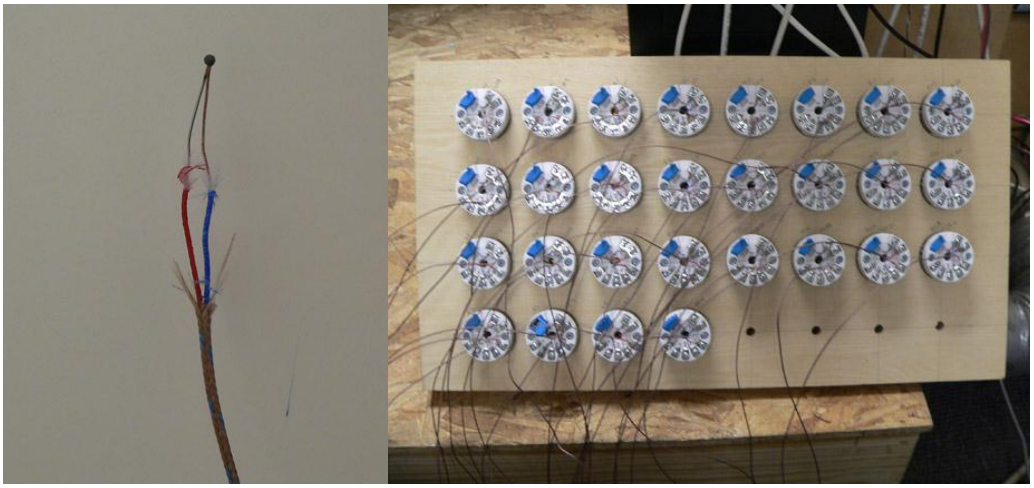

Figure 4.5. T-type thermocouple and INOR Transducers.

Figure 4.6. Medical mesh to secure thermocouples.

#### *4.2.2. Globe Temperature Sensor*

A globe thermometer is a device that is used to measure globe temperature which can be converted to mean radiant temperature for a given point inside a space. Globe temperatures combine the three important comfort parameters in one index which are air velocity, air temperature and thermal radiation (Pereira et al., 1967). A traditional globe thermometer consists of 150mm (6") diameter thin copper globe which is painted in flat black to maximize absorptivity of light in the infrared section of the spectrum (Graves, 1974; McIntyre, 1980). However, alternative methods of constructing globe thermometers exist. Humphreys (1977) suggested that a table tennis (ping-pong) ball which has a diameter of 38mm has half the response time of a 150mm ball and can be used instead. Similarly, Pereira et al. (1967) stated that table tennis balls are satisfactorily used as the globe thermometer in environmental studies. Pereira et al. also explained the procedures for building the globe thermometers from table tennis ball which was adapted to build the thermometers of this study. The conventional globe thermometers were built with mercury thermometers as the temperature measuring device. Graves (1974) however found that thermocouples are twice as responsive as the mercury thermometers.

In order to build the globe thermometer, a small hole was drilled on a table tennis ball. A 2mm plastic pipe was placed with one end close to the center of the globe. A calibrated thermocouple placed through the plastic pipe with the welded junction in the center of the tennis ball (Figure 4.7). This plastic casing was needed for structural stability since thermocouple cannot be attached to the globe directly. Gaps around the thermocouple and the plastic casing were sealed with silicon. The globe was then painted with flat black paint with an emissivity ($\varepsilon$) of about 0.95.

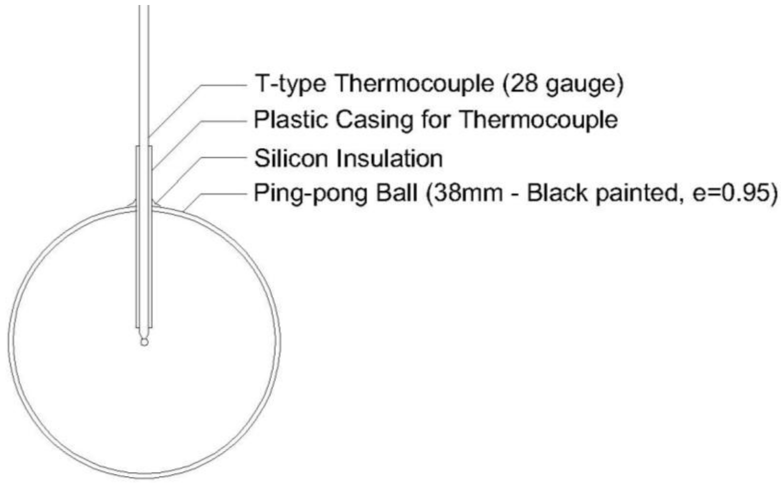


Figure 4.7. Schematics of the globe thermometer.

The determination of mean radiant temperature from globe temperature measurements requires simultaneous measurements of the air temperature, air velocity, and the globe temperature (McIntyre, 1980). The same principle was applied in our test setup by measuring the air temperature and the air velocity next to the globe thermometer (Figure 4.8). The thermocouple that measured air temperature was shielded from the airstream with the globe thermometer not to affect the temperature measurements by the increased airflow speed. The globe temperature was converted to mean radiant temperature using the following equations (ISO7726, 1998):

For natural convection:

$$\overline{t_r} = \left[ (t_g + 273)^4 + \frac{0.25*10^8}{\varepsilon_g} \left( \frac{|t_g - t_a|}{D} \right)^{1/4} * (t_g - t_a) \right]^{1/4} - 273 \qquad (4.1)$$

For forced convection:

$$\overline{t_r} = \left[ (t_g + 273)^4 + \frac{1.1*10^8 * {v_a}^{0.6}}{\varepsilon_g * D^{0.4}} (t_g - t_a) \right]^{1/4} - 273 \qquad (4.2)$$

where,

$t_r$ = mean radiant temperature, °C,

$t_g$ = globe temperature, °C,

$v_a$ = air velocity at the globe level, m/s,

$\varepsilon_g$ = emissivity of the globe,

$D$ = globe diameter, m,

$t_a$ = ambient temperature, °C.

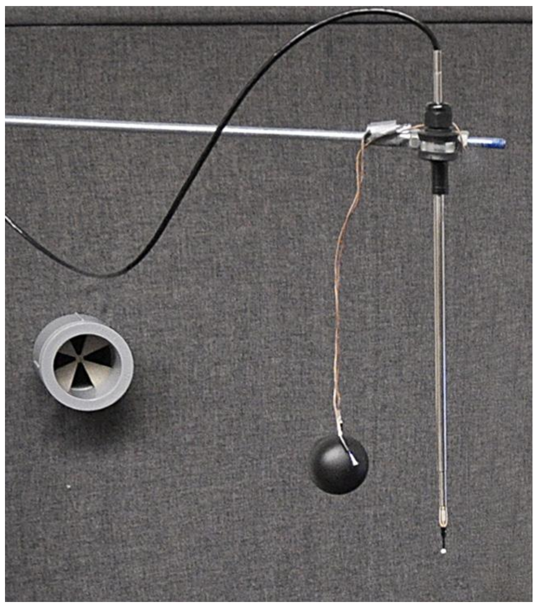

Figure 4.8. Air nozzle, globe thermometer, thermocouple for air temperature and the air velocity probe shown together in the test setup.

#### *4.2.3. Dew Point Temperature Measurement and Chilled Mirror Sensor*

The relative humidity was calculated from the dew point temperature. The dew point temperature was measured using General Eastern Dew-10 (Figure 4.9) wall-mounted chilled mirror sensor (GESensing, 2010), which was placed in the center of the room volume on the cubicle wall. Dew-10 has both a dew point sensor and a temperature sensor with accuracies of 1°F. The temperature sensor of Dew-10 was used as the reference for the room ambient temperature.

Chilled mirror sensors determine dew point temperature by cooling a mirror which is used to reflect a light beam. When dew occurs on the mirror, the light is not reflected and the temperature of the mirror is recorded as the dew point temperature. The dew point temperature was then converted to relative humidity using Excel 2003 spreadsheet functions.


Figure 4.9. Dew-10 chilled mirror sensor.

#### *4.2.4. Airflow Measurement*

A TSI 8475 omni-directional air velocity transducer was used for air velocity measurements (TSI, 2010). This specific instrument has a response time of 5 seconds and an accuracy of 3%. The transducer was configured to measure 0-400 ft/m of air velocity with 4-20 mA signal. The airflow transducer was used to measure the airflow velocity at the head level during the tests.

***4.2.5. Physiological Measurements: Electrodermal Activity (EDA), Heart Rate, Tympanic Temperature, Weight Loss***

The electrodermal activity was measured at the thenar and hypothenar eminences of the palm (Cacioppo et al., 2007) using Coulbourn Lablinc V Isolated Skin Conductance Coupler (Coulbourn, 2010) (Figure 4.10). In this measurement, *phasic* responses, which are the momentary fluctuations of the skin conductance level was recorded (Andreassi, 2000) rather than the *tonic* level to avoid a potential interference of physiological sweat with the psychological sweat. To determine the level of EDA, we used the *magnitude* measure which is the most commonly used method as suggested by Cacioppo et al. (2007). In this method a mean value was derived across all the stimulus presentations in which the stimulus frequency and the amplitude were combined in one variable. This was useful for our purposes since we were estimating the EDA activity for a given period of time.


Figure 4.10. Coulbourn Lablinc V Isolated Skin Conductance Coupler and Bioamplifier.

The tympanic temperature was measured with an infrared thermometer to estimate the core temperature (Heusch et al., 2006, Kistemaker et al., 2006). The temperature of the eardrum reflects the arterial blood flow temperature which is also the temperature utilized for thermoregulation (ISO 9886, 2004). Tympanic temperature was measured four times (e.g. before the test, after the first session, after the second session, after the test ended) during the test to determine the change in core body temperature. A Braun Thermoscan ear thermometer (Model IRT4520) was used for the measurements (Kaz, 2010). Each measurement was repeated three times to avoid measurement errors and the median of the three was accepted as the correct reading. The best effort was shown to measure the temperature of the eardrum, not the temperature of the auditory meatus as suggested by ISO 9886 (2004). The test conditions were within the range of 18°C to 30°C room air temperature with air velocity less than 0.2 m/s as required by ISO 9886-2004 for accurate readings.

The subject's weight was measured before and after the test using a digital scale with the precision of ±0.1 lbs (45 gr.). This scale satisfies the minimum precision requirement of ISO 9886 (2004). There was no intake of food or liquids during the test. Therefore, weight difference is solely due to the activity during the test.

Heart rate was recorded using a Polar (2010) heart rate monitor with T31 Wireless Coded Transmitters every 5 seconds. The heart rate transducer was interfaced to the MagneTrainer small bicycle ergometer which was used to increase the metabolic heart rate during the test (MagneTrainer, 2010) (Figure 4.11). Therefore, heart rate and the speed of the bicycle were recorded within the same binary file. This data set was matched to the DAQ data in the Excel spreadsheet by matching the time stamps.

Figure 4.11. MagneTrainer bicycle ergometer.

### *4.2.6. Backpack Design*

Subjects wore a backpack which was designed to house the thermocouples that were attached to the skin surface (Figure 4.12). All the skin thermocouples entered the backpack from the bottom and were distributed to the different parts of the body through the openings around the backpack. This backpack design allowed a non-intrusive way of accommodating the thermocouples.

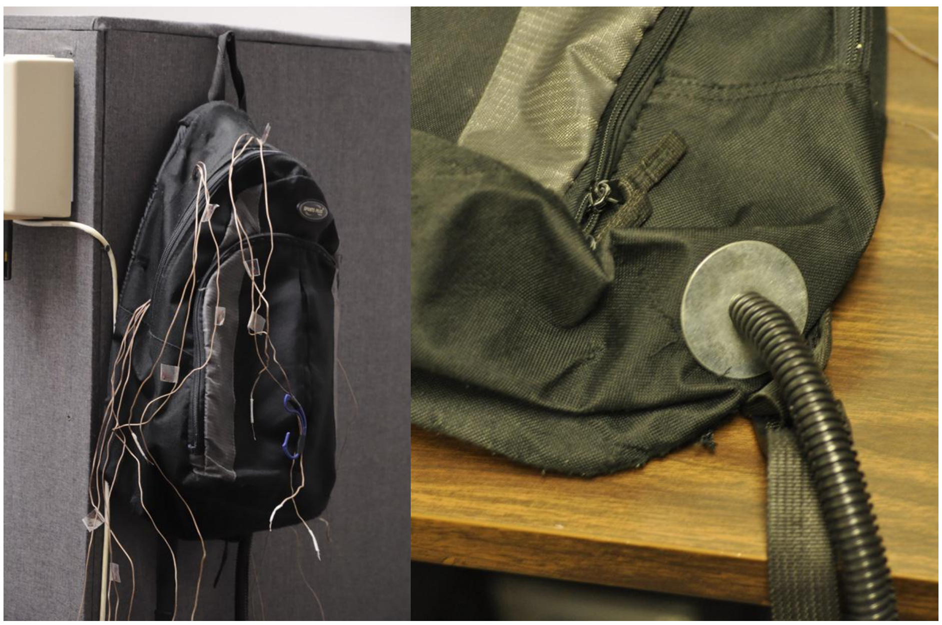

Figure 4.12. The modified backpack to accommodate the skin thermocouples.

## 4.3. Test Room Design

Human subject tests were conducted in a 12ft*11ft*10ft (3.7m*3.4m*3.05m) (W*D*H) environmentally controlled test room which is located at the Center for Housing and Urban Design (CHUD) of the Texas A&M University. A literature survey was conducted for test room design. A classification can be made based on the resemblance of the room design to the real life environments. The first group consists of test room designs with a clear sense of a laboratory environment (Gagge et al., 1967; Jones et al., 1986; Toftum and Nielsen, 1996; Conceicao et al., 2006). Activities carried out during the tests, such as walking up and down the steps, resting on a bed, or using arms to increase metabolic rate, are not necessarily related to a specific type of environment or activity. In this approach, no additional variables from the room design are introduced and subjects accept the fact that they are in a laboratory environment. The downside of this approach is the reduced applicability of the results to the real world. The second group consists of room designs with resemblance to real world environments (Kacmarczyk et al., 2004; Atthajariyakul and Leephakpreeda, 2004; Zhang, 2003a; Zhang et al., 2008a). The advantages are reduced feeling of a laboratory environment and more natural activities during the test, such as carrying out an office task, and increased applicability of the results to the real world.

The test room that was used for this study was furnished as a regular office environment to alleviate the feeling of being in a laboratory (Figures 4.13 and 4.14). To further support this concept, a regular office room in CHUD was converted into an environmentally controlled room. The test subjects used a 5 ft (1.53m) wide cubicle as a workstation. The cubicle was designed for this study and built from wooden structure and plywood. It consisted of a base and two sidewalls. Sidewalls of the cubicle were 6 inches (150 mm) wide hollow boxes which had air nozzles at the head, hands and feet level on both sides (Figure 4.15). The nozzles were designed to fully open or close with a 90° turn to control the airflow. The side walls were supplied with air through the ductworks which were placed inside the raised floor (250 mm / 10 inches) of the cubicle. The construction photos of the cubicle are presented in Appendix A. Subjects elevated their activity level by exercising on a bicycle ergo-meter which was placed under the desk. This configuration eliminated the need to leave the workstation to exercise, thus eliminated the potential disturbance of the subject.

The air temperature next to the subject was measured at the foot, hand and the head level. Black globe temperature was measured at the head and hand levels and was converted to mean radiant temperature. Room surface temperatures were measured using the thermocouples.

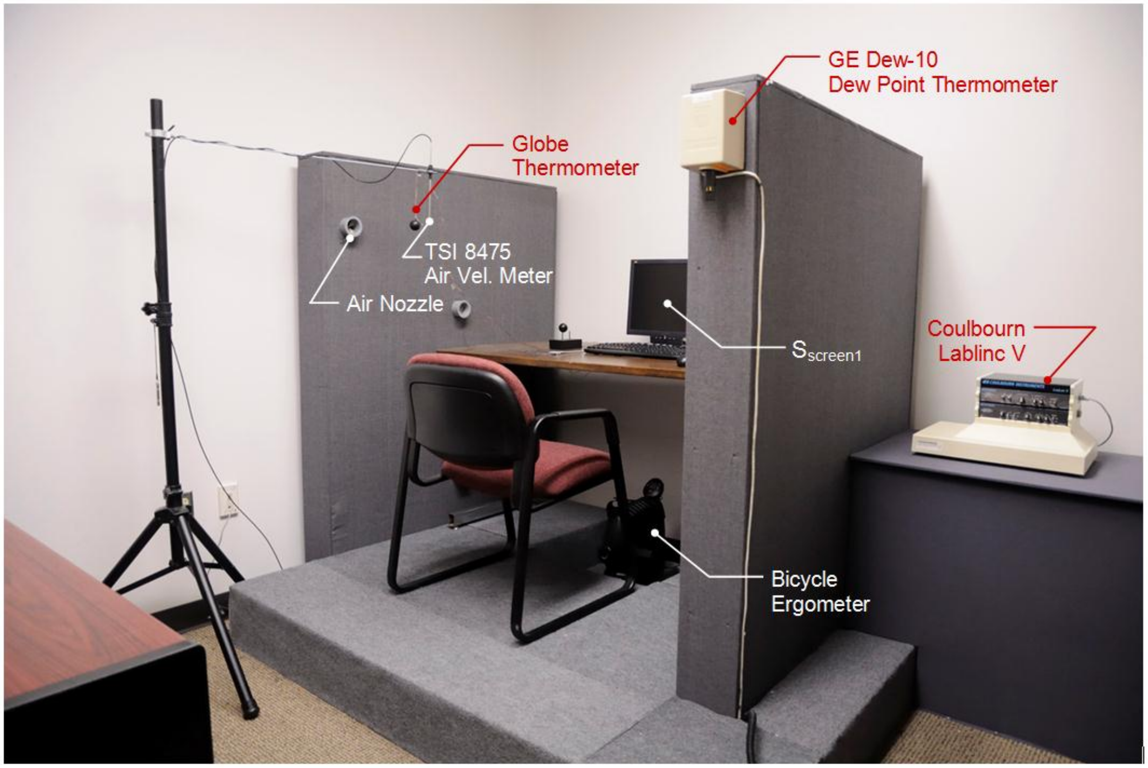


Figure 4.13. Test subject’s workstation with the bicycle ergometer.

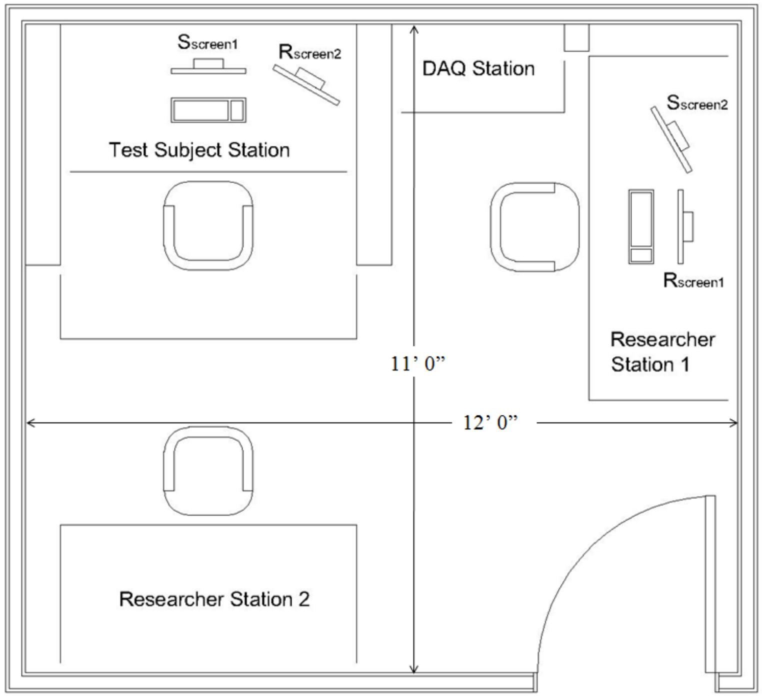


Figure 4.14. Plan of the test room.

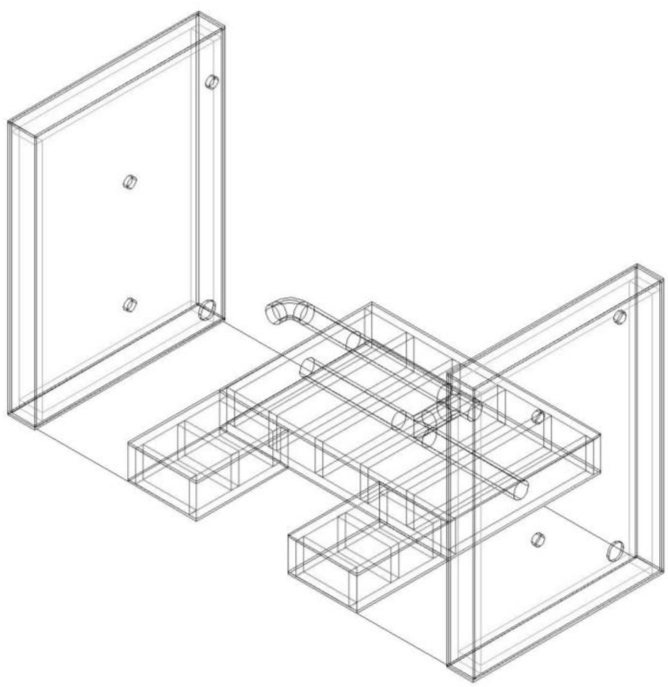

Figure 4.15. Three-dimensional drawing of the cubicle design.

The test room layout has a researcher side and a subject side (Figure 4.16). There is no direct visual connection between the researchers and the subject. Figure 4.17 shows the subject at the workstation. Both the subject side and the researcher side had one computer ($PC_{Sub}$ and $PC_{Res}$) with one main and one secondary screen. Secondary screens were cross-connected and were used for communication purposes between the subject and the researcher. Subjects filled out the online surveys and read the magazines or played the games on their main screen ($S_{screen1}$). The researcher could monitor the subject's computer activity through $S_{screen2}$ which is located on researcher's side but connected to the subject's computer ($PC_{Sub}$). The researcher monitored the DAQ data collection on his main screen ($R_{screen1}$). The researcher remotely turned on/off the secondary screen ($R_{screen2}$) of the subject to signal the subject to start/stop exercising. The subject was able to follow his/her instantaneous heart rate on $R_{screen2}$ during the exercise session.

All the data except the *Online Survey* responses were collected on $PC_{Res}$. Online Survey responses were collected on $PC_{Sub}$ and copied to the $PC_{Res}$ after the test ended. Two types of data were combined based on their time stamps. The clocks of the two PCs were synchronized before each test to avoid lags between the time stamps of the data.

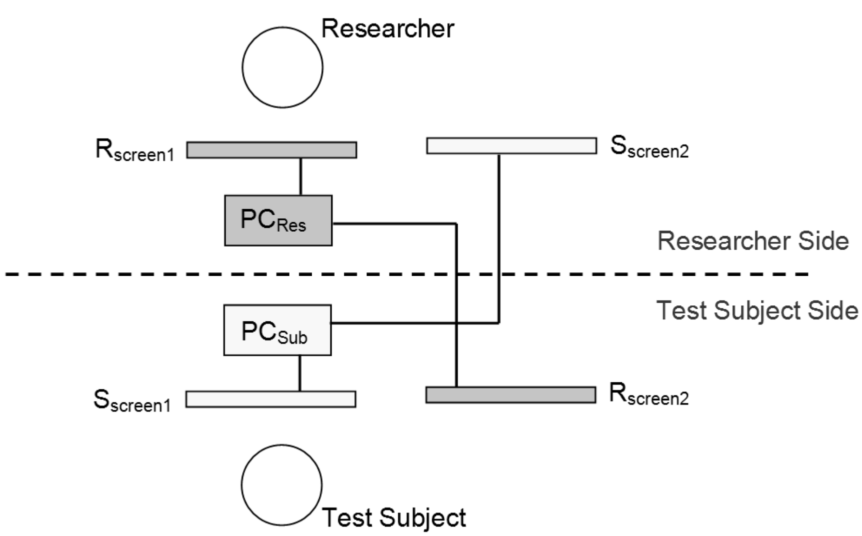


Figure 4.16. The connection diagram of PCs and PC screens of the researcher and the test subject on both sides of a hypothetical line.

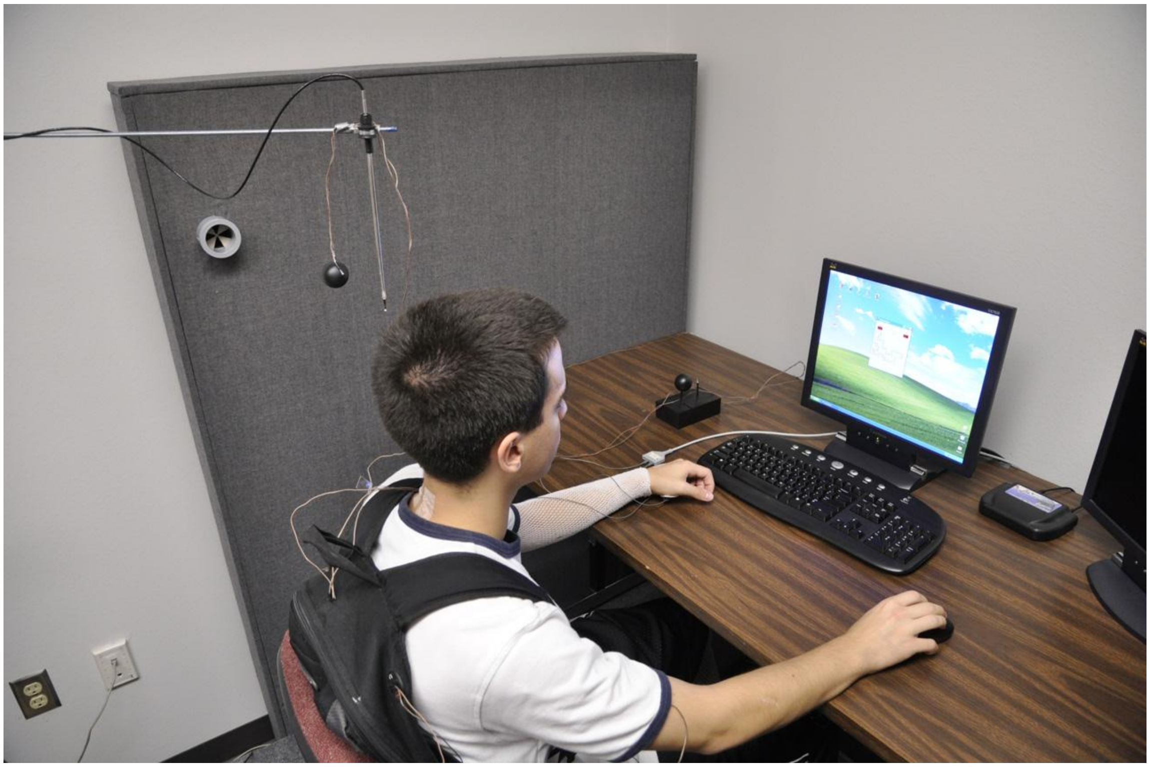

Figure 4.17. Subject's workstation with sensor backpack.

## 4.4. Sensor Calibration

Calibration is the set of procedures which establish the relationship between the values gathered from the measuring equipment and the corresponding known values of a measurand. Traceability is the procedure of relating the property of measurements to the appropriate standards (Nicholas and White, 1994). This section presents the calibration procedures and the data for thermocouples, globe thermometers, thermal comfort airflow speeds, heart rate sensors and the weight scale.

### *4.4.1. Thermometer and Thermocouple (TC) Calibration*

Thermocouples (TCs) were fabricated and calibrated at the laboratory before the tests started. The calibration procedure had three steps. Step 1 was to check the quality of the fabricated TCs by comparing the output results of all TCs with each other. Step 2 was the processing of the data to determine the offset errors. Random errors were filtered by oversampling and averaging. Calibration was done using auxiliary temperature devices which were also calibrated at our laboratory following the procedures from Nicholas and White (1994). Step 3 required a correction to eliminate the systematic error for the temperature regions of interest. Uncertainty in a measurement can be characterized by the standard deviation of the repeated measurements for the same temperature. This is also called the *standard uncertainty* (Nicholas and White, 1994).

*4.4.1.1. Auxiliary Mercury Thermometer Calibration*

Auxiliary measurement is an integral part of the systematic error analysis. Calibration of a thermometer was conducted by exposing it to a known fixed-point temperature environments such as melting or boiling point of some substances. Doebelin (2004) stated that calibration of a sensor is done by placing the auxiliary measuring device and the uncalibrated sensor, in intimate thermal contact, into a temperature controlled bath. A correction factor can be established by varying the temperature of the bath over a desired range while recording the measurements. A similar methodology was applied in the calibration of our mercury thermometers. Three certified thermometers from Brooklyn Inc. were used as the auxiliary measurement devices (Serial Numbers 79369, 67264, 79433).

The calibration of the thermometers was checked using the two fixed point calibration method. An ice-bath and the boiling point of distilled water were used to ensure that thermometers were usable as auxiliary measuring device (Figures 4.18 and 4.19). The ice-bath stabilized for 2.5 hours and the boiling water for 30 minutes. Measurements were taken every 15 minutes during the process. The final thermometer readings are presented in Table 4.1. The time constant of the thermometers were also determined during the cool-down period from the boiling point. All thermometers measured identical values for a wide range of temperature conditions (Figure 4.20).

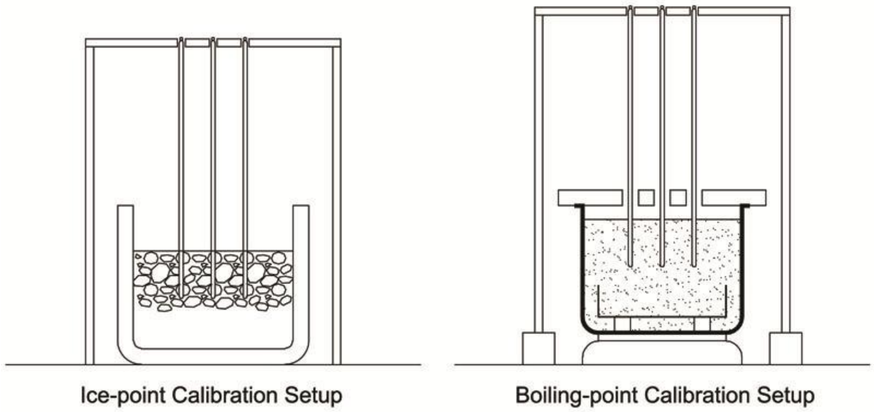


Figure 4.18. Schematics of the ice bath and the boiling point calibration setups.

Figure 4.19. Images from the actual ice bath and the boiling point calibration setups.

Table 4.1. Ice bath and boiling point measurements after stabilization of the water.

| | **Thermometers** | | |
|---|---|---|---|
| | **79369** | **67264** | **79433** |
| Ice Bath Test (after 2.5 hours) | 32.10 | 32.10 | 32.00 |
| Boiling Point Test (After 30 minutes): | 211.8 | 211.7 | 211.9 |

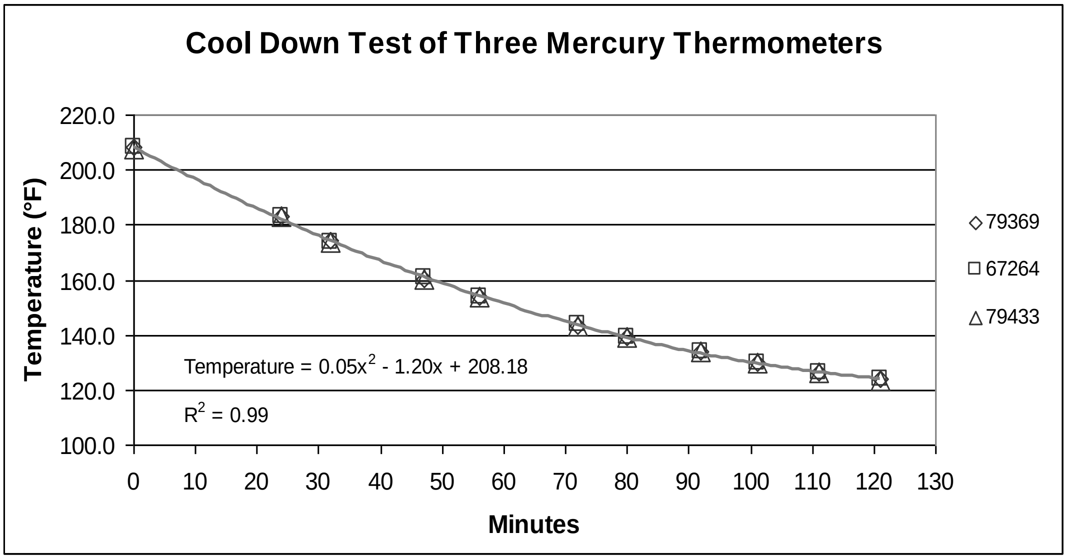


Figure 4.20. Thermometer measurements during cool-down period.

*4.4.1.2. Thermocouple (TC) Calibration for Random Errors (Noise) and Systematic Errors (Offsets)*

The next step in the calibration process was determining the systematic errors of the TCs by comparing them to the auxiliary temperature devices which were calibrated in the previous step. The true temperature, to which the TCs were compared, was determined by averaging the two thermometer measurements that were closest to each other. A running temperature calibration of TCs was conducted for temperatures ranging from 40°F to 105°F. Ensuring that thermometers and TCs were exposed to same temperature during the calibration process was the most critical problem. A refrigerator was modified and used as the temperature chamber (Figure 4.21). A 40W lamp supplied the heat to increase the temperature inside the chamber. It was shielded with aluminum foil not to radiate heat directly onto the thermometers. A personal computer CPU fan mixed the air and created a homogenous temperature environment. A webcam and a LED light source were used to record the thermometer reading without having to open the refrigerator door during the calibration. Webcam snapshots of the thermometers provided readings of the thermometers. The values were then manually entered in a spreadsheet. All TCs were placed on a copper-block between the mica and the plastic washers (Figure 4.22). Silicone thermal paste was applied between the copper block and the mica washers to ensure good thermal contact between the TCs and the copper block. The thermometers were also thermally coupled with the thermal block using the thermal paste.

During the calibration, the temperature of the chamber was first raised to 105°F by keeping the 40W light on. Once the temperature reached to the 105°F, the light was turned off and the chamber cooled down to the room temperature in 4.5 hours. The cool-down process was slower than the time constant of the mercury thermometers. In the second phase, chamber was cooled down to 40°F and was let to warm up to the room temperature. The warm-up process took 3 hours. A total of 54 thermometer readings (snapshots) were taken for the complete range of temperatures.

Figure 4.21. Modified refrigerator that was used as calibration chamber.

Figure 4.22. TC copper calibration block.

TC temperatures were recorded every 0.5 seconds during the calibration. Different levels of filtering were applied to the data to eliminate the random errors. Running averages of 10 seconds, 30 seconds and 60 seconds were calculated. Figure 4.23 shows that 10-second filter reduced the majority of the random errors and 30-sec filter eliminated the large fluctuations in the 10-second data. The 30-second filtering was decided to be an accurate representation of the data without the random errors.

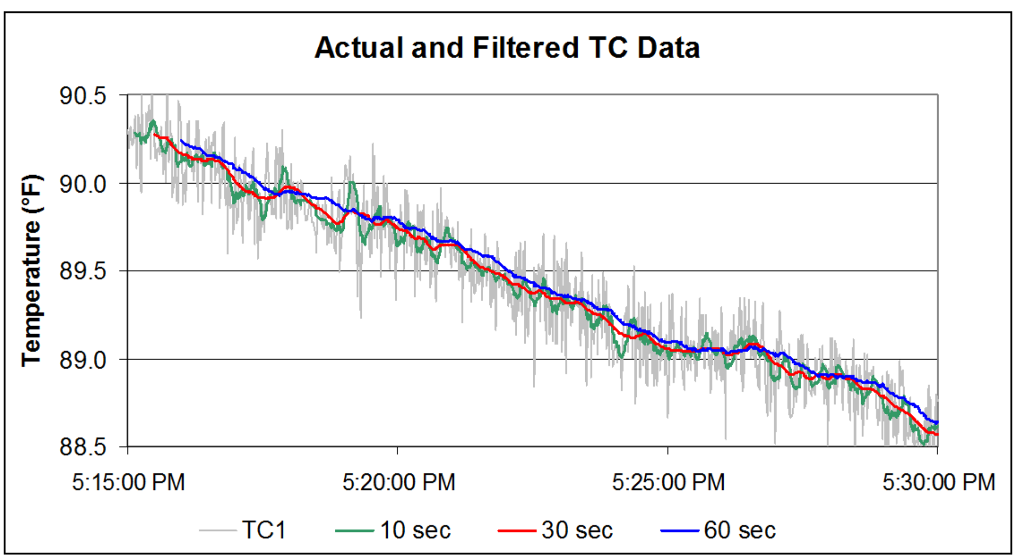


Figure 4.23. Raw data and different levels of filtering for reducing the random errors (noise).

An inspection of data showed that each TC has an offset from the true temperature, which is an indicator of systematic error (Figure 4.24). A regression equation between each TC and the thermometer data was determined. Each TC had a high correlation ($R^2 > 0.99$) with the thermometer data. The mean error and the standard deviation for the mean error between the thermometers and the TCs were calculated. An average offset for each TC was determined and are presented in Table 4.2. The offsets were then used to correct the readings of each thermocouple.

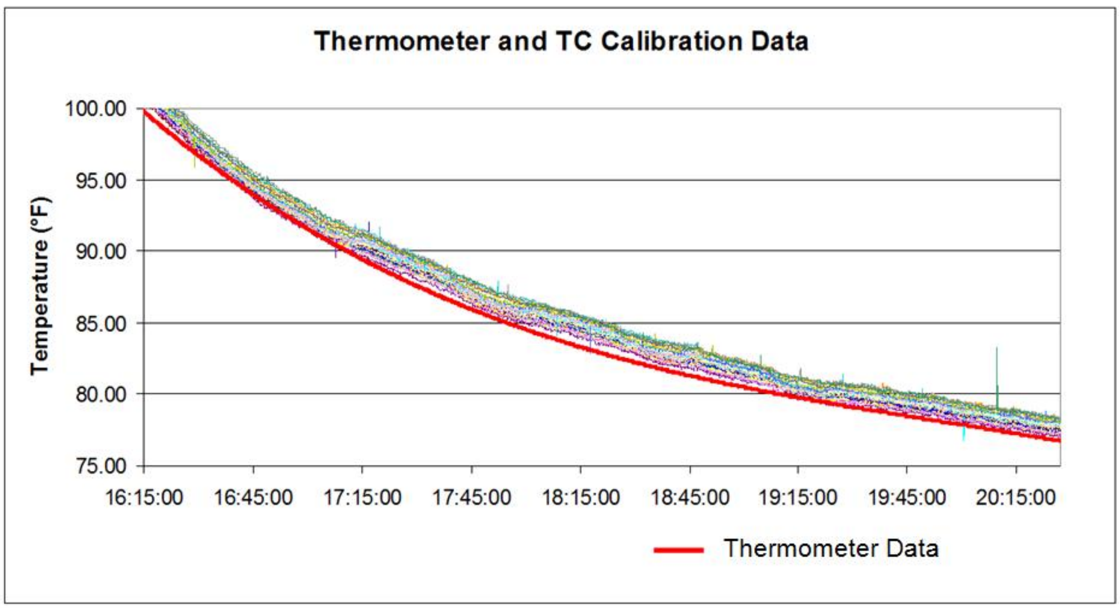


Figure 4.24. TC measurements compared to the thermometer data.

Table 4.2. Average systematic errors (offsets) between the thermocouples and the thermometer data in Fahrenheit.

| **Thermocouple** | **Offset (°F)** | **Thermocouple** | **Offset (°F)** |
|---|---|---|---|
| TC 01 - Thermometer | 0.667 | TC 15 - Thermometer | 0.799 |
| TC 02 - Thermometer | 0.882 | TC 16 - Thermometer | 0.833 |
| TC 03 - Thermometer | 0.421 | TC 17 - Thermometer | 1.215 |
| TC 04 - Thermometer | 1.014 | TC 18 - Thermometer | 1.471 |
| TC 05 - Thermometer | 0.505 | TC 19 - Thermometer | 1.548 |
| TC 06 - Thermometer | 1.105 | TC 20 - Thermometer | 1.657 |
| TC 07 - Thermometer | 1.110 | TC 21 - Thermometer | 1.332 |
| TC 08 - Thermometer | 0.927 | TC 22 - Thermometer | 1.494 |
| TC 09 - Thermometer | 0.338 | TC 23 - Thermometer | 1.480 |
| TC 10 - Thermometer | 1.168 | TC 24 - Thermometer | 1.592 |
| TC 11 - Thermometer | 0.753 | TC 25 - Thermometer | 1.620 |
| TC 12 - Thermometer | 1.197 | TC 26 - Thermometer | 1.433 |
| TC 13 - Thermometer | 0.860 | TC 27 - Thermometer | 0.507 |
| TC 14 - Thermometer | 0.480 | TC 28 - Thermometer | 1.053 |

### *4.4.2. Globe Thermometer Calibration*

Globe temperature sensor is composed of a T-type thermocouple placed inside a ping-pong ball (38mm) which was painted flat black (Krylon Flat Black Paint, ε=0.95) on the outside. The calibration setup is composed of a sealed wooden box (11/16" thick) with the interior dimensions of 20"x20"x20". The interior surfaces of the wooden box were also painted black paint with the same paint as the ping-pong ball (Figure 4.25). Interior surface temperatures of the calibration box were measured with the thermocouples. The surface temperatures were used to calculate a true mean radiant temperature for the center of the box where the globe thermometer was placed. Another thermocouple and the airflow sensor were placed next to the globe thermometer to measure air temperature and the airflow speed for forced convection conditions. A computer fan was placed inside the box to ensure homogenous distribution of air inside the box. A 1000W hot plate was placed under the box to increase the surface temperature. A homogenous distribution of temperature on the bottom surface was ensured by covering the perimeter of the gap between the box and the hot plate and using a fan to distribute the air in that gap.

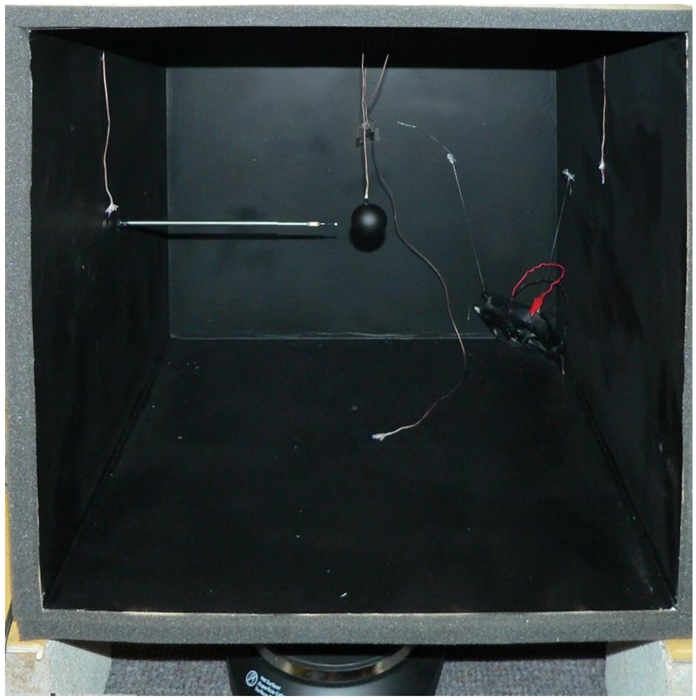

Figure 4.25. Globe thermometer calibration setup.

The calibration procedure was based on the comparing the measured mean radiant temperature (MRT) to the calculated MRT from the globe temperature measurement (Figure 4.26). Measured mean radiant temperature was determined by averaging the six surface temperatures of the calibration box (Equation 4.3). Calculated MRT is determined by converting the measured globe temperature to MRT by using Equations 4.4 and 4.5 (ISO 7726, 1998). Two offsets for forced convection ($v > 0.2$ m/s) and natural convection ($v < 0.2$ m/s) were determined for each globe temperature sensor (TC26, TC27 and TC28). In the actual thermal comfort test data, one of the two offsets was used depending on the air velocity on the globe thermometer.

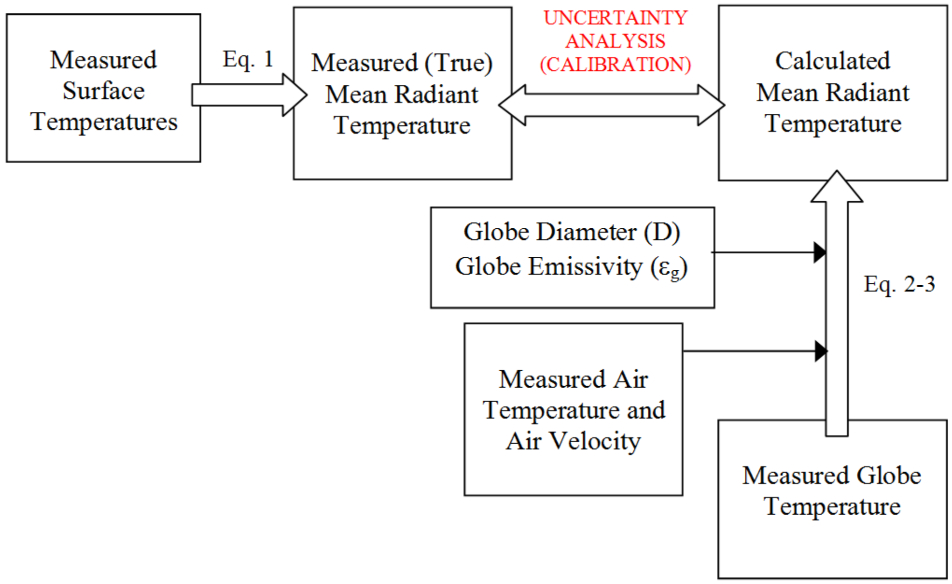


Figure 4.26. Procedure diagram of the globe thermometer calibration.

MRT from the surface temperatures:

$$MRT = \frac{\sum_{n=1}^{6} T_n}{n} \tag{4.3}$$

where,

*MRT* = Mean Radiant Temperature, °C,

$T_n$ = Surface Temperature of the n$^{th}$ surface, °C.

MRT from Globe Temperature under natural convection:

$$\bar{t}_r = \left[ \left(t_g + 273\right)^4 + \frac{0.25 * 10^8}{\varepsilon_g} \left( \frac{\left|t_g - t_a\right|}{D} \right)^{1/4} * \left(t_g - t_a\right) \right]^{1/4} - 273 \tag{4.4}$$

MRT from Globe Temperature under forced convection

$$\bar{t}_r = \left[ \left(t_g + 273\right)^4 + \frac{1.1 * 10^8 * v_a^{0.6}}{\varepsilon_g * D^{0.4}} \left(t_g - t_a\right) \right]^{1/4} - 273 \tag{4.5}$$

where,

$t_r$ = mean radiant temperature, °C,

$t_g$ = globe temperature, °C,

$v_a$ = air velocity at the globe level, m/s,

$\varepsilon_g$ = emissivity of the globe,

$D$ = globe diameter, m,

$t_a$ = ambient temperature, °C.

*4.4.2.1. Calibration Conditions*

The calibration of the globe thermometers were conducted for four different scenarios:

Case 1: All surface temperatures are approximately equal and *Calculated MRT = Tg*

Case 2: One surface temperature increased and Equation 4.4 applies with *Calculated MRT*

Case 3: All surface temperatures are approximately equal and air velocity increased, Equation 4.5 applies with *Calculated MRT*

Case 4: One surface temperature and air velocity increased, Equation 4.5 applies with *Calculated MRT*

*4.4.2.2. Globe Thermometer Calibration Data*

Four calibration conditions were applied to each globe thermometer and the differences between the measured and calculated MRTs were presented in Table 4.3. These differences were used as offsets in the thermal comfort test data depending on the airflow conditions.

Table 4.3. Offsets between the measured and the calculated MRTs in Fahrenheit.

| | **Air Velocity Condition**<br>**High: V ≥ 0.2 m/s**<br>**Low: V < 0.2 m/s** | **$MRT_{measured} - MRT_{calculated}$ (°F)** | **Standard Deviation (°F)** | **Number of Cases** |
|---|---|---|---|---|
| TC 26 | High | -2.434 | 0.187 | 252 |
| | Low | -3.101 | 0.409 | 372 |
| TC 27 | High | 0.508 | 0.175 | 252 |
| | Low | 1.045 | 0.231 | 491 |
| TC 28 | High | -2.054 | 0.188 | 252 |
| | Low | -2.360 | 0.468 | 492 |

***4.4.3. Thermal Comfort Station Airflow Calibration***

*4.4.3.1 Software Calibration for Target Airflow Speeds*

The custom designed data acquisition (DAQ) software was used to control the start and stop sequences of the fan as well as the speed of the airflow. A calibration of the thermal comfort unit was conducted based on the airflow settings of the DAQ software. The target airflow speed on at the subject's neck was 160 ft/min (0.8 m/s). At the target airflow speed, the comfort unit provided 22.96 cfm of air onto the subjects' body.

A 12" 12V direct current (DC) radiator fan was used to supply air to the comfort unit. DAQ software controlled the fan speed within range of the full scale of the power supply voltage. A power supply of 7.5V and maximum 4.5Amps was used to run the fan. DAQ software setting of 1 to 10 corresponded with 0V to 7.5V of power for the fan speed. Actual measurements showed that fan voltage changes linearly for different software settings except around 7V region (Figure 4.27). The power consumption of the fan was plotted against the software settings for various nozzle conditions. Figure 4.28 shows that the energy consumption of the fan doesn't change for different nozzle opening conditions.

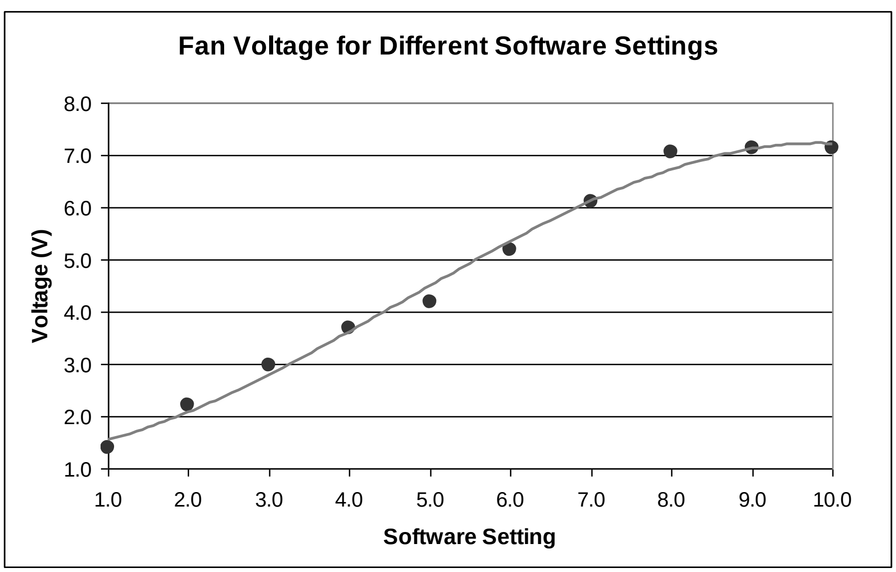


Figure 4.27. Fan voltage for different software settings.

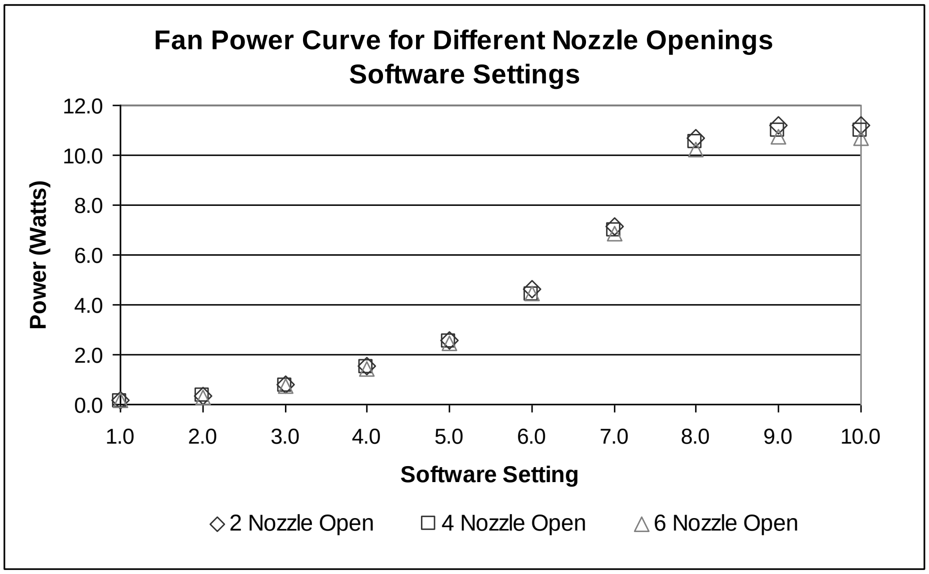


Figure 4.28. Power consumption of the fan for various nozzle opening conditions

Comfort unit airflow calibration was conducted for two nozzle conditions. In the first condition, only the head nozzles were open providing airflow to the head of the subject slightly from behind to avoid eye dryness due to the direct airflow into the eye. A sitting manikin was used as the human figure (Figure 4.29). Figures 4.30 and 4.31 show the first set of measurements with only the head nozzles open. Measurements were taken at the nozzle exit to determine the nozzle leaving airflow speed. The airflow meter was set to measure up to 400 ft/m. Therefore, the measurements were maxed out at the 80% of the full speed of the fan (Figure 4.30). Figure 4.31 shows the airflow speeds behind the subject's neck. During the actual thermal comfort tests, software setting that provided 160 ft/min airflow at the subject's neck was used.

Second set of measurements were taken when all six nozzles were open delivering air to the head, hands, and feet simultaneously. Airflow in simultaneous cooling was lower than the head-only condition. Figures 4.32 and 4.33 show the airflow speeds at the nozzle exit and behind the manikin's neck.

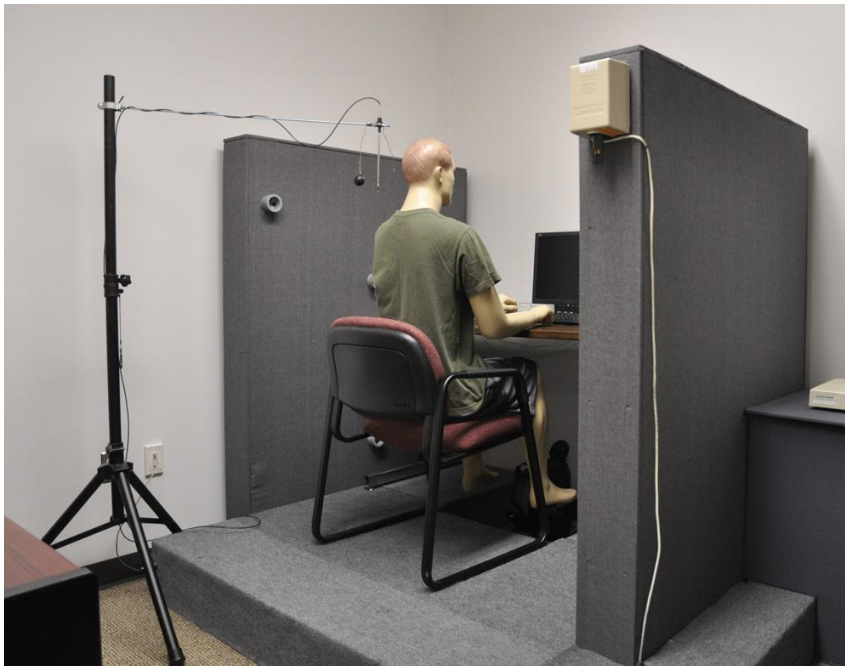

Figure 4.29. The manikin that was used as the human figure during airflow measurements.

Measurement Specifications:

Only head nozzles are open. Airflow was measured on the head nozzle axis 1” away from the nozzle.

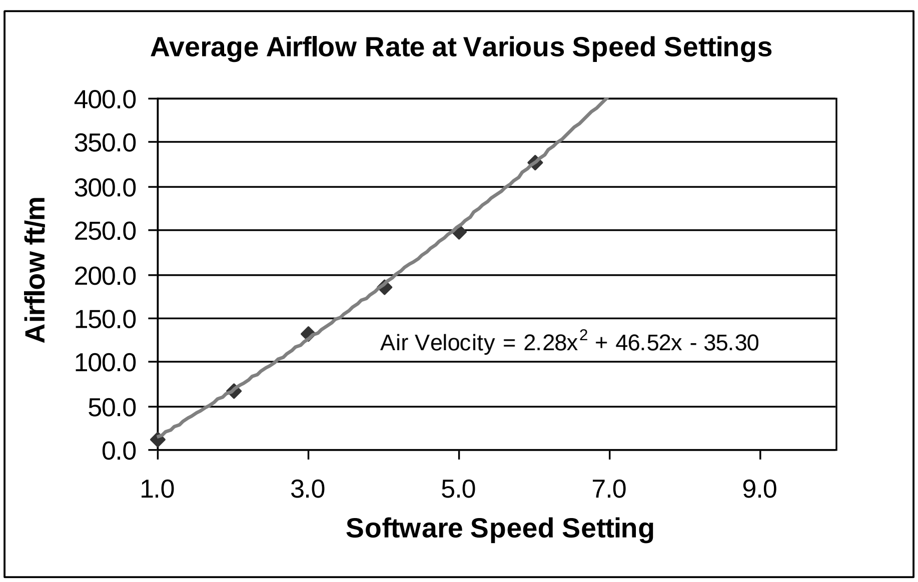


Figure 4.30. Airflow speeds at the nozzle exit.

Measurement Specifications:

Only head nozzles are open. Airflow was measured at 50" from the floor, in the middle of the head axis 1" off towards the front and 1" behind the manikin's neck.

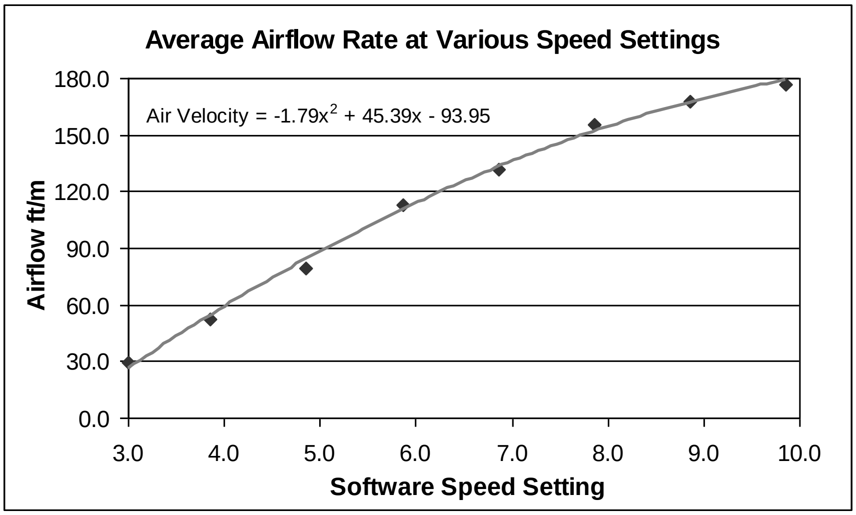


Figure 4.31. Airflow speeds behind the manikin's neck at different software settings.

Measurement Specifications:

All nozzles are open. Airflow was measured on the head nozzle axis 1" away from the nozzle.

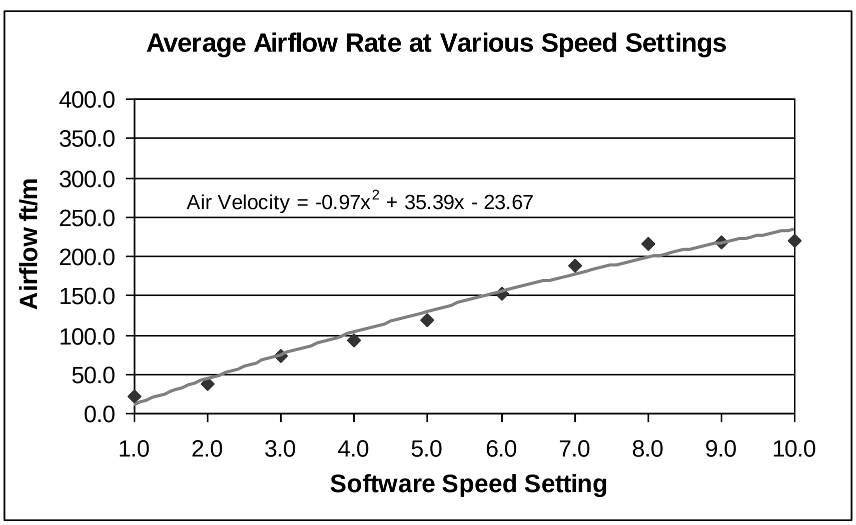


Figure 4.32. Airflow speed at the head-nozzle exit when all the nozzles are open.

Measurement Specifications:

All nozzles are open. Airflow was measured at 50” from the floor, in the middle of the head axis 1” off towards the front and 1” behind the manikin’s neck.

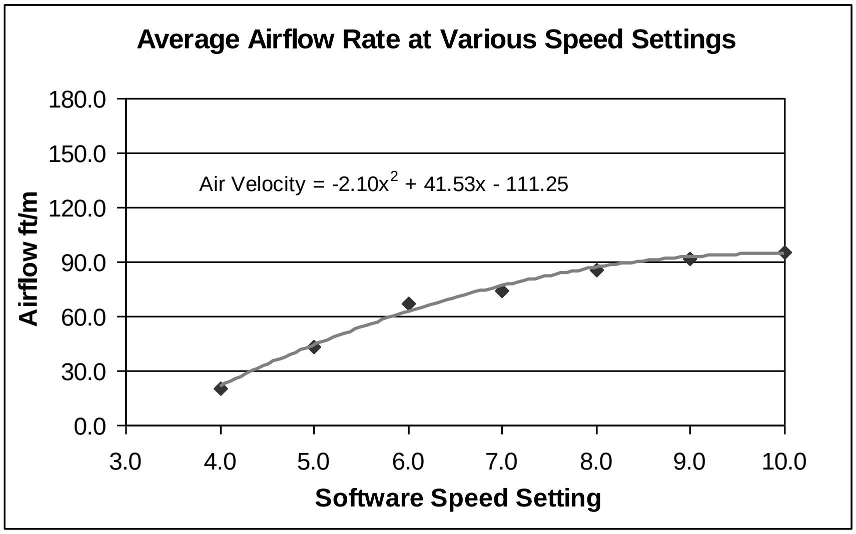


Figure 4.33. Airflow speed behind manikin’s neck when all nozzles are open.

*4.4.3.2. Thermal Comfort Station Airflow Measurements*

Airflow measurements around the human body were conducted for two nozzle conditions: head-only, and head/hands/feet simultaneously. A manikin was also used as the human figure during the measurements. Figures 4.34 and 4.35 show the measurement locations in elevation and in plan of the comfort unit. Points X1 through X24 are on the head nozzle axis with the numbers denoting the distance from the nozzle in inches. Points Z1 through Z24 are on the hand nozzle axis. XY12B through XY30B are on the head nozzle level with a 30 degrees angle to the nozzle axis towards the back of the comfort station. Numbers denote the distance on the head nozzle axis. XY12F through XY30F are the same as the previous ones with an angle towards the front. XW201 through XW207 are the vertical points which are located on the head nozzle axis 18" from the nozzle. YX1 is located 1" next to the neck and XZ1 is placed 1" next to the face both on the head nozzle height.

Analysis in 4.4.3.1 showed that 0.8 m/s airflow at the neck is achieved with 80% speed of the fan, which provided 22.96 cfm. The measurements in this section used the same fan speed which represented maximum airflow that would occur during the test. Same fan speed was used for both head-only and simultaneous airflow to ensure a constant amount of airflow delivered to the subject regardless of the nozzle conditions. Airflow measurement for each location was taken for 2 minutes with 100 millisecond sampling and 1 second recording frequency. A two minute idle time was given before the actual measurements for the airflow to stabilize at the specific measurement location. The 2-minute data was then averaged to determine the airflow values that are presented in Table 4.4.

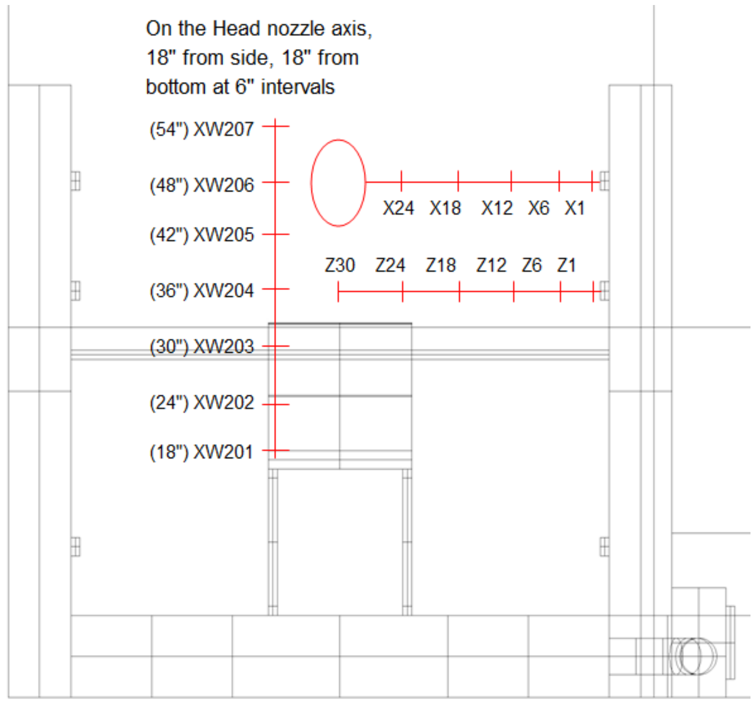


Figure 4.34. Elevation of the thermal comfort unit showing the airflow measurement locations.

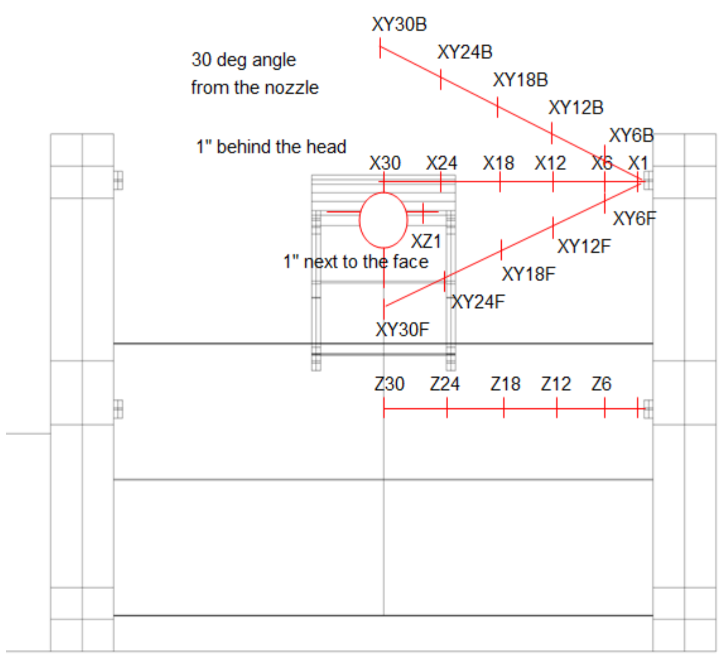


Figure 4.35. Plan of the thermal comfort unit showing the airflow measurement locations.

Table 4.4. Average airflow speeds at various locations around the human body.

| **Head-only Airflow** | | **Whole-body Airflow** | |
|---|---|---|---|
| **Measurement Site** | **Average Airflow Speed (ft/m)** | **Measurement Site** | **Average Airflow Speed (ft/m)** |
| X1 | > 400.0 | X1 | 220.0 |
| X6 | > 400.0 | X6 | 213.6 |
| X12 | 323.5 | X12 | 128.1 |
| X18 | 155.9 | X18 | 80.8 |
| X24 | 100.3 | X24 | 54.6 |
| YX1 (X30) | 152.2 | YX1 (X30) | 71.3 |
| XZ1 | 66.5 | XZ1 | 56.9 |
| XY6F | 37.4 | XY6F | 35.2 |
| XY12F | 76.0 | XY12F | 64.2 |
| XY18F | 58.6 | XY18F | 74.2 |
| XY24F | 50.9 | XY24F | 61.9 |
| XY30F | 50.7 | XY30F | 60.2 |
| XY6B | 46.3 | XY6B | 41.4 |
| XY12B | 51.4 | XY12B | 39.4 |
| XY18B | 41.5 | XY18B | 32.8 |
| XY24B | 26.4 | XY24B | 27.4 |
| XY30B | 28.8 | XY30B | 33.7 |
| XW201 | N/A | XW201 | N/A |
| XW202 | N/A | XW202 | N/A |
| XW203 | 58.5 | XW203 | 41.1 |
| XW204 | 56.9 | XW204 | 54.1 |
| XW205 | 68.4 | XW205 | 53.9 |
| XW206 | 99.5 | XW206 | 73.6 |
| XW207 | 96.2 | XW207 | 85.2 |
| | | Z1 | 300.0 |
| | | Z6 | 133.0 |
| | | Z12 | 142.7 |
| | | Z18 | 90.5 |
| | | Z24 | 58.7 |
| | | Z30 | 73.5 |

### *4.4.4. Heart Rate Sensor Calibration*

Heart rate data from Polar T31 wireless transmitters and the MagneTrainer proprietary software was calibrated using an oscilloscope. Calibration was conducted by comparing the data from the Polar to the oscilloscope data and by determining the offset. Oscilloscope time was set to read 0.5 seconds per division on its screen.

A volunteer subject exercised at a steady pace at different metabolic rates. When the heart rate was stable for 5-10 seconds, the reading on the oscilloscope was frozen using the "save" button. The distance between each R wave of the heart rate signal was recorded in terms of # of divisions. As an example, when distance between two R waves was 1.6 divisions, this means at that moment heart pulsed once every 0.8 seconds. This means that the corresponding heart rate was 60/0.8 or 75. The distances between the R waves are tabulated next to the Polar transmitter reading in Table 4.5.

The heart rate data from the Polar system closely matched to the real heart rate measurements from the oscilloscope at different metabolic rates. The differences were within 2 beats per minute which is negligible for the purposes of this study. Therefore, heart rate data from the Polar system was used as is.

Table 4.5. Heart Rate (HR) data as calculated from the oscilloscope readings and from the Polar system.

| | **Oscilloscope Readings and Corresponding HR** | | | | | | | | **Average HR from Oscilloscope** | **HR from Polar** |
|---|---|---|---|---|---|---|---|---|---|---|
| # of Divisions | 1.55 | 1.55 | 1.60 | 1.60 | 1.58 | | | | 76 | 75 |
| Corresponding HR | 77 | 77 | 75 | 75 | 76 | | | | | |
| # of Divisions | 1.45 | 1.45 | 1.40 | 1.45 | 1.35 | 1.45 | | | 85 | 83 |
| Corresponding HR | 83 | 83 | 86 | 83 | 89 | 83 | | | | |
| # of Divisions | 1.00 | 1.05 | 1.05 | 1.03 | 1.03 | 1.03 | | | 116 | 117 |
| Corresponding HR | 120 | 114 | 114 | 116 | 116 | 116 | | | | |
| # of Divisions | 0.92 | 0.88 | 0.90 | 0.90 | 0.90 | 0.90 | 0.90 | 0.90 | 133 | 132 |
| Corresponding HR | 128 | 135 | 133 | 133 | 133 | 133 | 133 | 133 | | |

#### *4.4.5. Weight Scale Calibration*

A digital scale with a precision of ±0.1 lbs (45 gr) was used to measure weight loss of the subjects due to the test. The load cells that are used in digital scales are prone to drift which may affect the readings. An hourly drift and a daily measurement drift tests were conducted to ensure the reliability of the weight measurements. A concrete block weighing 87.0 lbs were used as the load in these tests.

In the hourly drift test, the scale was loaded with the block and the weight was measured. The block was left on the scale. At the end of one hour, the scale was turned on and the measurement was read without moving the block. The scale was then unloaded and loaded immediately and the measurement was read the third time. The readings were stable at 87.0 lbs (Table 4.6).

In the daily drift test, the weight of the block was measured every 15 or 30 minutes by loading the scale each time. The test was repeated twice one from morning through afternoon, and from noon through the evening. The weight measurements were stable in both cases (Table 4.7).

Table 4.6. Hourly drift test of the digital scale.

| | **Time** | **Weight (lbs)** |
|---|---|---|
| Beginning of the Test | 5:30 PM | 87.0 |
| End of the Test | 6:30 PM | 87.0 |
| End of the Test (re-loading) | 6:30 PM | 87.0 |

Table 4.7. Daily drift test of the digital scale.

| Time | Weight (lbs) |
|---|---|
| 12:30 PM | 87.0 |
| 1:00 PM | 87.0 |
| 1:30 PM | 87.0 |
| 2:00 PM | 87.0 |
| 2:30 PM | 87.1 |
| 3:00 PM | 87.0 |
| 3:30 PM | 87.0 |
| 4:00 PM | 87.1 |
| 4:30 PM | 87.0 |
| 5:00 PM | 87.0 |
| 5:30 PM | 87.0 |
| 6:00 PM | 87.0 |
| 6:30 PM | 87.0 |

| Time | Weight (lbs) |
|---|---|
| 9:45 AM | 87.0 |
| 10:00 AM | 87.0 |
| 10:15 AM | 87.0 |
| 10:30 AM | 87.0 |
| 10:45 AM | 87.0 |
| 11:00 AM | 87.0 |
| 3:45 PM | 87.0 |
| 4:00 PM | 87.0 |
| 4:15 PM | 87.0 |
| 4:30 PM | 87.0 |
| 4:45 PM | 87.0 |

# 5. GENDER DIFFERENCES OF THERMAL ENVIRONMENT PERCEPTION

Differences of thermal comfort perception between males and females are evident in previous laboratory tests in which environmental and personal factors are controlled (Griefahn and Kunemund, 2001a; Fanger, 1972; Parsons, 2002, McNall et al., 1968; Tanabe et al., 2007; Beshir and Ramsey, 1981). On the other hand, field studies show less significant differences between the genders due to the variations in the environmental factors (Toftum, 2002, Erlandson et al., 2003). Toftum (2002) addressed this problem of field studies as the respondents' difficulty in balancing their thermal preferences with other factors. In effect, the complexity of the field study environment makes the relationship between thermal sensation and draught less evident. In this study, gender differences of thermal responses were investigated in realistic controlled environment for individual and two-way effects of environmental and personal factors.

The objective of this section is to characterize differences in thermal sensation and thermal comfort as well as temperature and airflow preferences between males and females in transient airflow and metabolic rate conditions at two constant room temperatures. This section covers the environmental and personal conditions that were presented in the literature and extends the conditions to the high metabolic rates with very warm room temperatures with the added complexity of dynamic airflow.

## 5.1. Thermal Comfort

### *5.1.1 Gender Differences of Thermal Comfort*

Thermal comfort votes showed significant differences ($p<0.001$) between the males and the females. Note that the p-value needs to be less than 0.05 to be accepted as significant. On average, males felt more comfortable than females. This result was consisted with Karjalainen's study (2007). On the 7-point scale, mean thermal comfort vote for males was 1.12, whereas for females it was 0.57 (Table 5.1). The difference between the genders is more pronounced for high metabolic rate conditions during which male mean comfort vote was 0.82 as opposed to the female mean comfort vote of 0.16. The average thermal comfort votes for both males and females were on the comfortable half of the scale (Mean Votes > +0). Figure 5.1 shows that metabolic rate has the same effect on both genders. Therefore, gender and metabolic activity level has no interaction effect on thermal comfort (p=0.768).

Table 5.1. Mean thermal comfort votes under three metabolic activity conditions

| Gender | Metabolic Activity Level | Mean Thermal Comfort | Thermal Comfort Std. Dev. |
|---|---|---|---|
| Male | High (4 met) | 0.82 | 1.27 |
| | Low (1.2 met) | 1.36 | 0.99 |
| | Medium (2.6 met) | 0.99 | 1.23 |
| | Total | 1.12 | 1.16 |
| Female | High | 0.16 | 1.15 |
| | Low | 0.89 | 0.83 |
| | Medium | 0.40 | 1.03 |
| | Total | 0.57 | 1.02 |
| Total | High | 0.41 | 1.24 |
| | Low | 1.07 | 0.92 |
| | Medium | 0.63 | 1.14 |
| | Total | 0.78 | 1.10 |

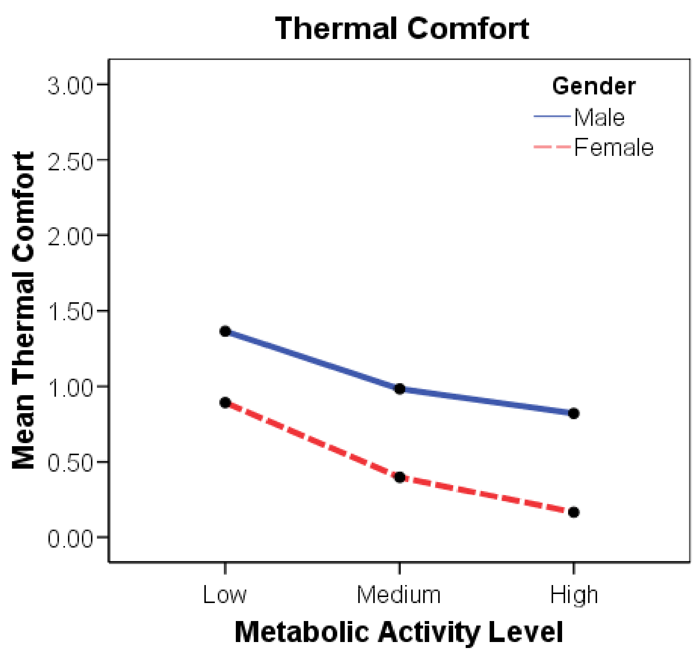


Figure 5.1. Thermal comfort responses of males and females under low (1.2 met), medium (2.6 met) and high (4 met) metabolic conditions.

### *5.1.2. Interaction Effects of Gender, Room Temperature, and Metabolic Rate on Thermal Comfort*

The second between-subjects variable is the room temperature which has a significant effect on thermal comfort of both genders ($p<0.001$). The interaction of metabolic activity level and room temperature is also significant at $\alpha=0.05$ ($p=0.022$). Under the low metabolic rate conditions, the females' thermal comfort responses were similar for 75°F and 83°F room temperatures (Table 5.2). This result is counter-intuitive to the established understanding of thermal comfort feelings. On the other hand, room temperature has a significant effect on male thermal comfort votes during the low metabolic rate conditions which are consistent with the literature.

Table 5.2. Mean thermal comfort votes under different temperature and metabolic rate conditions.

| Gender | Room Temperature | Metabolic Activity Level | Mean Thermal Comfort | Thermal Comfort Std. Dev. |
|---|---|---|---|---|
| Male | 75°F (24°C) | High (4 met) | 0.92 | 1.69 |
| | | Low (1.2 met) | 1.64 | 1.19 |
| | | Medium (2.6 met) | 1.36 | 1.55 |
| | | Total | 1.40 | 1.46 |
| | 83°F (28°C) | High | 0.75 | 0.83 |
| | | Low | 1.16 | 0.75 |
| | | Medium | 0.70 | 0.82 |
| | | Total | 0.91 | 0.82 |
| Female | 75°F (24°C) | High | 0.23 | 1.25 |
| | | Low | 0.89 | 0.84 |
| | | Medium | 0.67 | 0.78 |
| | | Total | 0.68 | 0.93 |
| | 83°F (28°C) | High | 0.10 | 1.07 |
| | | Low | 0.90 | 0.83 |
| | | Medium | 0.15 | 1.18 |
| | | Total | 0.47 | 1.08 |

The medium metabolic rate condition yielded the largest thermal comfort difference between the two room temperatures for both genders. Transient conditions of metabolic rate created a negative perception of thermal environment at 83°F room temperature (Figures 5.2 and 5.3). During the high metabolic conditions, room temperature had a minor effect on thermal comfort. There are two possible explanations to this. The first one is that the high metabolic rate creates anticipation for low comfort and this anticipation is more pronounced than the thermal effect of high temperature. The second explanation is that high metabolic activity saturates the thermal comfort feeling and increased temperature did not make difference for the saturated thermal comfort feeling.

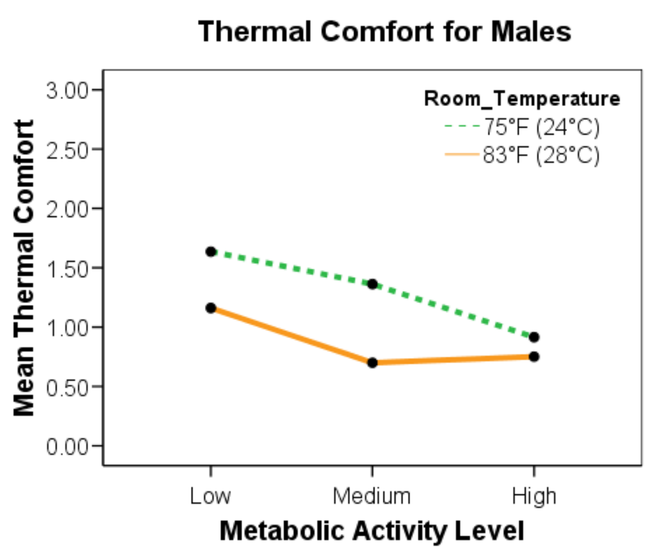


Figure 5.2. The combined effects of temperature and metabolic activity level on thermal comfort under low (1.2 met), medium (2.6 met) and high (4 met) metabolic conditions for males.

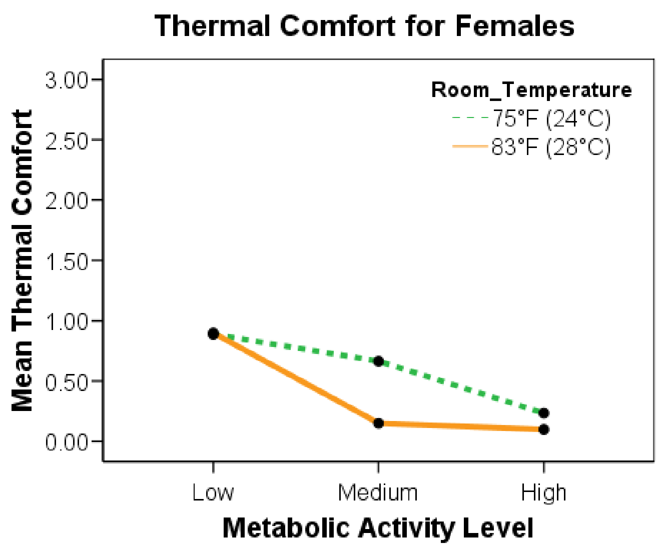


Figure 5.3. The combined effects of temperature and metabolic activity level on thermal comfort under low (1.2 met), medium (2.6 met) and high (4 met) metabolic conditions for females.

## 5.2. Thermal Sensation

### *5.2.1. Gender Differences of Thermal Sensation*

Thermal sensation votes showed significant differences between males and females ($p<0.001$). Females registered 0.72, 0.71, and 0.52 points (on 7-point scale) warmer than the males for high, medium and low metabolic rate conditions respectively (Table 5.3). Higher thermal sensation votes of females translated into lower thermal comfort votes as shown in the previous section. Figure 5.4 shows the relationship between thermal sensation and metabolic rate for males and females.

Table 5.3. Mean thermal sensation votes under different metabolic rate conditions.

| Gender | Metabolic Activity Level | Mean Thermal Sensation | Thermal Sensation Std. Dev. |
|---|---|---|---|
| Male | High (4 met) | 0.69 | 1.36 |
| | Low (1.2 met) | 0.09 | 1.26 |
| | Medium (2.6 met) | 0.52 | 1.42 |
| | Total | 0.37 | 1.36 |
| Female | High | 1.41 | 0.99 |
| | Low | 0.61 | 0.94 |
| | Medium | 1.23 | 0.97 |
| | Total | 1.00 | 1.02 |
| Total | High | 1.14 | 1.19 |
| | Low | 0.42 | 1.10 |
| | Medium | 0.96 | 1.21 |
| | Total | 0.76 | 1.20 |

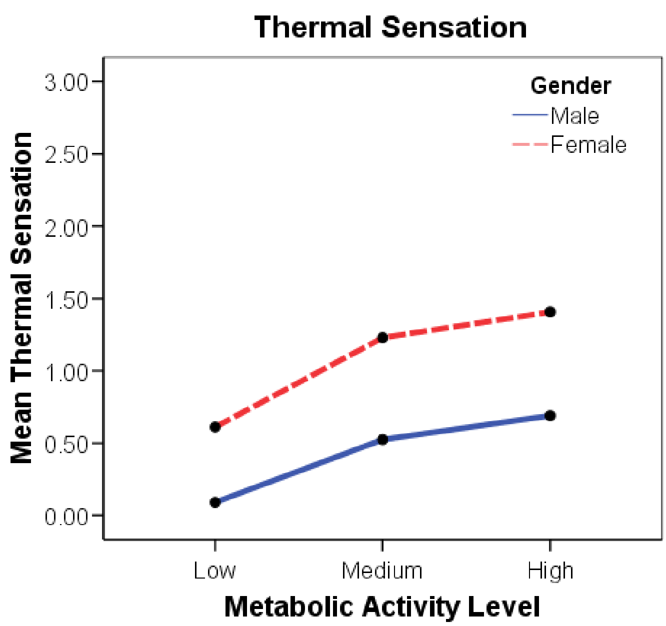


Figure 5.4. Thermal sensation responses under low (1.2 met), medium (2.6 met) and high (4 met) metabolic conditions.

### *5.2.2. Interaction Effects of Gender, Room Temperature, and Metabolic Rate on Thermal Sensation*

The analysis in this section shows that the room temperature is a confined variable and the interaction between the metabolic rate and the room temperature is significant at $\alpha=0.05$ ($p=0.014$). Thermal sensation is linearly correlated with metabolic rate under neutral (75°F) room conditions. However, thermal sensation saturated during medium metabolic conditions under warm temperatures (83°F) and yielded thermal sensation votes similar to the high metabolic conditions (Table 5.4, Figures 5.5 and 5.6). One possible explanation is that mental shift due to the stopping of the exercise increased the awareness towards the thermal conditions and resulted in unique evaluation of the thermal state of the body.

The combined averages of males and females yielded a maximum mean thermal sensation vote of 1.27 points for high metabolic rate conditions and 83°F room temperature. For the same conditions, PMV predicts the maximum thermal sensation which is 3.00. The average thermal sensation under low (sedentary) metabolic rate and neutral room temperature (75°F) was -0.2 points. For the same sedentary/neutral conditions PMV predicted -1.14 points. Therefore, thermal sensation of the subjects varied much less than PMV predictions in a dynamic environment. A dynamic component needs to be added to the PMV calculation to accurately predict transient conditions which are more likely in a given environment. Section 6 of this study presents the reasons for the difference between the real conditions and the PMV and suggests the improvements to the PMV calculation to account for the dynamic conditions.

Table 5.4. Mean thermal sensation votes under different temperature and metabolic rate conditions.

| Gender | Room Temperature | Metabolic Activity Level | Mean Thermal Sensation | Thermal Sensation Std. Dev. |
|---|---|---|---|---|
| Male | 75°F (24°C) | High (4 met) | 0.25 | 1.84 |
| | | Low (1.2 met) | -0.74 | 1.38 |
| | | Medium (2.6 met) | -0.26 | 1.71 |
| | | Total | -0.37 | 1.64 |
| | 83°F (28°C) | High | 1.02 | 0.70 |
| | | Low | 0.71 | 0.66 |
| | | Medium | 1.11 | 0.72 |
| | | Total | 0.92 | 0.71 |
| Female | 75°F (24°C) | High | 1.28 | 1.04 |
| | | Low | 0.33 | 1.04 |
| | | Medium | 0.89 | 0.87 |
| | | Total | 0.72 | 1.04 |
| | 83°F (28°C) | High | 1.52 | 0.93 |
| | | Low | 0.87 | 0.74 |
| | | Medium | 1.55 | 0.95 |
| | | Total | 1.25 | 0.92 |

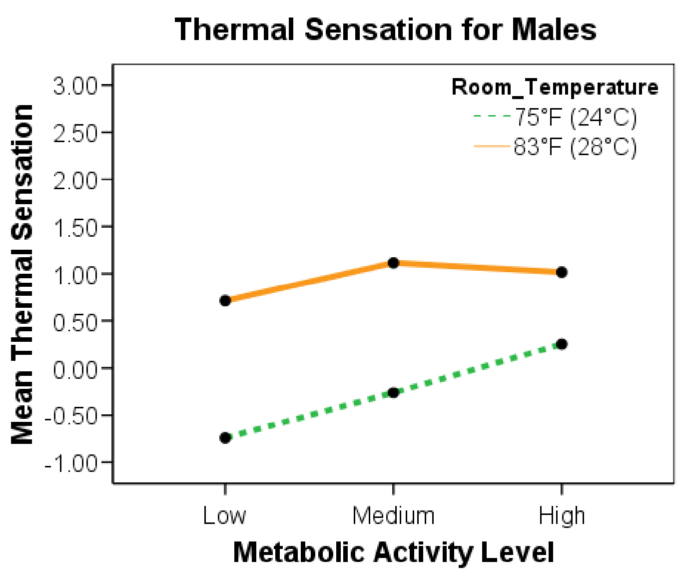


Figure 5.5. The combined effects of temperature and metabolic activity level on thermal sensation under low (1.2 met), medium (2.6 met) and high (4 met) metabolic conditions for males.

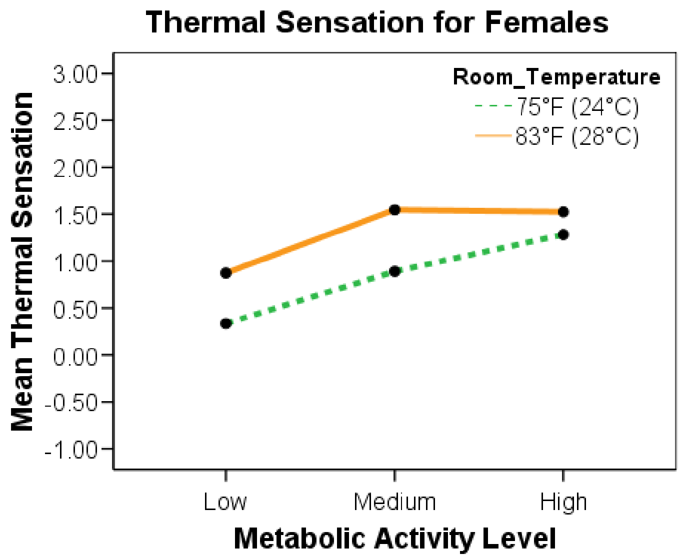


Figure 5.6. The combined effects of temperature and metabolic activity level on thermal sensation under low (1.2 met), medium (2.6 met) and high (4 met) metabolic conditions for females.

### 5.3. Neutral Temperatures for Males and Females

The neutral temperature is the temperature in which somebody feels neither cool nor warm. Therefore, it is the temperature that corresponds with the value zero on the thermal sensation scale. The thermal sensation results of this study were compared to the PMV values and two other studies from the literature (Beshir and Ramsey, 1981; Tanabe et al., 2007). For the purposes of this comparison, Tanabe et al.'s and Beshir and Ramsey's thermal sensation values were compensated for the clothing insulation difference using the PMV formula. Our average thermal sensation values showed close proximity to their PMV values and to Beshir and Ramsey's study for low metabolic and for 75°F and 83°F conditions (Figure 5.7), and to Tanabe's study for 83°F. Beshir and Ramsey's and Tanabe's studies showed lower thermal sensation for females than males. However, the current study showed higher thermal sensation for females above 76.6°F and lower thermal sensation below 76.6°F than the males. This is consisted with Parson's study (2002). Beshir and Ramsey found that neutral temperatures are 71.6°F (22.0°C) and 77.1°F (25.1°C) for males and females respectively. Our results showed neutral temperatures of 72.3°F and 74°F for males and females respectively. Possible explanations of the difference between males and females are given in the discussions section. The thermal sensation regression models of the current study for the given conditions are

For females, $$ThermalSensation = 0.065T_a - 4.82 \quad (5.1)$$

For males, $$ThermalSensation = 0.041T_a - 2.95 \quad (5.2)$$

where the mean radiant temperature is equal to ambient temperature and $T_a$ is the room temperature in Fahrenheit. These models assume that thermal sensation changes linearly with the temperature within the temperature conditions of this study.

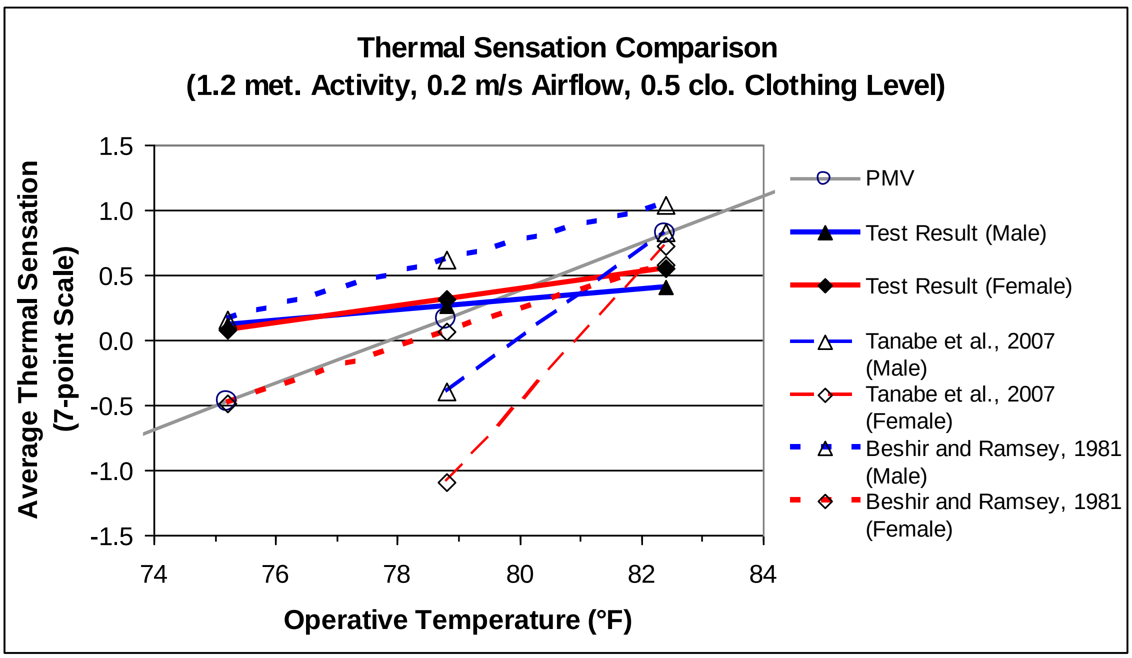


Figure 5.7. Comparison of thermal sensation models for the given conditions.

### 5.4. Temperature and Air Movement Preferences

Jones et al. (1986) found higher sensitivity to temperature in females than males under 2.3 metabolic rate conditions. The expected result, then, is a difference in temperature preference for two genders. However, our temperature preference results showed no significant differences (p=0.297) between males and females under three metabolic rate conditions although there is a marginal difference between the mean votes (Figures 5.8 and 5.9). The average temperature in these analyses was 79°F, which was higher than the neutral temperatures of both genders. There is also no interaction effects between the metabolic rate and the gender in terms of temperature preferences (p=0.684). No interaction effects between the metabolic rate and the gender exist for the airflow preference (p=0.768). However, there is a significant difference between the genders (p=0.009). Griefahn and Kunemund (2001a) found no difference of airflow perception between the genders in neutral (23°C) temperature conditions. It is hypothesized in our study that if both genders perceive air similarly, females should have a higher demand for more airflow to offset their high thermal sensation. Data showed that females preferred more airflow under all metabolic rate conditions. Both males and females wanted more airflow at all times regardless of the airflow conditions. The characteristic of transient conditions, which acts similar to high metabolic conditions, is evident for both temperature and air movement preference.

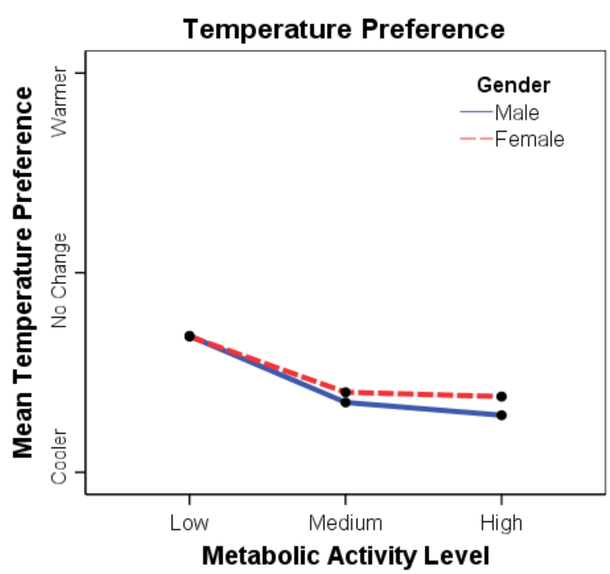


Figure 5.8. Mean temperature preference under low (1.2 met), medium (2.6 met) and high (4 met) metabolic conditions.

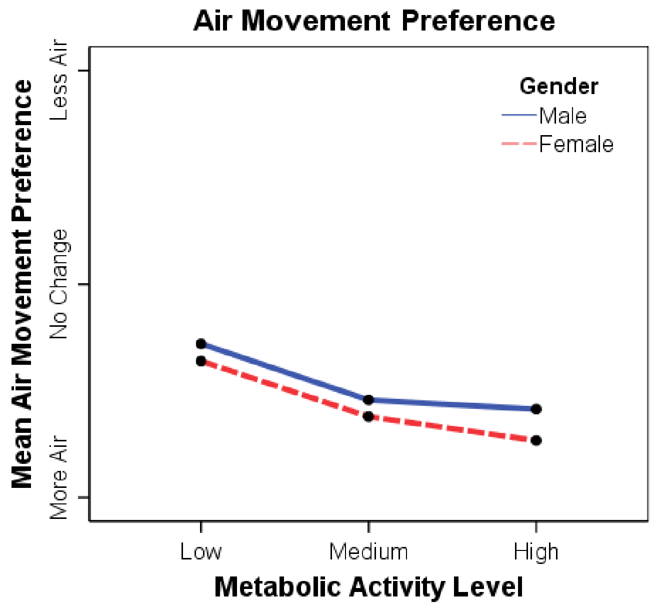


Figure 5.9. Mean air movement preference under low (1.2 met), medium (2.6 met) and high (4 met) metabolic conditions.

### 5.5. Gender Differences of Transient Thermal Comfort and Thermal Sensation

A transient analysis of thermal comfort and thermal sensation responses were conducted. Pulsing airflow with 30-seconds or 60-second periods were applied starting with the 45$^{th}$ minute in Figure 5.10. The 40$^{th}$ through 45$^{th}$ and 75$^{th}$ through 80$^{th}$ minutes were the resting times between the test sessions and were not considered as part of the actual test. Females consistently felt less comfortable than the males throughout the test. Thermal comfort increased within the first fifteen minutes which was the relaxed period with low metabolic and mental activity levels. Thermal comfort consistently dropped during the exercise due to the increased metabolic activity. The sudden increase in thermal comfort votes after the end of the exercise suggests a psychological effect due to exercise. Therefore, the drop in thermal comfort votes during the exercise may be partially thermal and partially psychological. Based on the recovery time after the exercise, the time constant for the subjective thermal comfort responses is approximately six minutes.

After each exercise period, subjects returned to the same if not higher pre-exercise thermal comfort levels although they experienced an increased thermal comfort drop at each consecutive exercise session (Table 5.5). This result suggests that there is a short-term memory effect (< 1 hour) of past experiences which effect current thermal comfort. The short-term memory effect of comfort is similar for both males and females. After the 1st exercise session, during which only constant minimum airflow (24 ft/min) was used, thermal comfort increased by 0.293 points for males and by 0.187 points for females until the next exercise session. After the 2nd, 3rd, 4th and 5th exercise sessions, during which dynamic (pulsing) airflow existed, the average increase in thermal comfort was 1.066 points for males and 1.232 for females. The mean preference for airflow was for more air movement at all times during the test.

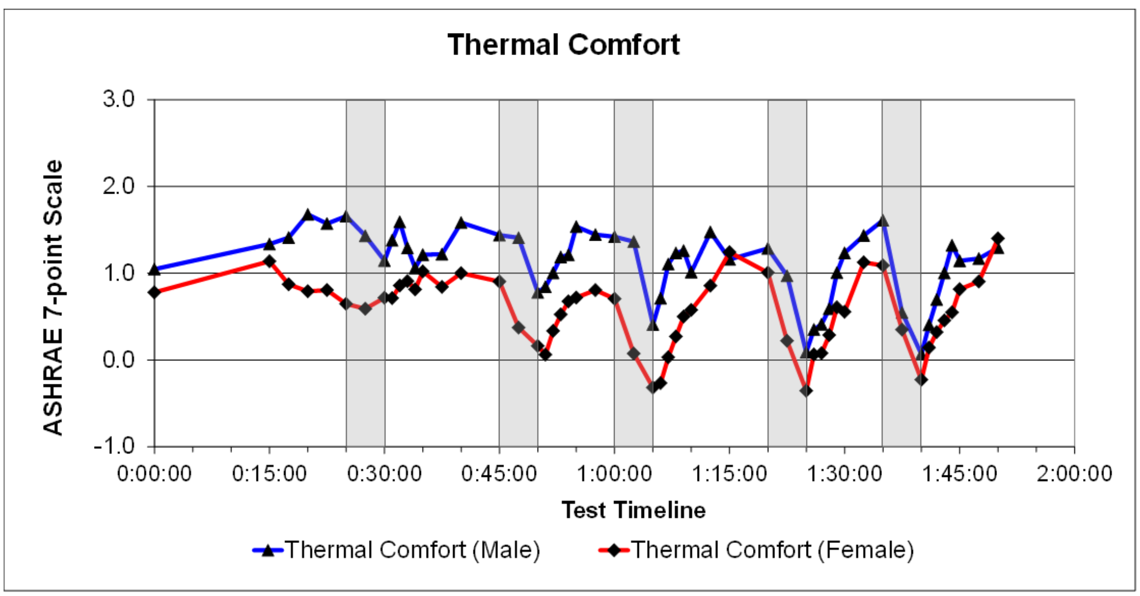


Figure 5.10. Thermal comfort votes for males and females for the duration of the test.

Table 5.5. Thermal comfort drop during the 5-minute exercise sessions (7-point scale).

| | | **1st Exercise** | **2nd Exercise** | **3rd Exercise** | **4th Exercise** | **5th Exercise** |
|---|---|---|---|---|---|---|
| Male | At the Onset | 1.659 | 1.439 | 1.421 | 1.287 | 1.610 |
| | At the Offset | 1.146 | 0.780 | 0.409 | 0.090 | 0.067 |
| | Difference | 0.513 | 0.659 | 1.012 | 1.197 | 1.543 |
| Female | At the Onset | 0.647 | 0.904 | 0.704 | 1.007 | 1.089 |
| | At the Offset | 0.717 | 0.163 | -0.318 | -0.355 | -0.228 |
| | Difference | -0.070 | 0.741 | 1.022 | 1.362 | 1.317 |

Thermal sensation responses are consistent with the thermal comfort findings. Subjects experienced an increase in thermal sensation (warmth feeling) during the consecutive exercise periods (Figure 5.11). Short-term memory effect of previous experiences also existed for thermal sensation. The increase in thermal sensation due to the exercise was more pronounced for females (Table 5.6). They experienced maximum thermal sensation earlier than males which indicates a higher sensitivity of thermal sensation. On the other hand, males experienced a gradual increase in peak thermal sensation during the exercise sessions which suggests a more linear relationship between the metabolic rate and the thermal sensation. A sharp drop was also evident for thermal sensation after each exercise session. The third survey instance after each exercise session showed an increase in thermal sensation which interrupted the sudden drop. This is typical to transient systems in which sudden changes occur. A similar discussion of transient responses of thermal sensations and thermoreceptor responses can be found in the literature (Gagge et al., 1967; Ring and De Dear, 1991; De Dear et al., 1993; Fiala et al., 2003; Zhao, 2007).

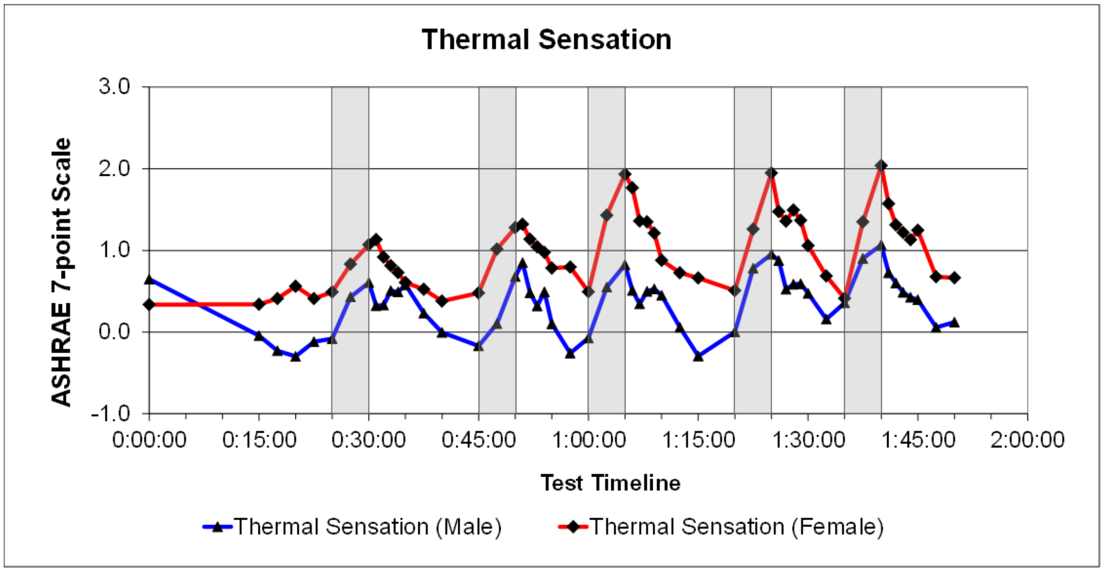


Figure 5.11. Thermal sensation votes for males and females for the duration of the test.

Table 5.6. Thermal sensation decrease during the 5-minute exercise sessions (7-point scale).

| | | 1st Exercise | 2nd Exercise | 3rd Exercise | 4th Exercise | 5th Exercise |
|---|---|---|---|---|---|---|
| Male | At the Onset | -0.080 | -0.169 | -0.071 | 0.003 | 0.360 |
| | At the Offset | 0.606 | 0.681 | 0.826 | 0.953 | 1.069 |
| | Difference | 0.686 | 0.850 | 0.897 | 0.950 | 0.709 |
| Female | At the Onset | 0.491 | 0.478 | 0.494 | 0.510 | 0.412 |
| | At the Offset | 1.070 | 1.280 | 1.933 | 1.948 | 2.038 |
| | Difference | 0.579 | 0.802 | 1.439 | 1.438 | 1.626 |

Metabolic rate, based on the heart rate, returned to pre-exercise levels within approximately 4 minutes after the exercise session ended. However, subjective responses did not return to the pre-exercise levels until the 10th minute of resting. Therefore, a residual response exists between the 3rd minute and the 10th minute. Cacioppo et al. (1987) explained this phenomenon with a residual arousal theory. Residual response findings of the current study are consistent with Cacioppo et al. This is explained in more detail in Section 8.3.

### 5.6. Discussion

Subjective thermal responses of males and females were investigated under low (1.2 met), medium (2.6 met), and high (4 met) metabolic rate conditions, and under 75°F and 83°F room temperatures. Thermal comfort and thermal sensation of males and females differ significantly under all metabolic conditions such that females consistently felt less comfortable and felt warmer than the males. Room temperature was a confined variable and different temperature conditions affected the relationship of thermal sensation and thermal comfort to metabolic rate. The thermal conditions of this test ranged from neutral room temperatures and sedentary conditions to high room temperatures and high metabolic conditions. According to ISO 7730 (2005) and ASHRAE Standard 55 (2004), subjects should feel uncomfortably warm. However, our results show that average subjective responses are on the slightly warm and on the comfortable side of the scale.

The relationship between metabolic rate and the subjective responses were linear for 75°F room temperature. On the other hand, medium activity level generated subject responses similar to or higher than high metabolic conditions for 83°F temperature. This cannot be explained with the heat balance of the body but may be explained with psychological factors. Subjects' expectations of the thermal environment were shifted during the transient conditions. However, thermal conditions did not meet subjects' expectations of improving thermal conditions which created a negative feeling towards the thermal environment for short periods of time. The negative feeling disappears once the thermal conditions were steady, and subjects' expectations were consistent with the thermal environment.

Analysis of transient conditions showed that the memory of earlier thermal experiences affected thermal comfort and thermal sensation of the subjects. The time constant for the subjective responses was approximately six minutes. Subject responses showed that their comfort and sensation returned to their baseline conditions within nine minutes after the end of the exercise. In this study, room air was re-directed onto the subject's body. A time component was added to the airflow by varying it in 30-second or 60-second periods. During the existence of the dynamic airflow, higher thermal sensations (warm feelings) were compensated. This finding suggested that people feel comfortable under conditions which is considered outside the comfort zone by the standards as long as the environment is dynamic and people's thermoregulation systems are actively working with the environment to provide comfort. Zhou et al. (2006) stressed the same idea by stating that varying thermal environments can change people's expectations and perception of the thermal environment.

Subjects found the thermal environment acceptable 83.1% and unacceptable 14.8% of the time (Figure 5.12) using an "acceptable" or "unacceptable" choice. A15% dissatisfaction with the thermal environment is acceptable even for neutral and sedentary conditions. Although our test conditions were more extreme than the neutral and sedentary conditions, a similar dissatisfaction percentage was achieved. This may be due to the presence of airflow in the second and the third sessions of the test.

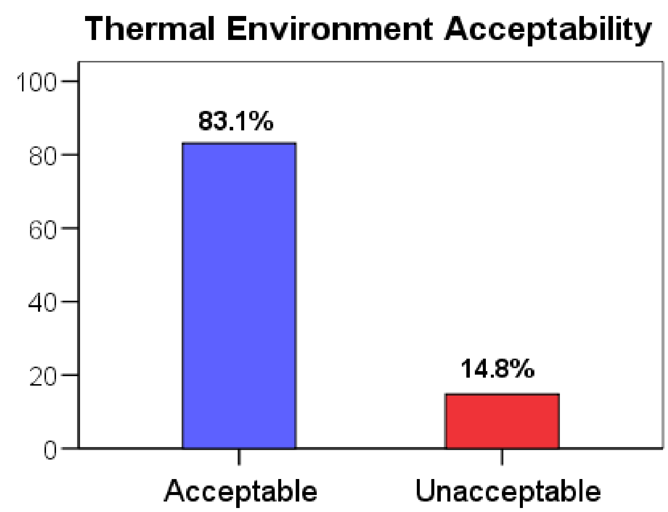


Figure 5.12. Average thermal environment acceptability for the whole test.

Cunningham et al. (1978) reported that during the heat exposure, female test subject's tympanic temperature and skin temperature rose more than the males because women store more heat. McIntyre (1980) suggested that during the heat exposure, conduction through the fat layer is relatively unimportant because heat is transported to the skin surface by the blood. Our study showed that women's skin temperature fluctuated more than men's during transient metabolic conditions which indicates a more sensitive thermoregulation for women under neutral and warm conditions. In addition, females showed an initial skin temperature rise of 1.1°F compared to males which was 0.8°F. These results supported the arguments of both Cunningham et al. (1978) and McIntyre (1980) such that more heat needs to be carried to the skin surface in females in order to overcome the extra fat layer's insulation. Women's electrodermal activity was higher than the male's which indicated higher mental stress. Higher mental stress together with higher heat storage can explain the higher thermal sensation in females above 76.6°F room temperatures.

# 6. THERMAL COMFORT AND TRANSIENT METABOLIC CONDITIONS

The current approach to thermal environment design deems the metabolic conditions steady for a given type of activity. Metabolic level for office environments is considered around 1.2 met and evaluation of the thermal sensation is based on this value. However, as presented previously, metabolic rate in sedentary environments is variable such that office workers are away from their workstations 30% of the time (Bauman et al., 1994) or metabolic rate changes with the psychological stress. This section focused on the thermal comfort responses of people under dynamic conditions in which metabolic rate changes with respect to time in a typical office environment. The test conditions employed in this study vary between steady state, neutral, sedentary to transient, warm, and high-metabolic rate conditions.

The first objective of this section is to characterize thermal responses under transient metabolic conditions and warm temperatures. The second objective is to improve the existing thermal comfort evaluation methods in order to include transient metabolic conditions. Three methods of estimating thermal sensation were compared to each other for accuracy to predict actual thermal sensation. A short term and a long term correction for thermal sensation were presented in the case of repeated high metabolic conditions.

## 6.1. Overall Thermal Comfort and Thermal Sensation

### *6.1.1. Predicted Mean Vote (PMV) and Predicted Percentage Dissatisfied (PPD) Results*

Thermal comfort standards specify comfort for the majority of the occupants in a given space. ASHRAE Standard 55 (2004) defines majority as 80% of the occupants. It assumes that 10% will experience discomfort due to general thermal sensation and another 10% due to local thermal sensation. Thermal sensation data of our study also showed high correlation with the thermal comfort of the subjects (Pearson correlation 0.931). A mathematical relationship was constructed between thermal comfort and thermal sensation (Equation 6.1) (Figure 6.1).

$$ThermalComfort = -0.86 * ThermalSensation + 1.24 \qquad (6.1)$$

Similar studies were found in the literature (Zhang and Zhao, 2008b; Zhang et al., 2008a). Minor differences in correlation coefficients and mathematical fits between the previous studies and our study exist which maybe due to the complex nature of thermal environments and subjective responses. However, all the studies including ours show that the maximum thermal comfort corresponds with neutral (0) thermal sensation and thermal comfort decreases as the subjects feel warmer. The data of this study was also compared to the predicted percentage dissatisfied (PPD) formula of Fanger which is also based on the human subject tests. We generated the same graph of 'percentage dissatisfied' versus thermal sensation to validate our data. The percentage of 'unacceptable thermal environment' votes was calculated for different levels of thermal sensation. Our data matches well with the PPD calculation (Figure 6.2).

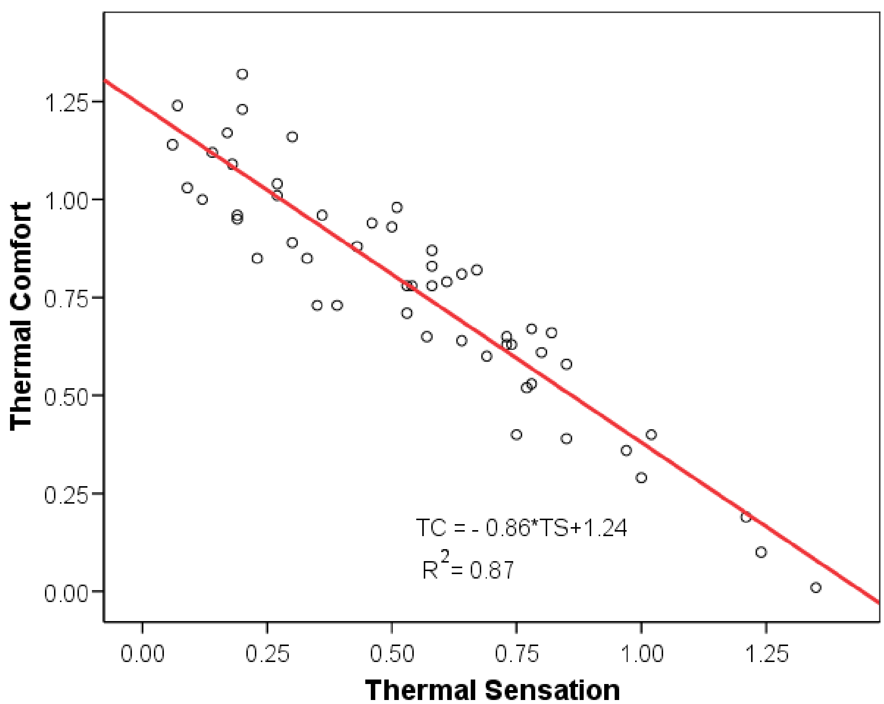


Figure 6.1. Correlation between thermal sensation (TS) and thermal comfort (TC).

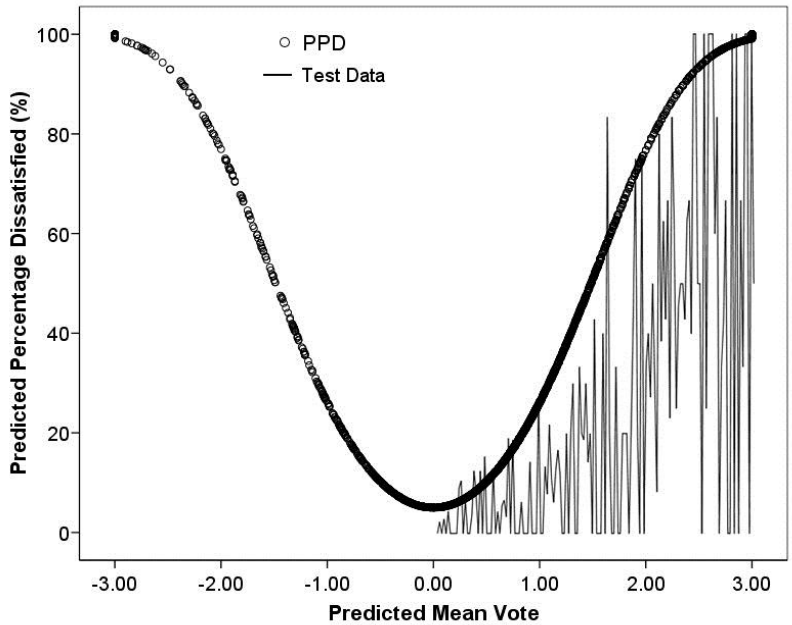


Figure 6.2. PPD from Fanger's equation and the percentage of dissatisfaction results from the test data plotted together.

### *6.1.2. Three Methods of Mean Thermal Sensation Prediction*

Three average thermal sensation values for the whole test were calculated with the results shown in Table 6.1. The thermal sensation and the PMV values are based on ASHRAE 7-point scale.

Method 1: PMV from time-averaged variable,

Method 2: Average PMV of the discrete PMV values from actual data,

Method 3: Average thermal sensation votes.

Table 6.1. Results from three methods of determining average thermal sensation for 75°F and 83°F room temperatures.

| **Room Temperature** | **Method 1: PMV from time-averaged variables** | **Method 2: Average PMV from actual data** | **Method 3: Mean Thermal Sensation** |
|---|---|---|---|
| 75°F | 0.61 | 0.55 | 0.31 |
| 83°F | 1.47 | 0.91 | 0.74 |

Method 1 was calculated using the air-velocity, metabolic rate, ambient and mean radiant temperature values which were averaged for the whole test. This is the common method that is used to evaluate the comfort conditions in buildings. The time-averaged metabolic rate was calculated as 1.9 met (1.2 met for 75% of the time and 4 met for 25% of the time) based on ISO 8996 (2004). The average air velocity was 43.4 ft/m (0.2 m/s). Average relative humidity was approximately 50% and clothing level was constant at 0.5 clo. Room temperature was either 75°F or 83°F while mean radiant temperature was equal to the room temperature at all times. PMV was 0.61 and 1.47, while PPD was 12.7% and 49.4% for 75°F and 83°F respectively.

In the Method 2, a PMV value was calculated for each discrete time-step using the actual data and an average PMV value for the whole test was calculated from the discrete PMV values. This method takes into account transient conditions and presents a more accurate approximation to the actual thermal sensation conditions. The actual mean thermal sensations of the subjects were also calculated as the third method.

Method 3 is the average of the thermal sensation responses of the test subjects. The comparison between the thermal sensation calculations shows that PMV from time-averaged variables (Method 1) over-estimates the sensation of people under neutral and warm conditions. Since this method uses one value for each comfort variable which was averaged for the whole test, the resulting PMV didn’t represent the detailed conditions. Method 1 is more suitable for environments with steady conditions for long periods of time. Method 2 takes into account dynamic conditions by calculating PMV at each time step. However, the average value is still over-estimating the conditions compared to the thermal sensation data (Method 3). Therefore, detailed time-based analysis is required for spaces with dynamic conditions. Subjective thermal sensation votes show that people find higher than predicted temperatures comfortable. Nicol (2004) reached a similar conclusion after finding that people in the field studies have a larger range of comfort temperatures. Both laboratory and field studies showed that thermal comfort can be achieved with temperatures higher than the presumably neutral temperatures.

## 6.2. Subjective Thermal Responses for Transient Metabolic Conditions

### *6.2.1. Thermal Comfort and Thermal Sensation*

An analysis of thermal comfort and thermal sensation based on the metabolic rate is summarized in Figure 6.3. Medium metabolic rate responses were calculated from the average of the five online survey instances after the exercise periods. Mean thermal sensation votes are less than "slightly warm" (+1) in all metabolic conditions. It was previously stated that a thermal sensation vote between +1 and -1 is accepted as comfortable. Thermal comfort votes supported this assumption. Mean thermal comfort of the subjects were always above zero, which is the "comfortable" zone. Thermal comfort and sensation votes during the medium metabolic rate were closer to the high metabolic rate responses than the low metabolic rate. Section 8.3 of this study shows that thermal responses were sustained at an elevated level for up to 10 minutes after the exercise period ended.

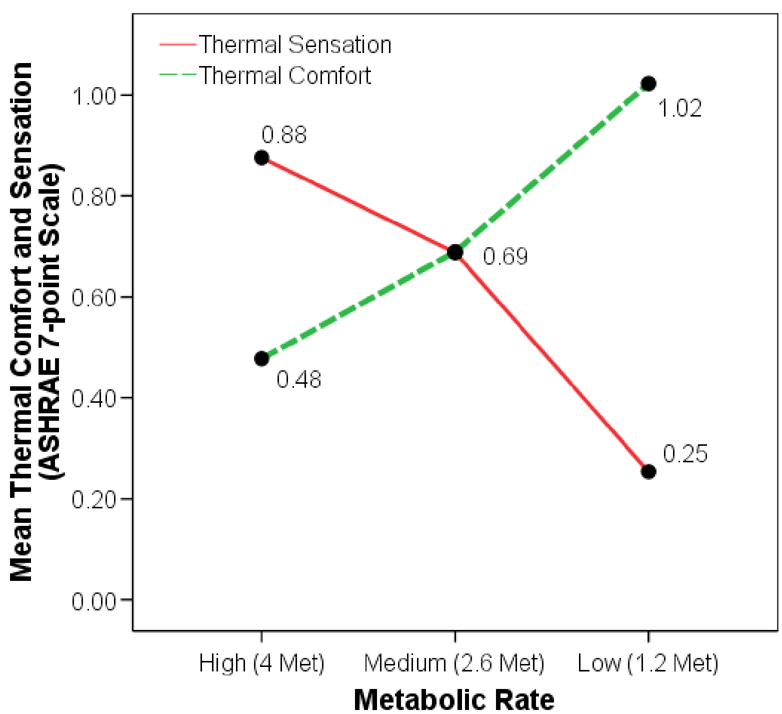


Figure 6.3. Mean thermal comfort and thermal sensation based on metabolic rate.

### *6.2.2. Temperature and Air Movement Preferences*

Mean temperature and airflow preferences of subjects were plotted against the metabolic rate conditions (Figures 6.4 and 6.5). In mean temperature preference responses, -1, 0, and +1 represents preferences for ‘cooler temperature’, ‘no change’, and ‘warmer temperature’ respectively. Similarly, in mean airflow preference responses, -1, 0, and +1 represents ‘less air’, ‘no change’, and ‘more air’ respectively. The mean temperature in these tests was 79°F which was the simple average of 75°F and 83°F test room temperatures.

Subjects preferred cooler temperatures and more airflow in all metabolic conditions. This is expected since the average temperature was warmer than neutral. However, as shown previously, subjects reported that they were comfortable in all metabolic conditions. This can be explained with a shift in people’s expectations of the thermal environment. People’s thermal sensation, which was based largely on the thermoreceptor response, was always on the warm side. However, subjects adjusted their thermal comfort evaluation based on the dynamic conditions of the test.

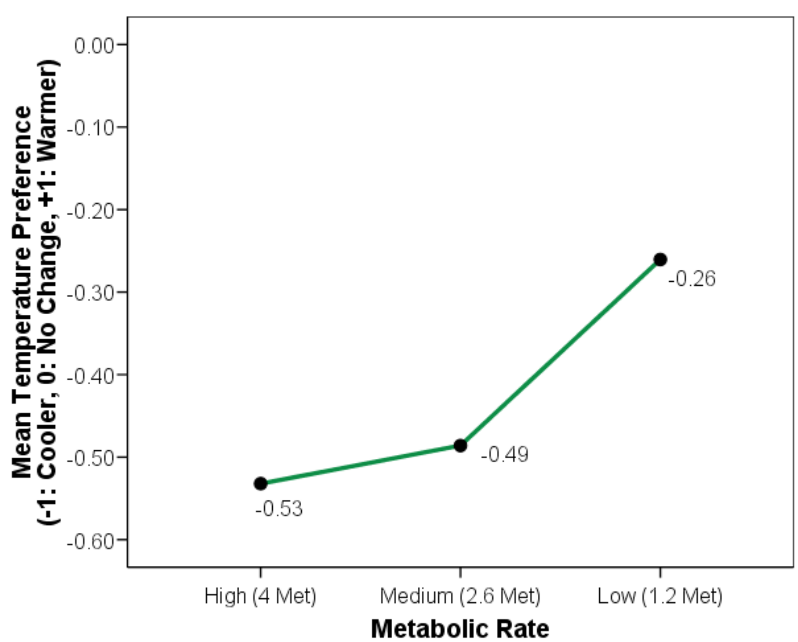


Figure 6.4. Mean temperature preference for three metabolic rate conditions.

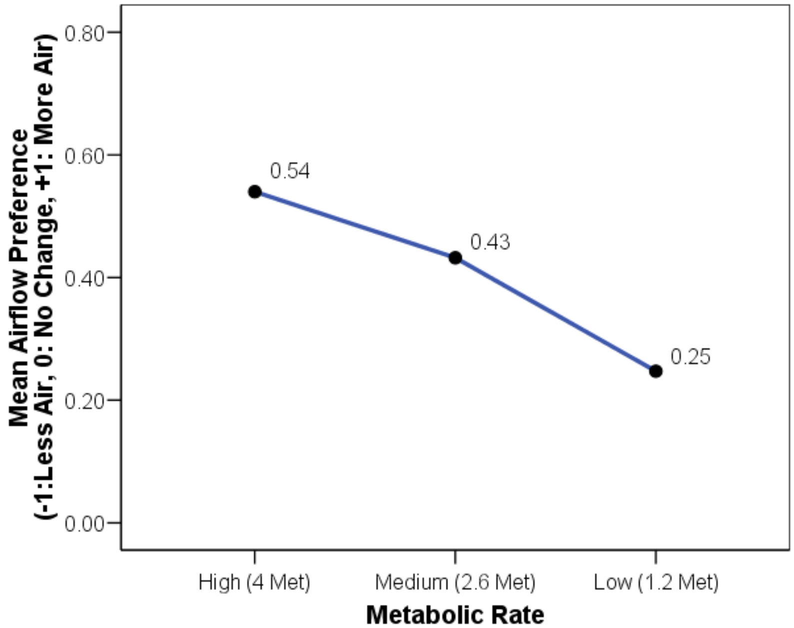


Figure 6.5. Mean airflow preference for three metabolic rate conditions.

### *6.2.3. Environmental Acceptability*

Mean environmental satisfaction of the subjects was plotted in Figure 6.6. In this figure, +1 and -1 represents 'satisfied' and 'dissatisfied' votes of the subjects respectively. The mean satisfaction value was above zero in all metabolic conditions. These results support the previous analysis on the thermal comfort which also showed that mean thermal comfort of the subjects were on the comfortable side of the scale. Subjects were able to accurately evaluate the objective properties of the thermal environment (nonsedentary and warm conditions) by stating that it was warm. Although the subjects' responses indicated that they preferred cooler temperatures and more air movement, they also reported thermal comfort and satisfaction with the thermal environment. It is therefore concluded that thermal comfort and satisfaction are the secondary processing of the thermal sensation evaluation. A two stage model of thermal environment perception is proposed.

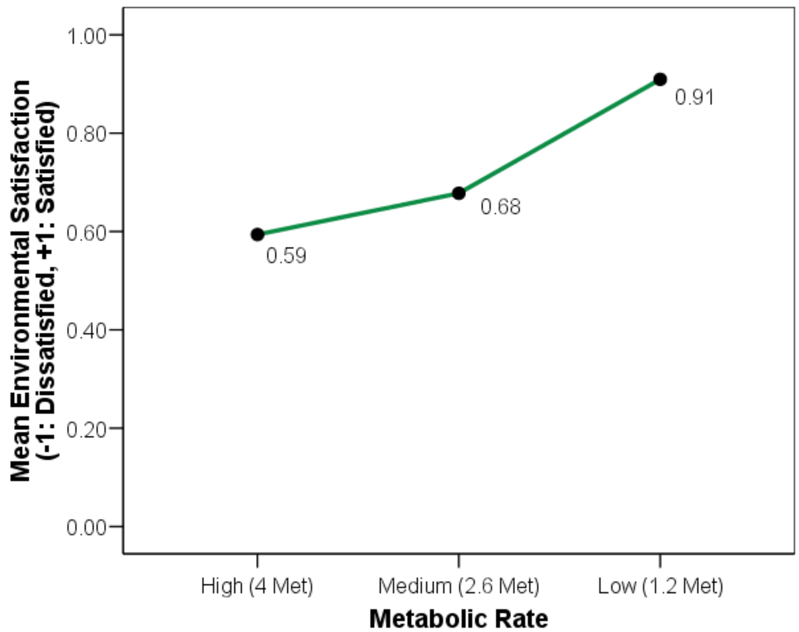


Figure 6.6. Mean environmental satisfaction votes for three metabolic conditions.

In the first stage of the proposed two-stage thermal evaluation model (Figure 6.7), people evaluate the thermal environment based on the physical factors and the associated physiological factors such as skin temperature and metabolic rate. This stage is the objective processing of the thermal information (Gagge et al., 1967; Tanabe and Kimura, 1994) which generates a thermal sensation response (level of warmth or coolness). In the second stage, people evaluate the thermal sensation which was generated in the first stage. After this evaluation, thermal comfort and satisfaction responses are generated. This is a more subjective than the previous stage and several psychological factors may affect the output. Nikolopoulou and Steemers (2003) listed naturalness, expectations, experience, time of exposure, perceived control, and environmental stimulation as some of the psychological adaptation factors which may affect thermal comfort. A practical example is that two persons can perceive the same conditions cold, while one of them thinks that it is comfortable while the other person perceives it uncomfortable.

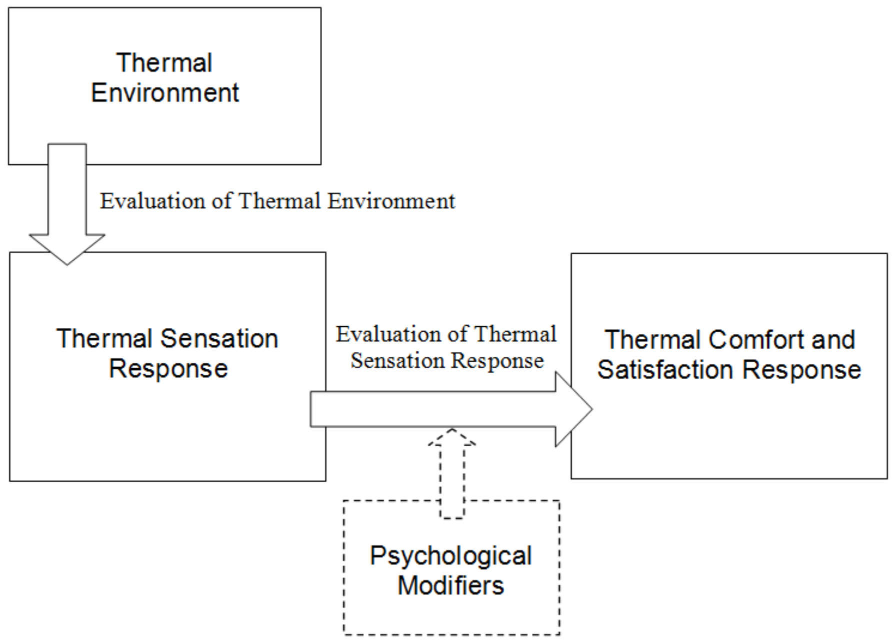


Figure 6.7. The proposed two-staged model of thermal environment perception.

The percent of people dissatisfied is a significant indicator of the thermal conditions of a given environment and is part of the PMV-PPD model of Fanger. The percentage of satisfied and the dissatisfied people were tabulated in Table 6.2 and plotted in Figure 6.8. In the worst case scenario, which is high metabolic rate conditions, subjects reported satisfaction 80% of the time. 80% is on par with what thermal comfort standards suggests as the target satisfaction level. In this study, this target was achieved under high metabolic conditions and higher than neutral average temperatures (79°F). This suggests that people have higher tolerances for thermal environments. The 5% dissatisfaction or 95% satisfaction achieved in this study for low metabolic conditions is also the theoretical maximum satisfaction of the PPD model.

Table 6.2. Percentage of people dissatisfied in three metabolic conditions (1 Met = 58.15 $W/m^2$).

| | **High (4 Met)** | | **Medium (2.6 Met)** | | **Low (1.2 Met)** | |
|---|---|---|---|---|---|---|
| | **Satisfied** | **Dissatisfied** | **Satisfied** | **Dissatisfied** | **Satisfied** | **Dissatisfied** |
| Number of Responses | 310 | 79 | 656 | 126 | 865 | 41 |
| Percentage (%) | 80% | 20% | 84% | 16% | 95% | 5% |

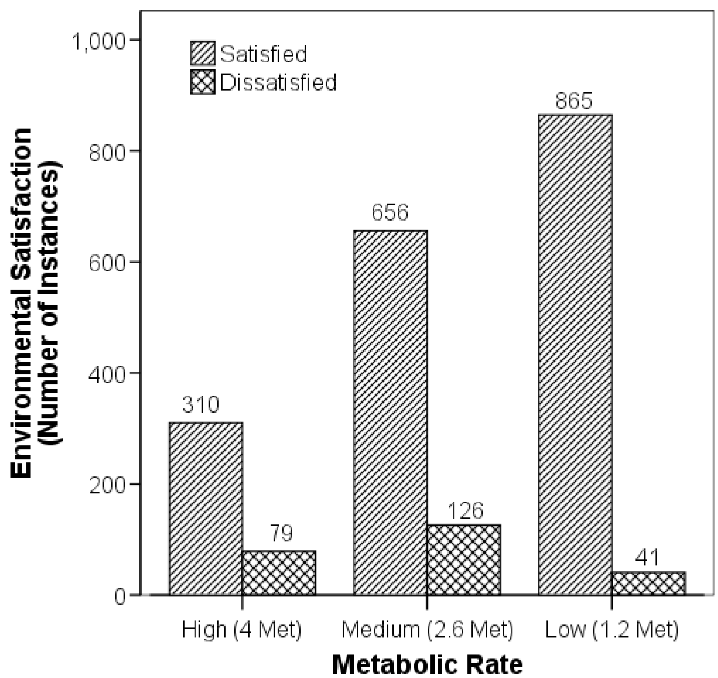


Figure 6.8. Number of instances in which people reported satisfaction or dissatisfaction.

### 6.3. Empirical Models for Dynamic PMV

A comparison between the thermal sensation votes and the PMV calculation based on the actual test data showed discrepancies up to 2.2 points on a 7-point scale (Figure 6.9). Despite the discrepancy, thermal sensation and PMV are well-correlated (Pearson correlation 0.61). Average thermal sensation of subjects varied between 0.06 and 1.35. Whereas, PMV results varied between 0.06 and 3.00 which is the maximum value in the scale. Temperature and the metabolic rate had the largest impact on the final PMV values. According to the PMV method, the thermal conditions of our test clearly deviate from what is considered acceptable. However, thermal sensation votes rarely (<10% of the time) exceeded the comfort limit (+1) which infers that the PMV calculation over-estimates the impact of the thermal conditions. This is due to the steady state nature of the PMV method which is based on subjective response data collected after more than one hour of exposure to the same thermal conditions. Temperature and the metabolic rate were the major factors of the final PMV values. In our test conditions, the metabolic rate has the biggest impact on the PMV variations (Pearson correlation 0.99) since temperature was fairly constant and average air velocities were the same for all subjects.

The high correlation between the thermal sensation data and the PMV results suggests that the PMV formula can be modified to reflect dynamic conditions. Our thermal sensation results suggested that two types of transient conditions occurred during the course of the test. The first one is the short-term transients (up to 10 minutes) which occurred within a 10-minute time frame particularly around transient metabolic conditions. The second one is the long-term transients (up to 1.5 hours) which shows in the average thermal sensation change in the course of the test. Short-term (up to 10 minutes) and long-term (up to 1.5 hours) improvements to the PMV calculation are presented in this study.

### *6.3.1. Short-term Time Dependent Model*

A time-averaged PMV method is proposed to account for the short-term transient nature of the thermal environments. Rowe (2001) suggested that a weighted averaging of activity level (in 10 minute increments) can be used to reflect the effect of previous activity levels on current thermal state. Our test results suggested that the short-term time constant of the subjective responses due to the activity level is approximately six minutes. Subjects reported thermal sensations similar to sedentary votes within 10 minutes after stopping exercising (Figure 6.9). For this reason, a 5-minute and a 10-minute time-averaging the PMV data were applied to account for the short-term past experiences. The 10-minute averaging of the PMV data matched closer to the thermal sensation data than the steady PMV model and the 5-minute averaging. The time-averaged model better represents the transient character of the thermal sensation during the ascending and descending votes around the peak thermal sensations compared to the steady PMV model.

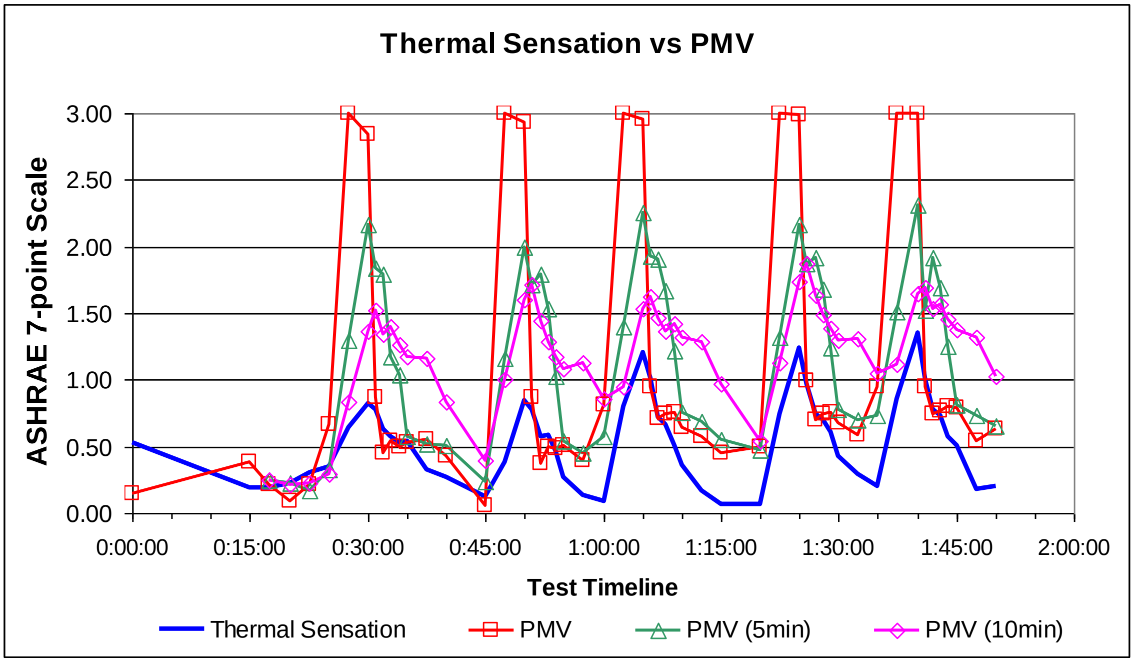


Figure 6.9. Thermal sensation, PMV and time-averaged PMVs for the duration of the test.

### *6.3.2. Long-term Time Dependent Model*

The test data showed that thermal sensation of the subjects steadily increased in time although they reported steady-like thermal sensations within 10 minutes after each exercise session. This was possibly due to the thermally unpleasant past memory, and the resulting increased sensitivity of the subjects towards the thermal environment. Therefore, a long-term time component of the thermal sensation was calculated (Figure 6.10). According to our data, the thermal sensation of a person after 1.5 hours of repetitive high metabolic activity can be 0.30 points higher than the sedentary thermal sensation. According to the PMV under neutral conditions, 0.30 point can be compensated by dropping the ambient temperature by 2°C (3.6°F), or by increasing the air velocity to 0.55 m/s from 0.20 m/s. If the work environment of a person requires moving around for short durations of time (which is typical even for office type of work) the thermal environment should be designed to respond to the changing thermal perception of the person. This could be accomplished by providing personal control over the thermal environment. This is likely to have significant impact on both productivity and energy consumption of a building.

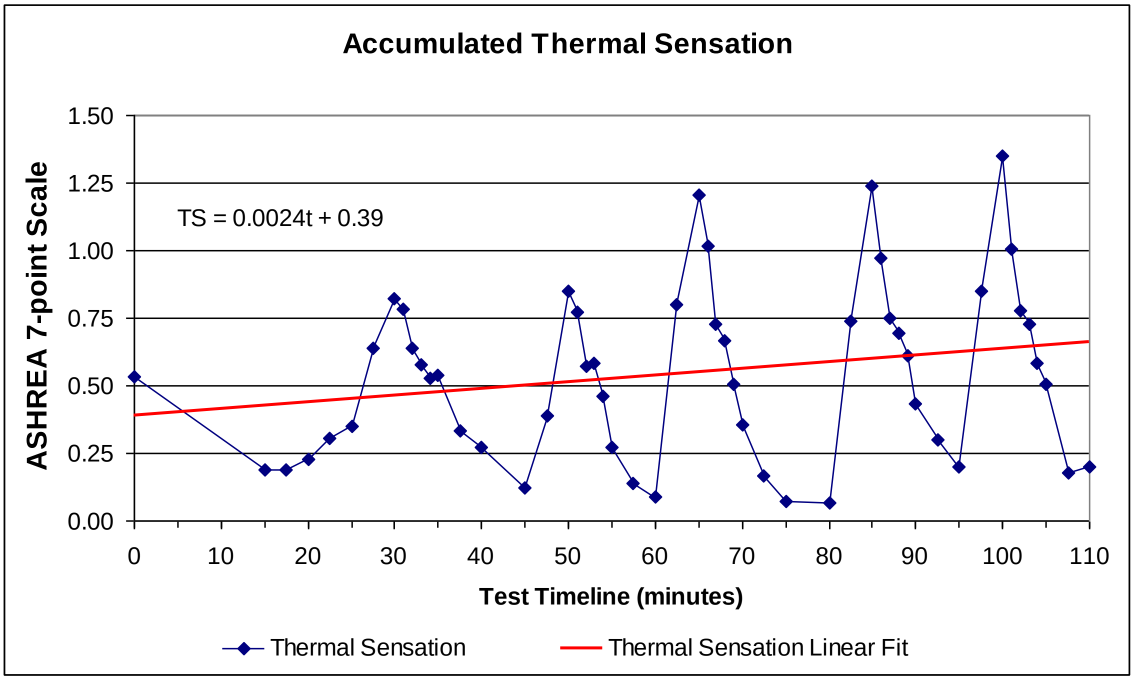


Figure 6.10. Long-term (up to 1.5 hours) time effect due to repeated high metabolic rate.

### 6.4. Increase in Thermal Sensation Based on Short Durations of High Metabolic Activity Periods

The existence of the high metabolic activity in a thermal environment is proved to be significant. Wang et al. (2005) determined an average of approximately 65% occupancy at the workstation throughout a typical work day. Similarly, Bauman et al. (1994) also determined that workers are away from their stations 30% of the time. Since high metabolic conditions are common in a workspace, an analysis was conducted to determine the increase in thermal sensation as a function of percentage of high metabolic activity period. This analysis assumes that people are experiencing high metabolic conditions, such as walking at medium speed or climbing stairs when they are away from their workstations. Figure 6.11 presents the increase in average thermal sensation, peak thermal sensation, and PMV as a function of percentage of high metabolic activity. PMV for each data point was calculated by keeping all the variables neutral except the metabolic rate which was time-averaged between the high metabolic and sedentary conditions (Equation 6.2).

$$AverageMet = \left[ActiveTime\% * 4Met + (100 - ActiveTime\%) * 1.2Met\right]/100 \quad (6.2)$$

Time factors in Figure 6.12 show the factor of increase in thermal sensation over sedentary thermal sensation. In essence, a person who is vacant 25% of the time in repeated periods will vote two times higher compared to his/her sedentary thermal sensation. The conventional method of calculating PMV by time-averaging different metabolic rates as suggested by ISO 8996 (2004) over-estimates the thermal conditions. Building engineers and designers should account for short durations of high metabolic activity in work environment even though the type of environment suggests sedentary conditions.

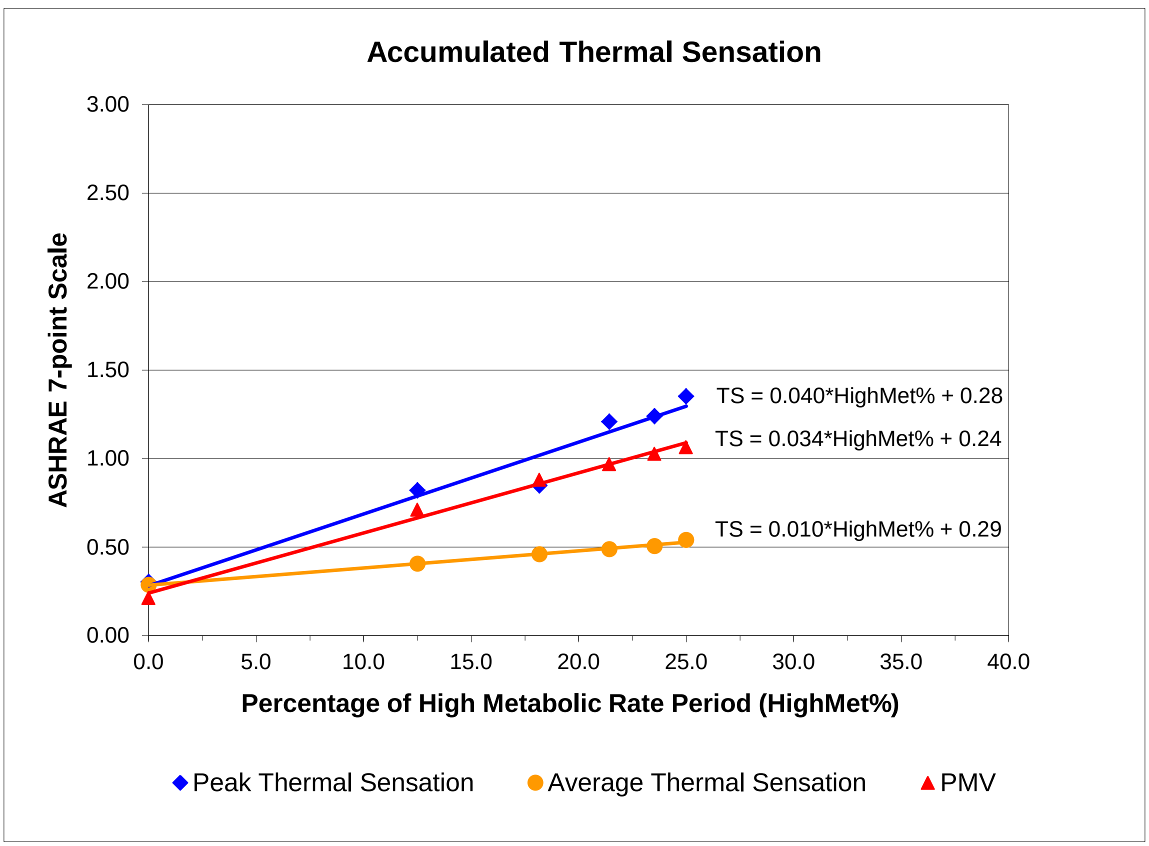


Figure 6.11. Increase in thermal sensation as a function of percentage of high metabolic activity period.

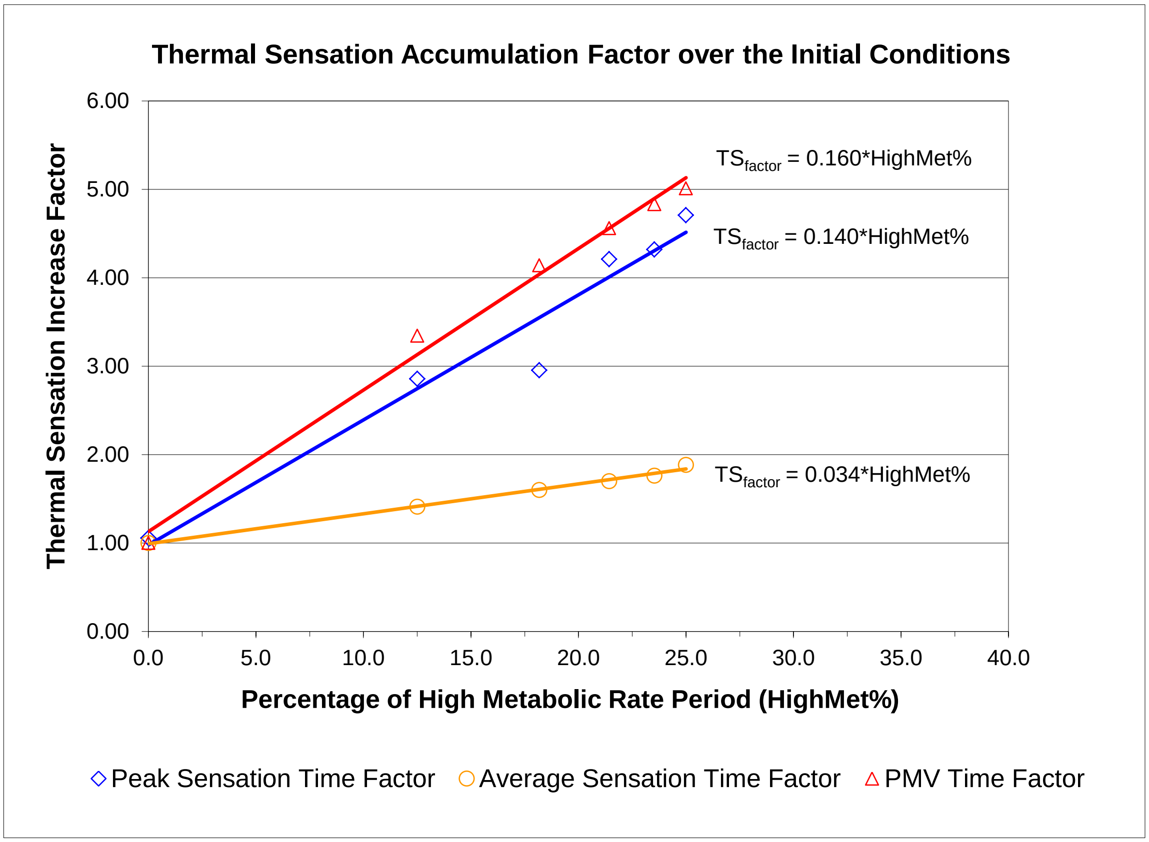


Figure 6.12. Thermal sensation increase factor over the initial thermal sensation.

## 6.5. Discussion

This section focuses on the predictability of subjective thermal responses under transient metabolic conditions for neutral (75°F) to warm (83°F) temperatures. The subjective thermal response data of this study was first compared to the similar studies from the literature for validation purposes. Thermal sensation and thermal comfort responses in our study were found to be similar to the previous studies. In addition, the percent of dissatisfied subjects was compared to the PMV-PPD graph and an almost identical response behavior was discovered. Validation of the data suggested that our test results can be compared to the previous studies and the PMV-PPD index.

PMV-PPD index has been widely in use since its introduction in the early 1970s. It was developed by Fanger (1970) as a steady state heat balance calculation method which was fitted to the extensive subjective thermal comfort test data. PMV is a steady state method and does not reflect the transient conditions since its data is based on test subjects' responses after more than one hour exposure to the steady thermal environments. In addition, the final PMV formula is lacking a time component which can enable transient calculations.

The philosophy behind the PMV model is based on a deterministic approach of finding the optimal comfort conditions for the maximum possible number of people. This "one-size-fits-most" approach provides a description of thermal comfort by combining all the basic comfort variables in one simple-to-understand and easy-to-use index. The real-life application of the PMV index has been in the form of determining one average value for each comfort variable and calculating an average PMV value which reflects average thermal conditions. This value represents the average thermal sensation of the majority of the occupants. However, several studies in the literature showed that the thermal environment is transient in nature and changes in the thermal environment occur in a shorter time than the current PMV calculations can capture.

The conventional PMV approach was applied as PMV Method 1 in our study and was compared to a second method (Method 2) of PMV calculation and to the actual thermal sensation data (Method 3). Method 1 of the PMV calculation over-estimated the average thermal sensation by a factor of two in both 75°F and 83°F ambient temperatures when compared to the actual thermal sensation data (Method 3). Over-estimation of the thermal sensation often results in cold interior environments which are perceived as unpleasant by the occupants. The Method 2 of the PMV calculation was presented which is the average of PMV values calculated at the individual time-steps in the course of the test. Thermal comfort variables vary at each time-step and the Method 2 can reflect the transient conditions to a limited degree since a PMV value was calculated at each time-step. A final PMV value was determined from the average of individual PMVs (a total of 53 time-steps). Although more accurate than the first method, this second method still over-estimates the thermal conditions between 20% and 80%. A time component to the PMV calculation is required to match the predicted values to the real thermal sensation data.

Wang et al. (2005) and Bauman et al. (1994) found that people are periodically away from their workstations for 30% to 35% of the time. Repetitive higher metabolic conditions in our study simulated this behavior. Thermal sensation data revealed two types of transient conditions under repetitive high metabolic conditions: short-term (up to 10 minutes) and long-term (up to 1.5 hours). Short-term transient conditions occurred around peak thermal sensation response which corresponds with the end of the each exercise session.

The PMV calculation estimated a maximum value prior to the peak actual thermal sensation and a lower than actual thermal sensation value immediately after the end of the exercise period. This was because the PMV calculation was determined by the metabolic rate which was calculated through the heart rate. Heart rates of the subjects were very responsive and quickly reached to the target level at the onset and to the base level after the stopping of exercise period. However, human thermal sensation acted like a capacitor-resistor which introduced a time-delay while ascending to and descending from the peak as an exponential function. In order to simulate this capacitor-resistor effect, we introduced short-term (5 minute) averaging of the thermal sensation data to represent the subjective responses in transient metabolic conditions.

The thermal sensation data revealed a second type of transient response behavior which occurred between 15 minutes and 1.5 hours. In this long-term transient behavior, mean thermal sensation of the subjects at each exercise period increased in time. This increase in sensation is due to the psychological processes rather than the physiological processes because thermal sensation always returned to the neutral levels after each exercise period. The increase in subject's sensitivity to the heat stress is most probably due to the memory of the immediate past experiences.

In a final analysis, we correlated the percentage of the high metabolic period to the increase in thermal sensation. In this analysis, we assumed that the high metabolic period encompasses the time away from the workstations. The mean thermal sensation linearly increased at a rate of 0.034 (times the percentage of the high met period), whereas peak thermal sensation increased at a rate of 0.16. This analysis also supports the previous conclusion that the sensitivity of the subjects to the heat stress increased.

# 7. LOCALIZED AND DYNAMIC AIRFLOW FOR TRANSIENT THERMAL CONDITIONS

This section focused on the localized dynamic airflow conditions which have the potential to improve thermal comfort with transient metabolic conditions and warm temperatures. The literature survey of thermoreceptor responses showed that it is possible to provide thermal comfort by positively influencing the thermoreceptors even though the conditions are outside the comfort limits. When stimulated, the thermoreceptors show a peak transient response which settles down to the steady levels. One of the objectives of this study is to periodically stimulate cold sensors on the skin surface to create transient responses and sustain an awareness of coolness while preventing thermoreceptor adaptation.

Dynamic airflow with high power spectrum, varying air velocity and a high turbulence intensity provide more cooling sensation than the steady airflow. Also, Section 2.2.3 of the literature survey showed that local airflow directed at thermally sensitive parts of the body significantly affect the overall thermal sensation. This section presents the concept of *Localized Dynamic Airflow* in which different combinations of airflow frequencies and airflow locations on the body were tested as treatments to correct the thermal discomfort. This approach also has the potential to create cooling sensation more economically since less air is required to cool a relatively small region of the body. A variable thermal environment was created by using two factors. The first one is creating transient airflow conditions by pulsing the air every 30 seconds (10 seconds on, 20 seconds off) or 60 seconds (10 seconds on, 50 seconds off). The second variable is the location of the airflow stimulus: head only or head/hands/feet simultaneously. Tests were conducted for 75°F (24°C) and 83°F (28.3°C) ambient temperature conditions. In addition, thermal responses of the participants were taken for varying metabolic rate conditions ranging from sedentary (1.2 met) to high metabolic conditions (4 met).

A second focus point of this study is the draught discomfort and the airflow preferences of the subjects for different airflow, temperature, and metabolic rate conditions. ASHRAE Standard 55 (2004) defines draught as the unwanted cooling of the body due to air movement and specifies an allowable airflow of 40 ft/min (0.2 m/s) for neutral temperatures to avoid draught discomfort. However, previous literature (Zhang et al., 2007a) shows that people want more airflow even their thermal sensation is cool. This looks contradictory considering the fact that a cooling stimulus is felt unpleasant when general thermal sensation is on the cool side (Zhang, 2003a). These two opposing facts imply that airflow affects people not only physically but also psychologically and that airflow yields positive comfort sensation in a variety of conditions. Analyses were conducted to determine subjects' perception of airflow in multiple thermal conditions and results were compared to the ASHRAE Standard 55 and the previous studies.

## 7.1. Airflow Perception

### *7.1.1. Airflow Preferences of Test Subjects*

The mean thermal sensation of our test subjects when they were satisfied with the air movement was 0.24 (on 7-point scale). Tanabe and Kimura (1994) found that the mean thermal sensation of the subject under preferred air velocity conditions was -0.5. This means that subjects in Tanabe and Kimura's study preferred slightly cool conditions contrary to the test subjects of our study who preferred slightly warm conditions under the same environmental conditions. Tanabe and Kimura also found that at thermal neutrality, the preferred air velocity was 0.33 m/s, which shows that people like to feel airflow even at thermal neutrality. Fountain et al. (1994) investigated the draught discomfort for temperatures ranging from 77°F (25°C) to 82.4°F (28°C) and found that approximately 50% of the people demand more airflow. Our test conditions varied between neutral/sedentary (75°F/24°C) conditions to warm/high metabolic rate (83°F/28.3°C) conditions and demand for more air movement to compensate the warm feeling is somewhat expected. However, even 30% of the sedentary subjects, of which 13% belong to the 75°F group and 17% belong to the 83°F group, demanded more air (Figures 7.1 and 7.2). This supports Tanabe and Kimura's (1994), Fountain et al.'s (Fountain, 1994) and Zhang et al.'s (2007a) conclusions. Figure 7.1 shows the airflow preferences as a function of metabolic rate. Preference for more air increased from 30% in low metabolic conditions to 58% in high metabolic conditions. This shows that people prefer to feel airflow around them in the case of heat stress. Huda and Homma (2005) conducted human subject tests and asked the participants about their airflow perception in summer (room temperature 78.8°F/26°C to 82.4°F/28°C) and winter seasons (room temperature 71.6°F/22°C to 75.2°F/24°C). The average airflow preference (for the neck and the ankle) was 0.53 (5-point scale from -2 to +2) for the summer season and was 0.04 for the winter season. This showed that people prefer airflow even in cool winter conditions. We analyzed the same conditions for our tests and found no significant differences of airflow preference between the 75°F (24°C) and 83°F (28.3°C) room temperatures (p=0.656) (Figure 7.3). In addition, mean airflow preferences of our subjects were higher than Huda and Homma's results. This may be due to the lower mean air velocities of our study. Nevertheless, there is overwhelming evidence for the demand for more air movement in majority of the conditions.

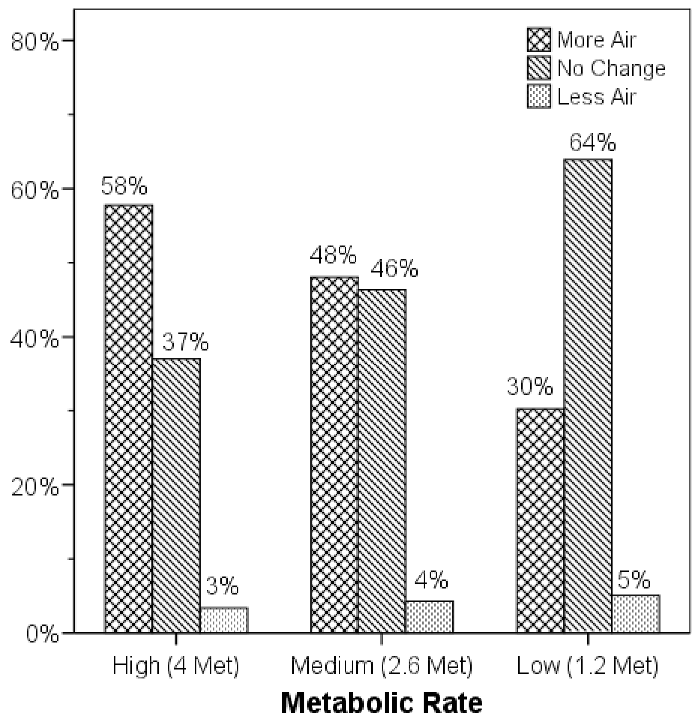


Figure 7.1. Airflow preference percentages grouped by the airflow preference class.

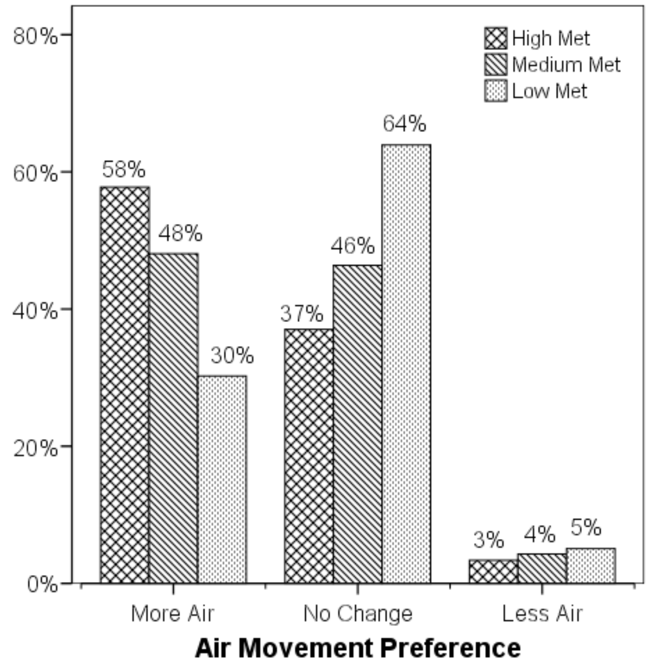


Figure 7.2. Airflow preferences as a function of metabolic rate.

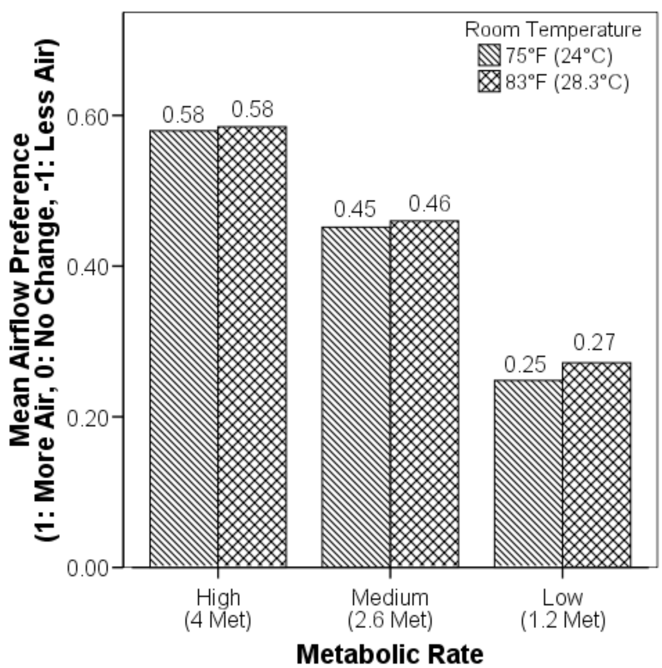


Figure 7.3. Mean air movement preference for various metabolic and room temperature conditions.

The preference for airflow was affected by the thermal sensation of the people. Since airflow increases the heat loss from the body, it is natural for people, who are feeling warm, to want more air, and people who are feeling cool to want less. However, our test results show that 17.9% of the people feeling slightly cool still preferred more air. Less than half of the people (42.1%) preferred less air. As expected, the preference for more air increased with the increased thermal sensation (Table 7.1). We compared air preference of our subjects to the study by Zhang et al. (2007a). Table 7.2 shows the airflow preference of Zhang et al.'s study for air velocities up to 0.2 m/s. The preferences for less air, no change and more air are more evenly distributed in our study with a preference for more air as the subjects felt warmer. In Zhang et al.'s study, airflow preference was concentrated around "No change" for thermal sensations below neutral. The preference for more air movement is evident for thermal sensations above the neutral.

Table 7.1. Airflow preferences for different thermal sensation votes and mean air velocity of 0.21 m/s.

| **Thermal Sensation** | **Percentage of Occupant Responses Preferring** | | | **N** |
|---|---|---|---|---|
| | **Less Air** | **No Change** | **More Air** | |
| Cold | 0.0[a] | 0.0[a] | 100.0[a] | 8 |
| Cool | 15.5[a] | 25.4[a] | 59.2[a] | 56 |
| Slightly Cool | 42.1 | 40.0 | 17.9 | 146 |
| Neutral | 38.2 | 31.8 | 30.0 | 842 |
| Slightly Warm | 30.1 | 34.0 | 35.9 | 657 |
| Warm | 27.4 | 31.6 | 41.0 | 290 |
| Hot | 0.0[a] | 62.0[a] | 38.0[a] | 49 |

[a] Not significant due to the small sample size.

Table 7.2. Airflow preferences for different thermal sensation votes and mean air velocity of less than 0.2 m/s (reproduced from Zhang et al. (2007a)).

| **Thermal Sensation** | **Percentage of Occupants Preferring** | | | **N** |
|---|---|---|---|---|
| | **Less Air** | **No Change** | **More Air** | |
| Cold | 38.0 | 62.0 | 0.0 | 13 |
| Cool | 39.8 | 59.6 | 10.6 | 47 |
| Slightly Cool | 10.0 | 79.0 | 11.0 | 329 |
| Neutral | 1.7 | 78.1 | 19.9 | 704 |
| Slightly Warm | 0.9 | 40.8 | 57.8 | 429 |
| Warm | 0.6 | 25.3 | 74.1 | 158 |
| Hot | 0.0 | 0.0 | 100.0 | 32 |

### *7.1.2. Draught Discomfort*

We calculated the draught discomfort as a continuous variable for our case and compared the mean draught rating (DR) prediction to the actual responses from the test subjects (Table 7.3). Following Toftum's (2002) methodology, preference for less air movement was taken as an indicator of the draught dissatisfaction. In this comparison, data corresponding to 83°F (28.3°C) room temperature was excluded since DR formula is limited to 80°F (26.7°C). We detected significant difference between the predicted and the actual dissatisfaction data. Part of the reason may be due to the lack of metabolic rate component in the DR formula. Our test includes high metabolic rate periods and it is known that airflow dissatisfaction decreases with the increased metabolic rate (Toftum and Nielsen, 1996). Section 6 of this study presented that people experience high metabolic rate periods during a typical day and the DR calculation should include a metabolic rate component to more accurately predict the real conditions.

Table 7.3. DR calculation based on Fanger et al.'s formula and the air movement dissatisfaction from the test data.

| **Mean DR for the test (from Standard 55-2004)** | **Air Movement Dissatisfaction (based on "Less Air" votes)** |
|---|---|
| 16% | 5% |

Toftum and Nielsen (1996), Toftum (2002) and Griefahn et al. (2001b) focused on the relationship between the metabolic rate and the draught discomfort and found that DR decreases with the increased metabolic rate. Toftum and Nielsen (1996) argued that when the deep body temperature is raised due to the increased physical activity, the influence of the impulses from thermoreceptors on the thermoregulation is decreased to maintain the heat balance. In other words, decreased sensitivity to draught in high metabolic conditions ensures utilization of the airflow to lose heat. We compared our results to those Toftum and Griefahn et al.'s and found that draught discomfort in our study is significantly lower than other two studies (Figure 7.4).

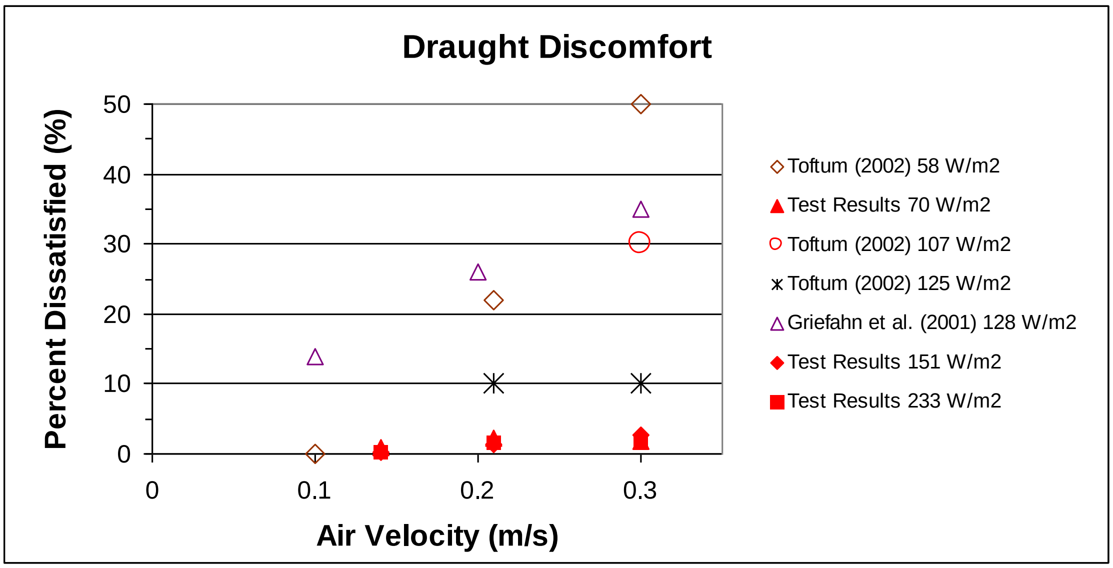


Figure 7.4. The relationship between draught discomfort and the metabolic rate.

### 7.2. Dynamic Airflow and Location of Airflow Stimulus on the Body

The thermal comfort and the thermal sensation data that are presented in Section 6 showed good agreement with the existing studies from the literature. Minor differences between studies exist within acceptable limits due to the slight differences in test conditions. Initial analysis of the subjective response data showed similar variability for each subject. However, offsets between subjects exist due to the differences in subjective interpretation of the online survey question scales. In the following airflow frequency and location analysis, z-normalization was applied to the subjective response data to eliminate the offsets and to better determine the overall response trends. The methodology is explained in Section 3.6. Both the absolute and the normalized responses are presented in the following analyses.

### *7.2.1. Dynamic Airflow and Thermal Comfort*

The literature survey showed that warm sensation can be compensated with the cold warnings from the skin thermoreceptors (Fiala et al., 2003; Zhou et al., 2006). We tested the hypothesis that stimulation of the cold receptors can provide comfort in warm temperatures and high metabolic conditions. Two dynamic airflow sequences (i.e. 30-second and 60-second pulsing) were used to prevent the skin thermoreceptors from adapting. The results for both cases were compared to the minimum constant airflow conditions of 24 ft/min (0.12 m/s).

We first compared the mean thermal comfort votes for Minimum Air, 30-second, and 60-second airflow conditions. The average metabolic activities were 1.55 Met (5 minutes of 4 Met and 35 minutes of 1.2 Met) during the Minimum Air condition, and 2.13 Met (5 minutes of 4 Met and 10 minutes of 1.2 Met) for the 30 and 60-second pulsing. The null hypothesis is that all three airflow conditions generate the same mean thermal comfort vote. The 30-second airflow was significantly different than the Minimum Air (p-value 0.013) and the 60-second (p-value 0.002) airflow. This means that 30-second pulsing was able to provide a more comfortable environment although the average metabolic rate was significantly higher (2.13 vs. 1.55 Met) than the Minimum Air conditions. On the other hand, there was no evidence to reject the null hypothesis for Minimum Air and 60-second comparison (p-value 0.647). This essentially means that 60-second airflow under 2.13 Met was able to generate similar thermal comfort to Minimum Air with near sedentary (1.55 Met) metabolic conditions. The mean thermal comfort for Minimum Air, 30-second, and 60-second airflow conditions were -0.04, 0.10, and -0.07 points respectively (Table 7.4).

Table 7.4. Normalized and actual thermal comfort votes for three airflow conditions.

| Airflow Condition | Normalized Thermal Comfort Votes | | Actual Thermal Comfort Votes | | N |
|---|---|---|---|---|---|
| | Mean | Std. Dev. | Mean | Std. Dev. | |
| Minimum Airflow (24 ft/min) | -0.04 | 1.05 | 0.81 | 1.03 | 585 |
| 30 Second Pulse | 0.10 | 0.95 | 0.82 | 1.22 | 734 |
| 60 Second Pulse | -0.07 | 0.98 | 0.71 | 1.26 | 729 |

We conducted a thermal sensation analysis for the three airflow conditions (Table 7.5). Statistically significant differences were found between the 30-second and the 60-second airflows (p-value 0.003). Subjects felt cooler (Thermal sensation: -0.06) during 30-second than the 60-second airflow (Thermal sensation 0.10). The 60-second airflow was still able to provide approximately neutral conditions given the higher-than-sedentary (2.13 Met) metabolic rate. The 30-second airflow under 2.13 Met was able to provide thermal sensation similar to near-sedentary (1.55 Met) conditions.

Table 7.5. Normalized and actual thermal sensation votes for three airflow conditions.

| Airflow Condition | Normalized Thermal Sensation Votes | | Actual Thermal Sensation Votes | | N |
|---|---|---|---|---|---|
| | Mean | Std. Dev. | Mean | Std. Dev. | |
| Minimum Airflow (24 ft/min) | -0.06 | 1.07 | 0.46 | 0.86 | 585 |
| 30 Second Pulse | -0.06 | 0.93 | 0.56 | 1.03 | 734 |
| 60 Second Pulse | 0.10 | 0.98 | 0.61 | 1.02 | 729 |

A theoretical analysis based on the PMV index was conducted to quantify the thermal sensation improvement that 30-second air provided. When the test conditions were kept constant (79°F mean radiant and room temperature, 45% RH, 24 ft/min airflow, 0.5 clo) PMV for 2.13 met is 0.55 points higher than the 1.55 Met. This means that 30-second pulsing was able to compensate for an expected 0.55 points increase in thermal sensation due to 2.13 Met activity level.

The airflow preference of the subjects also supports the above conclusions of cooling efficiency of the 30-second airflow. Table 7.6 shows that the average preference for more air was highest during the minimum airflow and lowest during the 30-second pulse. Given the fact that subjects were experiencing the highest volume of air during 30-second pulse and the lowest during minimum air means that subjects were able to differentiate between the different airflow patterns and they were able to assess personal and environmental thermal conditions consistently.

Table 7.6. Airflow preference for three airflow conditions (-1: Less Air, 0: No Change, +1: More Air).

| **Airflow Condition** | **Mean Airflow Preference** | **Airflow Preference Std. Dev.** | **N** |
|---|---|---|---|
| Minimum Airflow (24 ft/min) | 0.43 | 0.53 | 584 |
| 30 Second Pulse | 0.34 | 0.59 | 722 |
| 60 Second Pulse | 0.39 | 0.58 | 718 |

Tanabe and Kimura (1994) previously showed that a sine wave with a period of 30 seconds (Sin(30)) has the most cooling effect whereas pulsed air with the period of 60 seconds has the least. Section 3.3.2 showed that our airflow periods yielded similar airflow patterns to Tanabe and Kimura. In our study 30-second airflow was more desirable than the 60-second airflow which is consistent with Tanabe and Kimura who found that Sin(30) provided more cooling than the pulse air pattern.

### *7.2.2. Localized Airflow and Thermal Comfort*

Different regions of the human body have different level of sensitivity to the thermal conditions. Literature showed that head, hands, and feet are more sensitive than other regions of the body (Zhang et al., 2004; Zhang, 2003a; Arens et al., 2006b; Toftum and Nielsen, 1996; Wang et al., 2007; Pellerin et al., 2004; Huda and Homma, 2005). Among those three regions, neck and shoulders have the highest number of cold thermoreceptors and therefore are most sensitive to the cold stimulus. In this study, airflow was directed to the body in two different modes: head-only and combined (head/hands/feet simultaneously) airflow. In order to achieve the desired airflow condition, nozzles were placed at the head, hand and foot level on two sides of the test subject. The head nozzles were directed slightly from the back of the head towards to front to prevent eye dryness due to the direct airflow. Therefore, the head airflow covers the neck, and the sides of the face.

A main hypothesis of this study states that air directed to the head region would be more effective than splitting the same volume of air into three and directing it to head/hands/feet simultaneously. This hypothesis is based on the fact that head-only airflow is higher than simultaneous airflow in velocity therefore creates higher convection coefficient and more cold warnings. In addition, the turbulence intensity of the head-only airflow is slightly higher which has more potential to create cold warnings. Arens et al. (2006a) found that overall thermal sensation follows the coolest local sensation. Also, in slightly warm and warm conditions (which is similar to our conditions), overall thermal sensation follows the head region thermal sensation. Therefore, creating a strong local cooling at the head region of the body may create the coolest overall thermal sensation.

ANOVA was conducted to determine whether airflow location makes a difference in thermal comfort and thermal sensation responses. This analysis revealed that the difference between the head-only and the simultaneous airflow was significant at $\alpha=0.05$ (p-value 0.049). The average metabolic rate during the ‘Min. Air’ condition was 1.55 met, whereas during the two airflow treatments average metabolic rate was 2.13 met. Table 7.7 shows that the simultaneous airflow yielded higher thermal comfort votes than the ‘Min. Air’ condition, although metabolic rate was significantly higher. Head-only airflow was able to provide thermal comfort similar to the ‘Min. Air’ condition.

Table 7.7. Normalized and actual thermal comfort votes for three airflow conditions.

| | Normalized Thermal Comfort Votes | | Actual Thermal Comfort Votes | | |
|---|---|---|---|---|---|
| **Airflow Condition** | **Mean** | **Std. Dev.** | **Mean** | **Std. Dev.** | **N** |
| Minimum Air (24 ft/min) | -0.04 | 1.05 | 0.81 | 1.03 | 585 |
| Head-only | -0.03 | 0.95 | 0.70 | 1.23 | 741 |
| Simultaneous (Head/Hands/Feet) | 0.07 | 0.99 | 0.83 | 1.25 | 722 |

ANOVA of the normalized thermal responses showed that different airflow conditions yielded different thermal sensation votes (p-value 0.044) (Table 7.8). Simultaneous airflow was more effective in reducing the thermal sensation than the head-only airflow (p-value 0.054). There is not enough evidence to claim a difference between the 'Min. Air' and simultaneous airflow conditions (p-value 0.626). This means that simultaneous airflow under 2.13 met activity level was able to provide similar thermal sensation votes as 'Min. Air' conditions under 1.55 met activity. Simultaneous airflow condition compensated for the increase in metabolic rate.

Table 7.8. Normalized and actual thermal sensation votes for three airflow conditions.

| | Normalized Thermal Sensation Votes | | Actual Thermal Sensation Votes | | |
|---|---|---|---|---|---|
| **Airflow Condition** | **Mean** | **Std. Dev.** | **Mean** | **Std. Dev.** | **N** |
| Minimum Air (24 ft/min) | -0.06 | 1.07 | 0.46 | 0.86 | 585 |
| Head-only | 0.07 | 0.96 | 0.61 | 1.04 | 741 |
| Simultaneous (Head/Hands/Feet) | -0.03 | 0.95 | 0.56 | 1.02 | 722 |

An analysis of airflow preferences supports the above conclusions of the effectiveness of airflow location to provide thermal comfort and thermal sensation. Table 7.9 shows that the preference for more air was the highest during the 'Min. Air' conditions and the lowest during the simultaneous airflow condition. These results show that people perceived simultaneous air as more effective and responded with lower thermal sensation and higher thermal comfort. Our test conditions fall into the category of higher than sedentary metabolic activity (1.9 met according to ISO 8996) and warmer than neutral conditions (79°F average temperature). Under these conditions, the mean preference of airflow was always for “More Air” in all three airflow location conditions. This showed people’s inherent understanding of airflow as a corrective measure for thermal comfort. A biological evidence for this is the decrease in draught sensation with the increased metabolic activity as shown in this paper and by Toftum and Nielsen (1996). By decreasing the draught dissatisfaction, human body utilizes high air velocities to lose heat and to maintain thermal balance.

Table 7.9. Airflow preference for three airflow conditions (-1: Less Air, 0: No Change, +1: More Air).

| Airflow Condition | Mean Airflow Preference | Airflow Preference Std. Dev. | N |
|---|---|---|---|
| Minimum Air (24 ft/min) | 0.43 | 0.53 | 584 |
| Head-only | 0.39 | 0.58 | 722 |
| Simultaneous (Head/Hands/Feet) | 0.34 | 0.59 | 718 |

### *7.2.3. The Interaction Effects of Airflow Period and Location on the Body (Localized Dynamic Airflow)*

Different airflow frequencies and localized flow conditions yielded statistically significant results which are aligned with the previous studies from the literature. One hypothesis of this study was that the combination of localized air with varying flow speeds, which is called here the *Localized Dynamic Airflow*, can create a higher cooling sensation than the individual conditions. ANOVA for interaction effects of localized and dynamic air shows no significant difference between the different combinations (Table 7.10). In other words, different combinations of airflow frequency and the location resulted in similar thermal comfort sensations. However, it was proved in this study that airflow provided higher thermal comfort. Since, different combinations of airflow location and frequency yields similar thermal comfort results, the combination that used the least amount of air can be used to provide thermal comfort.

Table 7.10. ANOVA table for the individual and interaction effects of localized and dynamic airflow for thermal comfort.

| Source | Type III Sum of Squares | Degrees of Freedom | Mean Square | F score | Significance |
|---|---|---|---|---|---|
| Corrected Model | 15.003 | 4 | 3.751 | 3.843 | 0.004 |
| Intercept | 0.002 | 1 | 0.002 | .002 | 0.966 |
| Airflow Location | 3.621 | 1 | 3.621 | 3.710 | 0.054 |
| Airflow Frequency | 8.845 | 1 | 8.845 | 9.063 | 0.003 |
| Airflow Location * Airflow Frequency | 0.068 | 1 | 0.068 | 0.070 | 0.792 |
| Error | 1993.997 | 2043 | 0.976 | | |
| Total | 2009.000 | 2048 | | | |
| Corrected Total | 2009.000 | 2047 | | | |

An analysis of the effect of airflow on thermal responses was conducted for 83°F room temperature, 45% relative humidity, 0.5 clo insulation level, and 2.13 met activity. Thermal sensation and thermal comfort votes were averaged for distinct mean airflow periods of the test. Figure 7.5 shows that increasing the airflow from 27.5 ft/min to 60 ft/min decreased the average thermal sensation from 0.63 to 0.45 points. In addition, thermal comfort increased from 0.94 to 1.11 for the same amount of increase in airflow. Improvement in thermal responses is significant considering the fact that metabolic activity and room temperature are higher than neutral conditions. For the same conditions, PMV calculations predicted an average of 1.05 points higher in all three airflow conditions. These PMV calculations also underestimated the effect of increased airflow by predicting an improvement of 0.09 points compared to the actual improvement of 0.18 points when the airflow was increased from 27.5 ft/min to 60 ft/min.

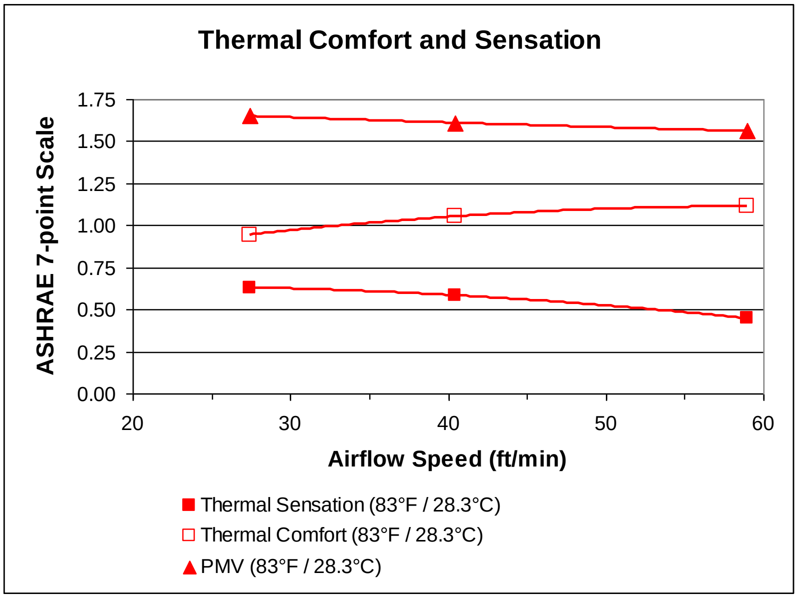


Figure 7.5. Thermal sensation and thermal comfort as a function of airflow (83°F Ta, 45% RH, 0.5 clo, 2.13 met).

### 7.3. Discussion

This section of this study focused on the dynamic localized airflow and its potential to provide comfort under varying metabolic rate and room temperature conditions. Previous studies showed that people demand more air even when their thermal sensation is cooler than neutral (Toftum, 2002; Zhang et al., 2007a). In this study, 17.9% of the subject who felt slightly cool still demanded more air. Only 42% of the same group of people preferred less air. This is counter-intuitive considering the fact that more airflow increases the heat loss making the person feel cooler. These results have two potential explanations. People either like to feel cool, therefore demand more air even when they feel cool, or airflow has a psychological function in yielding a comfort sensation. Section 6 of the study showed that the maximal thermal comfort votes occurred when thermal sensation was warmer than neutral. Combining the two results suggests that the second potential explanation is more likely since subjects in our study expressed maximum comfort when they felt slightly warm. These tests were conducted in the hot and humid region of the United States, where more air is usually felt as pleasant. Participants of our study might have developed a positive perception towards airflow during their residency in this region.

The average air velocity for the test was 43 ft/min during combined head/hands/feet cooling and 55 ft/min during the head-only cooling. These airflow speeds were slightly over the limits specified by ASHRAE Standard 55 (2004) for the same turbulence intensities and thermal conditions. Standard 55 predicted dissatisfaction due to draught (DR) of 16% for the overall test. However, only 4% of the subjects expressed dissatisfaction with the airflow and preferred less air. The possible reason is the higher than sedentary average metabolic rate of our test conditions. Previous studies documented the effect of metabolic rate on draught dissatisfaction (Toftum and Nielsen, 1996; Griefahn et al., 2001b). Our test results were aligned with those studies with 3% DR for high, 4% DR for medium and 5% DR for low metabolic rate conditions. However, these results were significantly lower than Toftum and Nielsen and Griefahn et al. who found higher dissatisfaction ratings for similar conditions. This may be due to the fact that the mean air velocity of this study is an average of constantly varying airflow rather than a constant stimulus on the body. Toftum measured the draught sensation for temperatures of 57.2°F (14°C), 62.6°F (17°C), and 68°F (20°C) and didn't find differences. Our study also showed no difference in airflow perception for 75°F (24°C) and 83°F (28.3°C) temperatures. Contrary to the common understanding, temperature had no effect on airflow perception under the test conditions we used.

One of the main variables of this study was the dynamic airflow (30-second and 60-second pulse) which was compared to the minimum constant air condition. Initial analyses showed that people interpret the analog thermal sensation and comfort scales differently. A z-normalization was applied to the data in order to isolate response characteristics from the individual differences. Results showed that 30-second pulsing yielded thermal sensation results similar to the minimum constant air conditions. This is significant considering the fact that metabolic rate was 2.13 met during the pulsed air testing compared to the 1.55 met during the minimum air testing. The mean thermal sensation during the 60-second pulse was higher than the minimum air condition while thermal comfort votes were similar. This suggested that while the 60-second airflow wasn't effective in reducing the heat stress, it provided a comfort sensation which was possibly due to the increased awareness for an airflow treatment. The 30-second airflow was the most effective in both reducing the heat stress and providing thermal comfort. Airflow preferences were consistent with the mean air velocities in which preference for more air is inversely related to the mean air velocity.

Another main variable of this study was the location of the airflow on the body. Two localized airflow modes were employed in this study: head-only and simultaneous head/hands/feet airflow. The hypothesis was that stronger airflow at the head level would be more effective in yielding a cooler thermal sensation than the simultaneous airflow. Analysis showed that the thermal sensation and thermal comfort votes were significantly different for two localized airflow modes. Simultaneous airflow yielded lower thermal sensation and higher thermal comfort votes. The thermal sensation votes of the simultaneous airflow with 2.13 met was similar to the no localized airflow condition with 1.55 met. The airflow mode being the only difference, it can be argued that simultaneous airflow compensated for the increase in metabolic rate. The head-only airflow yielded higher thermal sensation votes than the minimum airflow condition which means that it was not effective in dissipating the extra heat generated by the higher metabolic rate. However, thermal comfort votes of the head-only airflow were similar to the ‘Min. Air’ condition. This also supported an earlier conclusion that having an airflow treatment may have a thermally comforting effect.

Localized airflow and dynamic airflow proved to make statistically significant differences in thermal comfort and sensation. One of the hypotheses of this study was that more effective cooling can be provided by a localized dynamic airflow which combines the localized air with the dynamic airflow patterns. The results showed that different combinations of airflow frequency and location yielded similar thermal comfort results.

# 8. PSYCHOPHYSIOLOGICAL SIGNALS OF THERMAL COMFORT

The literature section presented the argument that thermal comfort depends on the heat exchange of the body with the environment. Cold and warm warnings from the thermoreceptors are sent to the hypothalamus which then activates the effector mechanisms of the body such as vasodilatation, vasoconstriction, sweating or shivering to maintain homeostasis (Cabanac, 1981; Parsons, 2003). McIntyre (1980), Prek (2006) and Sakoi et al. (2007) stated three conditions of thermal comfort as the heat balance, skin temperature and the sweat rate, all of which are directly physiological. In addition, thermal comfort is a psychological phenomenon which involves psychological adaptation, naturalness of the environment, expectations, short and long-term experience, and perceived control (Nikolopoulou and Steemers, 2003). Psychological aspect of thermal comfort is evident in the thermal comfort definition which refers to the 'state of mind'.

This section of the study had two objectives. The first objective focused on the relationship of three physiological signals (i.e. heart rate, skin temperature, and electrodermal activity) to the thermal comfort responses of people. The second objective focused on psychological stress, which is common in work environments, and its effect on thermal comfort.

Previous studies showed that psychological stress causes changes to the different physiological processes of the body. Heart rate, blood pressure, respiration rate and electrodermal activity increases with the increased mental load (Steele et al., 1968; Ettema and Zielhuis, 1971; Andreassi, 2000; Alderman et al., 2007). Andreassi also mentioned that epinephrine production and the heart rate increases with the difficulty of the psychological stressor or the task. The demand for high performance in stressful conditions results in an increased metabolic rate. Coronary heart disease is one consequence of the increased cardiovascular activity due to psychological stressors (Alderman et al., 2007; Spalding et al., 2004), which is beyond the scope of this study. However, the recovery time from the increased heart rate was analyzed in the following sections. Boregowda and Karwowski (2005) presented a study in which they focused on psychological stressors and their relationship to physiological signals. According to them, stress triggers multiple physiological systems and cannot be explained with a singular physiological signal. In this study, we extended it to investigate the relationship between the multiple physiological signals and the thermal comfort which is also an emotional response.

## 8.1. Skin Temperature

### *8.1.1. Mean Skin Temperature and Thermal Sensation Relationship*

This section focused, first, on the mean skin temperature and its relationship to thermal sensation and comfort in different metabolic conditions and, second, on the minimum feasible number of skin sites to determine mean skin temperature.

The relationship between the thermal comfort and the thermal sensation was established in previous sections. This section presents the relationship between the mean skin temperature and the thermal sensation which will also allow the prediction of thermal comfort. The literature section showed that thermal sensation is a function of mean skin temperature. An analysis regarding the relationship between the mean skin temperature and the thermal sensation was conducted in order to determine the effect of metabolic rate on that relationship. The data was grouped based on the metabolic rate of the subjects. A high metabolic rate condition was represented with two data points in the middle and at the end of each exercise session, during which the metabolic rate peaked at 4 met. A medium metabolic rate condition was represented with five data points after each exercise session, during which the metabolic rate dropped from 4 met to 1.2 met. A low metabolic rate condition was represented with the data points during which the subject was sedentary at 1.2 met.

Table 8.1 shows that different levels of mean skin temperature and metabolic rate generated different thermal sensation values ($p<0.001$). Figure 8.1 shows that thermal sensation increased with the mean skin temperature in all three metabolic conditions. For a given mean skin temperature, higher metabolic rate yielded a higher thermal sensation except around 94°F mean skin temperature (p-value $< 0.001$). Change in mean skin temperature yielded similar changes in thermal sensation for low and medium metabolic rate conditions. However, the change in thermal sensation during the high metabolic conditions was less than the other two conditions.

Table 8.1. ANOVA table for thermal sensation and mean skin temperature with metabolic rate as the grouping factor.

**Dependent Variable: Thermal Sensation**

| Source | Type III Sum of Squares | Degrees of Freedom | Mean Square | F Score | Significance |
|---|---|---|---|---|---|
| Corrected Model | 306.82 | 3 | 102.27 | 126.94 | 0.000 |
| Intercept | 159.89 | 1 | 159.89 | 198.45 | 0.000 |
| Mean Skin Temperature | 171.36 | 1 | 171.36 | 212.69 | 0.000 |
| Metabolic Rate Class | 133.48 | 2 | 66.74 | 82.84 | 0.000 |
| Error | 1674.20 | 2078 | 0.806 | | |
| Total | 2575.04 | 2082 | | | |
| Corrected Total | 1981.02 | 2081 | | | |

$R^2$= .155 (Adjusted $R^2$= .154)

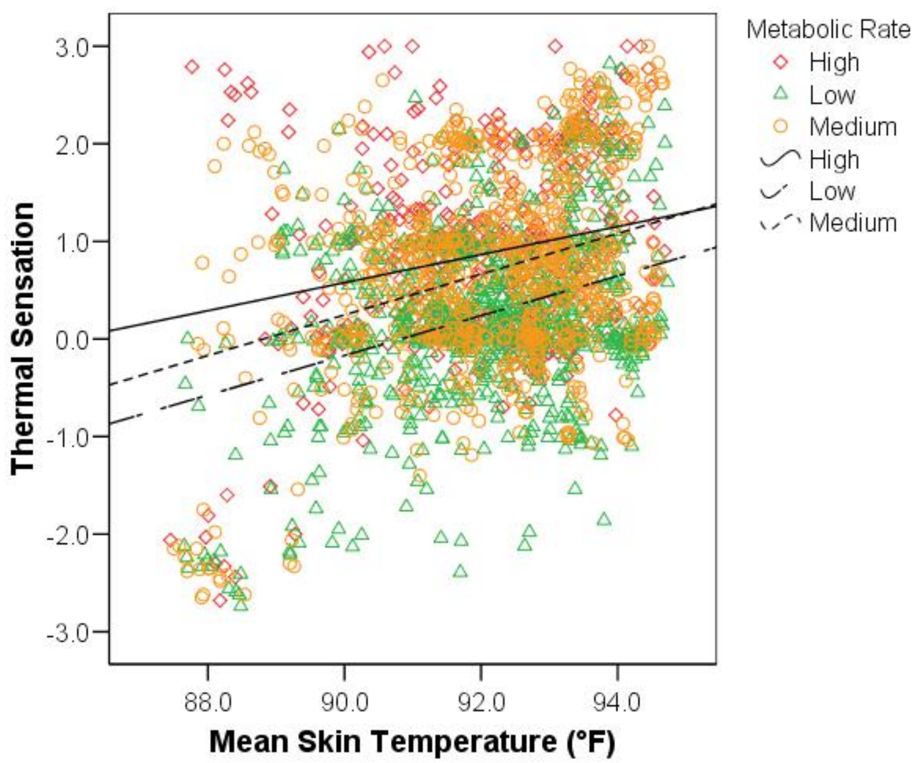


Figure 8.1. The relationship between mean skin temperature and the thermal sensation under three metabolic rate conditions.

### *8.1.2. Mean Skin Temperature Estimation*

Olesen (1984) conducted a stepwise regression analysis to determine the skin temperature sites that can accurately predict the mean skin temperature of the body. The same analysis was conducted in this study but for different metabolic rate conditions (low, medium, and high metabolic rate). First, the mean skin temperature was derived from the average of all fifteen skin temperature sites. Second, a stepwise regression analysis was conducted to determine which skin sites contribute the most to the mean skin temperature for different metabolic rate conditions. The regression equation with minimum number of sites that yield an $R^2$ of 0.990 with the mean skin temperature was recorded for each metabolic condition. Table 8.2 shows the skin temperature sites which are required in the regression analysis to achieve the target $R^2$.

Table 8.2. Skin temperature sites that are correlated with the mean skin temperature for three metabolic rate conditions.

| | **Low Met** | **Medium Met** | **High Met** |
|---|---|---|---|
| Forehead | | | |
| Neck | x | | x |
| Abdomen | x | x | |
| Lower Back * | x | x | x |
| Lower Arm | x | x | |
| Anterior Thigh | x | x | |
| Anterior Calf * | x | x | x |
| Instep * | x | x | x |
| Cheek * | x | x | x |
| Chest | | | |
| Upper Back | x | | x |
| Upper Arm * | x | x | x |
| Hand | | | x |
| Anterio-medial Thigh | x | x | |
| Posterior Calf | | | |

* Common skin temperature sites for three metabolic conditions

Table 8.2 shows that five of the fifteen locations (lower back, anterior calf, instep, cheek, and upper arm) were common skin temperature sites that contribute to the high correlation coefficient for the mean skin temperature. In a second analysis, a multiple regression analysis was conducted between the mean skin temperature and those five skin temperature sites for low, medium, and high metabolic conditions. The correlation coefficients ($R^2$) were 0.93, 0.95, and 0.93, respectively. This analysis showed that it is possible to estimate mean skin temperature, which can be used to determine thermal sensation, with acceptable accuracy by using the skin temperatures of lower back, anterior calf, instep, cheek, and upper arm in various metabolic conditions.

A similar test was conducted to determine the correlations between mean skin temperature and the individual skin sites for 75°F (24°C) and 83°F (28.3°C) room temperatures. Based on this analysis the common skin temperature sites for both temperatures were abdomen, lower arm, instep, cheek, chest, anterio-medial thigh, and posterior calf (Table 8.3). The anterior calf and upper arm of the 75°F (24°C) were replaced by the lower back and upper back in the 83°F (28.3°C) regression. The reason was that two additional torso skin temperature sites represent the general body thermal state better than the two limb locations. In the second step of this analysis, regression analysis between mean skin temperature and the above seven sites was conducted for 75°F (24°C) and 83°F (28.3°C) temperatures. The correlation coefficients ($R^2$) were 0.96 and 0.98 respectively.

Table 8.3. Skin temperature sites that are correlated with the mean skin temperature for two temperature conditions.

| | **75°F/24°C** | **83°F/28.3°C** |
|---|---|---|
| Forehead | | |
| Neck | | |
| Abdomen * | x | x |
| Lower Back | | x |
| Lower Arm * | x | x |
| Anterior Thigh | | |
| Anterior Calf | x | |
| Instep * | x | x |
| Cheek * | x | x |
| Chest * | x | x |
| Upper Back | | x |
| Upper Arm | x | |
| Hand | | |
| Anterio-medial Thigh * | x | x |
| Posterior Calf * | x | x |

* Common skin temperature sites for three metabolic conditions

Combining the analysis for different metabolic rate levels and temperatures, it was concluded that ten skin temperature sites (i.e. abdomen, lower back, lower arm, anterior calf, instep, cheek, chest, upper arm, anterio-medial thigh and posterior calf) can adequately represent mean skin temperature in a variety of temperature and metabolic rate conditions.

### *8.1.3. Skin Temperature Setpoints and Variations*

Zhang et al. (2004) defined a skin temperature setpoint for each body regions which was the skin temperature during the neutral body condition. The authors investigated the thermal sensation of each body segment's weight on the overall thermal sensation. Following the same methodology, we calculated the skin temperature setpoint for each body segment as well as the deviations from that setpoint for the course of the test. We hypothesized that a positive difference ($T_n$-$T_{setpoint}$) of skin temperature correlates with the warm sensation and a negative difference with the cool sensation. Toftum and Nielsen (1996) similarly stated that cold and warm receptors register the absolute skin temperature and the rate of change of skin temperature. Griefahn et al. (2001b) found a neck skin temperature drop of 3°F (1.7°C) with the increase of air velocity to 60 ft/min (0.3 m/s) from 20 ft/min (0.1 m/s). Similarly forearm temperature dropped by 0.7°F. General thermal sensation dropped by 0.25 (from -0.05 to -0.3) points for the same amount of increase in air velocity.

Figure 8.2 shows the difference between the skin temperature and the skin temperature setpoint for different regions of the body. The leg and the foot instep experienced the largest increase in temperature in the long term (up to 1.5 hours) due to the increased muscle activity for exercising. The foot instep, leg, and the hand showed the highest short-term (up to 10 minutes) variations around the exercise periods. This is expected since limbs are the most effective in maintaining homeostasis through vasodilatation and vasoconstriction. The chest skin temperature was relatively stable with some variations up to 0.3°F. This was also expected since torso region was slower to respond to the transient conditions. The neck temperature steadily increased during the first 45 minutes of the test during which no airflow treatment was applied. The airflow treatment started at the 45$^{th}$ minute which resulted in an overall decrease in neck skin temperature. The total drop in neck temperature after the start of airflow treatment was approximately 1°F (0.5°C) (Figure 8.3) which is lower than Griefahn et al. (2001b) who found 3°F drop in neck temperature. Figures 8.4 through 8.7 show the changes in the skin temperatures for all the body parts grouped by the region.

The head-only airflow was more effective in decreasing the neck temperature than the simultaneous airflow (p-value 0.004). This was expected since the neck region received higher air velocities during the head-only airflow. In general, by the end of the test, the airflow treatment effectively dropped the neck temperature to the same temperatures as the start of the test. This is significant considering the initial rise of temperature in the first 40 minutes of the test and the high metabolic rate in the last 70 minutes of the test.

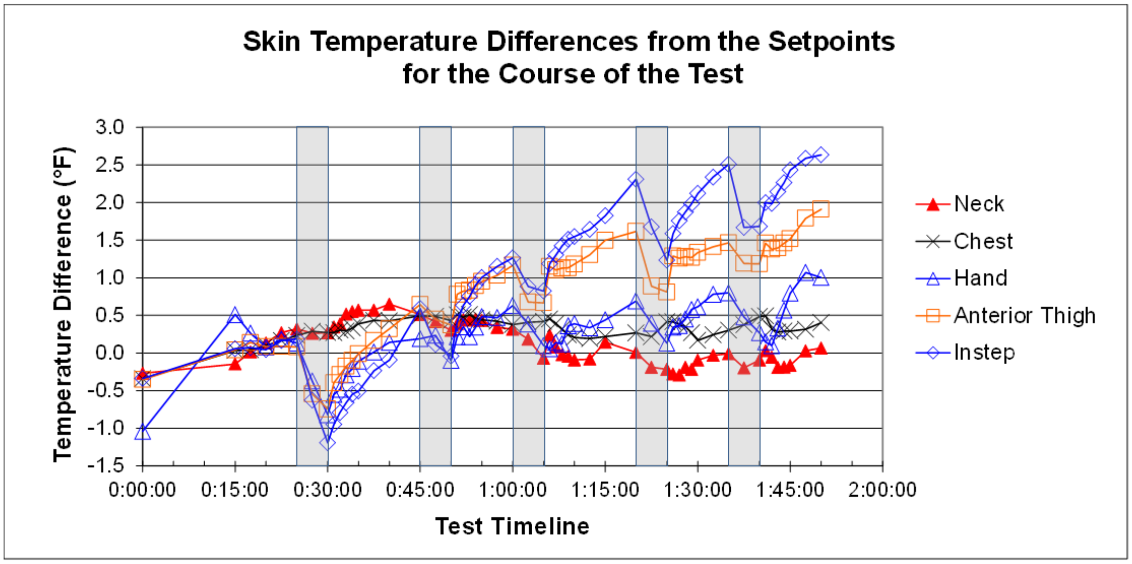


Figure 8.2. Differences between the skin temperatures and skin temperature setpoints for the course of the test.

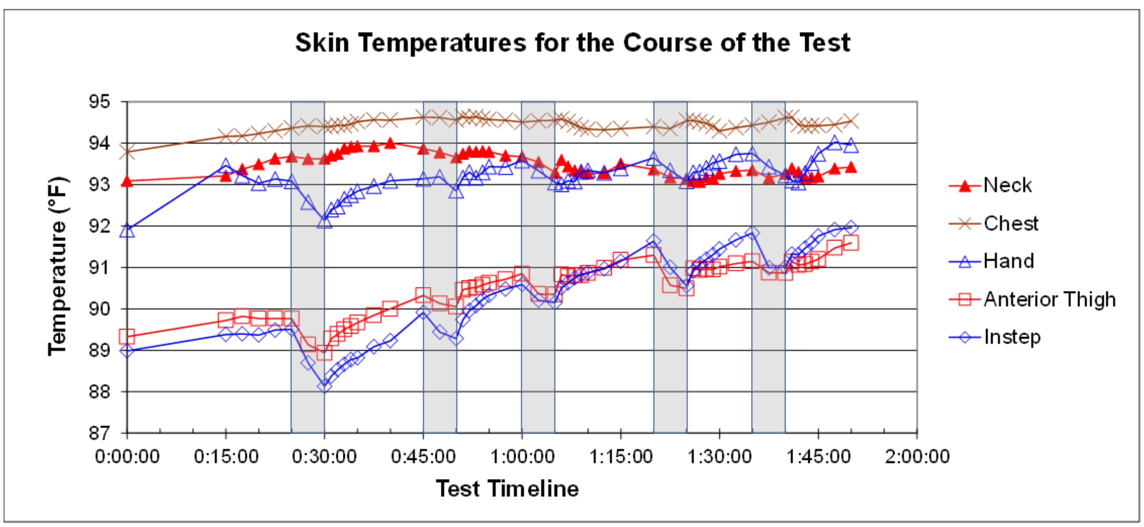


Figure 8.3. Skin temperatures for five locations.

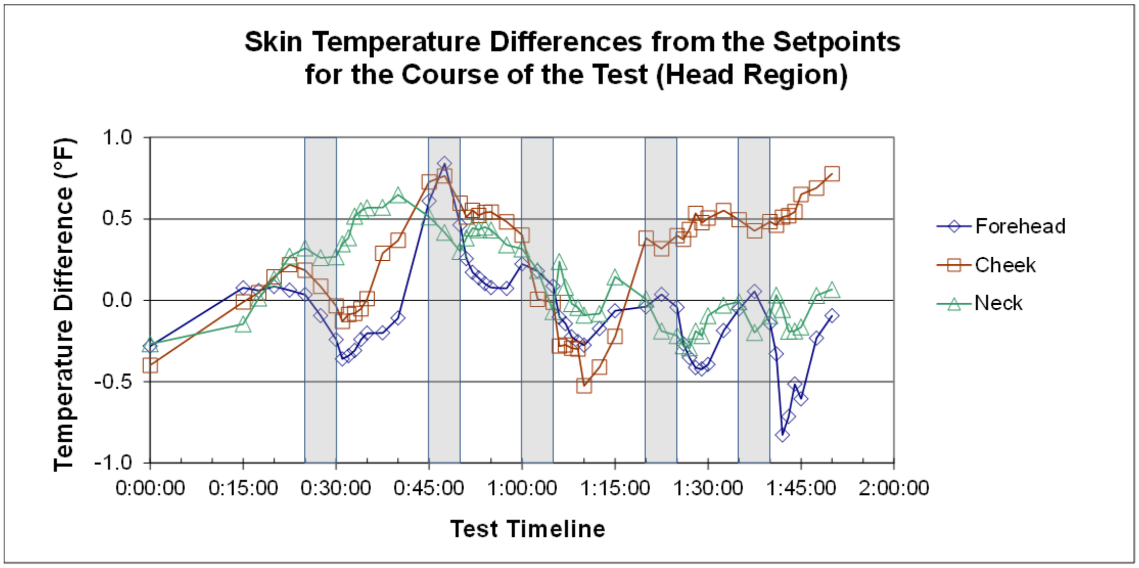


Figure 8.4. Head region temperature differences between the skin temperatures and skin temperature setpoints.

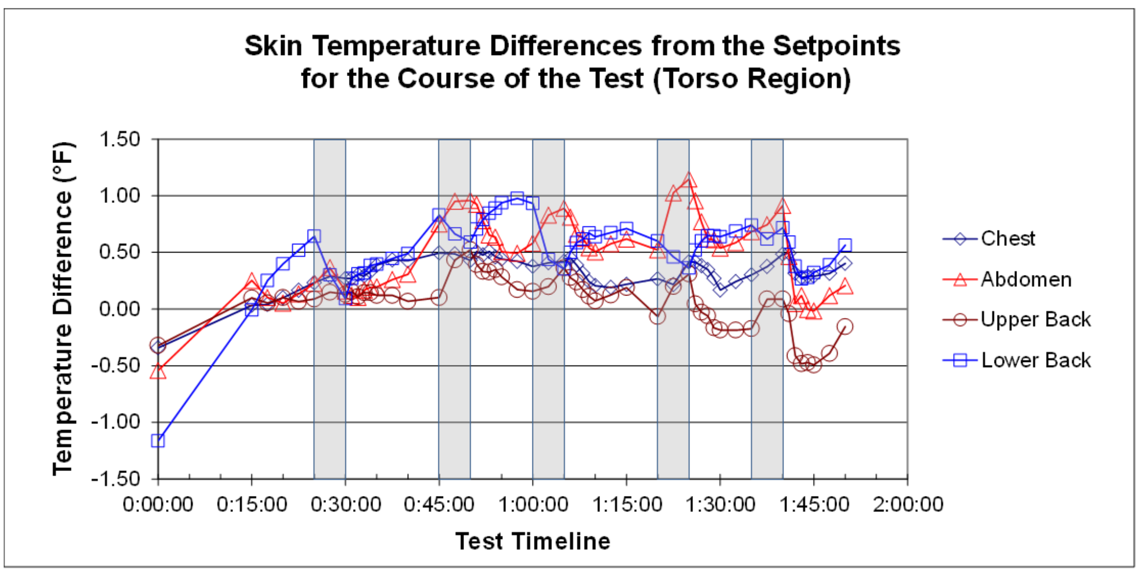


Figure 8.5. Torso region temperature differences between the skin temperatures and skin temperature setpoints.

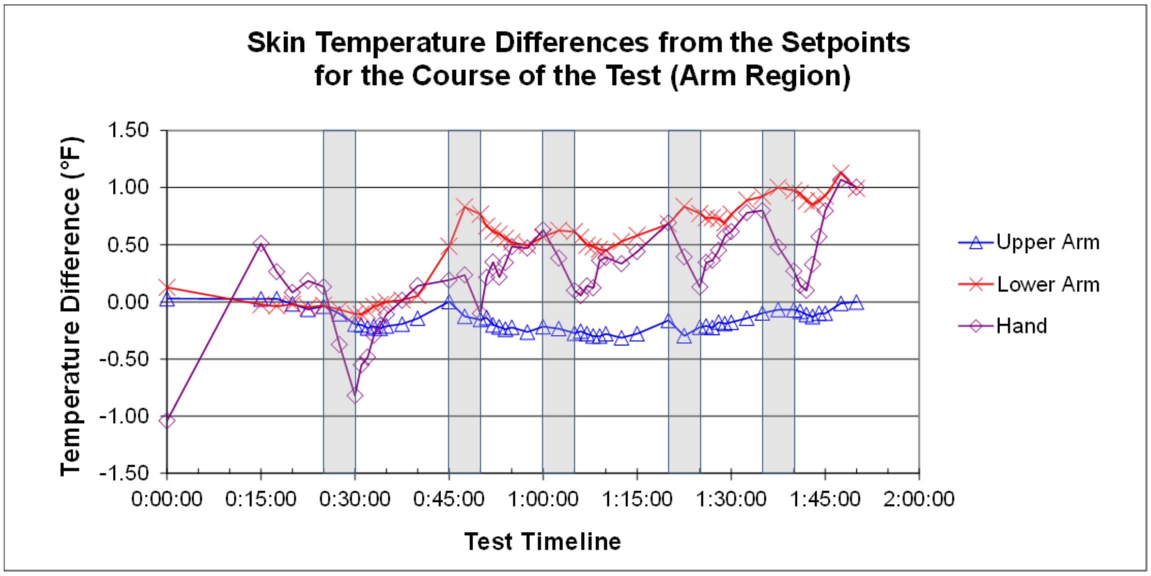


Figure 8.6. Arm region temperature differences between the skin temperatures and skin temperature setpoints.

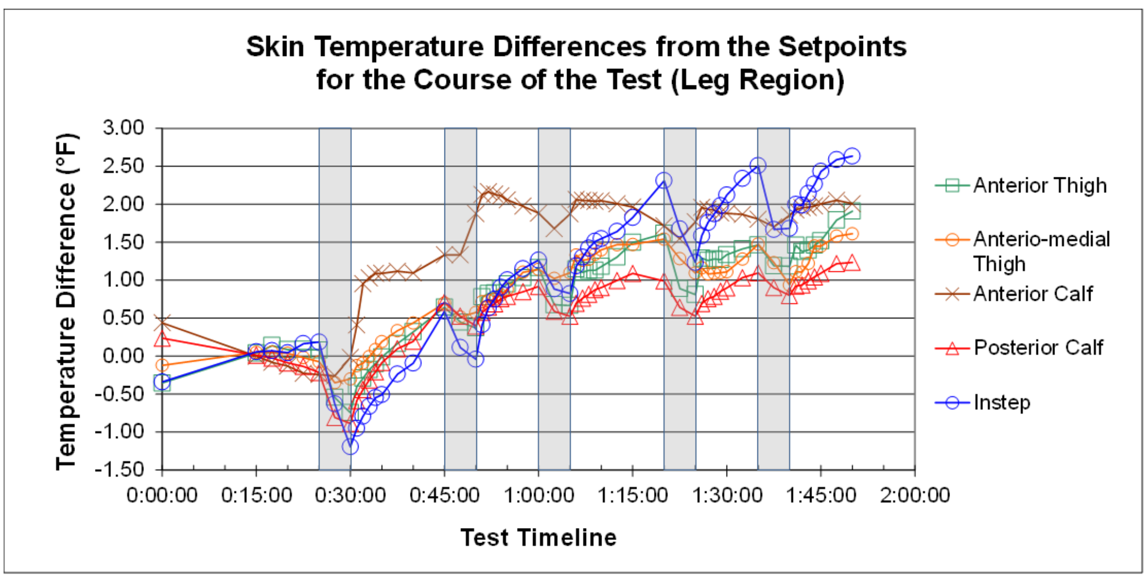


Figure 8.7. Leg region temperature differences between the skin temperatures and skin temperature setpoints.

A stepwise regression analysis of the thermal sensation's relationship to the deviations from setpoint temperature for each body region showed that eight of the fifteen body regions were the most effective in determining the thermal sensation ($R^2$= 0.431). Those body regions were the forehead, lower arm, instep, upper back, posterior calf, anterior thigh, anterior-medial thigh, and the chest (Table 8.4). It is worth noting that four out of eight locations belong to the leg and foot region. This result is meaningful considering the fact that the subjects pedaled to increase the metabolic activity. A second regression analysis between the thermal sensation and skin temperatures for the same sites showed a lower correlation ($R^2$: 0.186). This supported the fact that thermal sensation depends more on the deviations from the setpoints since more cold or warm warnings are generated as the skin temperature deviates from steady conditions.

Table 8.4. Regression coefficients of deviations of different skin temperatures from setpoints in determining the thermal sensation.

| **Differences between the skin temperatures and the setpoints** | **Unstandardized Coefficients** | | **Standardized Coefficients** | **t score** | **Significance** |
|---|---|---|---|---|---|
| | B | Std. Error | Beta | | |
| (Constant) | 0.380 | 0.035 | | 10.797 | 0.000 |
| ForeheadT - ForeheadSetpointT | -0.153 | 0.030 | -0.150 | -5.166 | 0.000 |
| LowerArmT - LowerArmSetpointT | 0.144 | 0.041 | 0.102 | 3.553 | 0.000 |
| InstepT – InstepSetpointT | 0.141 | 0.014 | 0.306 | 9.943 | 0.000 |
| UpperBackT - UpperBackSetpointT | 0.121 | 0.012 | 0.353 | 10.279 | 0.000 |
| PosteriorCalfT - PosteriorCalfSetpointT | -0.142 | 0.027 | -.152 | -5.271 | 0.000 |
| AnteriorThighT - AnteriorThighSetpointT | 0.103 | 0.023 | .162 | 4.505 | 0.000 |
| AntMedialThighT - AntMedialThighSetpointT | -0.052 | 0.019 | -0.080 | -2.742 | 0.006 |
| ChestT – ChestSetpointT | 0.116 | 0.037 | 0.118 | 3.174 | 0.002 |

Regression analysis showed that both mean skin temperature (MST) and the derivative of the mean skin temperature (dMST) have significant effect on thermal sensation (p<0.001) (Table 8.5). This is consistent with Zhang (2003a). The final model for thermal sensation on 7-point ASHRAE scale is

$$ThermalSensation = 0.20 * MST - 0.36 * dMST - 17.86 \quad (9.1)$$

where, *MST* is the mean skin temperature (°F), and *dMST* is the derivative of the mean skin temperature with respect to time (°F).

Table 8.5. Parameter estimates for thermal sensation based on MST and dMST.

| | | | | | 95% Confidence Interval | |
|---|---|---|---|---|---|---|
| **Parameter** | **B** | **Std. Error** | **t** | **Significance** | **Lower Bound** | **Upper Bound** |
| Intercept | -17.86 | 1.28 | -13.91 | 0.000 | -20.38 | -15.34 |
| MST | 0.20 | 0.01 | 14.34 | 0.000 | 0.17 | 0.23 |
| dMST | -0.36 | 0.09 | -3.93 | 0.000 | -0.54 | -0.18 |

We compared skin temperatures of body regions from our study to the skin temperatures from the literature (Houdas and Ring, 1982; Arens et al., 2006a; Yao et al., 2008). Figure 8.8 shows that the temperatures in our sedentary/neutral conditions were lower than the temperatures of Arens et al. This difference may be due to the higher evaporation rate at our subjects' skin surface since the average room temperature in our analysis was higher than that of Arens et al. Further research is required to determine the effect of skin wettedness on skin temperature. The comparison of overall and neutral/sedentary condition skin temperature averages for our test showed that the leg and foot regions of the body have the highest deviation from the neutral conditions. This conclusion also supports the previous argument of Kistemaker et al. (2006) and McIntyre (1980) who showed that the exercising muscle's temperature increases more than the other parts of the body.

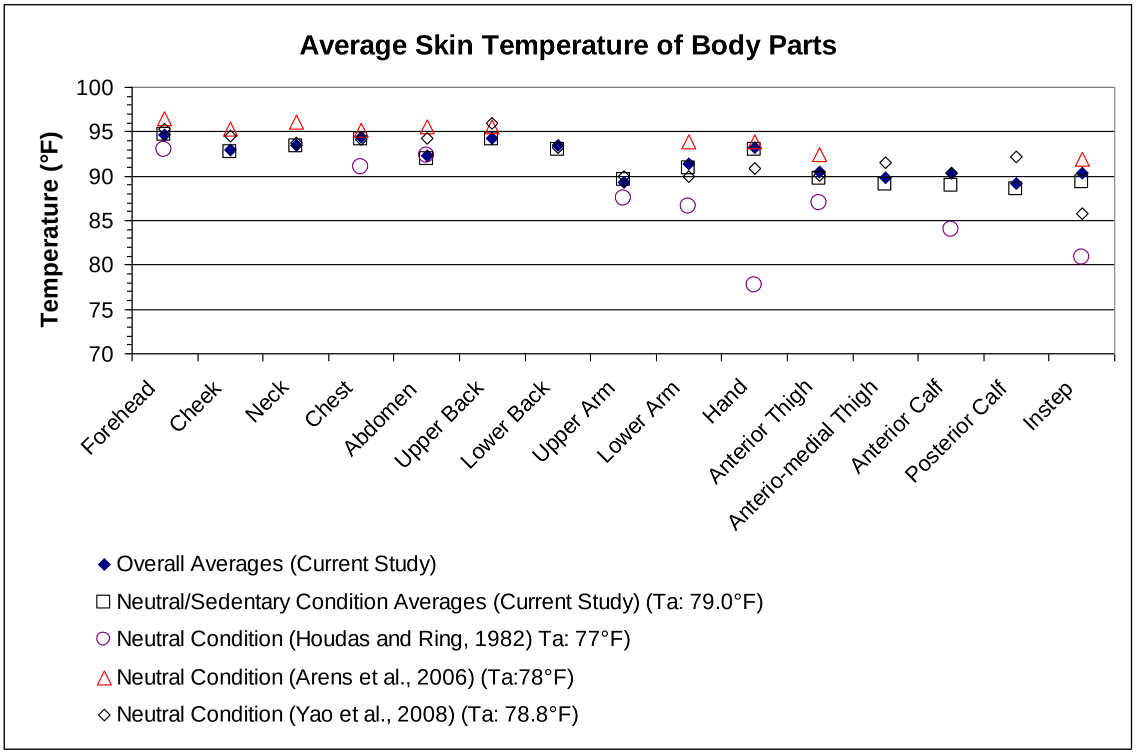


Figure 8.8. Comparison of average skin temperatures for the sedentary/neutral conditions and for the overall test of the current study with Houdas and Ring (1982), Arens et al. (2006a), and Yao et al. (2008).

## 8.2. Heat Balance and Local Heat Loss of the Human Body

An analysis was conducted to determine the heat balance of the body and its effect on thermal comfort. First, we determined whether there is heat storage within the body or not. Second, we determined the amount of heat that was transferred from the core to the skin and its effect on thermal comfort. In the last stage, we conducted an analysis of local and general heat loss to the environment and their effect on general thermal sensation.

### *8.2.1. Core Body Temperature*

A number of steady state and transient human thermal models were presented in the literature section. Those models are based on the heat balance of the human body with the environment, some of which have capabilities of calculating heat storage inside the body. In this section, a heat balance analysis of the human body based on the specific test conditions was presented.

The amount of heat stored inside the body is calculated through the increase in body temperature. The tympanic temperature measurements showed that the core body temperature is relatively stable throughout the test (Table 8.6) and the difference between the measurements was statistically insignificant. Therefore, there was no heat storage inside the body between the body temperature measurements and all the generated heat was dissipated to the environment through conduction, convection, radiation and evaporation.

Table 8.6. Body core temperature throughout the test.

| | **Mean Body Temperature (°F)** | **Body Temperature Std. Dev. (°F)** |
|---|---|---|
| Before the Test | 97.89 | 0.83 |
| After the 1st Session | 97.70 | 0.79 |
| After the 2nd Session | 97.74 | 0.87 |
| After the 3rd Session | 97.91 | 0.78 |

### *8.2.2. Evaporative Heat Loss*

Weights of the subjects were measured before and after the test and there was no food or liquid intake between the measurements. Male subjects lost 0.32 lbs, while female subjects lost 0.42 lbs on average (Table 8.7). The difference between the genders was significant at $\alpha$=0.05 (p-value < 0.001). There was no dripping of sweat during the tests and all the sweat was held by the clothing. Therefore, the weight loss was due to the evaporation of the sweat from the skin surface and the lungs. The total energy that was lost due to the evaporation of water was calculated by:

$$EvaporativeHeatLoss = F * m \tag{9.2}$$

where $m$ is the weight of water in lbs, and $F$ = 281.4 Wh/lbs which is the amount of energy required to vaporize 1 lb of water.

Table 8.7. Weight loss (lbs) of the subjects during the test.

| Gender | Mean Weight Loss (lbs) | Weight Loss Std. Dev. (lbs) |
|---|---|---|
| Male | 0.32 | 0.20 |
| Female | 0.42 | 0.35 |

Based on Equation 9.2, the evaporative heat losses for males and females were calculated as 90 Wh and 118 Wh respectively (Table 8.8). In this case, males' latent heat loss was 25% and sensible heat loss was 75%. For females, latent heat loss was 36% and sensible heat loss was 64% of the total heat loss.

Table 8.8. Evaporative and overall heat loss for males and females.

| Gender | Average Met | Average Surface Area ($m^2$) | Duration of Test (hour) | Total Energy Exerted (Wh) | Evaporative Heat Loss (Wh) |
|---|---|---|---|---|---|
| Male | 1.9 | 1.8 | 1.85 | 368 | 90 |
| Female | 1.9 | 1.6 | 1.85 | 327 | 118 |

### *8.2.3. Heat Transfer between the Body Core and the Skin Surface*

An analysis was conducted to determine the relationship between the heat conduction through the body and the thermal comfort. The difference between core temperature and the mean skin temperature ($\Delta T_{cr-sk}$) was normalized for body mass index (BMI) to take into account the insulation properties of the body. A significant correlation was detected between the $\Delta T_{cr-sk}$ and the thermal comfort at $\alpha$=0.05 (Pearson correlation: -0.254). Figure 8.9 shows the relationship between the two variables. The correlation was also significant without BMI normalization, however, with a lower correlation coefficient (Pearson correlation: -0.219). This shows that thermal discomfort increases with the increased thermal strain on the body, which is the difference between the core and the skin temperature.

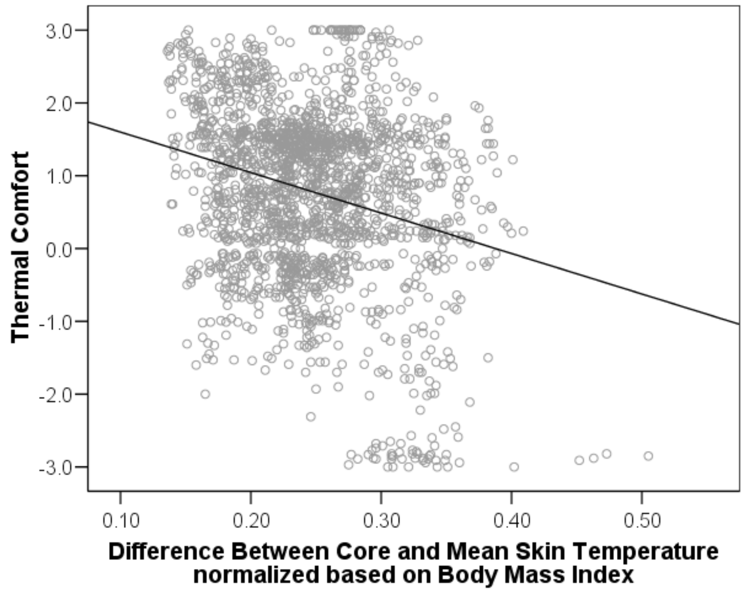


Figure 8.9. Correlation between thermal comfort and the difference between core and mean skin temperature as normalized based on body mass index.

### *8.2.4. Local Heat Loss from the Skin Surface to the Environment*

The thermal environment around the body is not uniform most of the time and different parts of the body are usually exposed to different thermal conditions. An analysis was conducted in order to test the effect of local heat loss on general thermal sensation. Ambient temperatures were measured at the head level, next to the hand, and next to the feet. Forehead, neck, and cheek skin temperatures were averaged to represent the head region. Lower arm and hand thermoreceptors were averaged to represent the hand region. Anterior calf, posterior calf, and instep skin temperatures were averaged to represent the foot region. The temperature difference between the skin and the environment was calculated for all three regions. Local temperature differences were then correlated to the general thermal sensation. Local temperature losses from all three locations have statistically significant correlation to the general thermal sensation. However, the strongest correlation was with the foot heat loss (Pearson correlation: -0.276). Although significant, correlations for hand heat loss (Pearson correlation: -0.102), and head heat loss (Pearson correlation: -0.142) were relatively weak. The result of this analysis suggests that local conditions can be designed to positively impact the thermal sensation of the people in buildings.

### 8.3. Heart Rate and Electrodermal Activity (EDA)

In this section, an analysis was conducted to determine the relationships between the heart rate, electrodermal activity (EDA), and the subjective thermal responses. For the analysis, data from the first 25 minutes of the test was used, during which subjects were sedentary. In the first 15 minutes, subjects were in a relaxed state with closed eyes and without any activity. The nonsedentary conditions were not included in this analysis since increased body activity triggers multiple physiological mechanisms which may interfere with the relationships between the previously mentioned variables. Tests were conducted in 75°F (24°C) and 83°F (28.3°C) room temperatures. We conducted ANOVA calculations to determine whether increased skin wettedness due to the higher room temperature has any effect on EDA measurements. Five-second integrated average EDA values were 1.18 µS and 1.10 µS for 75°F (24°C) and 83°F (28.3°C). The difference was significant ($p=0.004$) but negligible for the purposes of this study. It was concluded that increased sweat activity in higher temperatures do not interfere with the EDA measurements.

The traditional approach to determining metabolic conditions in thermal environment design is to assign a metabolic rate based on the nature of the activity in the environment. This approach assumes stable conditions so long as the activity remains the same. ISO 8996 (2004) suggests a time averaged approach if the type of activity is variable in an environment. In order to validate this assumption, we analyzed the heart rate and metabolic rate data. Results showed that even when there was minimal activity, the heart rate still fluctuated within ±7 beats per minute (bpm) which was equal to the momentary metabolic rate fluctuations of ±0.17 met. The average heart rate among all the subjects stayed relatively stable during the same period (±1 bpm). ANOVA showed no significant difference of average heart rate between different periods of the first 25 minutes of the test ($p=0.388$).

The effect of psychological stress on heart rate was presented in the previous studies (Andreassi, 2000; Spalding et al., 2004; Alderman et al., 2007). The psychological stress increases heart rate which increases energy expenditure. This assumption was tested for the sedentary first 25 minutes of the test and a significant ($p<0.001$) correlation between EDA and heart rate was detected (Pearson correlation: 0.333).

One of the hypotheses of this study was that thermal comfort is a psychological phenomenon; therefore, EDA can explain the variability in thermal comfort. ANOVA was conducted and no correlation was detected between the EDA and the thermal comfort ($p=0.385$). On the other hand, a statistically significant ($p<0.001$) but weak correlation was detected between the EDA and the thermal sensation.

Analysis of the EDA data together with the thermal comfort and the thermal sensation data for the duration of the whole test revealed significant information (Figure 8.10). The EDA was very sensitive to occurrences of events. There was a sudden increase at the 15$^{th}$ minute when the subject was asked to resume normal activity after the relaxed period. Similarly, there were sudden EDA responses at the onset of each exercise session which recovered towards the middle of the exercise session. It was clear that the onset of the exercise was perceived as a disturbance by the subjects. EDA increased in the second half of each exercise session due to the thermal strain. EDA recovered within 2.5 minutes after the exercise stopped. Onset of the second exercise period in session 2 and session 3 yielded a significantly higher EDA response than the onset of the first exercise periods. This can be explained with two theories. The first one is the short-term memory of unpleasant past experiences (which was the exercise in this case) which caused heightened response in the repeated occurrences. The second one is the residual arousal theory which was presented by Cacioppo et al. (1987). According to this theory, people present amplified responses to external stimulus, if that stimulus occurs during the recovery period from a psychophysiological stressor. The recovery period is usually 6-8 minutes. Based on this theory, it is possible for the subjects to show heightened response to the onset of the second exercise, if it fell under the recovery period of the previous exercise period. In the meantime, thermal comfort and thermal sensation recovered within 8-10 minutes after the ending of each exercise session.

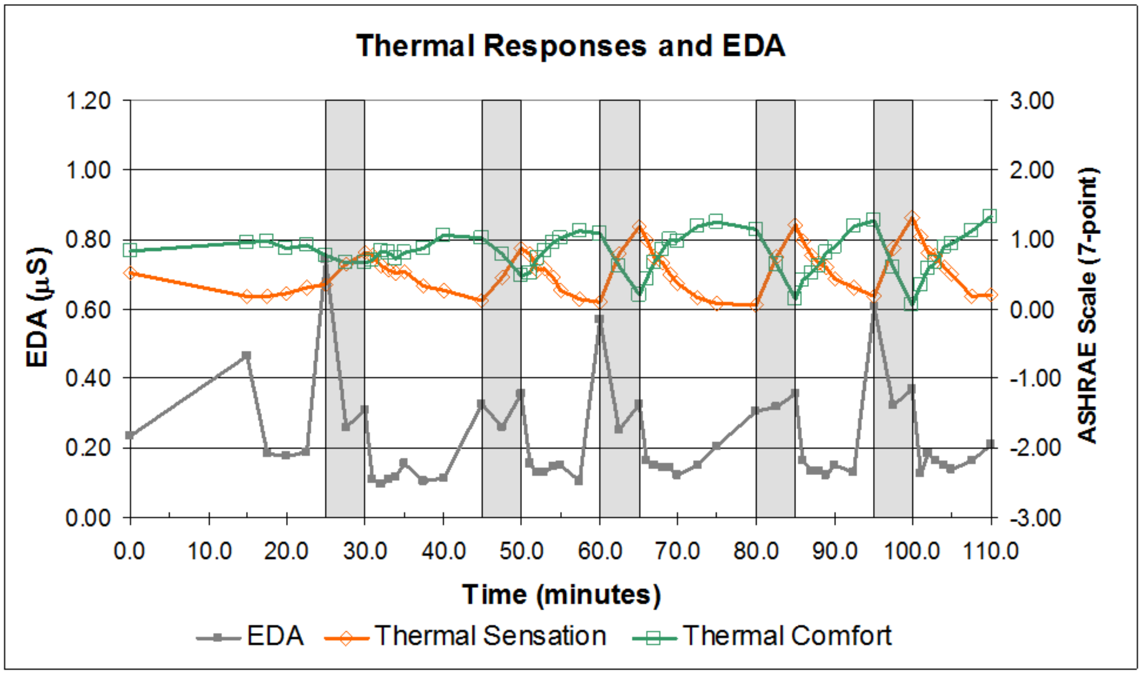


Figure 8.10. Thermal responses and EDA data for the duration of the whole test.

Detailed analyses of physiological variables were conducted for metabolic transients of the first exercise session (Figure 8.11). As mentioned previously, there exists a sudden EDA response at the onset of exercise which started recovering shortly after with a time constant of approximately 1.5 minutes. EDA started increasing towards the middle of the exercise session. This increasing behavior closely followed the heart rate pattern and was due to the physiological strain. EDA returned to pre-exercise values at the 9$^{th}$ minute after the exercise period ends. In some cases, this recovery period might overlap with the next exercise session which yielded amplified responses to external stimulus based on the residual arousal theory. Thermal comfort and thermal sensation values returned to pre-exercise values also at the 9$^{th}$ minute after the end of the exercise period, with a time constant of six minutes. The mean skin temperature dropped during the exercise period. This was expected since blood was directed to the exercising muscles which caused a drop in the skin temperature. The mean skin temperature returned to the pre-exercise level at the 6$^{th}$ minute after the exercise with a time-constant of four minutes. This was slightly shorter than the five minutes that Houdas and Ring (1982) found as the time constant for skin temperature recovery in transient environmental conditions.

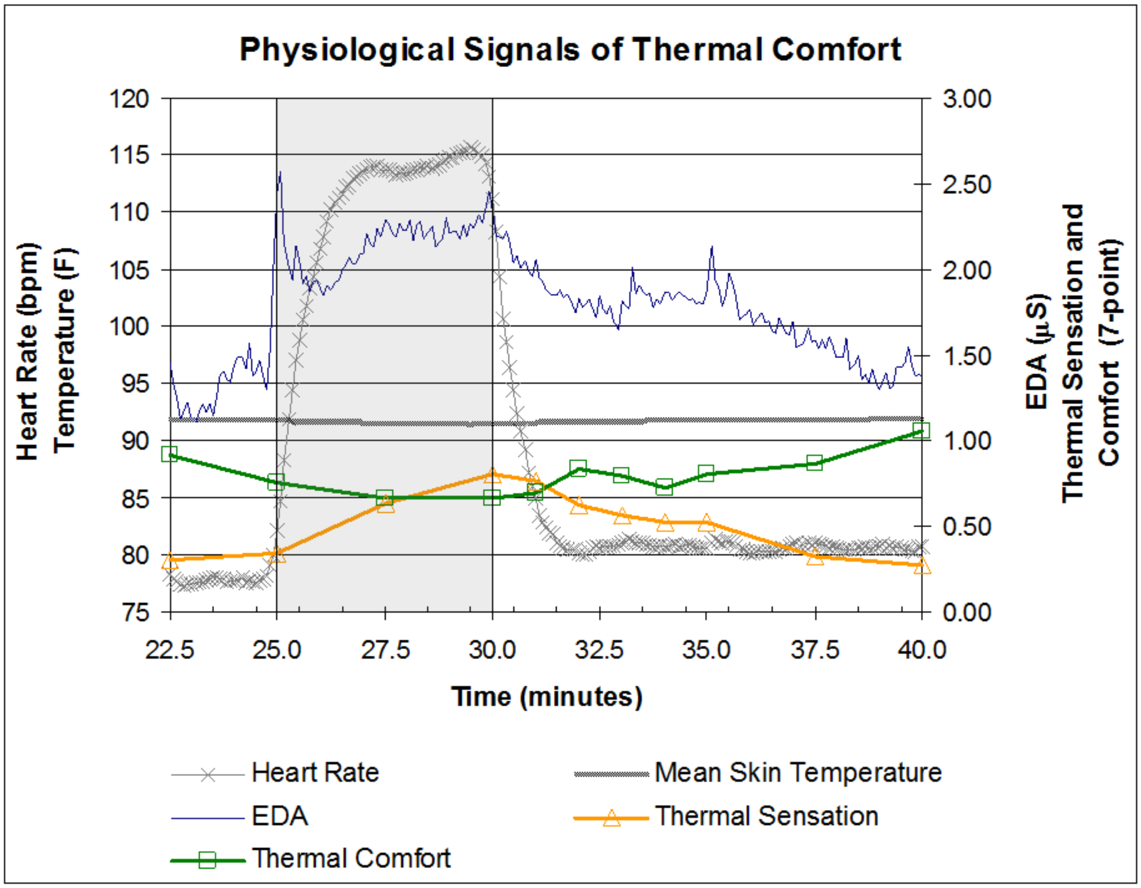


Figure 8.11. Transient behavior of physiological signals and thermal responses.

### 8.4. Diurnal Variations of Psychophysiological Factors

Thermal comfort tests were conducted at three different times during the day. Subjects arrived at the test location at 8:30 am, 11.30 am, or 2.30 pm. Diurnal variations of skin conductance level and skin temperature was documented in a previous study (Hot et al., 1999). We tested the diurnal variations of EDA, mean skin temperature, thermal comfort and thermal sensation. Figure 8.12 shows the values and the significant differences between the test times. EDA was significantly higher in the afternoon than in the morning or at noon. Mean skin temperature was the highest at noon and lowest in the morning. These results were similar to Hot et al.'s findings of skin conductance level and skin temperature. Following a similar trend of the mean skin temperature, thermal sensation was the warmest during the noon tests and the lowest during the morning tests. The relationship between thermal sensation and mean skin temperature was already presented earlier in this study. Thermal comfort, on the other hand, was significantly lower during the morning than at noon and during the afternoon. Results of this analysis suggested that people's physiological signals change throughout the day, which was supported with their subjective responses. Different thermal conditions are required depending on the time of the day regardless of the outdoor conditions. Therefore, air conditioning strategies should take into account this variability.

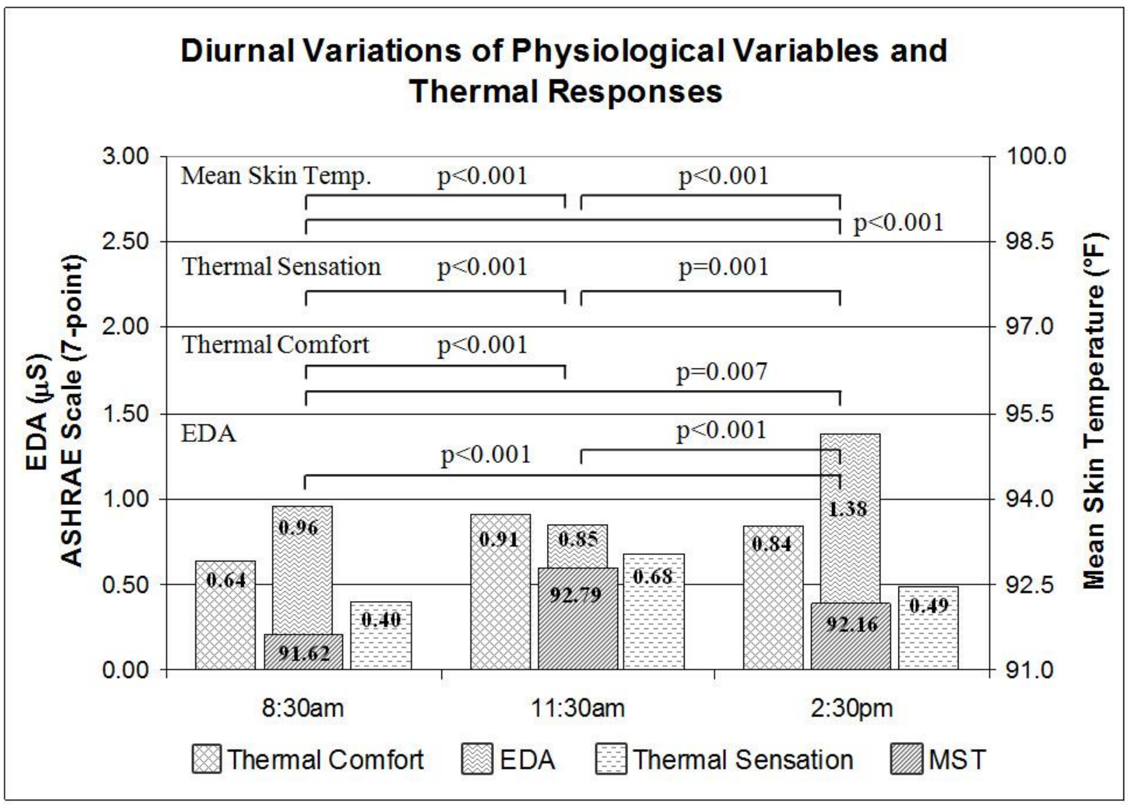


Figure 8.12. Diurnal variations of mean skin temperature, thermal sensation, thermal comfort and electrodermal activity.

## 8.5. Discussion

In this section, the psychophysiological signals and their relationship to subjective thermal responses were investigated. The human body responds to physical and psychological changes with different physiological signals. Heart rate, electrodermal activity (EDA), skin temperature, core temperature, and skin wettedness are among those signals which have direct relationship to the thermal environment perception. All the above variables, except the EDA, are parts of the human body heat balance with the environment.

Skin is the interface between the body and the environment, and is the most important sensory organ which houses cold and warm thermoreceptors. Thermoreceptor response is affected by both the condition of the body as well as the environment. Thermal sensation is the perception of the thermal conditions based on the integration of the skin and deep body thermoreceptors. This study showed a significant relationship between the mean skin temperature and the thermal sensation for different metabolic rate conditions. The relationship depends on both the absolute as well as the derivative of the skin temperature. These findings were also consistent with thermoreceptor responses which have a static and a dynamic component based on the absolute temperature and the change in the temperature.

Since thermal sensation is based on the skin temperature and thus the thermoreceptor response, it is possible to manipulate thermal sensation by changing the skin temperature conditions. Stimulating the cold receptors at varying levels is a strategy which can yield sensation of coolness while avoiding thermoreceptor adaptation. Thermoreceptor and thermal sensation adaptation occur when there is a constant stimulus on the skin (Greenspan et al., 2003; Ring et al., 1993). Preventing skin thermoreceptors to adapt improves the effectiveness of the external stimulus. Changing the skin temperature to desired conditions can be a viable strategy in thermal environment design. The same principles can be incorporated to the physical design of the occupied space in the form of cool or warm surfaces.

In this section, three analyses were conducted regarding the skin temperature. The first analysis focused on the relationship between thermal sensation and the mean skin temperature. It was shown that thermal sensation increases linearly with the increased mean skin temperature in all metabolic rate conditions. The second analysis focused on the determination of mean skin temperature from individual skin temperature sites. Following Olesen's (1984) methodology, correlations were developed between the skin sites and the mean skin temperature for three metabolic rates and two temperature conditions. Taking Olesen's method one step further, the minimum number of sites that generated a $R^2$=0.990 correlation with the mean skin temperature were determined. Five locations (i.e. lower back, anterior calf, instep, cheek, and upper arm) were determined as the common sites for all metabolic rate conditions. Therefore, these five sites can be used to determine mean skin temperature with $R^2$>0.93 in various metabolic conditions. A similar methodology was applied to determine common skin temperature sites for 75°F (24°C) and 83°F (28.3°C). The abdomen, lower arm, instep, cheek, chest, and the anterio-medial thigh were the sites which correlated with mean skin temperature ($R^2$>0.96). Therefore, depending on the character of the thermal environment, five or six (or ten when combined altogether) skin sites can give an accurate estimation of mean skin temperature. As a general rule skin temperature sites, which deviate more from their neutral temperature should be excluded in mean skin temperature calculations when only a small number of measurement sites are feasible. Because, skin sites that deviate more than average do not represent the average skin temperature conditions. The third analysis was conducted to determine the relationship between the thermal sensation and individual skin temperature sites. Individual skin sites showed unique behaviors for different metabolic conditions. The most prominent behavior was the highest temperature fluctuations in the exercising muscles (anterior thigh, instep). The same locations also experienced the most drop in skin temperature due to the highest evaporation rate of sweat. These results were consistent with Kistemaker et al. (2006) and McIntyre (1980). Hand skin temperature also fluctuated more than the other sites due to the thermoregulatory function of the limbs. Zhang (2003a) also found high temperature fluctuations for hands and feet but also stated that they contribute less to the overall thermal sensation. However, a stepwise regression analysis showed in this study that temperature deviations of forehead, lower arm, instep, upper back, posterior calf, anterior thigh, anterio-medial thigh, and chest correlate best with the thermal sensation. Four out of eight locations belong to the exercising sites of the body. Zhang's statement should be improved such that in the case of muscle activity, skin temperature sites in predicting thermal sensation should be biased towards the exercising muscle locations.

As stated previously, the neck and the shoulders have the highest number of cold thermoreceptors, and therefore are the most sensitive to the skin cooling (Wang et al., 2007). In addition, cold and warm thermoreceptors register rate of change and the absolute skin temperature (Toftum and Nielsen, 1996). A study by Arens et al. (2006a) showed that general thermal sensation in slightly warm environments followed the thermal sensation of the head region. Based on the these information from the literature, we decided that neck temperature was a significant indicator of the general thermal sensation and restoring it to its setpoint temperature would also mean restoring thermal sensation to the sedentary/neutral levels. An analysis was conducted of the different regions' skin temperatures and their deviations from their setpoints. The results showed that the neck skin temperature was effectively restored to its setpoint temperature at the end of the test which was consistent with the neutral thermal sensation. On the other hand, anterior thigh, hand, and instep skin temperatures consistently increased over their setpoints until the end of the test.

Heat balance analyses were conducted including heat generation, heat storage, and heat transfer between the body core and the skin surface and between the skin surface and the local environment. Tympanic temperature measurements showed that there was no significant change in the core body temperature. The body was able to release the generated heat; therefore, heat storage was neglected. This statement can also be supported with the skin temperature. The skin temperature kept rising during the metabolic transients and didn't reach a plateau. This means skin wettedness didn't reach unity (maximum skin wettedness, w=1.0) which would stabilize skin temperature at a steady temperature. Therefore, it was concluded that the body could handle more heat generation before it started storing heat. A second analysis on heat transfer between the core and the skin showed that thermal comfort was negatively correlated with the temperature difference between the core and the skin surface ($\Delta T_{cr-sk}$). A new index was proposed which is $\Delta T_{cr-sk}$ normalized based on body mass index (BMI). BMI in this index represented the insulation properties of the mass and the heat transfer surface from core to the skin. In the final analysis of the heat balance section, thermal sensation was correlated to the local heat loss from the head, hands and the feet. This analysis was based on the temperature difference between the local body section and the immediate local environment. All significant relationships were detected between the three body parts heat loss and the thermal sensation. However, the strongest relationship was with the feet heat loss (Pearson correlation: -0.276).

These results showed the potential for thermal environment design. Local conditions in the occupied spaces can be designed to control heat loss from specific parts of the body to change thermal sensations without having to cool or warm the whole space. This can have significant energy savings since less conditioned air would be used for comfort.

The final section of this study focused on the diurnal variations of the physiological signals and the thermal environment perception. Tests were conducted at three different times of the day starting at 8:30 am, 11:30 am, or 2:30 pm. Statistically significant differences of variables exist between the test times. The coolest thermal sensation and the lowest thermal comfort occurred during the morning test. This can be associated with the low metabolic heat generation in the morning hours than the afternoon hours. In the meantime, EDA was significantly higher during the afternoon test than the morning and the noon tests. This was associated with the higher mental activity during the afternoon hours. The human body was physiologically more active in the afternoon than in the morning hours. This was also supported by the heart rate measurements. The mean heart rate of the afternoon test subjects was 1.1 bpm higher than the morning test subjects. The difference was significant at $p=0.001$. Mean skin temperature was at highest during the noon compared to the other two test times. Hot et al. (1999) achieved similar results in their measurements of skin conductance level and skin temperature. Analysis of diurnal variations of physiological and subjective thermal variables clearly showed that people have different thermal comfort needs depending on the time of the day. Mechanical systems should be designed to allow changes during the day based not only on the outdoor conditions or interior thermal loads but also on the psychophysiological condition of the building occupants.

# 9. COMPUTATION FLUID DYNAMICS (CFD) SIMULATIONS OF THE THERMAL ENVIRONMENT

## 9.1. Simulated Human Geometry and the Benchmark Tests

### *9.1.1. Simulated Human Geometry*

Computational fluid dynamics (CFD) has been widely used to simulate the thermal and airflow conditions of the human environments. The representation of the human body in the simulation domains is one of the problems of the CFD models. Since human body is geometrically very complex, detailed representations in the CFD models significantly increase the computational intensity of the simulations. Literature survey presented human geometries of different complexities which were developed by researchers around the world.

In this section, a simplified human model is presented which was developed for the CFD simulations (Figure 9.1). A commercial CFD package (Star-CCM+ Version 5.02.009) was used for the simulations. In all simulations the solution is considered converged at 0.0001. The human geometry is a person of 5’10” tall with 1.70 $m^2$ of surface area and has the resemblance of a male figure. The advantage of this model over different computer simulated persons from the literature is threefold. First, the developed model is composed of simplified geometries which reduce the computational power required for the simulations. Despite the simplified geometry, the model still retains the definitions of the significant body segments such as such as feet, hands, arms, legs, neck, chin, and the head. The nose was also included in the model for the future studies which include the simulations of the breathing zone. The second advantage is that all the joints were designed as spherical elements which allow the change of body posture in minutes using the native program Rhinoceros. The third advantage is that the simplified geometries allow the use of structured grid schemes which are of higher quality than the unstructured grid schemes (Gao and Niu, 2004).

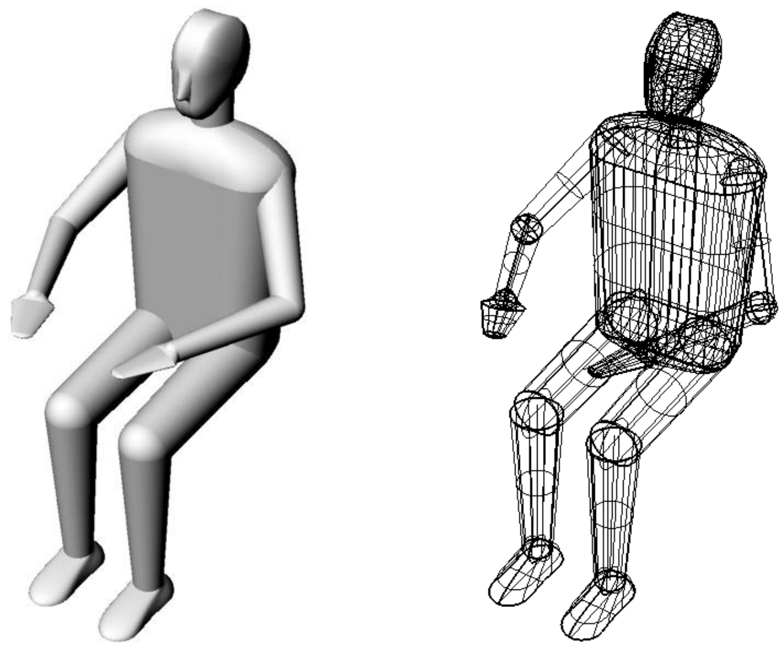

Figure 9.1. Simulated human model shown in rendered and wireframe modes.

### *9.1.2. Benchmark Tests for the Simulated Human Geometry*

Benchmark tests were conducted to test the usability of the simulated human model in the CFD simulations. Nielsen et al. (2003) presented two cases to validate the human geometries. The mixing ventilation case (Figure 9.2) was developed by the Aalborg University and the displacement ventilation case was developed by the University of Tokyo and Keio University (Figure 9.3). For the mixing ventilation scenario, Nielsen et al. suggested three cases with 0.05 m/s, 0.20 m/s, and 0.50 m/s inlet velocity with 22°C inlet temperature. For the displacement ventilation case, they suggested 0.20 m/s inlet velocity at 22°C temperature with 30% turbulence intensity. For the simulated person, they specified 76 W of heat flux from the body which corresponds with the 1 met metabolic activity. We used the same boundary conditions as Nielsen et al. for the benchmark tests. The results of our benchmark tests for the mixing ventilation case were compared to a previous study by Topp et al. (2002) and results of the displacement ventilation case were compared to a study by Deevy et al. (2006). Both studies used the guidelines which were summarized by Nielsen et al. (2003).

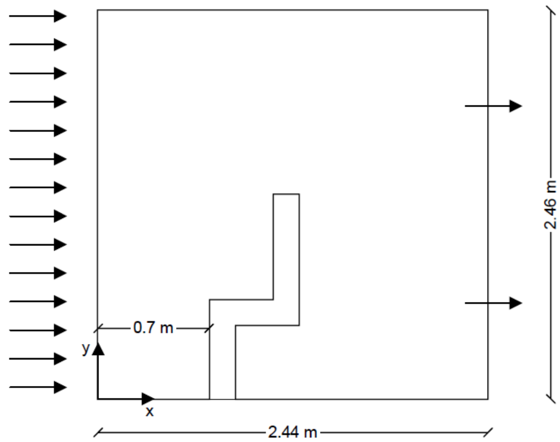


Figure 9.2. The mixing ventilation case of the CFD simulation (Nielsen et al., 2003).

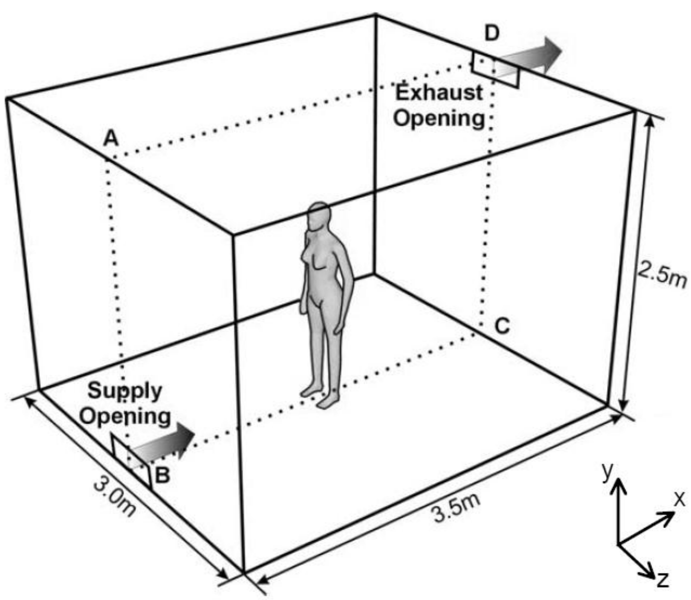


Figure 9.3. The displacement ventilation case of the CFD simulation (Nielsen et al., 2003).

*9.1.2.1. The Mixing Ventilation Case*

In a benchmark study, Topp et al. (2002) simulated two extreme cases for human geometries which are a cuboid and a realistic human figure (Figure 9.4). They used the mixing ventilation case which was summarized by Nielsen et al. (2003). The uniform inlet velocity was 0.05 m/s (10 ft/min), with an inlet turbulence intensity of 39% and a temperature of 22°C (71.6°F). For the human body, they used 38 W of heat flux from the body which corresponds with 1 met of activity level. Topp et al. used the standard k-ε turbulence model with near wall treatments.

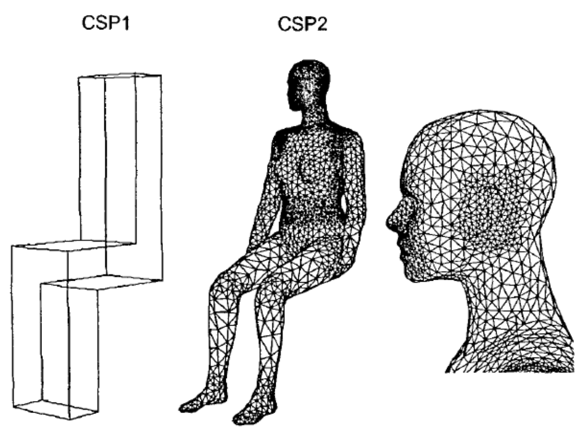


Figure 9.4. Computer simulated persons (CSPs) that were used by Topp et al. (2002).

The simulated human geometry of our study falls between the two extreme cases of Topp et al. (2002) (Figure 9.5). Therefore, our results are comparable through an interpolation of Topp et al.'s results. The boundary conditions of our simulations were similar to Topp et al.'s study and the standard k-ε turbulence model with wall treatment was used for the simulations. The results of our simulations were compared to Topp et al.'s results in order to validate our human geometry. Grid independence tests were also conducted and presented for 2.5 cm (1 inch), 2.0 cm (0.8 inches), and 1.5 cm (0.6 inches) grid sizes. Structural grids were used for the simulations. The minimum surface mesh size on the human geometry was 0.5 cm (0.2 inches). A velocity inlet boundary condition was used for the whole surface in front of the human figure. Pressure outlet boundary conditions were used for the two circular outlets.

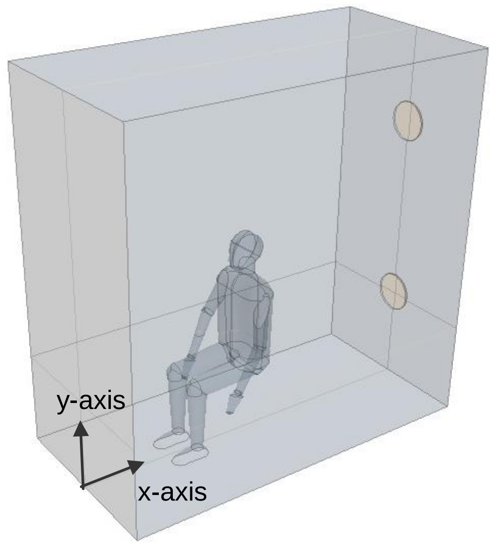


Figure 9.5. The simulation domain of the simulated human geometry for the mixing ventilation case.

Figure 9.6 presents Topp et al.'s velocity profiles at four different virtual vertical probes (data lines) on the x-axis located at 0.5 m, 1.5 m, 1.7 m, and 2.0 m from the origin. Topp et al.'s study showed that two geometries yield similar results for the global airflow. The solid configuration of CSP1 yielded lower velocity profiles in front of the legs (x=0.5 m) due to the separation of the flow. Since CSP2 allows airflow between the legs, the velocity profiles are higher in that region. The airflow profiles of our study at the same probes are presented in Figure 9.7. Velocity profiles at x=0.5 m and x=2.00 m show that the simulated human geometry of this study yielded airflow velocities similar to CSP2 which is the lifelike human figure. At x=1.5 m and x=1.7 m, the simulated human geometry yielded lower air velocities behind the human figure which is due to the larger torso section and the resulting larger leeward region. However, at x=2.00 m, both Topp et al.'s simulations and our study yielded almost identical velocity profiles.

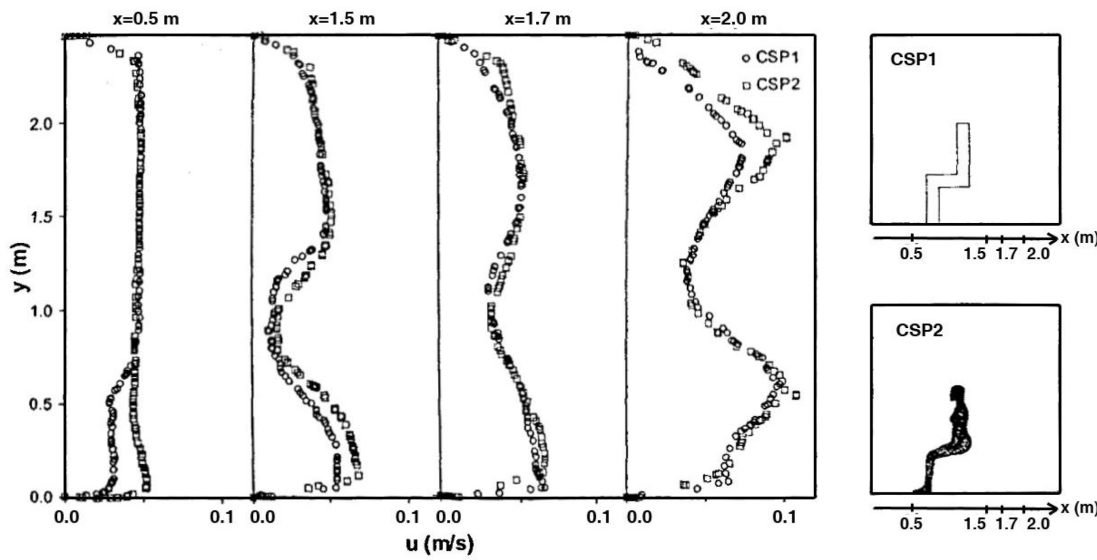


Figure 9.6. Velocity profiles at the virtual data probes located on the x-axis (Topp et al., 2002).

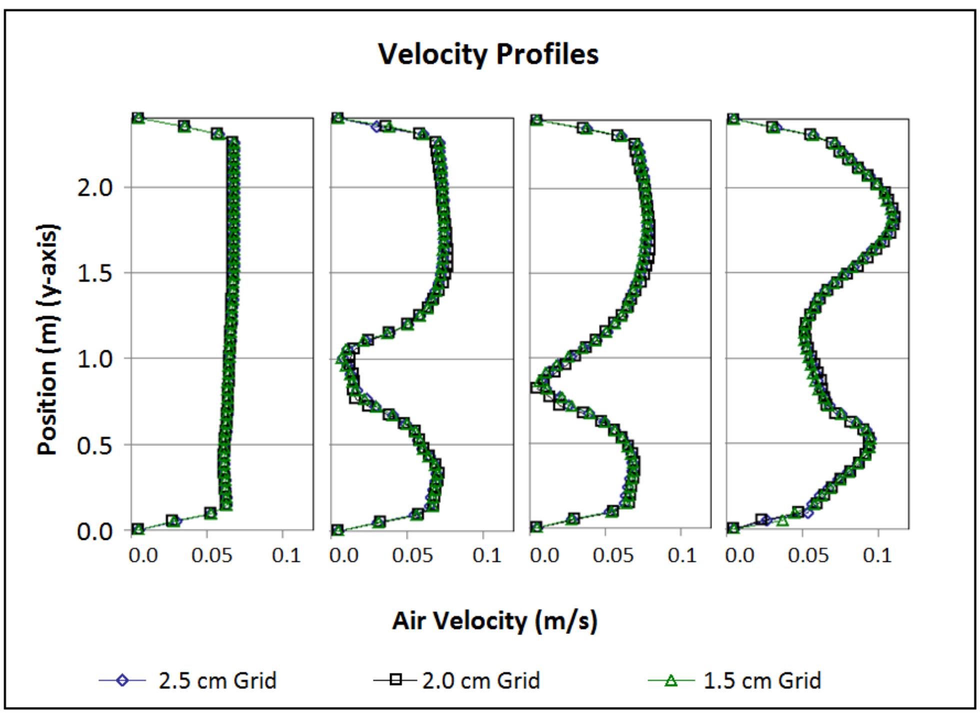


Figure 9.7. Velocity profiles of this study at the virtual data probes located on the x-axis.

A grid independence study was also conducted using 2.5 cm (1 inch), 2.0 cm (0.8 inches), and 1.5 (0.6 inches) cm grid sizes for the simulation domain. A 0.5 cm (0.2 inches) grid size was used for the surface of the human figure. Figure 9.7 showed that all three grid sizes yielded identical results which showed that CFD simulations of this study were grid independent for the grid sizes smaller than 2.5 cm. Grid sizes larger than 2.5 cm were not simulated since it is larger than the conventional grid size that was used for similar studies in the literature. The grid independence study is limited to the global airflow around the human body. A separate grid independence study may be required for microenvironment studies. The microenvironment characteristics of the thermal conditions are outside the scope of this study. The global air velocity patterns of the mixing ventilation case are presented in Figure 9.8. An inlet velocity of 0.5 m/s (98 ft/min) was used to show the effect of the simulated human geometry on the airflow patterns. Figure 9.8 also shows the separation of the flow at the wall region and the turbulent areas around the human body.

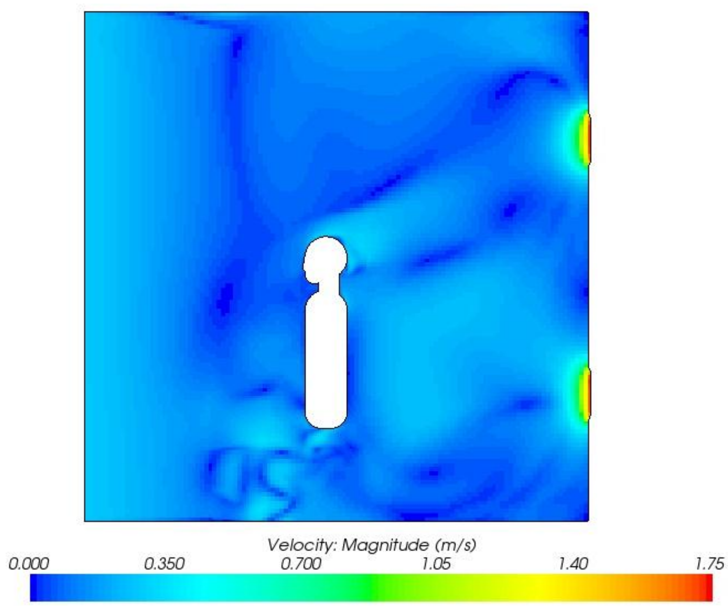


Figure 9.8. Air velocity profiles on the x-axis.

*9.1.2.2. The Displacement Ventilation Case*

The CFD technique and the simulated human geometry of this study were compared to a study by Deevy et al. (2006) for the displacement ventilation case which was summarized by Nielsen et al. (2003). Figure 9.9 shows the cross section of the simulation domain and the data probes (L1 through L6) from the original study by Nielsen et al. Deevy et al. simulated the displacement ventilation case using three human geometries: a cylinder, a simplified geometry and an experimental geometry. The experimental geometry is similar to the CSP2 of Topp et al. The realistic geometry and the measured data of Deevey et al. were used in this section. Figure 9.10 shows the simulation domain of our CFD model which was modeled based on the guidelines by Nielsen et al. An inlet velocity of 0.2 m/s (40 ft/min), temperature of 22°C (71.6°F), and turbulence intensity of 30% was used for the inlet boundary conditions. Pressure outlet boundary condition was used for the outlet. The radiation model was included in the simulations with 76 W of heat flux from the body which corresponds with 1 met of activity. Air velocity profiles at the L1, L2, L4, and L5 probes of the current study were presented in this section. Those probes are located on the central axis of the room which cuts through the inlet, outlet, and the human geometry.

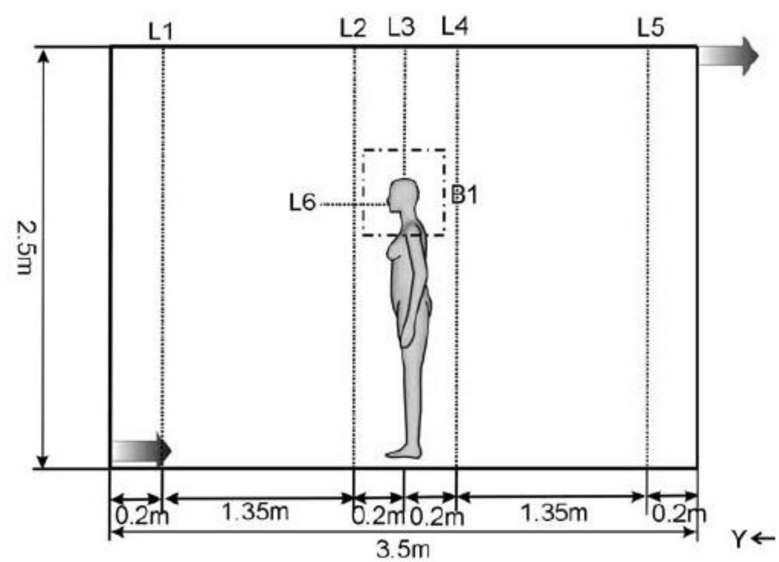


Figure 9.9. The cross section of the displacement ventilation case and the data probes (Nielsen et al., 2003).

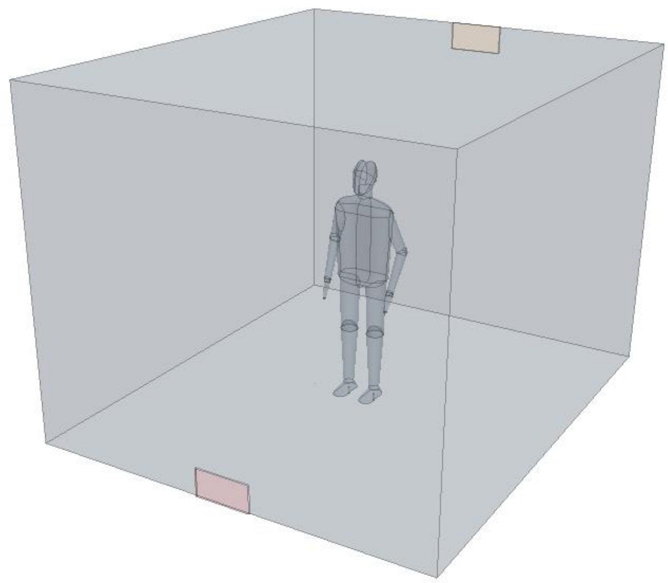

Figure 9.10. Human geometry and the simulation domain of the current study.

Figure 9.11 shows the air velocities at the L1 probe which is located 0.2 m (0.66 ft) away from the inlet boundary. The vertical axis is denoted as the z-axis in the following graphs. Simulations showed air velocities up to 0.25 m/s at the bottom of the room due to the placement of the inlet. The region above the inlet shows a relatively stable airflow condition.

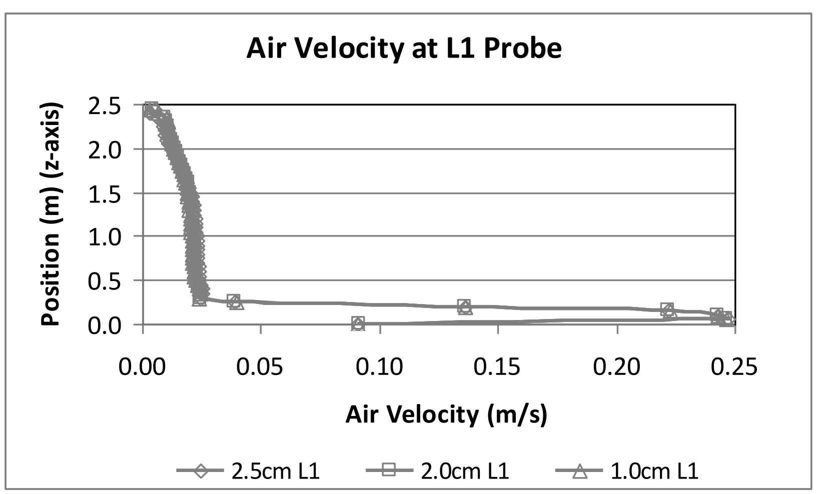


Figure 9.11. Velocity profiles for three grid sizes as simulated at the L1 probe.

Results of our simulations were compared to the measured and the simulated data of Deevey et al. (2006). Figure 9.12 was redrawn from the original study of Deevey et al. Deevey et al.'s simulation and measurements showed slight increase in airflow up to 0.2 m above the floor (Figure 9.12), while our simulations showed a high velocity region extending up to 0.75 m from the floor (Figure 9.13). Our simulation results are more likely considering the fact that the inlet is 0.25 m high and there is separation of flow from the ground which creates a high velocity region above 0.25 m from the ground.

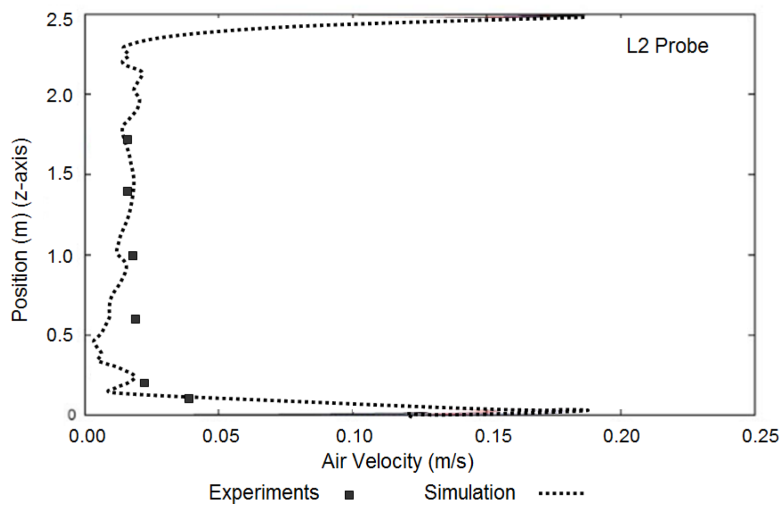


Figure 9.12. Velocity profiles at the L2 probe in Deevey et al. (2006).

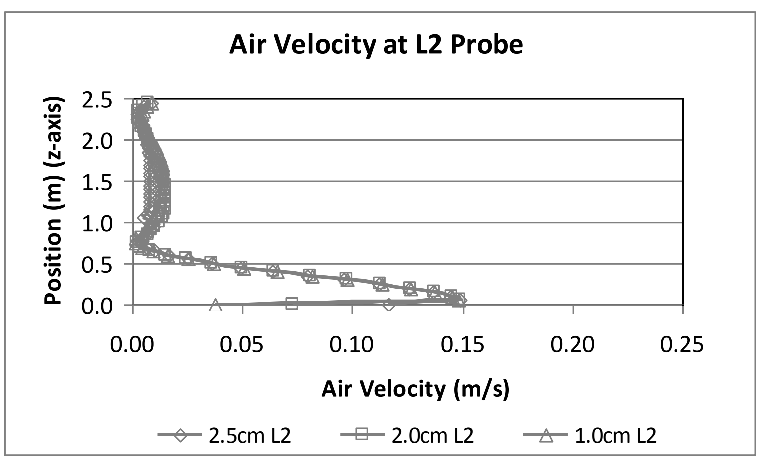


Figure 9.13. Velocity profiles for three grid sizes as simulated at the L2 probe.

Measured and simulated data of Deevey et al. for the L4 probe (Figure 9.14) were compared to our simulation results (Figure 9.15). Figure 9.14 was redrawn from the original study of Deevey et al. Both simulations showed air velocities close to 0.15 m/s on the ground and 0.2 m/s at 1.5 m from the ground. Deevey et al.'s data showed a high velocity point at 1.0 m, in both simulation and measurement. The same behavior was found in our case at 1.4 m. This is likely due to the slight geometrical differences between the models and the resulting air vortex.

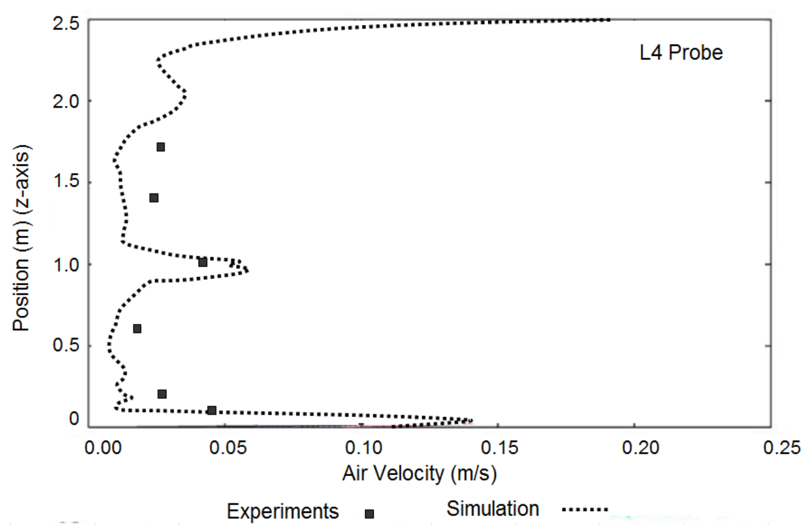


Figure 9.14. Velocity profiles at the L4 probe in Deevey et al. (2006).

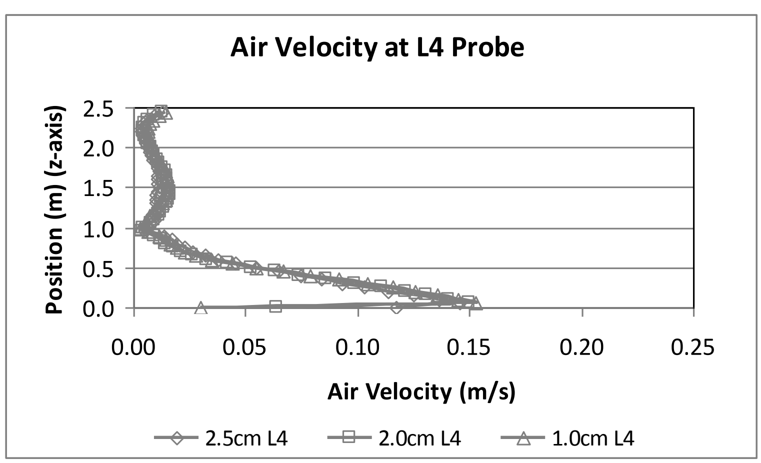


Figure 9.15. Velocity profiles for three grid sizes as simulated at the L4 probe.

In a final comparison, Deevey et al.'s measured data at L5 (Figure 9.16) was compared to the simulation results of our study (Figure 9.17). Figure 9.16 was redrawn from the original study of Deevey et al. The simulation results showed similar characteristics to the measured data. However, velocities predicted by the simulation were higher than the measured data. The differences are within 0.03 m/s which are negligible for this kind of study. Figure 9.18 show the velocity distribution on the central axis of the simulation domain with higher velocities between the inlet and the outlet.

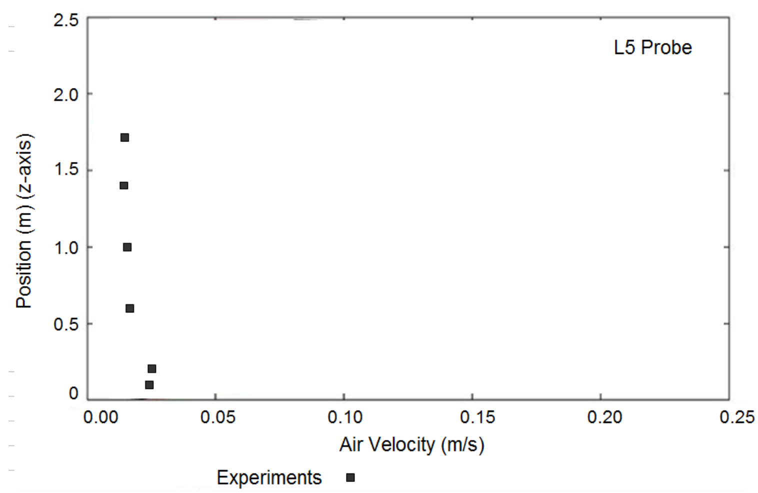


Figure 9.16. Velocity profiles at the L5 probe in Deevey et al. (2006).

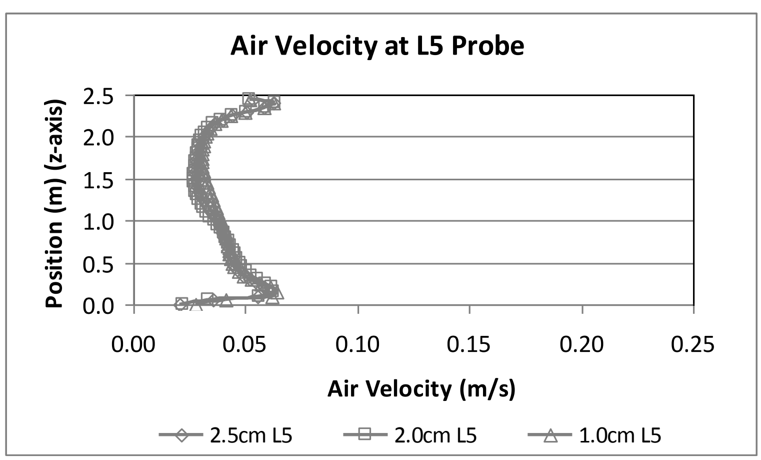


Figure 9.17. Velocity profiles for three grid sizes as simulated at the L5 probe.

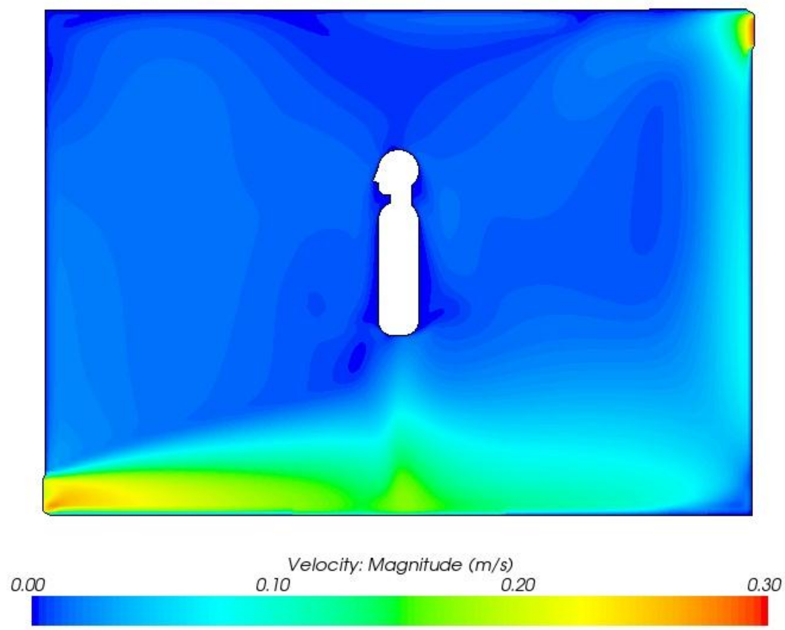


Figure 9.18. Velocity distribution on the central axis of the simulation domain.

A grid independence test was conducted together with the simulations of the displacement ventilation case. Figures 9.11, 9.13, 9.15, and 9.17 showed that 2.5 cm (1 inch), 2.0 cm (0.8 inches), and 1.5 cm (0.6 inches) grid sizes yielded almost identical results. Therefore, it was concluded that grid independence was achieved in our CFD simulations for grid sizes smaller than the 2.0 cm. This is also consistent with the mixing ventilation case.

The two benchmark studies showed that our simulated human geometry and the CFD model were able to simulate the general flow characteristics similar to the previous studies from literature and they can, therefore, be confidently used for the thermal analysis of the actual thermal comfort test conditions. The CFD simulations of the actual test room used boundary conditions and the grid sizes which were verified in the benchmark tests.

### 9.2 Airflow Simulations of the Thermal Comfort Test Conditions

The computational fluid dynamics (CFD) technique and the simulated human geometry of this study were validated using the similar studies from the literature. The purpose of this part of the study is to verify the CFD simulation techniques and the human which will be used to improve thermal conditions in future studies. In this section, the CFD analyses of the test thermal conditions were conducted following the methodologies presented in the previous section. The airflow measurements that were presented in section 4.4.3.2 were used to verify the simulation results. The simulated human geometry that was presented earlier was used as the human figure in these simulations. Figure 9.19 presents the simulation domain in which two researcher desks were simplified into boxes and subtracted from the domain. Head-only airflow and simultaneous head/hands/feet airflows were simulated separately.

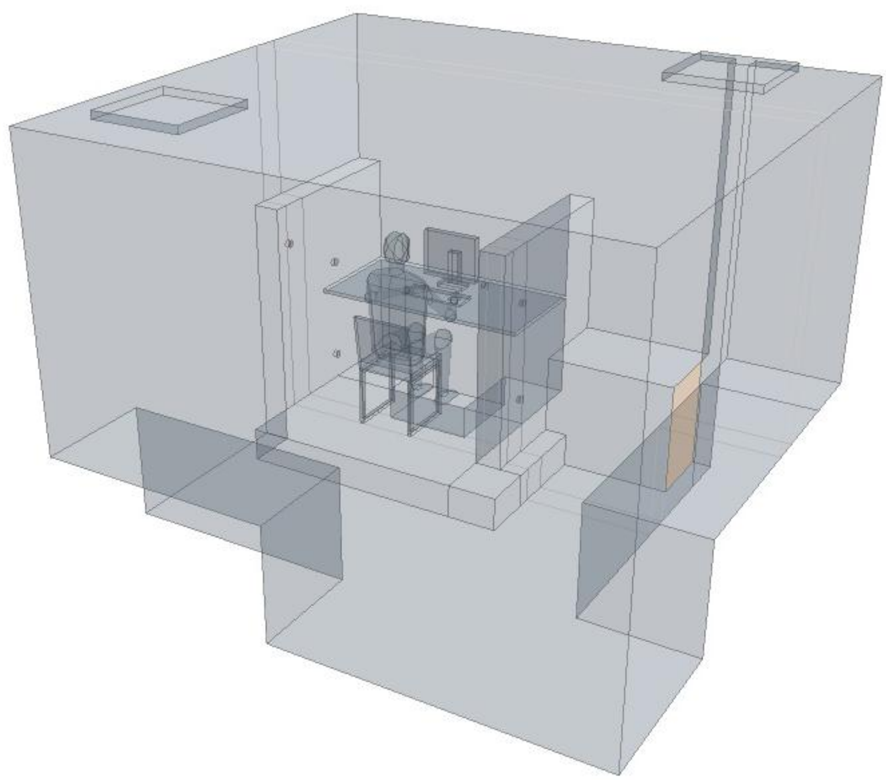

Figure 9.19. CFD model of the thermal comfort test room.

Velocity inlet boundary condition with 2.00 m/s (394 ft/min) and 1.15 m/s (226 ft/min) of inlet velocities were used for the head-only and simultaneous airflows respectively. Only the head nozzles were used as the inlet for the head-only airflow, and head, hand, and foot nozzles were used as inlet for the simultaneous airflow. A heat flux of 100 W from the simulated human figure was used which corresponds with 1.3 met metabolic activity. For the airflow measurements, a 100 W heat source was used to create the thermal plume around the human body. A structured scheme was used to generate the grid (Figure 9.20). The maximum grid size away from the human figure was 2.5 cm, and the minimum grid size on the human figure was 0.6 cm. The total number of cells was 7.3 million. The standard k-e model with wall treatment was used for the simulations. The y+ value, which is the dimensionless distance from the center of the first cell to the wall surface, on the manikin surface was less than 3.5. Soransen and Voigt (2003) suggested to use y+<1, while Gao and Niu's (2004) y+ values ranged between 10 and 29. Dygert et al. (2009) suggested that y+<3 is sufficient when enhanced wall treatment is used. We decided that y+=3.5 with wall treatment is sufficient enough to simulate conditions near the human geometry. All the simulations in this section were considered converged at 0.0001 level.

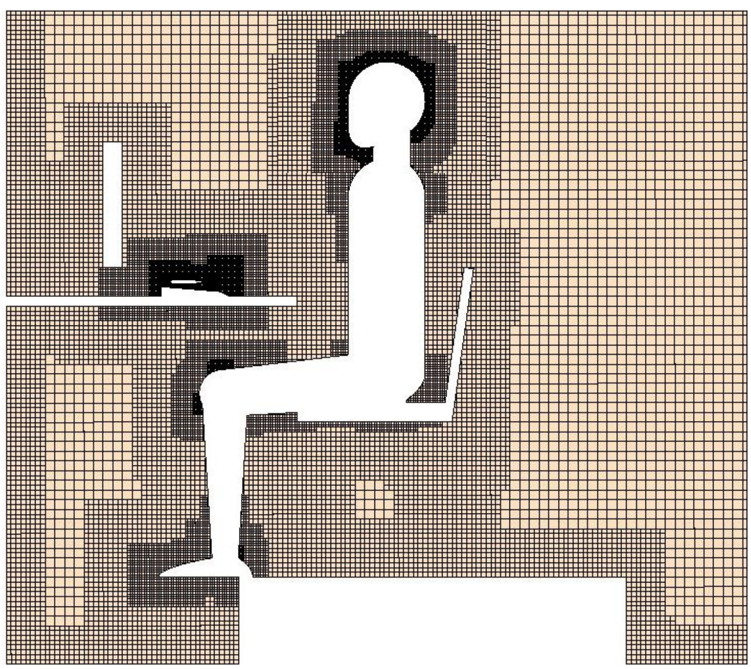

Figure 9.20. The structured grid scheme of the simulation domain.

Airflow velocities from the simulation results were compared to the measured data using the four probes (data measurement lines) whose locations were presented in section 4.4.3.2. X-probe, Z-probe, XYnB, and XYnF probes start at 1” from the nozzle and end in the middle of the cubicle (Figure 9.21). XYnF probe started at the head nozzle and was angled towards the front by 30 degrees, whereas XYnB probe was angled towards the back by the same amount. XW probe is located vertically next to the manikin. In the following sections, same probe notations were used for the naming of the graphs.

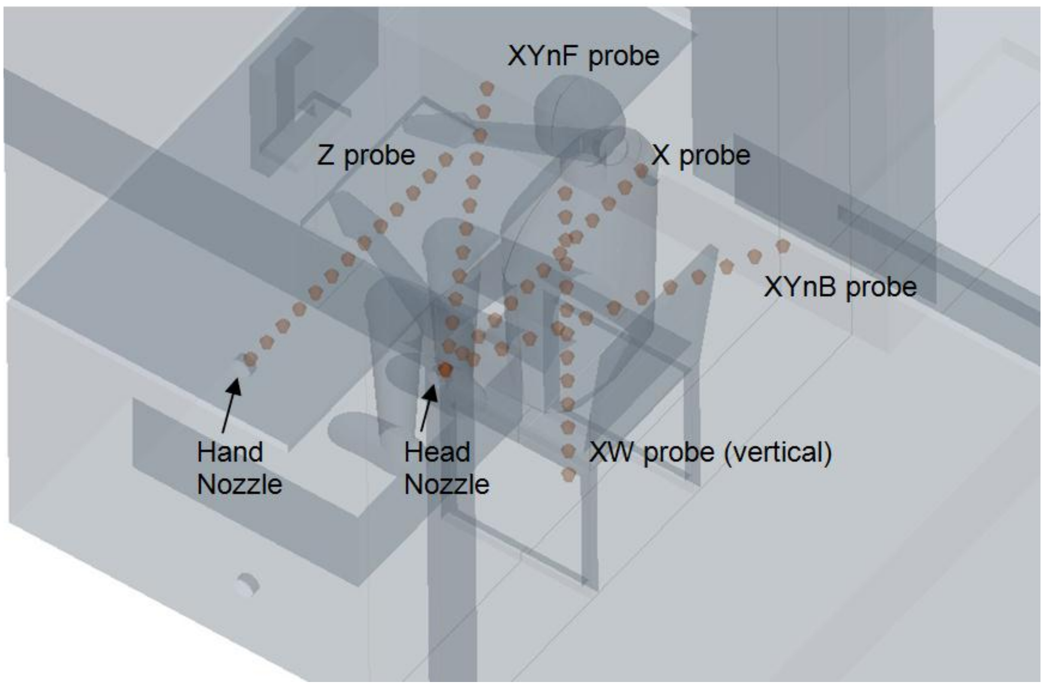


Figure 9.21. Probes around the manikin which were used to compare the measured and the simulated data.

### *9.2.1. Head-only Airflow*

Comparisons between the measured and the simulated data for the head-only airflow showed that simulations accurately replicated the general flow characteristics. Figure 9.22 shows that simulations predicted a linear air velocity drop whereas measurements showed an exponential drop until the $18^{th}$ inch. Figures 9.23 and 9.24 showed that the measured and the simulated data matched very closely for the probes that are angled towards to front and the back. In these regions, the air velocities were relatively low due to the dispersion of the air jet. Figure 9.25 shows that airflow velocities were relatively low (50 – 70 ft/min) on the XW probe which was located next to the manikin. This was due to the airflow blocked by the manikin. Airflow increased suddenly at z=48 inches which is the free flow stream above the shoulder line.

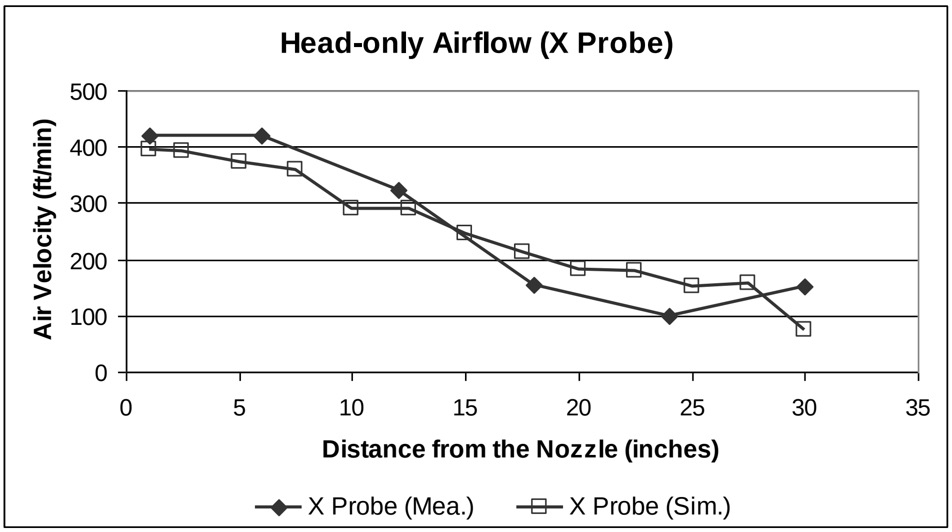


Figure 9.22. Measured and simulated data at the X-probe for the head-only airflow.

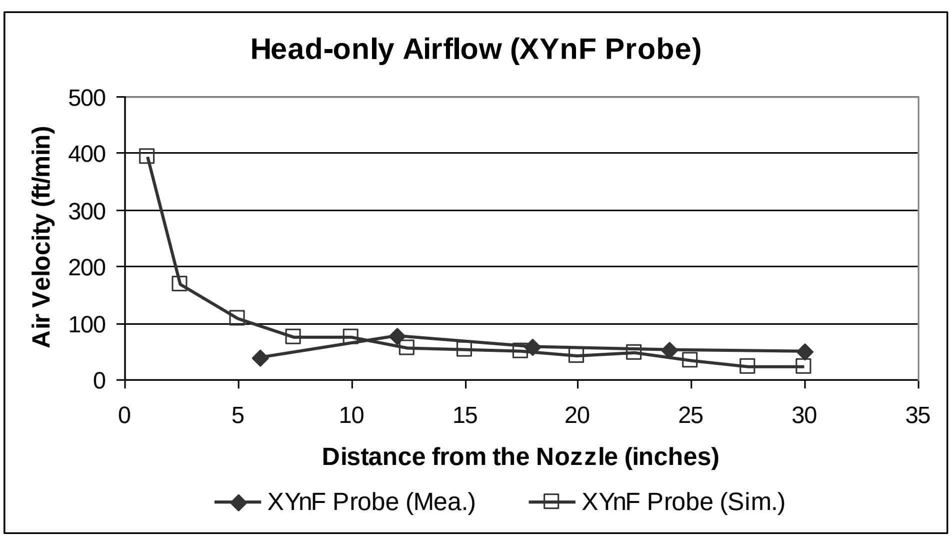


Figure 9.23. Measured and simulated data at the XYnF probe for the head-only airflow.

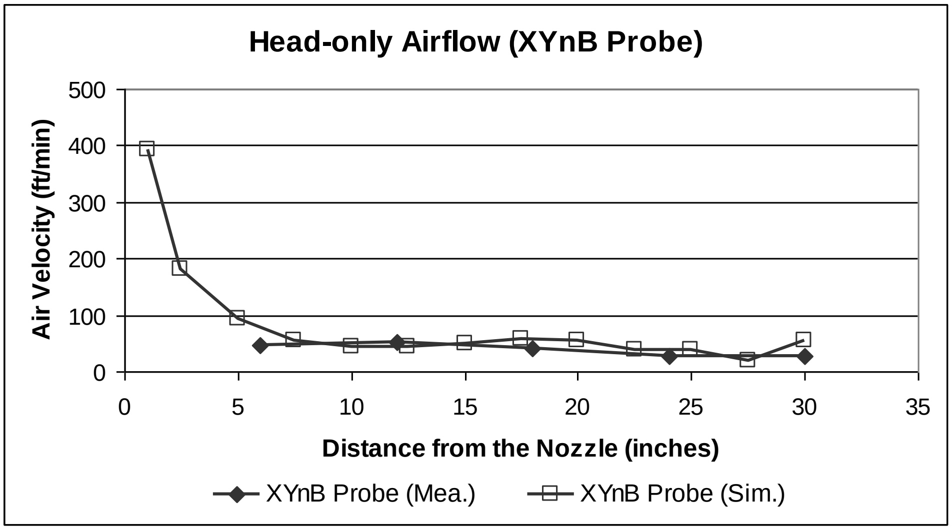


Figure 9.24. Measured and simulated data at the XYnB probe for the head-only airflow.

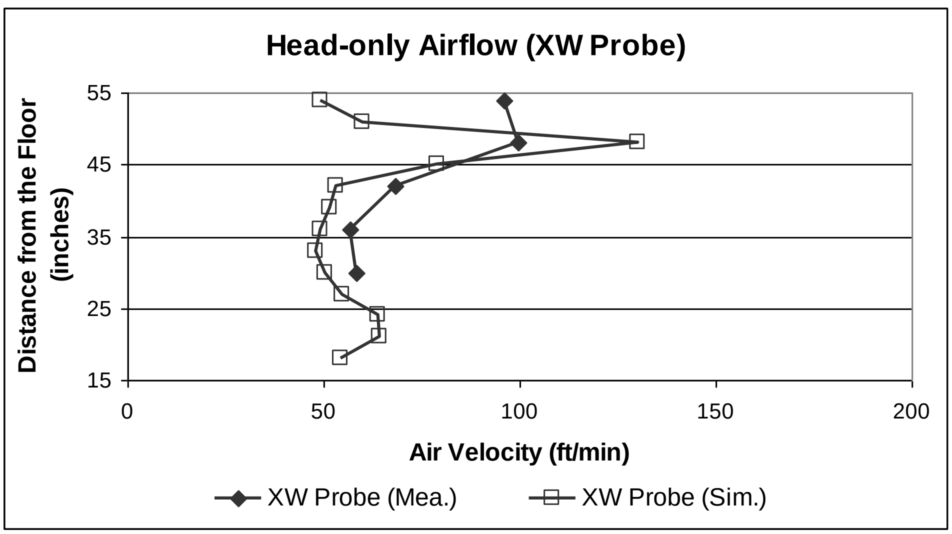


Figure 9.25. Measured and simulated data at the XW probe for the head-only airflow.

### *9.2.2. Simultaneous Head/Hands/Feet Airflow*

Comparisons of the measured and the simulated data for the simultaneous airflow showed similar characteristics to the head-only airflow. Simulated data was higher than the measured data up to 60 ft/min for the X probe (Figure 9.26) and up to 50 ft/min for the Z probe (Figure

9.27). However, Z probe showed closer agreement between the measured and the simulated data. In general, simulations predicted linear air velocity drops, whereas measured data showed quadratic air velocity drops.

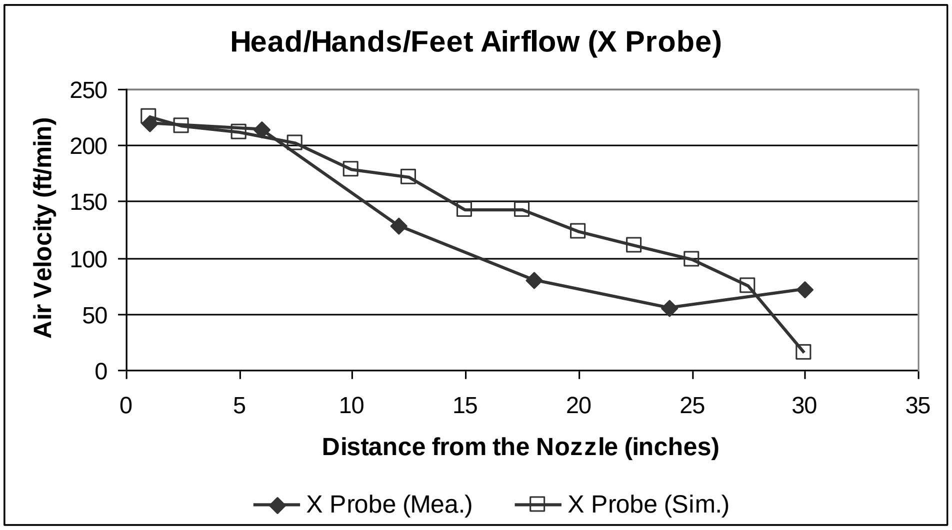


Figure 9.26. Measured and simulated data at the X probe for the simultaneous airflow.

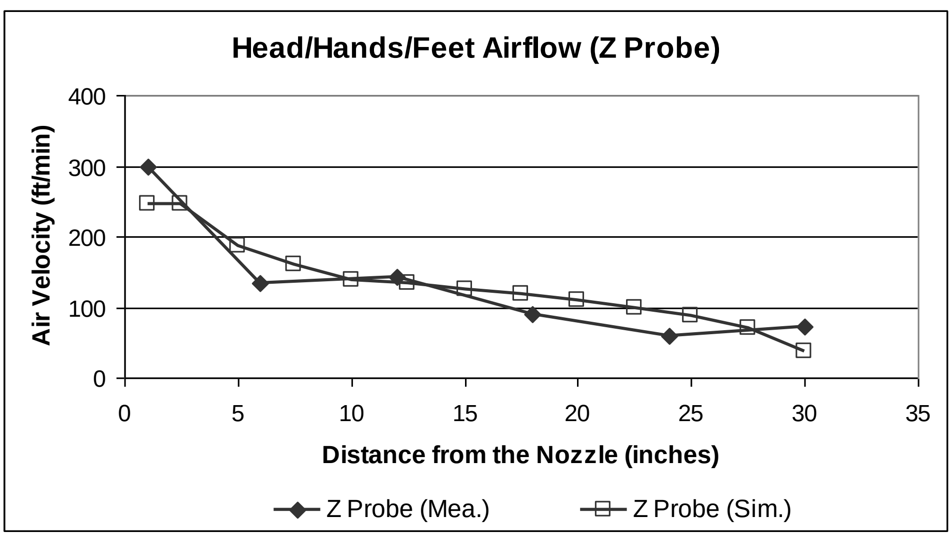


Figure 9.27. Measured and simulated data at the Z probe for the simultaneous airflow.

Simulations for the XYnF probe replicated the measured flow characteristics with an average offset of 20 ft/min (Figure 9.28). Velocities increased towards the manikin because manikin's head obstructed the flow and created a high velocity region. A similar phenomenon didn't occur for the XYnB probe since manikin's head was located between the head nozzle axis and the XYnF probe (Figure 9.29). Simulation results for the XYnF probe was 15 ft/min higher than the XYnB probe on average.

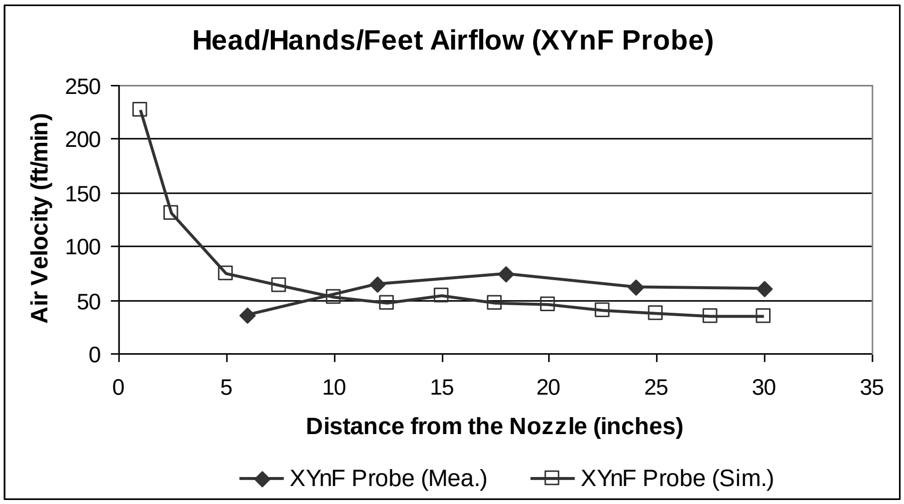


Figure 9.28. Measured and simulated data at the XYnF probe for the simultaneous airflow.

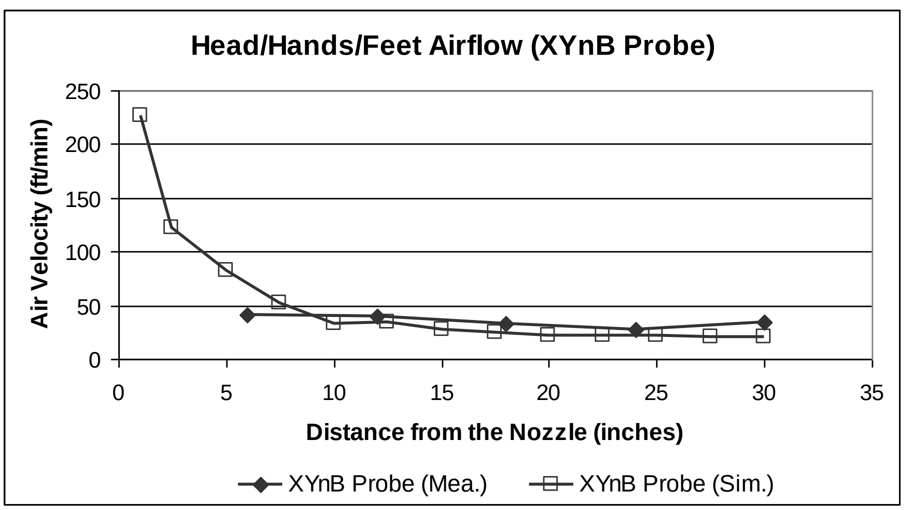


Figure 9.29. Measured and simulated data at the XYnB probe for the simultaneous airflow.

Figures 9.30 and 9.31 show the air jets from the nozzles for the simultaneous airflow. Air jets of the hand and foot nozzles show higher dispersion due to the obstructing elements such as the table, hands, and legs. The air jet in Figure 9.30 is located behind the manikin's neck.

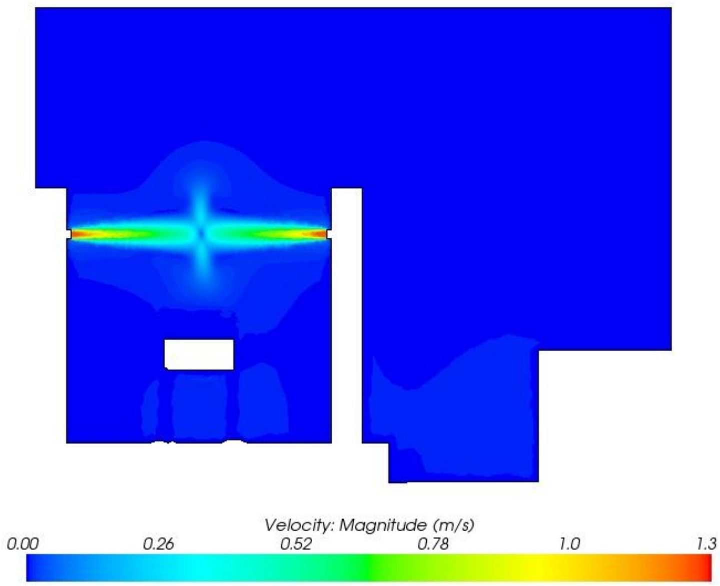


Figure 9.30. Air velocity profiles on the head nozzle cross section.

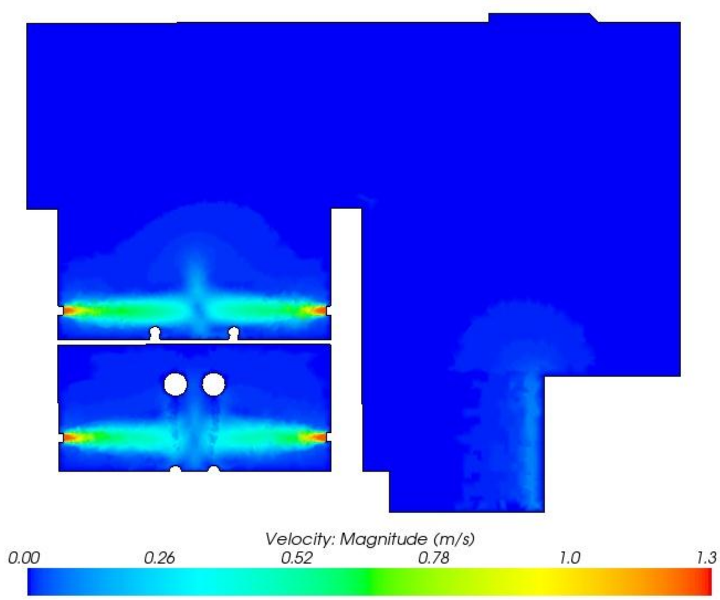


Figure 9.31. Air velocity profiles on the hand and foot nozzle cross section.

## 9.3. Discussion

In thermal environment studies, computational fluid dynamics (CFD) simulations emerged as an alternative to the experimental methods which are more costly and less practical. Section 9 of this study focused on the development of the CFD models and techniques to accurately simulate the environmental conditions of the thermal comfort test.

In the first part of this section, the development of the simulated human geometry was explained. The developed human geometry used simplified geometric components while still providing an accurate definition of the human body with head, neck, arms, hands, legs and feet. The developed geometry was simulated using two benchmark ventilation cases which were the mixing ventilation and the displacement ventilation cases. Air velocity profiles at different locations of the simulation domains of our study were compared to the two studies from the literature which also used the same benchmark guidelines. Simulation results of our study matched closely with the two existing studies which validated the developed human geometry and the CFD methodology. Grid independence studies were also conducted for the two benchmark cases.

In the second part of this section, simulation results of the thermal comfort test conditions were presented. Head-only and the simultaneous head/hands/feet airflow conditions were simulated separately. The air velocity profiles from the simulation results were compared to the measured data. The comparisons showed that CFD simulations were able to successfully replicate the physical conditions. It is concluded that the developed human geometry and the CFD methods can be confidently used in the future studies of thermal comfort.

# 10. CONCLUSIONS

## 10.1. Summary

A thermal comfort study was designed to determine people's responses to transient thermal conditions. Human subject tests were conducted to test the thermal comfort response differences for various thermal comfort variables including gender, ambient temperature, metabolic rate, local airflow, and airflow frequency. Gender (male and female) and ambient temperature (75°F and 83°F) were considered between-subjects variables since their effects are more definitive in terms of subjective responses. Airflow location (head-only, head/hands/feet simultaneously), airflow frequency (30s and 60s), and metabolic rate (high, low, and transient) were considered within-subject variables. Thermal factors and physical conditions of this test was designed to emulate real conditions such as short durations of high metabolic rate, local airflow as in draught, dynamic airflow, and real office environments. This approach has more external validity than the purist laboratory studies which aim at isolating one or two variables.

Thermal sensation and thermal comfort responses of the test subjects showed similar tendencies as the previous studies from literature with more tolerance for warmth. The predicted mean vote (PMV) and the predicted percent dissatisfied (PPD) values of this study had the same distribution as the thermal comfort standards, which validated the responses of this test. PMV calculations determine the average thermal sensation for given thermal conditions based on the six conventional thermal comfort variables. PPD calculations determine the percentage of dissatisfied people corresponding to that PMV value.

The first part of the analyses focused on the gender differences of thermal comfort requirements. Test results showed significant thermal comfort and thermal sensation differences between the genders for various combinations of environmental and metabolic conditions. Females reported warmer thermal sensation and lower thermal comfort than males for all metabolic conditions. Temperature and metabolic rate had interaction effects in producing thermal sensation and comfort. ASHRAE Standard 55 (2004) and ISO 7730 (2005) predicted uncomfortably warm sensation for the test conditions. However, average thermal comfort responses of both genders were on the comfortable side of the scale.

Thermal comfort and sensation changed linearly for different metabolic conditions under the 75°F room temperature. On the other hand, thermal responses saturated at medium activity level under the 83°F room temperature. This suggested decreased tolerance for increased heat stress when the body is under considerable heat stress. Higher thermal sensations were compensated with the localized dynamic airflow. Under dynamic airflow conditions, females and males felt neutral at 74°F and 72.3°F respectively, although these temperatures together with the high average metabolic rate are considered outside the comfort zone. Test results showed that thermal environment design should include not only the conditions but how people respond to those conditions in time when the metabolic rate is changing. Expectations play a significant role in thermal environment evaluation and dynamic conditions shift people's expectations and increase their comfort tolerances.

Physiological differences of thermoregulation exist between males and females. Females' skin temperatures increased more than the males' skin temperatures which means that more heat was transferred from the body core to the skin surface of the females. This may be a result of decreased conduction due to the additional fat layer in females. In addition, average electrodermal activity level was higher for females. High mental stress with extra heat capacity can explain the higher thermal sensation of females. Although the subjects felt warm throughout the test, the majority found the thermal environment more acceptable than the thermal comfort standards predict. This was noted as a secondary proof of the effectiveness of the dynamic conditions in providing thermal comfort.

An analysis of the PMV approach was conducted to determine the accuracy of the method in determining the thermal sensations of this comfort test. In real world applications, average values of the thermal conditions are used for the PMV calculations. ISO 8996 suggests time-averaging different metabolic rates in order to obtain an average metabolic rate for a given period of time. Calculating the PMV from this time averaged value assumes that throughout the high metabolic period thermal sensation was at its peak value. However, people's thermal sensation worked like a capacitor which took approximately five minutes to reach its peak value while heart rate was at its target rate within one minute into the exercise period. This will result in over-estimation of the thermal conditions, which will lead to over-design of the thermal environments and the mechanical systems. However, this study showed that calculating the PMV from the average thermal factors yield significant discrepancies between the PMV and the actual thermal sensation votes. This study showed that thermal sensation doesn't have linear relationship to metabolic rate during sudden metabolic transients. However, due to its steady-state nature, PMV calculations cannot model the transient components of the comfort factors which are largely responsible of the discrepancy.

A second PMV calculation (Method 2) was proposed which accounted for the transient conditions that occur for short durations of time. In this approach, a PMV value was calculated at each time-step and an average value was calculated from individual time-steps. This approach had a higher accuracy than the conventional method of PMV calculation when compared to the actual thermal sensation votes.

Thermal sensation of subjects revealed two types of transient conditions when they are exposed to the repetitive transient conditions. The first type of transient conditions occurred within 10 minutes after each exercise period ended. During this period, heart rate returned to the base level within 4 minutes, while thermal sensation returned to the base level around the $9^{th}$ minute. A modification to the PMV was required for transient conditions since estimating PMV based on heart rate yields erroneous results. The second type of transients occurred within 1.5 hours of the test time. The peak and the mean thermal sensation of the subjects increased at each exercise session although thermal sensation votes returned to the base level after each exercise. This increase in thermal sensation was then attributed to the psychological processes, more specifically to the immediate past disturbances due to exercising.

Analyses were conducted to determine subjects' perception of and preference for the airflow conditions. Same series of tests with counterbalancing were conducted with each subject during which combinations of airflow location and frequency were applied as treatments for thermal comfort. Average preference for airflow was always for 'more air' for all metabolic conditions even when the subjects reported 'cool' thermal sensation. This is most likely due to the subjects' inherent understanding of airflow as a thermal comfort provider in a hot and humid climate in which the tests were conducted. In addition, the subjects reported discomfort due to draught much less than the previous studies from the literature. Subjects voted in favor of more air although the average airflow speeds were slightly higher than the comfort standards. This can be attributed to the effectiveness of dynamic airflow to provide comfort without creating a negative feeling of draught. A rather counter-intuitive result was that people's airflow preference was independent of the room temperature. This was also consistent with another study from the literature.

Detailed analyses were conducted to determine the effectiveness of airflow frequency and location to provide thermal comfort. The 30-second and 60-second airflow periods were compared to a minimum airflow condition. Thermal comfort and sensation votes suggested that 30-second airflow was more effective in providing thermal comfort. The 60-second air pulse provided a feeling of thermal comfort without reducing the heat stress. Therefore, it was not as effective as the 30-second pulse. A comparison of airflow location showed that simultaneous head/hands/feet airflow was more effective than the head-only airflow although airflow speed was higher during the head-only airflow. Since the volume of airflow did not change between the two modes, removal of the heat from body was proved to be more important than the strong feeling of air on the body. As a result of these analyses, a *Dynamic Localized Airflow* was proposed as the new concept which accounts for varying airflow conditions at specific locations on the body. Results suggested that 30-second airflow located to head/hands/feet simultaneously was the most effective in providing thermal comfort while reducing the heat stress.

Thermal comfort response is the result of subjective evaluations of the physical and physiological conditions that are related to the thermal environment. Thermal conditions as well as the nature of the activity in an environment yield physiological signals. It is the integration of these physiological signals by the human body that generates a thermal response. For this reason, analyses were conducted regarding the mean skin temperature (MST), core temperature, heart rate, electrodermal activity, as well as thermal comfort and sensation together with different levels of metabolic rate and ambient temperatures.

Analyses showed that MST was positively correlated with the thermal sensation and thermal sensation was a function of the absolute value as well as the derivative of the MST. This was consistent with the thermoreceptor characteristic which has a static and a dynamic response. Thermoreceptors, therefore, can be stimulated while preventing adaptation for improved thermal sensation. Determining thermal sensation from the MST provided the missing link between the human physiology and the thermal response. One of the challenges in determining the MST is to decide which local skin temperatures should be included in the calculation. Analysis showed that five locations (i.e., lower back, anterior calf, instep, cheek, and upper arm) for all metabolic rate conditions and six locations (i.e., abdomen, lower arm, instep, cheek, chest, and anterio-medial thigh) for the two ambient temperatures correlated well with the MST. Additional analysis on the skin temperature measurements showed that exercising muscles experienced the highest deviation from the normal skin temperature. Analysis also showed that the hand skin site was actively involved in thermoregulation which was also consistent with the literature.

The heat balance of the body with the environment is the basis for the conventional approach in thermal comfort research. A heat balance analysis of the human body was conducted which took into account the heat generation and storage inside the body, the heat transfer from the body core to the skin, and from the skin to the environment. Core temperature measurements showed that body temperatures were steady throughout the test and subjects were able to fully dissipate the heat generated inside the body. However, increased heat generation inside the body resulted in increased blood flow to the skin and therefore higher skin temperatures. An analysis of body's thermal strain was conducted based on the temperature difference between the body core and the skin surface. Thermal comfort was negatively correlated to the $\Delta T$ between the core and the skin surface. A new index was proposed which is the temperature differential between the core and the skin divided by the body mass index (BMI). The BMI normalization took into account the insulation properties of the body in relation to the body composition. Heat transfer between the skin surface and the environment was also calculated. Heat loss from the skin surface to the environment occurred at different rates. This was calculated by the temperature differential between the local body part and the immediate surrounding. Heat loss from the foot had a higher correlation to thermal sensation than the heat loss from the hands and the head. A final analysis of physiological signals showed diurnal variations of physiological signals and thermal comfort responses. People felt cooler and less comfortable during the morning hours than the afternoon hours. Mental stress was highest in the afternoon which might negatively impact thermal environment perception. MST was highest during the noon hours. Skin temperature and the electrodermal activity measurements of this study were consistent with another study from the literature.

The focal point of this study was thermal comfort and the interaction effects of thermal factors which have transient components. The interacting and time-based properties of the thermal variables can be simulated using the computation fluid dynamics (CFD) methods. As a part of this study, a human geometry was developed which provides the necessary details of the human body by using simplified geometric components. The result is an optimal model in terms of geometric definitions of the human body and the computational efficiency. Benchmark studies and the comparisons with the measured data showed that the human geometry and the overall CFD methodologies can be confidently used in the future thermal comfort studies.

In conclusion, this research study covered multiple aspects of thermal comfort to provide a research methodology and information on the transient environmental and personal conditions. The methodology was designed to investigate the interaction effects of several thermal comfort variables. In this study, first, relationships between the five subjective responses as presented in the *Online Survey* were investigated. Second, relationship between the transient metabolic conditions and the subjective responses were studied. Third, the effectiveness of the transient and localized airflow on thermal comfort for different metabolic rate and room temperature conditions was examined. Fifth, the physiological signals which are related to thermal comfort and the human body heat balance were studied. Finally, CFD methodologies were developed to simulate the thermal environment of the comfort test.

### 10.2. Practical Applications

The conventional approach to thermal environment design targets at maintaining an average comfort level for the majority of the occupants. Using the method of averaging in thermal environment analysis and design provides useful information about the general trends in a thermal environment. However, the designed average conditions become a result of a theoretical mathematical formula which does not satisfy individual differences. The difference between the individual thermal comfort requirements and the average thermal conditions is the fundamental problem of the conventional thermal comfort approach. Thermal comfort problem can be solved by personalizing the thermal microenvironment. The results of this research study showed that the conventional methods of thermal environment design and controls are not sufficient to provide the thermal comfort levels that are required by each individual. This section provides several practical applications which illustrate controlling the immediate thermal environments around individuals. These include accounting for gender differences and time-dependency of thermal comfort, creating microenvironment zones with temperature and airflow control, and designing energy management and control systems (EMCS) with diurnal adaptability.

The first analysis of this study provided the gender differences of thermal comfort requirements. Significant differences exist between the males and females, and the neutral temperature for males was 1.7°F lower than the males. Based on this finding, thermal environments should be personalized to take into account the neutral temperature differences. If thermal environmental design for each gender is not possible, enough flexibility and user control over the conditioning system should be provided for any given space which would allow users to adjust the settings.

The second analysis proved that metabolic conditions in a given environment should be calculated from the average of smaller time-steps (less than 5 minutes) rather than assigning an average value for the type of activity and thermal conditions. Therefore, different potential metabolic conditions should be anticipated in an environment even though the general character of the activity is fairly constant. This is more pronounced when there are short durations of high metabolic activity periods since it has extended effects on thermal responses.

The results of this study have potential environmental design applications. Physical environment can be designed to create transient localized heat loss from the body. Cool or warm localized surfaces around the body can be incorporated to the workstation design to control heat loss from the feet which had high correlation to the thermal sensation. The same strategy can be applied to influence the local skin temperatures which had a significant effect on thermal sensation. The immediate environment of a person can be designed to increase mean skin temperature under neutral conditions to avoid thermal discomfort.

Localized airflow was an efficient method of utilizing the convective heat loss while minimizing the volume of air needed for comfort. Flexible work environments can be designed relatively inexpensively which allow local airflow conditions. The strategy presented in this study de-couples the room air distribution from the air handling unit. Less pressure is adequate at the diffusers which will result in reduced fan power at the air handling units. Room air diffusers can be redesigned since their primary function becomes delivering the air to the room rather than distributing the air inside the room.

Analysis on the diurnal variations of thermal comfort and sensation showed that people's comfort requirements differ significantly between the morning and the afternoon hours. Mechanical systems should be designed to be flexible enough to allow hourly changes in operation and energy management and control systems (EMCS) should account for the diurnal variations of the building occupants.

Conventional thermal environment management solely depends on keeping the temperature and the humidity within an acceptable margin. The most fundamental aspects of thermal comfort which are physiological signals and subjective responses of building occupants are missing from the thermal environment control strategies. Work environments are increasingly depending on computers. Building occupants' thermal responses can be collected by computerized surveys similar to the *Online Survey* and fed into the EMCS as a direct measure of comfort. This would create spatial arrays of thermal comfort perception inside the buildings which would allow detection of comfort problems and equipment failure by direct input from the users. The second missing component is the physiological measurements. With the advent of measuring equipment and wireless technologies, sensors on building occupants, which measure physiological variables such as heart rate and skin temperature, can be used to control the environmental systems. This requires designing personalized comfort systems which can be fine tuned for each individual's comfort requirements.

### 10.3. Limitations and Future Research

The thermal comfort tests of this study were conducted in the hot and humid climate of the Southern United States, where airflow is naturally perceived as a thermal comfort strategy. The results of this study may be limited to this climate although the tests were conducted during the cool and temperate season with normal humidity levels. The same study for Northern climates is noted as a future research opportunity. This study was conducted with subjects whose ages ranged between 18 and 34 years old. Therefore, the applicability of the results to the ages below 18 and above 34 is also noted as a limitation of the study.

This study was designed for indoor climates in which humidity is controlled within comfort levels. However, thermal comfort is a significant problem in hot and humid regions of the world where people heavily depend on natural ventilation. It is also known that high humidity conditions increase skin wettedness which results in lowered thermal comfort. A similar study is noted as future research opportunity to investigate the effect of high humidity for transient environmental and metabolic conditions.

This study proposed and analyzed thermal environment design strategies based on the characteristics of the airflow around the human body. The key variables studied were metabolic rate, temperature, airflow pulse frequency, airflow location, and the airflow velocity were predetermined and were not adjusted during the test. It is known that providing individuals with environmental controls to adjust these variables can have a significant positive effect on the comfort of the individuals. Therefore, a future study is noted which is based on the same environmental and personal variables with an added user control over the thermal environment.

## REFERENCES

Abanto, J., Barrero, D., Reggio, M. and Ozell, B. (2004) Airflow modelling in a computer room, *Building and Environment*, **39**, 1393-1402.

Alderman, B.L., Arent, S.M., Landers, D.M. and Rogers, T.J. (2007) Aerobic exercise intensity and time of stressor administration influence cardiovascular responses to psychological stress, *Psychophysiology*, **44**, 759-766.

Andreassi, J.L. (2000) *Psychophysiology: Human Behavior and Physiological Response,* L. Erlbaum, Publishers, Mahwah, N.J.

Arens, E., Zhang, H. and Huizenga, C. (2006a) Partial- and whole-body thermal sensation and comfort - Part I: Uniform environmental conditions, *Journal of Thermal Biology*, **31**, 53-59.

Arens, E., Zhang, H. and Huizenga, C. (2006b) Partial- and whole-body thermal sensation and comfort - Part II: Non-uniform environmental conditions, *Journal of Thermal Biology*, **31**, 60-66.

ASHRAE (2004) Standard 55, *Thermal Environmental Conditions for Human Occupancy*, ASHRAE, Atlanta.

ASHRAE (2010) Standard 62.1, *Ventilation for Acceptable Indoor Air Quality*, ASHRAE, Atlanta.

Astrand, P.-O., Rodahl, K., Dahl, H.A. and Stromme, S.B. (2003) *Textbook of Work Physiology,* Human Kinetics, Champaign, IL.

Atmaca, I. and Yigit, A. (2006) Predicting the effect of relative humidity on skin temperature and skin wettedness, *Journal of Thermal Biology*, **31**, 442-452.

Atthajariyakul, S. and Leephakpreeda, T. (2004) Real-time determination of optimal indoor-air condition for thermal comfort, air quality and efficient energy usage, *Energy and Buildings*, **36**, 720-733.

Badagliacca, A. (2002) Theoretical approach to the global comfort problem in the man-environment interactions, *Building and Environment*, **37**, 975-982.

Bauman, F., Arens, E., Fountain, M., Huizenga, C., Miura, K., Xu, T., Akimoto, T., Zhang, H., Faulkner, D., Fisk, W. and Borgers, T. (1994) *Localized Thermal Distribution for Office Buildings; Final Report - Phase III, Indoor Environmental Quality*, University of California, Berkeley, 115 pp.

Berggren, G. and Hohwu Christensen, E. (1950) Heart rate and body temperature as indices of metabolic rate during work, *Arbeitsphysiologie*, **14**, 255-260.

Beshir, M.Y. and Ramsey, J.D. (1981) Comparison between male and female subjective estimates of thermal effects and sensations, *Applied Ergonomics*, **12**, 29-33.

Boregowda, S.C. and Karwowski, W. (2005) Modeling of human physiological stresses: A thermodynamics-based approach, *Occupational Ergonomics*, **5**, 235-248.

Bouden, C. and Ghrab, N. (2005) An adaptive thermal comfort model for the Tunisian context: A field study results, *Energy and Buildings*, **37**, 952-963.

Brager, G.S., Paliaga, G. and De Dear, R. (2004) Operable windows, personal control, occupant comfort, *ASHRAE Transactions*, **110**, 17-35.

Burton, A.C. (1934) A new technic for the measurement of average skin temperature over surfaces of the body and the changes of skin temperature during exercise, *Journal of Nutrition*, **7**, 481-496.

Cabanac, M. (1981) Physiological Signals for Thermal Comfort, In: Cena, K. and Clark, J. A. (eds) *Bioengineering, Thermal Physiology and Comfort*, Elsevier Scientific Publishing Company, New York, 181-192.

Cacioppo, J., Tassinary, L.G. and Berntson, G.G. (ed) (2007) *Handbook of Psychophysiology*, Cambridge University Press, Cambridge, UK.

Cacioppo, J.T., Tassinary, L.G., Stonebraker, T.B. and Petty, R.E. (1987) Self-report and cardiovascular measures of arousal: Fractionation during residual arousal, *Biological Psychology*, **25**, 135-151.

Cena, K. and De Dear, R. (1998) *ASHRAE RP-921 - Field Study of Occupant Comfort an Office Thermal Environments in a Hot-arid Climate*, ASHRAE, Atlanta.

Chen, Q. (2004) Using computational tools to factor wind into architectural environment design, *Energy and Buildings*, **36**, 1197-1209.

Conceicao, E.Z.E., Lucio, M.M.J.R., Lourenco, T.M.C. and Brito, A.I.P.V. (2006) Evaluation of thermal comfort in slightly warm ventialted spaces in nonuniform environments, *HVAC&R Research*, **12**, 451-475.

Coulbourn (2010) Lablinc V Isolated Skin Conductance Coupler, Coulbourn Instruments, Whitehall, PA.

Cunningham, D.J., Stolwijk, J.A.J. and Wenger, C.B. (1978) Comparative thermoregulatory responses of resting men and women, *Journal of Applied Physiology*, **45**, 908-915.

De Dear, R. (2004) Thermal comfort in practice, *Indoor Air*, **14**, 32-39.

De Dear, R., Brager, G. and Cooper, D. (1997) *Developing an Adaptive Model of Thermal Comfort and Preference: Final Report ASHRAE RP-884*, Macquarie University, Sydney, Australia.

De Dear, R. and Brager, G.S. (2001) The adaptive model of thermal comfort and energy conservation in the built environment: Final report ASHRAE RP-884, *International Journal of Biometeorology*, **45**, 100-108.

De Dear, R.J., Ring, J.W. and Fanger, P.O. (1993) Thermal sensations resulting from sudden ambient temperature changes, *Indoor Air*, **3**, 181-192.

Deevy, M. (2006) *CFD Modelling of the Benchmark Displacement Ventilation Test Case*, Health & Safety Laboratory, Derbyshire, UK.

Deevy, M., Sinai, Y., Everitt, P., Voigt, L. and Gobeau, N. (2008) Modelling the effect of an occupant on displacement ventilation with computational fluid dynamics, *Energy and Buildings*, **40**, 255-264.

Doebelin, E.O. (2004) *Measurement Systems,* McGraw Hill, Boston.

Drori, U., Dubovsky, V. and Ziskind, G. (2005) Experimental verification of induced ventilation, *Journal of Environmental Engineering*, **131**, 820-826.

Dygert, R.K., Dang, T.Q., Russo, J., S and Khalifa, E.H. (2009) Modeling of the human body to study the personal micro environment, *ASHRAE Transactions*, **115**, 407-420.

Edelberg, R. (1972) Electrical activity of the skin: Its measurement and uses in psychophysiology, In: Greenfield, N. S. and Sternbach, R. A. (eds) *Handbook of Psychophysiology*, Holt, Rinehart and Winston, New York.

EIA (2006) Total Energy Consumption by Major Fuel for Non-Mall Buildings, 2003, In: EIA-Table-C1.xls, Energy Information Administration, Washington, DC.

Epstein, Y. and Moran, D.S. (2006) Thermal comfort and the heat stress indices, *Industrial Health*, **44**, 388-398.

Erlandson, T., Cena, K., Dear, R.D. and Havenith, G. (2003) Environmental and human factors influencing thermal comfort of office occupants in hot-humid and hot-arid climates, *Ergonomics*, **46**, 616-628.

Ettema, J.H. and Zielhuis, R.L. (1971) Physiological parameters of mental load, *Ergonomics*, **14**, 137-144.

Fanger, P.O. (1970) *Thermal Comfort,* Danish Technical Press, Copenhagen.

Fanger, P.O. (1972) *Thermal Comfort: Analysis and Applications in Environmental Engineering,* McGraw-Hill, New York.

Fanger, P.O., Melikov, A.K., Hanzawa, H. and Ring, J. (1988) Air turbulence and sensation of draught, *Energy and Buildings*, **12**, 21-39.

Fiala, D., Lomas, K.J. and Stohrer, M. (2003) First principles of modeling of thermal sensation responses in steady-state and transient conditions, *ASHRAE Transactions*, **109**, 179-186.

Fluent Inc. (2005) *Fluent 6.2 User's Guide*, Fluent Company, Ann Arbor, MI.

Fountain, M., Arens, E., De Dear, R., Bauman, F. and Miura, K. (1994) Locally controlled air movement preferred in warm isothermal environments, *ASHRAE Transactions*, **100**, 937-952.

Gagge, A.P., Stolwijk, J.A.J. and Hardy, J.D. (1967) Comfort and thermal sensations and associated physiological responses at various ambient temperatures, *Environmental Research*, **1**, 1-20.

Gagge, A.P., Stolwijk, J.A.J. and Nishi, Y. (1970) An effective temperature scale based on a simple model of human physiological regulatory response, *ASHRAE Transactions*, **77**, 247-262.

Gagge, A.P., Stolwijk, J.A.J. and Saltin, B. (1969) Comfort and thermal sensations and associated physiological responses during exercise at various ambient temperatures, *Environmental Research*, **2**, 209-229.

Gao, N. and Niu, J. (2004) CFD study on micro-environment around human body and personalized ventilation, *Building and Environment*, **39**, 795-805.

GE Sensing (2010) Dew10 Series Precision Chilled Mirror Transmitter, General Electric Company, Billerica, MA.

Graves, K.W. (1974) Globe thermometer evaluation, *AIHA Journal*, **35**, 30-40.

Greenspan, J.D., Roy, E.A., Caldwell, P.A. and Farooq, N., S. (2003) Thermosensory intensity and affect throughout the perceptible range, *Somatosensory & Motor Research*, **20**, 19-26.

Griefahn, B. and Kunemund, C. (2001a) The effects of gender, age and fatigue on susceptibility to draft discomfort, *Journal of Thermal Biology*, **26**, 395-400.

Griefahn, B., Kunemund, C. and Gehring, U. (2001b) The impact of draught related to air velocity, air temperature and workload, *Applied Ergonomics*, **32**, 407-417.

Griffiths, I.D. and McIntyre, D.A. (1974) Sensitivity to temporal variations in thermal conditions, *Ergonomics*, **17**, 499-507.

Hanqing, W., Chunhua, H., Zhiqiang, L., Guangfa, T., Yingyun, L. and Zhiyong, W. (2006) Dynamic evaluation of thermal comfort environment of air-conditioned buildings, *Building and Environment*, **41**, 1522-1529.

Hashiguchi, N., Feng, Y. and Tochihara, Y. (2010) Gender differences in thermal comfort and mental performance at different vertical air temperatures, *European Journal of Applied Physiology*, **109**, 41-48.

Havenith, G., Holmer, I. and Parsons, K. (2002) Personal factors in thermal comfort assessment: Clothing properties and metabolic heat production, *Energy and Buildings*, **34**, 581-591.

Hensel, H. (1981) *Thermoreception and Temperature Regulation,* Academic Press, London.

Heusch, A.I., Suresh, V. and Mccarthy, P.W. (2006) The effect of factors such as handedness, sex and age on body temperature measured by an infrared 'tympanic' thermometer, *Journal of Medical Engineering & Technology*, **30**, 235-241.

Hot, P., Naveteur, J., Leconte, P. and Sequeira, H. (1999) Diurnal variations of tonic electrodermal activity, *International Journal of Psychophysiology*, **33**, 223-230.

Houdas, Y. and Ring, E.F.J. (1982) *Human Body Temperature,* Plenum Press, New York.

Huda, L.N. and Homma, H. (2005) Thermal sensation of local airflows with different temperatures and velocities: Comparison between summer and winter, *ASHRAE Transactions*, **111**, 123-131.

Huizenga, C., Hui, Z. and Arens, E. (2001) A model of human physiology and comfort for assessing complex thermal environments, *Building and Environment*, **36**, 691-699.

Humphreys, M.A. (1977) The optimum diameter of a globe thermometer for use in indoors, *Annals of Occupational Hygene*, **20**, 135-140.

INOR (2010) IPAQ-HLP Transmitter, INOR Company, Malmo, Sweden.

ISO 7726 (1998) *Ergonomics of the Thermal Environment - Instruments for Measuring Physical Quantities, ISO 7726*, The International Organization for Standardization, Geneva.

ISO 7730 (2005) *Ergonomics of the Thermal Environment - Analytical Determination and Interpretation of Thermal Comfort Using Calculation of the PMV and PPD Indices and Local Thermal Comfort Criteria, ISO 7730*, The International Organization for Standardization, Geneva.

ISO 8996 (2004) *Ergonomics of the Thermal Environment - Determination of Metabolic Rate, ISO 8996*, The International Organization for Standardization, Geneva.

ISO 9886 (2004) *Ergonomics - Evaluation of Thermal Strain by Physiological Measurements, ISO 9886,* The International Organization for Standardization, Geneva.

ISO 9920 (1995) *Ergonomics of the Thermal Environment - Estimation of the Thermal Insulation and Evaporative Resistance of a Clothing Ensemble, ISO 9920*, The International Organization for Standardization, Geneva.

Iyoho, A.E., Jang, T.S. and Nair, S.S. (2004) Human thermal model with extremities for asymmetric environments. In: *Proceedings of 2004 American Control Conference*, June 30-July 2, Boston, MA, pp. 4366-4371.

Jang, T.S., Berglund, L.G., Iyoho, A.E. and Nair, S.S. (2009) Modeling individual variations in thermal stress response for humans in transient environments, *ASHRAE Transactions*, **115**, 552-564.

Jay, O., Reardon, F.D., Webb, P., Ducharme, M.B., Ramsay, T., Nettlefold, L. and Kenny, G.P. (2007) Estimating changes in mean body temperature for humans during exercise using core and skin temperatures is inaccurate even with a correction factor, *Journal of Applied Physiology*, **103**, 443-451.

Jones, B.W. (2002) Capabilities and limitations of thermal models for use in thermal comfort standards, *Energy and Buildings*, **34**, 653-659.

Jones, B.W., Hsieh, K. and Hashinaga, M. (1986) The effect of air velocity on thermal comfort at moderate activity levels, *ASHRAE Transactions*, **92**, 761-768.

Jones, B.W. and Ogawa, Y. (1992) Transient interaction between the human and the thermal environment, *ASHRAE Transactions*, **98**, 189-195.

Kacmarczyk, J., Melikov, A. and Fanger, P.O. (2004) Human response to personalized ventilation and mixing ventilation, *Indoor Air*, **14**, 17-29.

Karjalainen, S. (2007) Gender differences in thermal comfort and use of thermostats in everyday thermal environments, *Building and Environment*, **42**, 1594-1603.

Kaynakli, O. and Kilic, M. (2005) Investigation of indoor thermal comfort under transient conditions, *Building and Environment*, **40**, 165-174.

Kaz Inc. (2010) Braun Thermoscan Ear Thermometer IRT4520. Braun Company, Kronberg, Germany.

Kistemaker, J.A., Den Hartog, E.A. and Daanen, H.A.M. (2006) Reliability of an infrared forehead skin thermometer for core temperature measurements, *Journal of Medical Engineering & Technology*, **30**, 252-261.

Kosonen, R. and Tan, F. (2004) Assessment of productivity loss in air-conditioned buildings using PMV index, *Energy and Buildings*, **36**, 987-993.

Lin, Z., Chow, T.T. and Tsang, C.F. (2007) Effect of door opening on the performance of displacement ventilation in a typical office building, *Building and Environment*, **42**, 1335-1347.

Lin, Z., Chow, T.T., Tsang, C.F., Fong, K.F. and Chan, L.S. (2005) CFD study on effect of the air supply location on the performance of the displacement ventilation system, *Building and Environment*, **40**, 1051-1067.

Lv, Y.-G. and Liu, J. (2005) Interpretation on thermal comfort mechanisms of human bodies by combining Hodgkin-Huxley neuron model and Pennes bioheat equation, *Forschung im Ingenieurwesen*, **69**, 101-114.

Lv, Y.-G. and Liu, J. (2007) Effect of transient temperature on thermoreceptor response and thermal sensation, *Building and Environment*, **42**, 656-664.

Mabuchi, K., Genno, H., Kunimoto, M., Kanbara, O., Suzuki, T. and Chinzei, T. (1996) Use of skin sympathetic nerve activity for the automatic control of an air-conditioning system. In: *Proceedings of the 18th Annual International Conference of the IEEE Engineering in Medicine and Biology Society*, Oct 31-Nov 3, Amsterdam.

Magnetrainer (2010) Mini Exercise Bike, 3D Innovations Company, Greeley, CO.

Mayer, E. (1987) Physical causes for draught: Some new findings, *ASHRAE Transactions*, **93**, 540-548.

Mayer, E. (1993) Objective criteria for thermal comfort, *Building and Environment*, **28**, 399-403.

McIntyre, D.A. (1980) *Indoor Climate,* Applied Science Publishers Ltd., London.

McNall, P.E., Jaax, J., Rohles, F.H., Nevins, R.G. and Springer, W.E. (1967) Thermal comfort (thermally neutral) conditions for three levels of activity, *ASHRAE Transactions*, **73**, I.3.1-I.3.14.

McNall, P.E., Ryan, P.W., Rohles, F.H., Nevins, R.G. and Springer, W.E. (1968) Metabolic rates of four activity levels and their relationship to thermal comfort, *ASHRAE Transactions*, **74**, IV.3.1-IV.3.17.

Melikov, A.K. and Knudsen, G.L. (2007) Human response to an individually controlled microenvironment, *HVAC&R Research*, **13**, 645-660.

Mifflin, M.D., St Jeor, S.T., Hill, L.A., Scott, B.J., Daugherty, S.A. and Koh, Y.O. (1990) A new predictive equation for resting energy expenditure in healthy individuals, *American Journal of Clinical Nutrition*, **51**, 241-247.

Mitchell, D. and Wyndham, C.H. (1969) Comparison of weighting formulas for calculating mean skin temperature, *Journal of Applied Physiology*, **26**, 616-622.

Mui, K.W. and Chan, W.T. (2005) Application of the Building Environmental Performance Model (BEPM) in Hong Kong, *Energy and Buildings*, **37**, 897-909.

Murray-Smith, A.I., Stewart, J.M. and Cohen, M.H. (1984) Dependence of human physiological conductance on metabolic rate, In: Hales, J. R. S. (ed) *Thermal Physiology*, Raven Press, New York, 239-242.

Nachtigal, C.L. (1990) Instrumentation and Control, New York, John Wiley & Sons Inc.

National Instruments (2010) PCI 6031E DAQ System, NI Company, Austin, TX.

Neghabat, M., Ringuest, J.L. and Gullege Jr, T.R. (1989) A model to the controller responses of the human temperature regulating system to changes in air temperature, *Mathematical and Computer Modeling*, **12**, 277-288.

Nicholas, J.V. and White, D.R. (1994) *Traceable Temperatures,* New York, John Wiley & Sons.

Nicol, F. (2004) Adaptive thermal comfort standards in the hot-humid tropics, *Energy and Buildings*, **36**, 628-637.

Nielsen, P.V. (2004) Computational fluid dynamics and room air movement, *Indoor Air*, **14**, 134-143.

Nielsen, P.V., Murakami, S., Kato, S., Topp, C. and Yang, J.-H. (2003) *Benchmark Tests for a Computer Simulated Person*, Aalborg University, Aalborg, Denmark.

Nikolopoulou, M. and Steemers, K. (2003) Thermal comfort and psychological adaptation as a guide for designing urban spaces, *Energy and Buildings*, **35**, 95-101.

Olesen, B. (1984) How many sites are necessary to estimate a mean skin temperature?, In: Hales, J. R. S. (ed) *Thermal Physiology*, Raven Press, New York, 33-39.

Olesen, B.W. and Brager, G.S. (2004) A better way to predict comfort, *ASHRAE Journal*, **46**, 20-28.

Olesen, B.W. and Parsons, K.C. (2002) Introduction to  thermal comfort standards and to the proposed new version of EN ISO 7730, *Energy and Buildings*, **34**, 537-548.

Omega (2010) T-type Thermocouple (GG-T-28-SLE), Omega Engineering, Inc., Stamford, CT.

Ott, L.R. and Longnecker, M. (2001) *An Introduction to Statistical Methods and Data Analysis,* Wadsworth Group, Pacific Grove, CA.

Parsons, K.C. (2002) The effects of gender, acclimation state, the opportunity to adjust clothing and physical disability on requirements for thermal comfort, *Energy and Buildings*, **34**, 593-599.

Parsons, K.C. (2003) *Human Thermal Environments : The Effects of Hot, Moderate, and Cold Environments on Human Health, Comfort, and Performance,* Taylor & Francis, New York.

Pellerin, N., Deschuyteneer, A. and Candas, V. (2004) Local thermal unpleasantness and discomfort prediction in the vicinity of thermoneutrality, *European Journal of Applied Physiology*, **92**, 717-720.

Pereira, N., Bond, T.E. and Morrison, S.R. (1967) Ping-pong ball into black-globe thermometer, *Agricultural Engineering*, **48**, 341-345.

Polar (2010) T31 Coded Transmitter, Polar Electro, Inc., Lake Success, NY.

Prek, M. (2006) Thermodynamical analysis of human thermal comfort, *Energy*, **31**, 732-743.

Ring, J.W., De Dear, R. (1991) Temperature transients: A model for heat diffusion through the skin, thermoreceptor response and thermal sensation, *Indoor Air*, **1**, 448-456.

Ring, J.W., De Dear, R. and Melikov, A. (1993) Human thermal sensation: Frequency response to sinusoidal stimuli at the surface of the skin, *Energy and Buildings*, **20**, 159-165.

Rowe, D.M. (2001) Activity rates and thermal comfort of office occupants in Sydney, *Journal of Thermal Biology*, **26**, 415-419.

Sakoi, T., Tsuzuki, K., Kato, S., Ooka, R., Song, D. and Zhu, S. (2007) Thermal comfort, skin temperature distribution, and sensible heat loss distribution in the sitting posture in various asymmetric radiant fields, *Building and Environment*, **42**, 3984-3999.

Seppanen, O., Fisk, W.J. and Faulkner, D. (2004) *Control of temperature for health and productivity in offices*, Lawrence Berkeley National Laboratory, Berkeley, CA.

Soransen, D.N. and Voigt, L.K. (2003) Modelling flow and heat transfer around a seated human body by computational fluid dynamics, *Building and Environment*, **38**, 753-762.

Spalding, T.W., Lyon, L.A., Steel, D.H. and Hatfield, B.D. (2004) Aerobic exercise training and cardiovascular reactivity to psychological stress in sedentary young normotensive men and women, *Psychophysiology*, **41**, 552-562.

Stamou, A. and Katsiris, I. (2006) Verification of a CFD model for indoor airflow and heat transfer, *Building and Environment*, **41**, 1171-1181.

Steele, W.G. and Lewis, M. (1968) A longitudinal study of the cardiac response during problem solving task and its relationship to general cognitive function, *Psychonomic Science*, **11**, 275-276.

Stolwijk, J.A.J. (1971) *A Mathematical Model of Physiological Temperature Regulation in Man*, Yale University, New Haven, CT.

Strigo, I.A., Carli, F. and Bushnell, C. (2000) Effect of ambient temperature on human pain and temperature perception, *Anesthesiology*, **92**, 699-707.

Tanabe, S.-I., Hasebe, Y., Kimura, K.-I. and Haga, Y. (1993) Estimation of thermal sensation using PMV and SET* under high air movement conditions, *Journal of Thermal Biology*, **18**, 551-554.

Tanabe, S.-I. and Kimura, K.-I. (1994) Effects of air temperature, humidity, and air movement on thermal comfort under hot and humid conditions, *ASHRAE Transactions*, **100**, 953-969.

Tanabe, S.-I., Kobayashi, K., Nakano, J., Ozeki, Y. and Konishi, M. (2002) Evaluation of thermal comfort using combined multi-node thermoregulation (65MN) and radiation models and computational fluid dynamics (CFD), *Energy and Buildings*, **34**, 637-646.

Tanabe, S.-I., Nishihara, N. and Haneda, M. (2007) Indoor temperature, productivity, and fatigue in office tasks, *HVAC&R Research*, **13**, 623-633.

Toftum, J. (2002) Human response to combined indoor environment exposures, *Energy and Buildings*, **34**, 601-606.

Toftum, J. (2004) Air movement - good or bad?, *Indoor Air*, **14**, 40-45.

Toftum, J. and Nielsen, R. (1996) Impact of metabolic rate on human response to air movements during work in cool environments, *International Journal of Industrial Ergonomics*, **18**, 307-316.

Topp, C., Nielsen, P.V. and Sorensen, D.N. (2002) Application of computer simulated persons in indoor environmental modeling, *ASHRAE Transactions*, **108**, 1084-1089.

Tse, W.L. and So, A.T.P. (2007) The importance of human productivity to air-conditioning control in office environments, *HVAC&R Research*, **13**, 3-21.

TSI (2010) The Model 8475 Omnidirectional Air Velocity Transducer, TSI, Inc., Shoreview, MN.

Ugursal, A. and Culp, C.H. (2007) Comparative analysis of CFD deltaP vs. measured deltaP for compressed flexible ducts, *ASHRAE Transactions*, **113**, 462-469.

Van Den Heuvel, C.J., Ferguson, S.A., Gilbert, S.S. and Dawson, D. (2004) Thermoregulation in normal sleep and insomnia: The role of peripheral heat loss and new applications for digital thermal infrared imaging (DITI), *Journal of Thermal Biology*, **29**, 457-461.

Van Hoof, J. and Hensen, J.L.M. (2007) Quantifying the relevance of adaptive thermal comfort models in moderate thermal climate zones, *Building and Environment*, **42**, 156-170.

Wang, D., Federspiel, C.C. and Rubinstein, F. (2005) Modeling occupancy in single person offices, *Energy and Buildings*, **37**, 121-126.

Wang, D., Zhang, H., Arens, E. and Huizenga, C. (2007) Observations of upper-extremity skin temperature and corresponding overall-body thermal sensations and comfort, *Building and Environment*, **42**, 3933-3943.

Wessel, A., Peinke, J. and Lange, B. (2006) Verification of a new model to calculate turbulence intensity inside a wind farm. In: *Proceedings of European Wind Energy Conference & Exhibition*, Feb 27-Mar 2, Athens, Greece.

Wissler, E.H. (1985) Mathematical simulation of human thermal behavior using whole body models, In: Shitzer, A. and Eberhart, R. C. (eds) *Heat Transfer in Medicine and Biology*, Vol. 1, Plenum Press, New York, 325-373.

Woods, J.E. (1989) Cost avoidance and productivity in owning and operating buildings, *Occupational Medicine*, **4**, 753-770.

Yao, Y., Lian, Z., Liu, W. and Shen, Q. (2008) Experimental study on physiological responses and thermal comfort under various ambient temperatures, *Physiology & Behavior*, **93**, 310-321.

Zhai, Z., Zhang, Z., Zhang, W. and Chen, Q.Y. (2007) Evaluation of various turbulence models in predicting airflow and turbulence in enclosed environments by CFD: Part 1--Summary of prevalent turbulence models, *HVAC&R Research*, **13**, 853-870.

Zhang, H. (2003a) *Human Thermal Sensation and Comfort in Transient and Non-Uniform Thermal Environments*. PhD Dissertation, University of California, Berkeley.

Zhang, H., Arens, E. and Arens, C. (2003b) Using a driving game to increase the realism of laboratory studies of automobile passenger thermal comfort, *SAE Technical Paper Series* **2003-01-2710**, 1-7.

Zhang, H., Arens, E., Fard, S.A., Huizenga, C., Paliaga, G., Brager, G. and Zagreus, L. (2007a) Air movement preferences observed in office buildings, *International Journal of Biometeorology*, **51**, 349-360.

Zhang, H., Huizenga, C., Arens, E. and Wang, D. (2004) Thermal sensation and comfort in transient non-uniform thermal environments, *European Journal of Applied Physiology*, **92**, 728-733.

Zhang, H., Kim, D., Arens, E., Buchberger, E., Bauman, F. and Huizenga, C. (2008a) *Comfort, perceived air quality, and work performance in a low-power task-ambient conditioning system*, University of California, Berkeley, CA.

Zhang, L. (2005) Turbulent three-dimensional air flow and heat transfer in a cross-corrugated triangular duct, *Journal of Heat Transfer*, **127**, 1151-1158.

Zhang, Y. and Zhao, R. (2008b) Overall thermal sensation, acceptability and comfort, *Building and Environment*, **43**, 44-50.

Zhang, Y.F., Wyon, D.P., Fang, L. and Melikov, A.K. (2007b) The influence of heated or cooled seats on the acceptable ambient temperature range, *Ergonomics*, **50**, 586-600.

Zhang, Z., Zhang, W., Zhai, Z. and Chen, Q.Y. (2007c) Evaluation of various turbulence models in predicting airflow and turbulence in enclosed environments by CFD: Part 2--Comparison with experimental data from literature, *HVAC&R Research*, **13**, 871-886.

Zhao, B., Li, X. and Yan, Q. (2003) A simplified system for indoor airflow simulation, *Building and Environment*, **38**, 543-552.

Zhao, R. (2007) Investigation of transient thermal environments, *Building and Environment*, **42**, 3926-3932.

Zhao, R., Sun, S. and Ding, R. (2004) Conditioning strategies of indoor thermal environment in warm climates, *Energy and Buildings*, **36**, 1281-1286.

Zhou, X., Ouyang, Q., Lin, G. and Zhu, Y. (2006) Impact of dynamic airflow on human thermal response, *Indoor Air*, **16**, 348-355.

# APPENDIX A
# COMFORT STATION DRAWINGS AND CONSTRUCTION PHOTOS

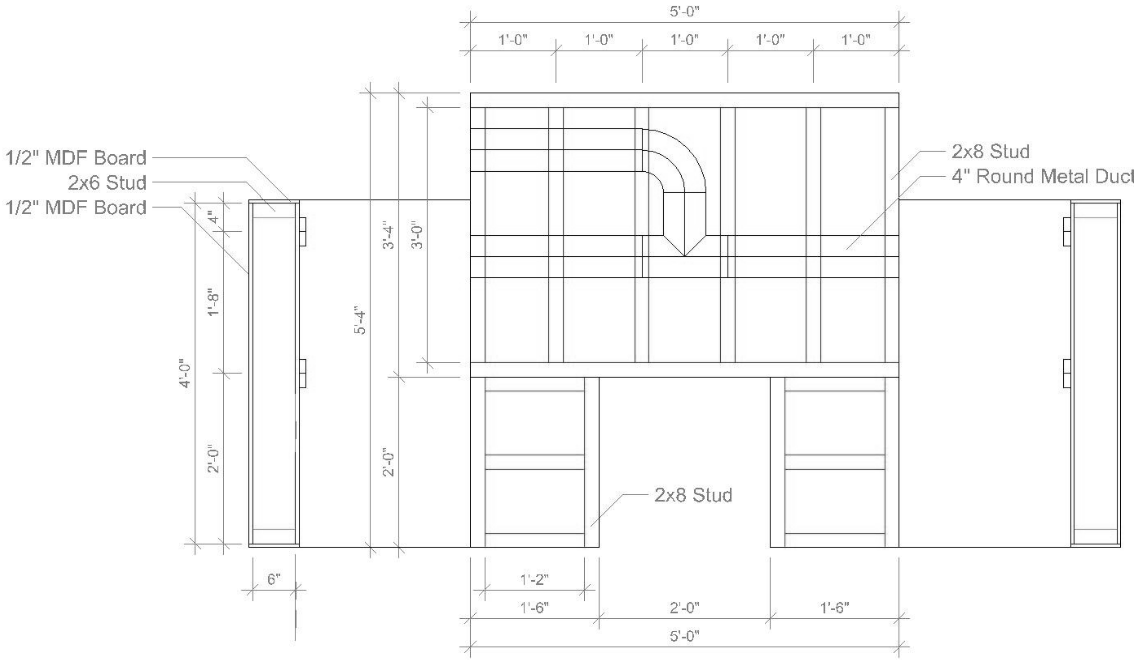


Figure A.1. Plan drawing of the Thermal Comfort Station.

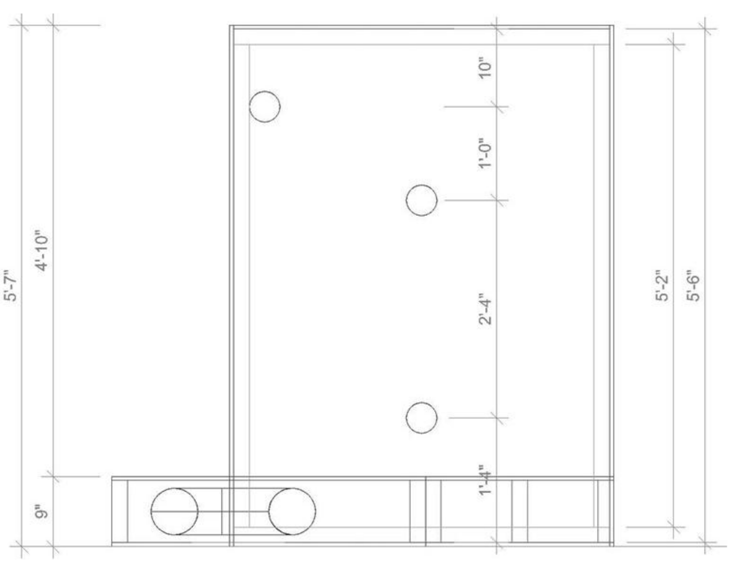


Figure A.2. Section drawing of the Thermal Comfort Station

Figure A.3. Construction of the Comfort Station wall.

Figure A.4. Connection of the fan to the Comfort Station for the test run.

Figure A.5. Connection of the wall to the Comfort Station base.

Figure A.6. Completed Comfort Station before the test runs.

# APPENDIX B
# TEST PROTOCOL

Before the Participant Arrives

- ☐ Test monitor turns on the computers, heaters and the power supplies.
- ☐ Test monitor turns on the white noise generator.
- ☐ Test monitor adjusts the vents for the initial conditions.
- ☐ Test monitor starts the necessary programs on monitor's and subject's computers.
    - Monitor's computer: Background Survey, Timer, Ergometer, Magnifier, Start-Stop Slides, Online Survey
    - Subject's computer: Online Survey, Games
- ☐ Test monitor prepares a test log on the monitor's computer from the *Excel* template in which *Background Survey* and *Online Survey* results will be copied.
- ☐ Test monitor prepares a blank *Excel* document on the subject's computer with participant code as the name of the file.
- ☐ Test monitor enters the survey sampling times and chooses the prepared excel document on the *Online Survey* initial screen.
- ☐ Test monitor sanitizes the TCs with alcohol and prepares the medical tapes.

After the Participant Arrives

- ☐ Participant arrives at the lab and time is recorded *Arrival Time*: ___________
- ☐ Test procedure explained
- ☐ Consent form signed
- ☐ Participant fills out the *Activity Readiness Questionnaire*
- ☐ Participant is asked to use the restroom
- ☐ Participant is asked to turn off his/her cell phone.
- ☐ Participant is given 3 oz. water
- ☐ Participant changes clothing.
- ☐ Participant's weight is measured. *Weight:*___________ *lbs*
- ☐ Test monitor adjusts the bike's position so that the subject can comfortable pedal.
- ☐ Test monitor marks the clothing types in the *Clothing Ins* workbook of the *Test Record Excel* sheet.

☐ EDA electrodes are attached to the hypothenar and thenar eminences

☐ Participant familiarizes himself with the computer and physical environment.

- Test monitor explains how to use the online survey form
- The monitor explains the participant how to communicate using the computer screens.
- The monitor explains the heart rate indicator and the target heart rate which will be shown on the computer screen message.

☐ Participant fills out the *Background Survey* form.

☐ Test monitor copies the *Background Survey* results to the test log file created on the monitor's computer.

☐ Heart rate sensor is attached to the chest.

- The textured surfaces has to be in good contact with the skin
- Wet the textured surfaces with the Saline Solution.
- Check that heart rate signal is correct.

☐ TCs are attached to the participant.

☐ EDA cables are attached to the participant and Coulbourn Equipment is started.

- Test monitor checks the EDA activity on the monitor's computer.

☐ Test monitor checks the TC measurement to make sure that they are attached correctly.

☐ Participant's core temperature is measured with tympanic IR thermometer.

*Temperature:_________ °F* *Time:___________*

Session I

☐ Test monitor chooses "Test-1" from the initial screen of the *Online Survey* and starts the program

☐ Phase I of the test starts *Time:_____________*

☐ Monitor starts the timer with the first instance of the survey.

☐ Test monitor averages the heart rate between 12$^{th}$ and the 14$^{th}$ minutes and records it as basal heart rate

*Basal Heart Rate: ________ bpm* *Target Heart Rate: _________ bpm*

☐ At the 15$^{th}$ minute, monitor asks the subject to start playing games.

☐ At the 25$^{th}$ minute, monitor starts the exercise sequence by projecting the target heart rate on the screen which was calculated based on the basal heart rate taken.

- ☐ At the 30th minute, monitor stops the exercise sequence.
- ☐ 5 min break between the tests. Participant's core temperature is measured.

  *Temperature:_________ °F* *Time:___________*

Session II

- ☐ Test monitor chooses "Test-2" from the initial screen of the *Online Survey* and starts the program.
- ☐ Phase II of the test starts *Time:_____________*
- ☐ Monitor starts the timer at the first instance of the survey
- ☐ Test monitor starts the initial vent sequence at the first instance of the *Online Survey*.
- ☐ Monitor starts the exercise sequence at the first instance of the survey
- ☐ At the 5th minute, monitor stops the exercise sequence.
- ☐ At the 15th minute, monitor changes the vent sequence and starts the exercise sequence.
- ☐ At the 20th minute, monitor stops the exercise sequence.
- ☐ 5 min break between the tests. Participant's core temperature is measured.

  *Temperature:_________ °F* *Time:___________*

Session III

- ☐ Test monitor adjusts the vents and chooses "Test-3" on the initial screen of the *Online Survey* and starts the program.
- ☐ Phase III of the test starts *Time:_____________*
- ☐ Monitor starts the timer at the first instance of the survey
- ☐ Test monitor starts the initial vent sequence at the first instance of the *Online Survey*.
- ☐ Monitor starts the exercise sequence at the first instance of the survey
- ☐ At the 5th minute, monitor stops the exercise sequence.
- ☐ At the 15th minute, monitor changes the vent sequence and starts the exercise sequence.
- ☐ At the 20th minute, monitor stops the exercise sequence.
- ☐ Test ends *Time:_____________*
- ☐ Participant's core temperature is measured.

  *Temperature:_________ °F* *Time:_____________*

<u>After the Test</u>

☐ Electrodes and sensors are detached from the participant.

☐ Participant's weight is measured. *Weight:___________ lbs*

☐ Participant's overall experience of the test is asked

| Very Negative | Negative | Slightly Negative | Neutral | Slightly Positive | Positive | Very Positive |
|---|---|---|---|---|---|---|

☐ Participant leaves the lab. *Time:_____________*

☐ Test monitor copies the *Online Survey* responses to the test log file created on the monitor's computer.

☐ Test monitor converts the HR data and copies the results to the test log file created on the monitor's computer.

☐ Test monitor copies the DAQ data to the test log file created on the monitor's computer.

☐ Test monitor sanitizes the TCs with alcohol.

# APPENDIX C

# TEST SEQUENCES FOR COUNTERBALANCING

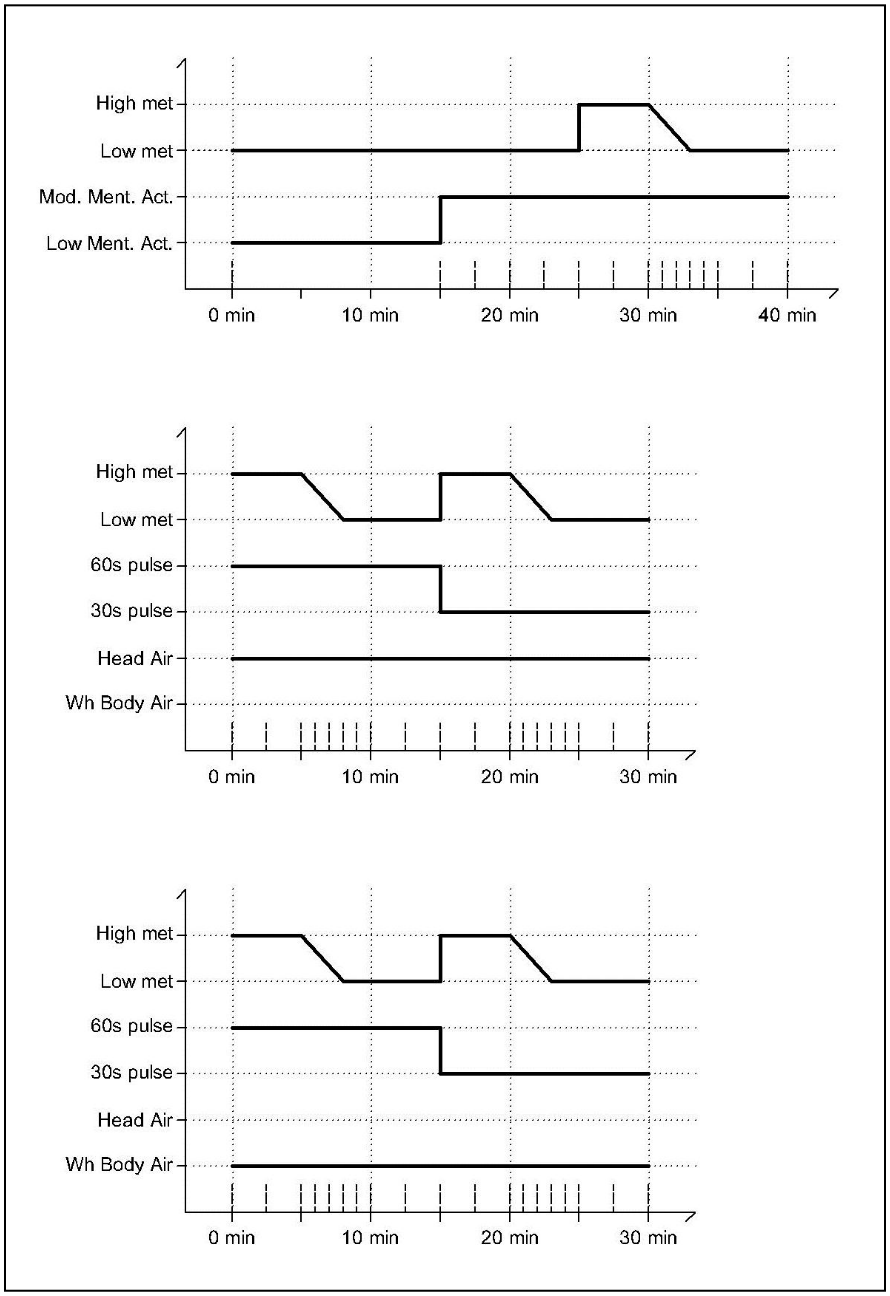


Figure C.1. The first test sequence used for counterbalancing the treatment effect.

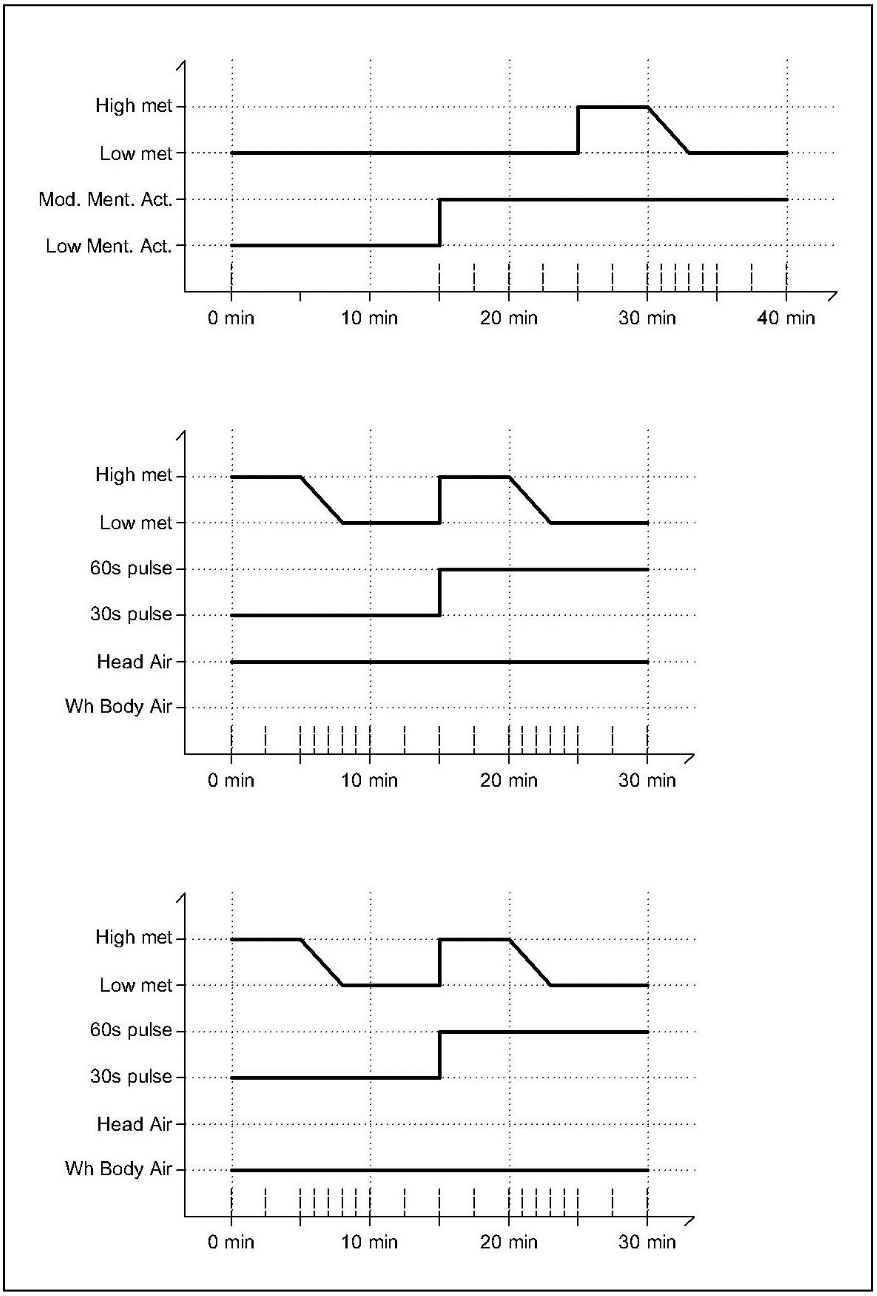


Figure C.2. The second test sequence used for counterbalancing the treatment effect.

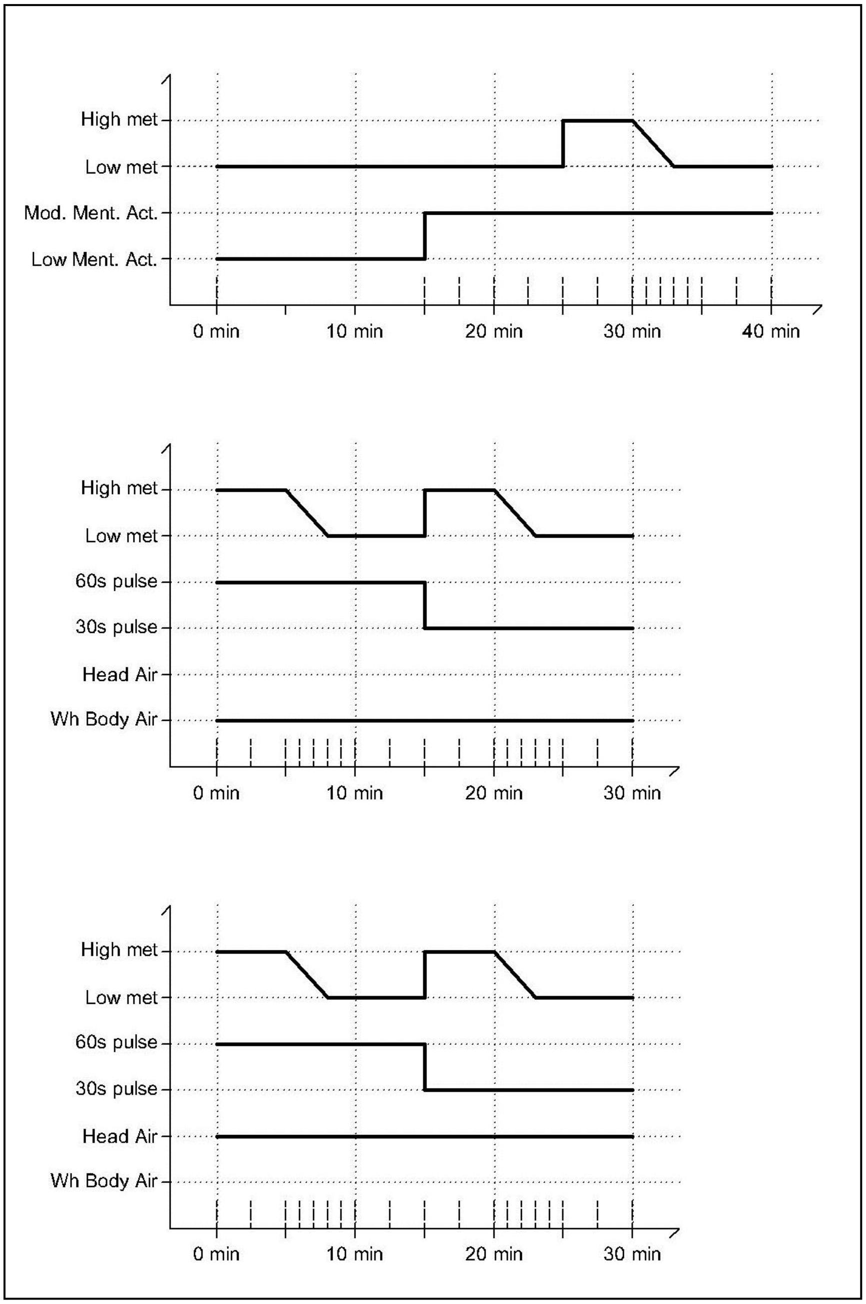


Figure C.3. The third test sequence used for counterbalancing the treatment effect.

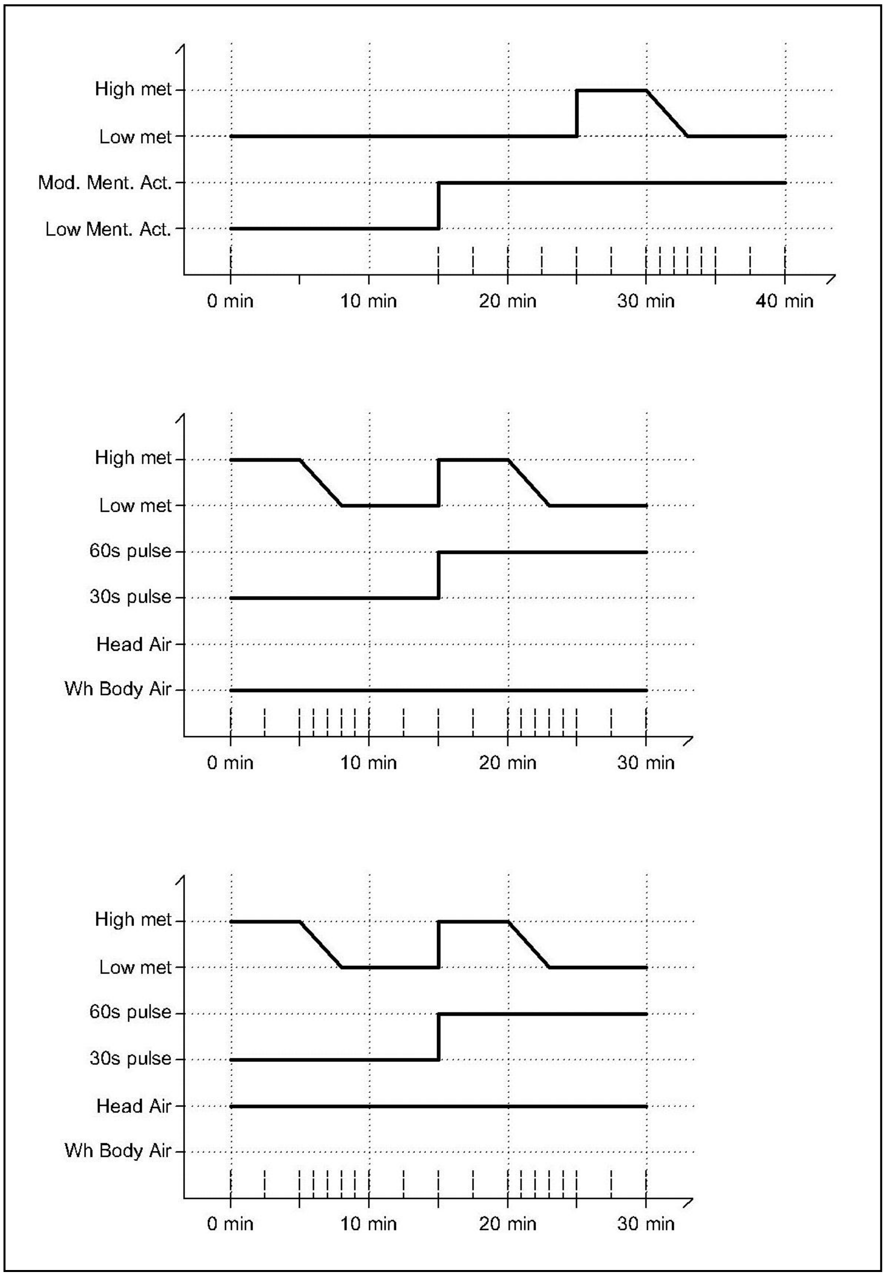


Figure C.4. The fourth test sequence used for counterbalancing the treatment effect.

# VITA


| | |
|---|---|
| Name: | Ahmet Uğursal |
| Address: | 3137 TAMU, Department of Architecture, Texas A&M University,<br>College Station, TX, 77843-3137 |
| Email Address: | augursal@gmail.com |
| Education: | B.Arch., Middle East Technical University, 2000<br>M.S., Building Science, Middle East Technical University, 2003<br>M.Arch., Ball State University, 2005<br>Ph.D., Texas A&M University, 2010 |